The Late Cretaceous and Cenozoic Geological History of the Outer Continental Margin off Nova Scotia, Canada: Insights into Margin Evolution from a Mature Passive Margin

by

D. Calvin Campbell

Submitted in partial fulfilment of the requirements
for the degree of Doctor of Philosophy

at

Dalhousie University
Halifax, Nova Scotia
November 2011

DALHOUSIE UNIVERSITY

DEPARTMENT OF EARTH SCIENCES

The undersigned hereby certify that they have read and recommend to the Faculty of Graduate Studies for acceptance a thesis entitled "The Late Cretaceous and Cenozoic Geological History of the Outer Continental Margin off Nova Scotia, Canada: Insights into Margin Evolution from a Mature Passive Margin" by D. Calvin Campbell in partial fulfilment of the requirements for the degree of Doctor of Philosophy.

Dated: November 4, 2011

Co-Supervisors: _____

_____

External Examiner: _____

Readers: _____

_____

Departmental Representative: _____

DALHOUSIE UNIVERSITY

DATE: November 4, 2011

AUTHOR: D. Calvin Campbell

TITLE: The Late Cretaceous and Cenozoic Geological History of the Outer Continental Margin off Nova Scotia, Canada: Insights into Margin Evolution from a Mature Passive Margin

DEPARTMENT OR SCHOOL: Department of Earth Sciences

DEGREE: Ph.D. CONVOCATION: May YEAR: 2012

_____

Signature of Author

TABLE OF CONTENTS

List of Tables

List of Figures

Abstract

The continental margin off Nova Scotia (the Scotian margin) forms the northern edge of the North American Basin. The Cenozoic stratigraphy and geological history of the outer margin is not well known. This study examines aspects of the Upper Cretaceous-Cenozoic geological history of the outer Scotian margin addressing the following objectives: 1) determine the geological history of a large deep-water depocenter, 2) investigate processes that led to deep-water unconformity formation in the study area, 3) determine the role of deep-ocean circulation in margin evolution, 4) examine the effects of morphological heritage on subsequent depositional patterns. High quality 2-D and 3-D seismic reflection data along with lithostratigraphic and biostratigraphic data from hydrocarbon exploration wells provide the basis for this investigation.

The seismic stratigraphy of a large deep-water depocenter along the western Scotian margin was broadly divided into four units. Unit 1 (Upper Cretaceous-Upper Eocene) is attributed to repeated, widespread erosion events interspersed with periods of hemipelagic and pelagic, carbonate-rich sedimentation. Unit 2 (Lower Oligocene-Middle Miocene) consists of a variety of seismic facies overprinted by dense, small-offset faults. Unit 3 (Middle Miocene-Upper Pliocene) is dominated by sediment drift deposition. Unit 4 (Upper Pliocene-present) is characterized by channel development and gravity flow deposition. The processes that led to regional seismic stratigraphic horizons were complex. Both large mass-wasting events and along-slope bottom currents contributed to the formation of unconformities in the study area. Most of the succession preserved in the depocenter belongs to seismic units 2 and 3. These deposits are mainly confined to the area seaward of the Abenaki carbonate bank and landward of shallow salt structures below the slope. Locally, however, modification of the slope profile through mass-wasting and bottom current processes greatly influenced subsequent depositional patterns. The Cenozoic geological evolution of the study area was strongly affected by northeast-to-southwest flowing bottom currents. The earliest indication of bottom current activity was in the Eocene. Upper Miocene and Pliocene sediment drifts represent >50% of the preserved stratigraphic section in the thickest part of the depocenter. It is clear that along-slope sedimentary processes were far more important in shaping the margin than previously understood.

List of Abbreviations Used

$+f$	Coriolis parameter (northern hemisphere)
2D	two-dimensional
3D	three-dimensional
AABW	Antarctic Bottom Water
CCD	Carbonate Compensation Depth
CLSW	Classic Labrador Sea Water
DSOW	Denmark Strait Overflow Water
DSDP	Deep-Sea Drilling Program
DWBC	Deep Western Boundary Current
Fm	Formation
HEBBLE	High Energy Benthic Boundary Layer Experiment
ISOW	Iceland-Scotland Overflow Water
km	kilometre
m	metre
Ma	Million years
Mbr	Member
ms	millisecond
MTD	Mass transport deposit
ODP	Ocean Drilling Program
OW	Overflow Water
RMS	Root mean square
s	second
SI	Système international
SWC	Sidewall core
twtt	two-way travel time
ULSW	Upper Labrador Sea Water
U.S.	United States

Glossary

abraded surface: in contourite depositional systems, an extensive area dominated by erosional processes. Current-aligned scours, 2D and 3D bedforms, sediment waves, and sand banks are found on abraded surfaces (Hernández-Molina et al. 2008).

barchan bedform: in the marine realm, bedforms that have a crescentic shape in planview. The apex of the crescent points in the up-current direction and the horns point in the down-current direction. It is generally agreed that these bedforms form in sediment-starved settings.

calcite compensation depth: the depth in the oceans below which the rate of supply of calcite (calcium carbonate) lags behind the rate of solvation, such that no calcite is preserved.

cuttings: small pieces of rock that break away at the drill bit during the drilling of a well. Cuttings are circulated with the liquid drilling mud system and screened out for analysis of composition, size, shape, color, texture, hydrocarbon content and other properties.

detached drift: a type of giant elongate mounded sediment drift that appears elongated at an angle from the adjacent slope against which it first began to form. Such drift development can result from a change in the margin's trend (e.g. Eirik Ridge in the Labrador Sea), or from the interaction between surface and bottom currents (e.g. Blake Ridge in the U.S. Atlantic margin) (Faugères and Stow 2008).

helicoidal flow: the spiral flow of water in a moving water mass. It is one example of a secondary flow.

isochore: a contour connecting points of equal true vertical thickness of strata. A map that displays isochores is an isochore map. The terms isochore and isopach are sometimes incorrectly used interchangeably. Isopachs and isochores are equivalent only if the rock layer is horizontal.

isochron: A line joining points of equal time or age, such as a reflection in a seismic profile or contours in an isochron map.

isopach: a contour that connects points of equal thickness. Contours that make up an isopach map display the true stratigraphic thickness as opposed to the true vertical thickness (or isochore).

mass transport deposit: a deposit formed by submarine slope failure.

nepheloid layer: a layer of water in the deep ocean basin, above the ocean floor, that contains significant amounts of suspended sediment.

plastered drift: a type of giant elongate mounded sediment drift located along a gentle slope swept by fairly low-velocity currents. Deposition occurs on one side, both sides and/or directly below the current pathway, together with lateral migration of the drift axis (Faugères and Stow 2008).

receiving basin configuration: the geomorphological characteristics of an ocean basin that includes its gross morphology, types of submarine accommodation, and equilibrium profile (Steffens et al. 2003).

separated drift: a type of giant elongate mounded sediment drift elongated parallel to the slope. Separated drifts are associated with steeper parts of the slope where the contour current is restricted due to Coriolis force. The elongated body is separated from the adjacent margin by a distinct contourite moat along which the principal flow is focused. Erosion and non-deposition are dominant near the current axis, while deposition occurs laterally, where the velocity decreases. Such drifts show an up-slope lateral migration marked by oblique or sigmoidal reflector patterns in seismic lines (Faugères and Stow 2008).

sidewall core: a core sample, typically 2.5 cm wide by 5 cm long, taken from the side of a borehole, usually by a wireline tool.

water mass: an identifiable body of water with a common formation history which has physical properties (e.g. temperature, salinity, chemical - isotopic ratios) distinct from surrounding water.

Acknowledgements

I would like to acknowledge my supervisors Dr. David Mosher and Dr. Grant Wach, and committee members Dr. Mark Deptuck and Mr. John Shimeld, for allowing me to explore the various directions this study has taken. Their varied backgrounds were invaluable when providing feedback as the thesis evolved.

I would like to acknowledge the many companies who supplied data for this study including EnCana Corporation, TGS-NOPEC Geophysical Company L.P., and ION-GXT. Without these key datasets, this project would not be possible.

I would like to thank my managers and supervisors at the Geological Survey of Canada, particularly Gary Sonnichsen, David Piper and Jacob Verhoef, for supporting me in my decision to undertake this project and deflecting some of my regular workload during the last 4 years. Fruitful discussions with individuals at the Bedford Institue of Oceanography and fellow graduate students, particularly David Piper, Francky Saint-Ange, John Wade, Brian Todd, Gang Li, Rob Fensome, Virgina Brake, Shawn Goss, and Michael Giles helped to improve the thesis. Additionally, I would like to acknowledge the various individuals who provided critical reviews of manuscripts and extended abstracts, as well as those who provided constructive comments during conference presentations and poster sessions.

Financial support for this project was provided by a Pengrowth-Nova Scotia Petroleum Innovation Grant, an award from the Canadian Society of Petroleum Geologists, the Geological Survey of Canada, and an Offshore Energy Technical Research Association research grant to Dr. Mosher and Dr. Wach.

I would like to thank my parents, in-laws, and the rest of my family, all of whom demonstrate through example success from hard work. I would also like to thank my dog, Remington, for occasionally forcing me away from the laptop to stretch my legs.

Finally (and especially), I want to thank my wife, Lori, for her constant support, her ability to put things in perspective, and most importantly her patience during the last 4 years.

Chapter 1: Introduction

1.1 General Statement

Continental margins are the transition zones between the continents and the deep ocean basins. They often preserve a wealth of information about the geological history of the adjacent continent and basin (Mountain and Tucholke 1985; Tucholke and Mountain 1986; Keen and Piper 1990; Piper 2006; Nittrouer et al. 2009). Studies of continental margins that look at a sufficiently long record reveal fundamental details about the processes that drive margin evolution and can expose the effects of geological, climatic, and oceanographic conditions that are far different from those which prevail today (Mountain et al. 2007). Regional studies of outer continental margin evolution depict lateral or along-slope changes not apparent from narrow corridor, shelf to slope transects (e.g. Locker and Laine 1992; Poag and Ward 1993; Stoker et al. 2005). Such studies typically rely on the correlation of regionally mappable seismic stratigraphic horizons correlated with available boreholes. Seismic reflection stacking geometries and stratal relationships provide important information about sediment delivery systems and processes, as well as the complex interactions between sediment supply, local and regional tectonics, variations in eustatic and local sea-level, oceanographic conditions, and climate change (Mountain and Tucholke 1985; Stoker et al. 2005; Shannon et al. 2005; Carvajal et al. 2009).

The continental margin south of Nova Scotia, Canada (herein the Scotian margin) forms part of the northern margin of the North American Basin, a large oceanic basin in the Northwestern Atlantic Ocean (Jansa et al. 1979) (Figures 1.1-1.2). The geology of the outer Scotian margin below the modern continental slope and rise is not well known, particularly the pre-Quaternary, Cenozoic history (Wade and MacLean 1990; Piper 2005). The Scotian margin is situated immediately northeast of the comparatively well-studied United States Atlantic continental margin. Studies of the U.S. Atlantic margin have benefited from numerous scientific boreholes drilled during the last 40 years; however, a moratorium on hydrocarbon exploration since the 1980s has prevented

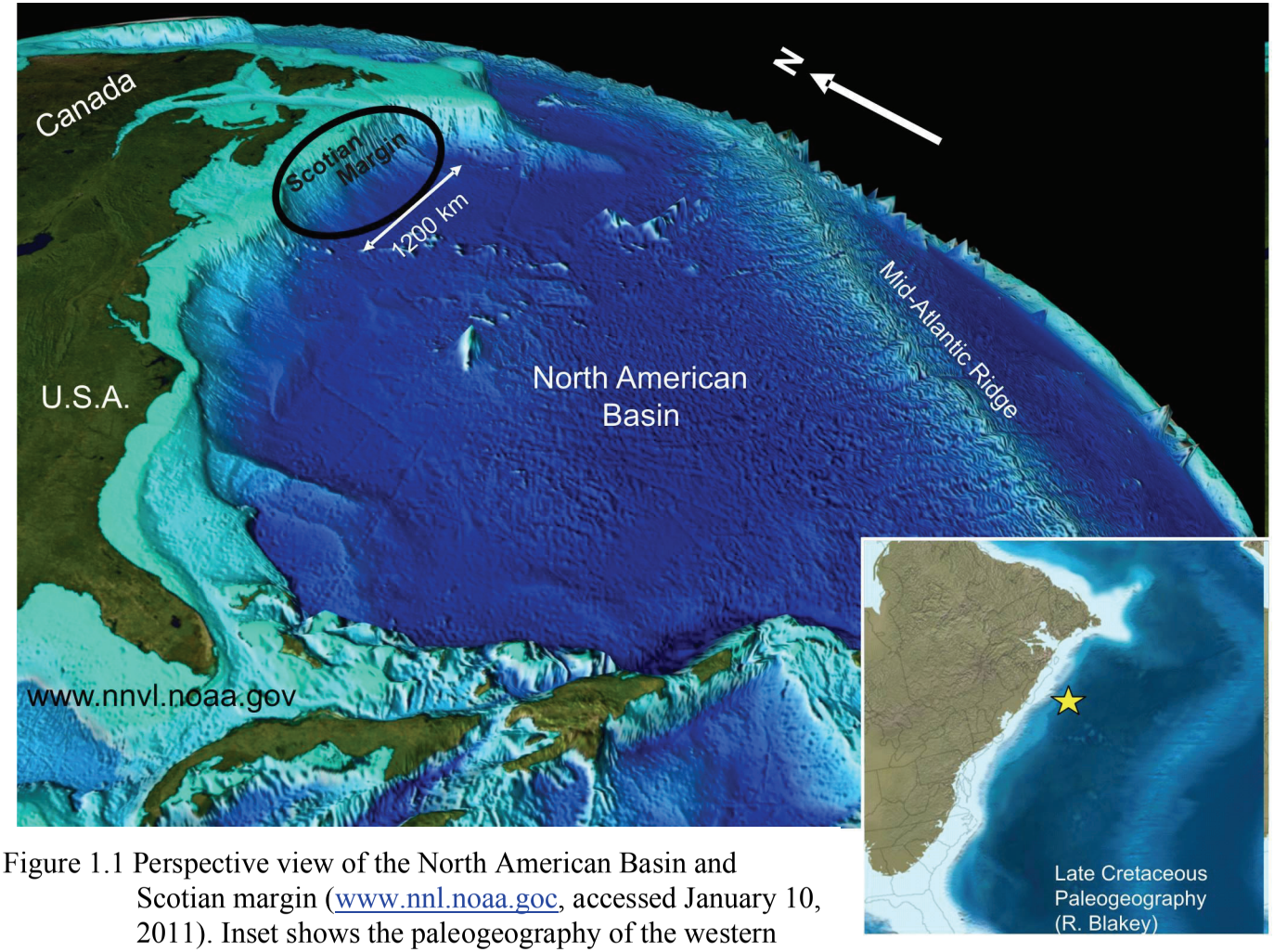

Figure 1.1 Perspective view of the North American Basin and Scotian margin (www.nnl.noaa.goc, accessed January 10, 2011). Inset shows the paleogeography of the western North Atlantic at the end of the Cretaceous (http://www2.nau.edu/rcb7/namK75.jpg, accessed January 10, 2011).

collection of modern petroleum industry seismic reflection data. During the late 1990s and early 2000s, a phase of hydrocarbon exploration along the outer Scotian margin resulted in the collection of an extensive database of regional two-dimensional and three-dimensional seismic reflection data. The new data not only provide a means to remedy the knowledge gap about the geological history of the Scotian margin, but permit a level of detailed investigation of the seismic geomorphology not currently achievable anywhere else along the North American Basin margin.

In this study, these new data are used to examine the last 70 Ma of evolution of the outer Scotian margin, spanning the Upper Cretaceous and Cenozoic succession. The results reveal changes in the depositional architecture of the margin long after the initial rifting of the Central Atlantic in the Late Triassic and Early Jurassic. This study makes comparisons between the Scotian margin and U.S. margin to the south, it provides new insights into the Cenozoic paleoceanography of the North Atlantic, and it provides insights into continental slope processes with a focus on mass wasting, unconformity formation, and along-slope processes.

Figure 1.2 A) Map of the western North Atlantic showing locations discussed in the text. B) Physiographic map of the modern continental margin off Nova Scotia (modified from Shaw and Courtney 2004). C) Map showing the geographical focus of each chapter, data used for this study, and major structural elements. Regional 2D seismic reflection data shown as a grid. 3D seismic datasets are shown as white polygons and consist of the Barrington (B), Torbrook (T), and Weymouth (W) survey areas. Structural elements were modified from Shimeld (2004).

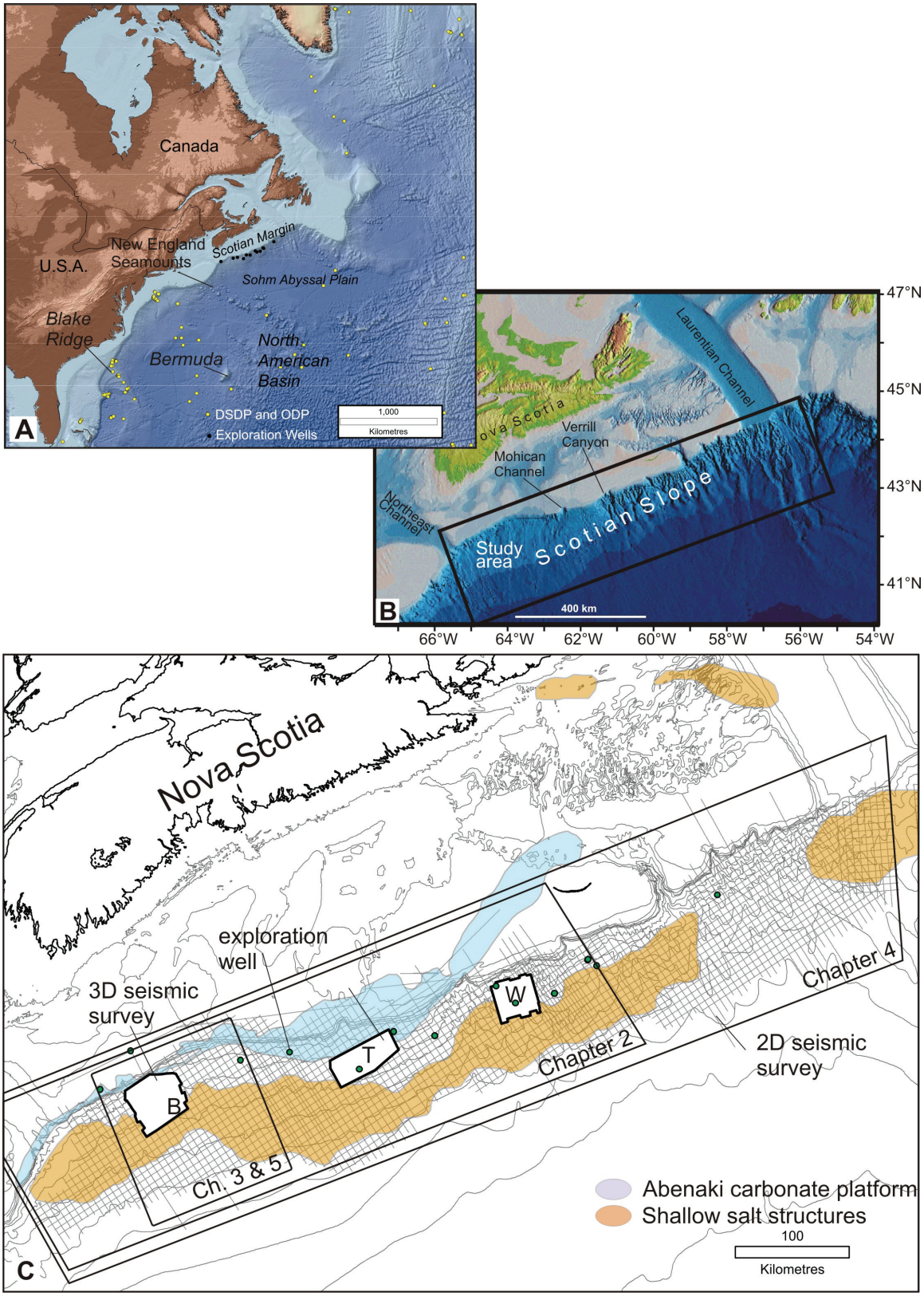
Canada
U.S.A.
New England Seamounts
Scotian Margin
Sohm Abyssal Plain
Blake Ridge
Bermuda
North American Basin
DSDP and ODP
Exploration Wells
1,000
Kilometres
A
Laurentian Channel
Nova Scotia
Verrill Canyon
Mohican Channel
Northeast Channel
Study area
Scotian Slope
400 km
B
47°N
45°N
43°N
41°N
66°W
64°W
62°W
60°W
58°W
56°W
54°W
Nova Scotia
exploration well
3D seismic survey
W
T
B
Chapter 4
Chapter 2
2D seismic survey
Ch. 3 & 5
Abenaki carbonate platform
Shallow salt structures
100
Kilometres
C

1.2 ORGANIZATION OF THESIS

The thesis begins with an introductory chapter that contains the objectives and rationale for the research, a summary of thesis chapters, an explanation of chapter authorship, as well as additional methods and background information not presented in subsequent chapters. The introductory chapter is followed by four individual manuscripts that address the research objectives (Chapters 2-5). The final chapter explains the significance of the research results, presents the main conclusions from this study, and provides suggestions for future research. Each chapter contains a list of references; a master bibliography is included at the end of the thesis.

1.3 OBJECTIVES

This study examines the Late Cretaceous and Cenozoic geological history of the outer Scotian margin with the following specific objectives:

1.3.1 Objective 1

To develop a new regional seismic stratigraphic framework for the outer Scotian margin integrated with the stratigraphy of the well-studied United States Atlantic margin to the south, and use this framework to elucidate the evolution of a large (~50 000 km^2) Upper Cretaceous and Cenozoic deep-water depocenter located along the southwestern Scotian margin.

Background and Rationale

The North American Basin is a large bathymetric depression in the northwest Atlantic Ocean centered on the Bermuda Rise (Figure 1.1). It is bounded to the west by the continental margin of the eastern United States and to the north by the Scotian and southwest Grand Banks margins. The Upper Cretaceous and Cenozoic deposits within the basin and along the basin margins preserve a geological record of important events that affected the northwest Atlantic during this period. These events include the opening and

closing of major oceanic gateways, fluctuations in relative and eustatic sea-level, the middle Cenozoic greenhouse to icehouse transition, marked increase in terrigenous input into the basin during the Neogene, bolide impacts on the U.S. and Canadian continental shelves during the Eocene, periodic pulses in bottom water circulation, among others (see summaries provided in Tucholke and Mountain 1986 and Poag and Ward 1993).

Along the U.S. Atlantic margin, the Upper Cretaceous and Cenozoic geology and seismic stratigraphy are well-studied (Emery et al. 1970; Jansa et al. 1979; Tucholke and Moutain 1979; Mountain and Tucholke 1985; Poag and Ward 1993). In fact, most of the geological and paleoceanographic history of the northwest Atlantic and concepts on how passive margins evolve are based on scientific drilling results and regional seismic reflection profiles collected along the margin and abyssal plain south of the New England Seamounts (Tucholke and Mountain 1986; McCave and Tucholke 1986; Miall et al. 2008). In contrast, apart from Late Quaternary deposits, the stratigraphy and geological history of the outer Scotian margin is not well known. This gap in knowledge is due to a number of factors that include historically sparse data coverage, limited interest from hydrocarbon exploration companies, difficulty extending the seismic stratigraphy of the North American Basin north of the New England Seamounts, and uncertainties of seismic correlation across areas highly deformed by salt diapirism (Schlee et al. 1985; Swift 1987; Ebinger and Tucholke 1988; Wade et al. 1995; Piper 2005).

Despite extensive scientific drilling and regional seismic reflection profiles on the U.S. Atlantic margin, a moratorium on hydrocarbon exploration in the area since the early 1980s has precluded the collection of modern two-dimensional (2D) and three-dimensional (3D) seismic reflection data. Conversely, on the Scotian margin a vast quantity of modern seismic reflection data were collected during the late 1990s and early 2000s in support of hydrocarbon exploration. These data provide an opportunity to investigate the seismic stratigraphy and seismic geomorphology of the continental slope at a level of detail not previously attainable anywhere along the North American Basin margin. Using these new data, this study addresses several questions: Do the new datasets alleviate the challenges faced by previous researchers with regards to regional seismic

correlation along the Scotian margin, and if so in what ways? What are the similarities and differences in the Upper Cretaceous and Cenozoic seismic stratigraphic architecture between the Scotian and U.S. Atlantic margins? Do the new data from the Scotian margin support or modify previous interpretations of seismic facies and depositional history? What new insights are revealed about the North American Basin margin and passive margins in general?

1.3.2 Objective 2

To determine the processes that led to the formation of a regional deepwater unconformity typical of Middle Cenozoic unconformities identified along the western North Atlantic margin.

Rationale

In general, deepwater erosional unconformities are attributed to either down-slope or along-slope processes. Down-slope processes include the spectrum of gravity-driven flows associated with sediment transport into deeper parts of a basin that lead to the formation of failure scars, gullies, channels and canyons (Stow and Mayall, 2000). Along-slope erosion processes are associated with bottom currents and occur when current velocities exceed the threshold for deposition and form erosional terraces, abraded surfaces, contourite channels, moats and furrows (Hernández-Molina et al., 2008). Other processes that potentially lead to erosion or non-deposition on the slope include downwelling or upwelling water masses, internal waves and turbulence caused at water mass boundaries, carbonate dissolution, and isolation of the basin from sediment supply (Poag and Ward 1993; Stoker et al. 2005). Determination of the processes that formed deepwater erosional surfaces, whether predominantly down-slope, along-slope, or mixed, has implications for understanding controls on margin evolution, paleoceanography, and sequence stratigraphy.

The global greenhouse to icehouse transition that occurred during the middle Cenozoic (Late Eocene to Middle Miocene) marked a major shift in the geological and

oceanographic conditions in the northwest Atlantic Ocean. During this transition, strong contour currents developed and sediment input to the North American Basin increased. These events were coeval with the development of regional unconformities within the basin and along the basin margins (Mountain and Tucholke 1985; Ebinger and Tucholke, 1988; Locker and Laine, 1992). In many cases, the relationship between abyssal plain and continental margin unconformities is unclear. As part of this study, 2D and 3D seismic reflection data from the southwestern Scotian Slope and Rise are used to investigate a previously undocumented, widespread deepwater angular unconformity, in turn addressing the following questions: How does the unconformity relate to erosional surfaces identified elsewhere along the Scotian and U.S. margins? What clues do the data provide about the origin of the unconformity?

1.3.3 Objective 3

To gain new insights into the paleoceanography of the western North Atlantic, as well as general along-slope processes, based on recognition and interpretation of sedimentary features indicative of contourite depositional systems along the Scotian margin.

Rationale

Contourite depositional systems develop when along-slope geological processes, driven by contour-following currents, dominate over down-slope geological processes, driven by gravity (Locker and Laine 1992; Hernandez-Molina et al 2008; Mulder et al. 2008; Hernandez-Molina et al. 2010). In the North Atlantic, contour-following bottom currents flow southward and westward along the continental margin of North America (Worthington 1976; Pickart 1992; Schmitz and McCarthy 1993). The interaction of these bottom currents with the seabed during the Cenozoic is demonstrated by the widespread presence of contourite drifts that flank the continental margins, from the Gulf of Cadiz to the northern Antilles margin (Heezen et al. 1966; McCave and Tucholke 1986; Faugères et al. 1993; Wold 1994; Faugères et al. 1999; Faugères et al. 2008). Additional evidence of these interactions is shown by the development of regional unconformities on the continental slope and rise when bottom current strength was sufficient to hinder

deposition or even erode the seabed (Tucholke and Mountain 1979; Mountain and Tucholke 1985; Laberg et al. 2005; Miller et al. 2009).

The paleoceanography of the western North Atlantic is largely based on the analysis of seismic reflection data, supplemented by ocean drilling data, from the United States Atlantic margin (Heezen et al. 1966; Tucholke and Mountain 1979; Mountain and Tucholke 1985; Tucholke and Mountain 1986; McCave and Tucholke 1986). Compared to the U.S. Atlantic margin, the Cenozoic paleoceanographic record along the continental margin off Nova Scotia has not been investigated to the same level of detail. Analysis of the modern bottom current regime along the Scotian margin suggests that modern conditions are suitable for contourite development. Although Holocene contourites are present on the lower Scotian Rise (Nowell and Hollister 1985), previous studies suggest that the Pleistocene geological record is dominated by gravity-driven processes (Hughes-Clarke et al. 1992). Additionally, previous researchers reported that pre-Quaternary sediment drifts are absent or of limited geographical extent compared to the continental margin to the south and north (Swift 1987; McCave and Tucholke 1986; Ebinger and Tucholke 1988; McCave et al. 2002). In fact, published maps of the distribution of large contourite drifts in the North Atlantic show that there are no large sediment drifts recognized between the Newfoundland Ridge seaward of the southern Grand Banks, and the Chesapeake Drift seaward of Chesapeake Bay (McCave and Tucholke 1986; Faugères et al. 1993; Faugères et al. 1999; Faugères et al 2008). This interval is the longest section of North America's Atlantic margin that lacks contourite drifts.

Through analysis of seismic reflection data, this study revisits the issue of the apparent lack of contourite depositional features along the Scotian margin and shows that contourite features *are* an important component of the preserved Cenozoic succession. The following questions are addressed: Does the orientation of the Scotian margin, such that opposing interactions occur between the Gulf Stream and western boundary currents, affect sediment drift development? Are there periods when a predominance of gravity-driven processes overpower or mask along-slope processes during the Cenozoic, preventing the development of sediment drifts? What was the dominant orientation of

ocean currents along the margin during the Cenozoic? What new insights into the paleoceanography of the western North Atlantic and along-slope processes do these features provide?

1.3.4 Objective 4

To determine the effects of morphological heritage on the development of an Upper Miocene and Pliocene mixed turbidite and contourite depositional system along the outer Scotian margin.

Rationale

Mixed turbidite and contourite depositional systems exist on many continental margins (e.g. Locker and Laine 1992; Carter and McCave 1994; Rebesco and Stow 2001; Knutz and Cartwright 2003; Hernández-Molina et al. 2006; Uenzelmann-Neben 2006). The interaction of gravity and bottom currents is most apparent where low frequency alternations of contourite and turbidite predominance are preserved (Mulder et al. 2008), and depositional elements are resolved in seismic reflection data. Pre-existing morphology likely influences the character of deposits originating from both down-slope gravity currents and along-slope bottom currents (Locker and Laine 1992; Uenzelmann-Neben 2006; Mulder et al. 2008). For instance, in the case of gravity flows, it is recognized that receiving basin configuration is one of the primary factors controlling lithofacies distribution as gravity flows transit from shelf areas into deeper water (Prather 2003; Steffens et al. 2003). Similarly for sediment drifts, pre-existing seafloor irregularities appear to be loci for the initiation of deepwater bottom current deposits (Faugères et al. 1999; Viana et al. 2007; Hopfauf and Spiess 2001; Wynn and Masson 2008).

Conceptual models of the interaction of sedimentary processes in mixed turbidite and contourite systems are proposed (Heezen et al. 1966; Locker and Laine 1992; Hernández-Molina et al. 2008; Viana 2008), however relatively few published studies use 3D seismic data to clearly demonstrate the effects of morphological heritage in alternating

gravity current and bottom current deposition. Recently, a number of authors demonstrated the effectiveness of applying such data to sediment drift studies (Knutz and Cartwright 2003; Hohbein and Cartwright 2006; Viana et al 2007) and emphasized the need for more detailed examination of these deposits.

In this study, a 3D seismic dataset located at the transition from the modern slope to continental rise is used to study in detail the seismic geomorphology and geological evolution of a mixed turbidite and contourite system. The following questions are addressed: What was the seismic geomorphology of the paleo-seabed immediately preceding the onset of drift construction? Is there a close association between inherited seabed relief and drift morphology? What is the seismic geomorphology of the sediment drift and how did the drift develop? What effect did the morphology of the sediment drift have on receiving basin configuration as the system switched back to downslope-dominated sediment transport?

1.4 Summaries of Individual Papers and Explanation of Authorship

This section provides summaries of the four manuscripts that make up the bulk of this thesis as well as an explanation of the authors' contributions to the manuscripts.

1.4.1 Chapter 2 – Paper 1

Title- "Seismic stratigraphic framework and depositional history of an Upper Cretaceous and Cenozoic depocenter off Southwest Nova Scotia, Canada." In prep.
Authors- D. Calvin Campbell, John W. Shimeld, Mark E. Deptuck, David C. Mosher

Summary

Chapter 2 presents the seismic stratigraphic framework and detailed Late Cretaceous to Present evolution of a large depocenter that spans the Shelburne Sub-Basin off southwest Nova Scotia. The difficulties experienced by previous researchers in

extending the North American Basin seismic stratigraphy into the area and in regional seismic reflection correlation are overcome by using extensive new seismic reflection data along the southwestern Scotian margin. In the study area, Upper Cretaceous through Quaternary sequences manifest four distinct phases in the interplay of down-slope versus along-slope depositional and erosional processes through time. The first phase, spanning the Late Cretaceous to Late Eocene, is characterized by widespread and repeated periods of gully erosion interspersed with periods of hemipelagic, carbonate-rich sedimentation. Extensive failure of outer shelf and upper slope regions, possibly related to the Montagnais meteorite impact, also occurred during this time. The second phase, spanning the Oligocene to Middle Miocene, is dominated by widespread erosion, deposition by gravity flow processes, and sediment re-working by bottom currents. Marked erosion and/or non-deposition along the mid- to lower slope is attributed both to down-slope and along-slope processes. The third phase, spanning the Late Miocene to Late Pliocene, is dominated by bottom current deposition including stacked sequences of giant sediment waves and large contourite drifts along the lower slope. The final phase, from the Late Pliocene to present, exhibits a return to predominance of gravity flows with deposition focused below the upper slope. The close similarity of the depositional phases preserved in the study area with those documented to the south, along the U.S. margin, demonstrates that regional scale slope geological processes share a common first-order history for this part of the North American Basin since at least the Late Cretaceous.

Author contributions

DCC conceived the initial concept and wrote the first version of the manuscript and drafted all the figures. The first draft was improved by suggestions from all co-authors. DCC loaded and interpreted all of the 3D seismic datasets in the study. DCC loaded all the well data and conducted all well to seismic correlations. JWS provided DCC with a digital seismic interpretation project that contained the regional 2D seismic reflection data, as well as regional seismic picks for the seabed and an Upper Cretaceous marker. JWS contributed to intellectual discussion on the stratigraphy of the margin, and to suggestions for technical approach for the well to seismic correlations. DCC defined and extended the remaining 8 seismic stratigraphic markers throughout the study area. MED

provided fruitful discussions about the Upper Cretaceous and Paleogene succession and the role of the upper slope instability zone. DCM provided guidance on the scientific approach, suggestions for depth conversion of isochron and isochore maps.

1.4.2 Chapter 3- Paper 2

Title- "Middle to Late Miocene slope failure and the generation of a regional unconformity beneath the western Scotian Slope, eastern Canada". Published (Submarine Mass Movements and Their Consequences Advances in Natural and Technological Hazards Research, 2010, Volume 28, IV, 645-655).
Authors- D. Calvin Campbell, David C. Mosher

Summary

Chapter 3 examines in detail the development of a pervasive erosional Middle to Late Miocene erosional unconformity along the outer western Scotian margin. The unconformity is interpreted to be equivalent to the "Merlin" seismic stratigraphic horizon along the U.S. margin (Mountain and Tucholke 1985) and to an unconformity termed "CS2" by Swift (1987) who recognised the same surface further east on the Scotian margin. This seismic surface is recognized along the entire U.S. and Canadian margin of the North American Basin and has an uncertain origin (e.g. bottom current erosion or gravity flows/ diagenetic boundary). This study represents the first time the 3D seismic geomorphology of the Merlin unconformity was examined and demonstrates that in the study area it is primarily the product of erosion by regional submarine mass movement, although bottom currents and channel development may have played a role in its formation. The mass-transport deposits that contributed to its formation are among the largest reported in the literature. Despite the presence of a steep upper slope in the study area, evidence from seismic reflection data suggests that the erosion was not due to mass-wasting initiated on the upper slope, but rather erosion and seabed failure initiated on the lower slope and continental rise, followed by failure retrogression. It is suggested that salt tectonics and bottom-current activity contributed to sediment failure.

Author contributions

DCC conceived the initial concept and was encouraged to pursue it by DCM. DCC wrote the first version of the manuscript and drafted all the figures. DCC loaded and interpreted all the seismic reflection data. DCM provided helpful discussion on mass transport deposits and made important improvements to the initial manuscript.

1.4.3 Chapter 4- Paper 3

Title- "Geological evidence for western boundary undercurrent activity throughout the Cenozoic from the continental margin off Nova Scotia, Canada" In prep.
Authors- D. Calvin Campbell, David C. Mosher

Summary

Chapter 4 presents evidence of widespread Cenozoic contourite depositional systems along the Scotian margin. The continental margins of the North Atlantic are flanked by widespread sediment drifts, the geological evidence of bottom current activity throughout the Cenozoic. Despite ubiquitous sediment drifts to the north and south, prior to this study, these features were thought to be absent or of limited extent along the continental margin off Nova Scotia (e.g. Hernandez-Molina et al. 2008; McCave et al. 2002; Faugeres et al. 1993; Swift 1987; McCave and Tucholke 1986). Recently collected 2D and 3D multichannel seismic reflection data allow detailed examination of the seismic reflection architecture and geomorphology of the Scotian margin and demonstrate that sediment drifts are a common feature in the Cenozoic succession. Large sediment drifts developed in the Late Eocene to Early Oligocene, and during the Late Miocene to Pliocene. Small sediment drifts developed locally throughout the late Paleogene and Neogene, either southwest and down-current of seafloor obstacles or within channels. Major erosional pulses form regional seismic markers, first along the continental rise in the Early Oligocene, then along the continental slope during the Late Miocene and Pliocene. 3D seismic data show that locally, erosion surfaces preserve along slope amplitude anomalies, barchan bedforms, and possible evidence of helical scour.

Author contributions

DCC conceived the initial concept for the paper and was encouraged to pursue it by DCM. DCC loaded and prepared all the 3D seismic data, conducted all the seismic data interpretation, and performed all well to seismic correlations. DCM provided helpful discussions about paleoceanography and deepwater processes. DCC wrote the initial version of the manuscript and drafted all the figures. DCM improved the manuscript by revising the initial draft of the text.

1.4.4 Chapter 5- Paper 4

Title- "Alternating bottom current dominated and gravity flow dominated deposition in a lower slope and rise setting- Insights from the seismic geomorphology of the western Scotian margin, Eastern Canada". Accepted. SEPM Special Publication on geomorphology of base of slope settings.
Authors- D. Calvin Campbell, Mark E. Deptuck

Summary

Chapter 5 examines the seismic geomorphology of a succession of alternating gravity flow- and bottom current-dominated deposits along the slope and rise off western Nova Scotia. It demonstrates the importance of inherited geomorphology on subsequent deposition patterns in mixed turbidite and contourite depositional systems. In the study area, widespread mass wasting and channel incision during the Miocene created a steep ramp with a complex geomorphology along the lower continental slope. In the Late Miocene and Pliocene, a sediment drift was constructed on the continental rise, forming a 50 km-wide terrace that onlapped the steeper slope. The location, style, and evolution of sediment waves associated with this sediment drift appear strongly linked to the morphology of the underlying surface. The orientation and extent of wave crests show strong correspondence to underlying geomorphic elements, with the most prominent sediment waves forming down-current of seafloor perturbations such as failure escarpments and salt diapirs. The erosive and constructional morphology of the contour-current-swept seafloor in turn strongly influenced the trajectory and response of

subsequent down-slope-oriented submarine sediment gravity flows later in the Pliocene and Pleistocene. Preferential accumulation took place above a regional terrace constructed as the sediment drift evolved, promoting deposition from sediment gravity flows that are otherwise transported into deeper water. The positive relief of wave crests guided sediment gravity flows down the slope, with erosion and deposition focused along wave troughs. This study highlights the complex feedback that exists between along-slope and down-slope constructional and degradational processes.

Author contributions

DCC conceived the initial concept for the paper and was encouraged to pursue it by MED. MED contributed helpful discussions about graded slopes, deepwater accommodation, and slope evolution. DCC loaded and prepared all the 3D seismic data. DCC conducted all the seismic interpretation, and generated all the time-thickness and time-structure maps. DCC wrote the initial version of the manuscript and drafted all the figures. Revisions of the initial draft by MED improved the manuscript.

1.5 METHODS

Each individual paper in the thesis provides a methods section with specific details on the methods applied in the particular manuscript. This section provides additional details on the methods utilized in this study.

1.5.1 Seismic reflection data and its interpretation

This study largely relies on the interpretation and seismic stratigraphic analysis of two-dimensional (2D) and three-dimensional (3D) marine multichannel seismic reflection data. The methods for collecting marine seismic reflection data involve ensonifying the seafloor and underlying deposits and recording the reflected signal. The sound source and reflection receiving equipment are towed behind a survey vessel. In the marine case, the sound source is typically an airgun or airgun array and the receiving equipment consists of a series of hydrophones contained within a streamer. The sound source generates

pulses at discrete intervals. As the sound propagates, some energy is reflected off layers and some energy is transmitted deeper. The returned energy of a source pulse is received as a seismic trace which represents the earth's response to sound traveling from the source through subsurface layers and returning to the receiver. The strength and polarity of subsurface reflection events of adjacent geological layers are dependant on the characteristics of the sound source (frequency and energy), as well as the difference in acoustic impedance, the product of the acoustic velocity and density, between layers. This relationship can be quantified as the reflection coefficient *R* (Equation 1.1) which is derived from the Zoeppritz equation for normal incidence acoustic energy (Yilmaz 1987).

[Equation 1.1] $$R = [(\rho_1 \cdot v_1) - (\rho_2 \cdot v_2)]/[(\rho_1 \cdot v_1) + (\rho_2 \cdot v_2)]$$

where *R* is the reflection coefficient, ρ_1 is the density of layer 1, v_1 is the acoustic velocity of layer 1, ρ_2 is the density of layer 2 and v_2 is the acoustic velocity of layer 2.

Seismic stratigraphic analysis is a method for analyzing seismic reflection data within a context of basin systems that uses reflection geometry and acoustic character of seismic reflection data. The method was developed in the 1960s and 1970s as a result of increased volume of seismic reflection data and developments by petroleum exploration companies in applying the data to resource exploration (Payton 1977). The technique applies concepts developed from established stratigraphic and depositional models (Boggs 1995). Recognizing that primary seismic reflections approximate chronostratigraphic surfaces (Vail et al. 1977), the method involves the correlation of erosional and unconformable surfaces and their conformable equivalents throughout the study area. The result is a stratigraphic framework that allows seismic geomorphological and structural analysis as well as a method for determining the relative timing of erosional and depositional elements. The internal reflection characteristics of the intervening data within the framework, along with the bounding unconformity relationships, provide important information about the depositional facies (Sangree and Windmier 1979; Ramsayer 1979) (Figure 1.3).

Early studies applied seismic stratigraphic analysis to 2D seismic reflection data, but with the increased availability of 3D seismic reflection data to researchers in the 1990s and 2000s, the methods were expanded and improved. 3D seismic data allow an unparalleled view of the deep-water depositional environment (Posamentier and Kolla 2003; Posamentier et al. 2007; Davies et al. 2007). The ability to analyse in plan-view horizontal time slices, shaded-relief surfaces, and seismic attributes affords a geomorphological approach to the interpretation of 3D seismic reflection data, leading to the development of the relatively new field of 3D seismic geomorphology.

1.5.2 Data resolution, visualization and seismic attributes

The resolution of seismic reflection data applies to both the vertical and horizontal domain. The vertical resolution of seismic reflection data is dependent on the frequency characteristics of the seismic source which impacts the frequency characteristics of the received signal. The acoustic frequency content of the 2D and 3D datasets in this study are similar for the interval examined (Figure 1.4). The Raleigh criterion states that for a geological layer to be resolved, its thickness must equal or exceed ¼ of the dominant wavelength of the data (Sheriff 1985). For this study, the result is a layer thickness resolution of ~18 m for the dominant frequency of ~25 Hz, with a maximum practical resolution of ~6.5 m for the peak frequency at ~70 Hz. These values are based on a 1500 m/s acoustic velocity, therefore resolution decreases with depth and increased velocity in the sub-surface.

The horizontal or spatial resolution of multichannel, migrated seismic reflection data is primarily dependant on the frequency of the source wavelet and the the aperture or hydrophone array length (Mosher et al. 2006; Chen and Schuster 1999). During the course of this study, digital seismic reflection files in SEG-Y format were loaded into an interpretation projects within commercial seismic reflection interpretation packages GeoFrame™ (Schlumberger Limited) and Kingdom Suite™ (Seismic Micro-Technology Incorporated). Seismic stratigraphic analysis was conducted in order to establish the seismic stratigraphic framework. The process of picking a reflection horizon produces a

set of discrete samples, one per seismic trace, with an X-Y location and a Z attribute (2-way travel time in most cases). This information is then interpolated into a continuous surface in the seismic interpretation software. Ideally, the appropriate interpolation method should give accurate results at observed data points, it should agree with the expected results (i.e., it should not create features not apparent from the data), and it should be independent from any arbitrary decisions by the operator (Hansen 1993).

Practical constraints of geophysical data collection often dictate that sample density is significantly higher in one direction versus another (Smith and O'Connell 2005). For example, a seismic reflection horizon interpreted over a 2D seismic reflection grid will have many "Z" values (either 2-way travel time or other attribute) in the survey or along-track direction, but will have few "Z" values in the cross-track direction. For this study, the 2D seismic data coverage is a regular grid, with line spacing of 6 kilometres over most of the area. The trace spacing along-track is 25 metres. The result is a highly anisotropic data distribution which in turn can lead to spatial aliasing of short-wavelength features. The data interpolation algorithms applied in most seismic interpretation software packages are designed to deal with highly anisotropic data. In the case of the 2D data, a convergent algorithm (GeoFrame™) was applied because of its suitability for modeling line-ordered and clustered random data. Most of the gridded surfaces from the regional 2D seismic reflection data shown in this thesis have a grid resolution of 1 km. Although data density along a seismic profile is much greater than this, gridding at a cell size smaller than 1 km resulted in the introduction of artifacts in the areas between seismic profiles. In the case of the 3D seismic data, data were typically binned at 12.5 m or 25 m intervals in both the x and y domains by the data provider. The bin dimensions for 3D seismic data are generally greater than the minimum spatial resolution derived from the source frequency and aperture length (Mosher et al. 2006). For the 3D data, a flex-gridding algorithm was applied (Kingdom Suite™), although there was little difference in the results from applying other gridding methods to the 3D data because of the isotropic and dense data point distribution.

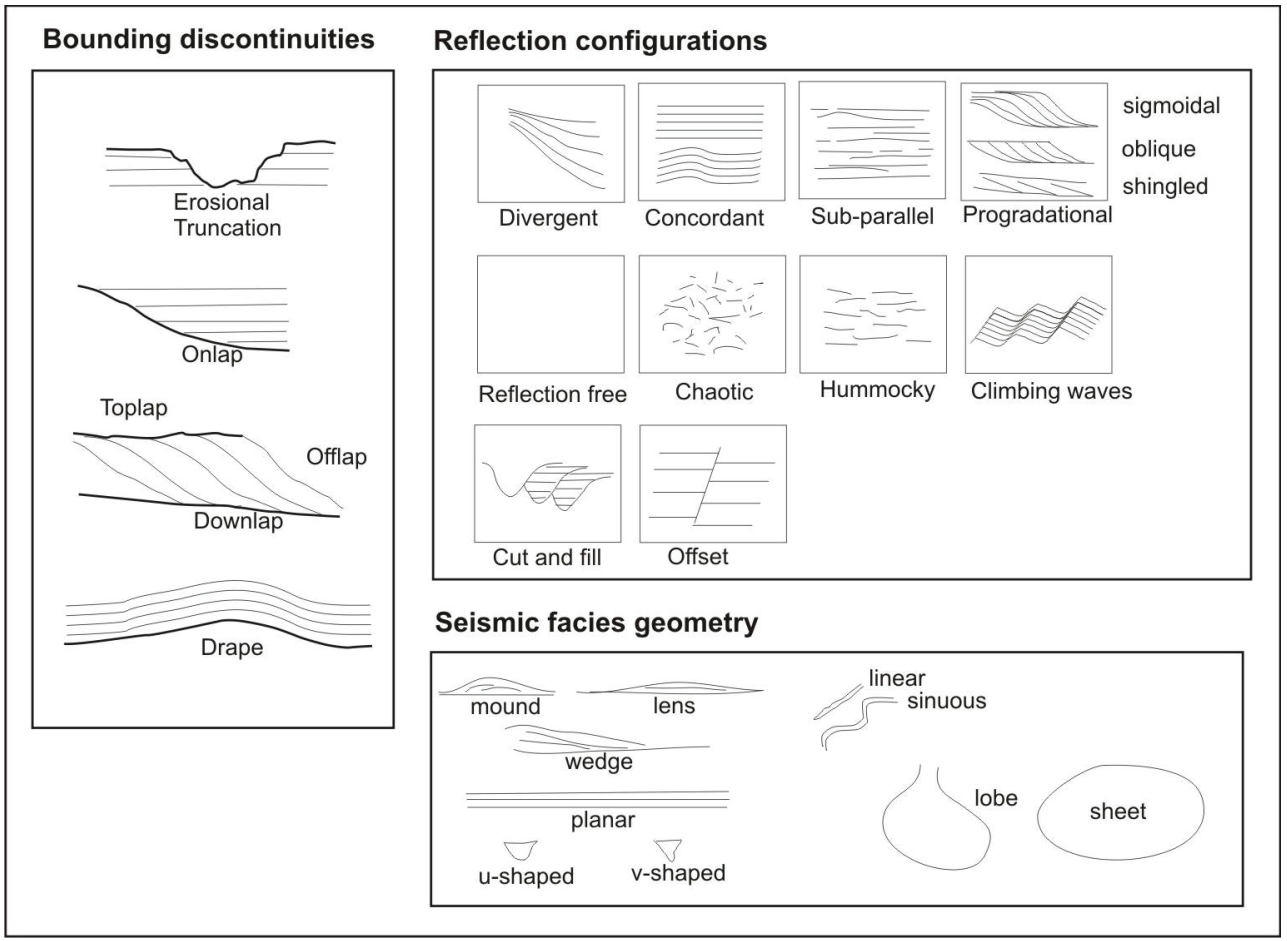

Figure 1.3 Relationship of reflection geometry, configuration, and continuity to depositional processes used in seismic interpretation. Modified from Deptuck (2003), Payton (1977) and Sangree and Windmier (1979).

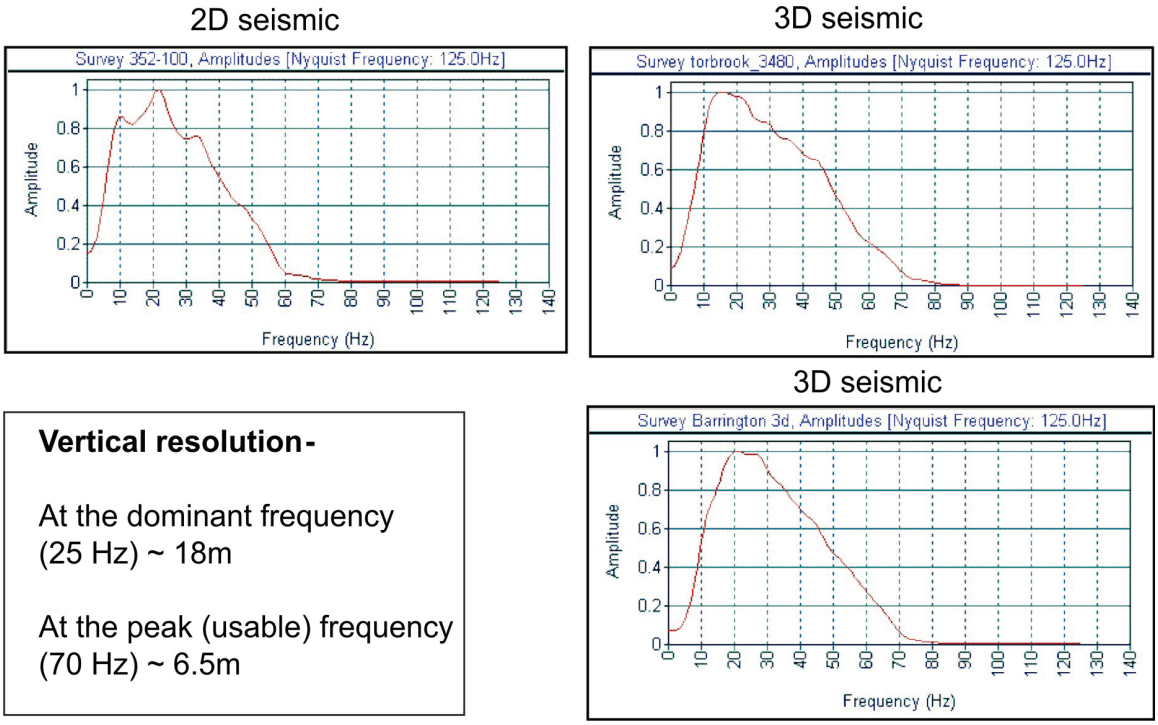

Figure 1.4 Examples of frequency spectrum histograms from 2D and 3D seismic datasets used in this study. Histograms were generated from seismic reflection data extracted from the depth interval of interest.

From the gridded surfaces, derivative maps such as structure and isochore (thickness between two surfaces) were generated to reveal structure and depositional patterns (Figure 1.5). Geometric or structural attributes were generated for the 3D seismic datasets. These attributes included similarity, which is analogous to coherence or the measurement of similarity between adjacent traces, as well as the dip of maximum similarity which is the first derivative of the similarity attribute. Along interpolated horizons, specific attributes at the level of the horizon were extracted to produce maps of amplitude, similarity, and dip of maximum similarity. The detailed seismic geomorphology revealed from the 3D seismic data was further enhanced using artificial shading of structure to enhance features, as well as overlaying attributes.

1.5.3 Petroleum exploration well data

Lithological information for the seismic stratigraphic framework was gathered from publicly available hydrocarbon exploration well data from 10 wells. Lithological information can be grouped into samples and instrumental well logs. Samples consist of conventional (vertical) drill cores at specific intervals targeted by the exploration company, sidewall cores taken at specific intervals down hole, as well as cuttings which are the chipped remains of the rock carried in the drilling fluid. Instrumental well logs consist of a broad range of data types that relate to the physical and lithological properties of the drilled interval. The data are collected either during or immediately after drilling by lowering logging instruments down the well bore and passing the instrument along the well. The instruments measure electrical resistivity, sound velocity, absorption and emission of nuclear radiation among other properties. The variations in these properties reflect large-scale changes in lithology, mineralogy, fluid content, and porosity (Boggs 1995). For this study, the most widely used logs were the gamma ray, acoustic velocity, and density logs.

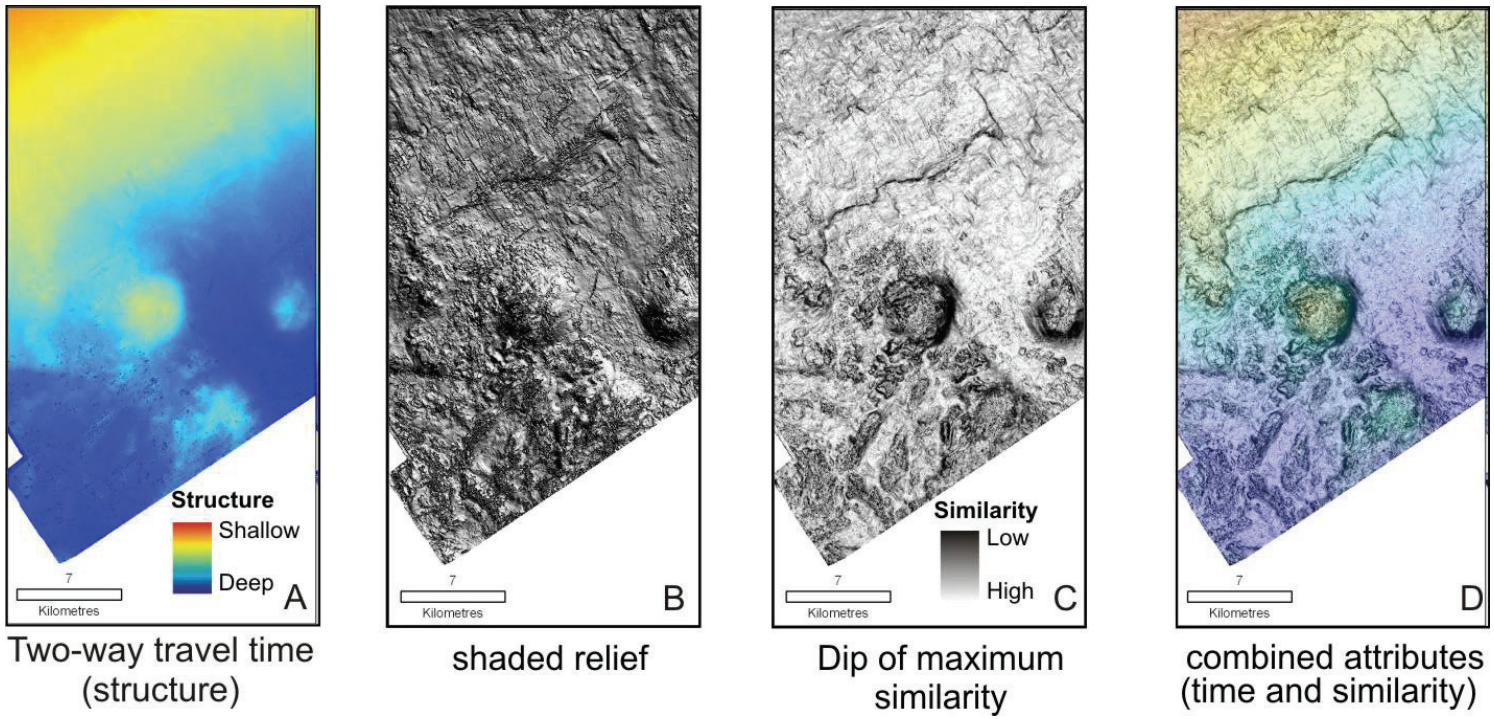

Figure 1.5 Examples of methods to visualize seismic reflection surfaces. A) Structure of interpolated seismic horizon coloured to reflect depth. B) Shaded relief of the same surface as (A) using artificial sun-illumination to highlight morphological features. C) Dip of maximum similarity attribute that detects similarity of adjacent traces on the structural surface. Areas of dissimilar reflections are darker (rougher relief) and areas of similar reflections are lighter (smoother relief). D) Combined structural and similarity attributes, in this case the dip of maximum similarity is draped as a semi-transparent surface over the colour-coded structure.

Correlation of seismic reflection data and coincident well data requires the definition of the relationship between time domain in the seismic data and depth domain in the well data and the generation of synthetic seismograms (Figure 1.6) (White and Simm 2003). This relationship was determined by first applying the time to depth relationships derived from the vertical seismic profile (VSP) or checkshot data available for each well, followed by the generation of synthetic seismograms using the well log data. For most of the wells used in the study, the VSP and checkshot data only existed in hardcopy tabular format, and were entered by hand into the seismic interpretation project. Using the same principles described by the Zoeppritz equations, reflection coefficient series were prepared for each well based on the well log sonic velocity and density information. This reflection coefficient series was then convolved with a seismic wavelet to produce a synthetic seismic trace in the depth domain. The seismic wavelet incorporates the frequency characteristics of the depth interval of interest and was modeled from seismic data nearest the well. The resultant synthetic trace was compared to the coincident seismic traces from the seismic reflection data and a qualitative assessment of the match between the well and seismic data was made through matching peaks and troughs.

1.5.4 Age control

Comparison of the erosion and deposition history in this study with published Atlantic and global records requires age control for the stratigraphic framework. Age control for this study is provided by published biostratigraphic information from exploration wells in the study area. The age estimates are corroborated by correlation of published deep ocean seismic reflection horizons from the Sohm Abyssal Plain dated at Deep Sea Drilling and Ocean Drilling Program sites. Where possible, dated horizons on the continental shelf, where there is much greater well control, were incorporated.

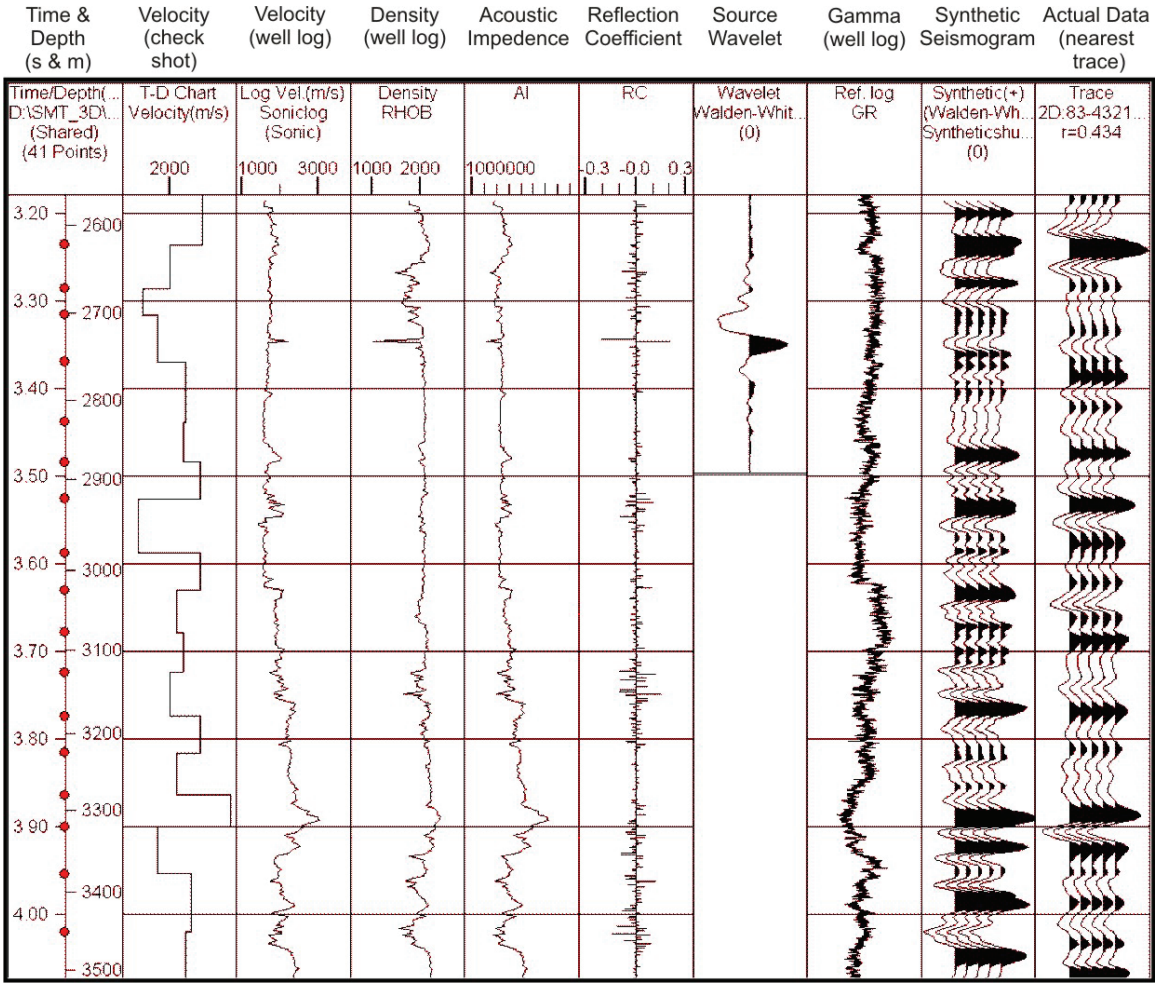

Figure 1.6 Example of synthetic seismogram genereated from well data from the Shubenacadie H-100 well.

1.5.5 Sources of error

Sources of error in this study include interpretive error and spatial error. Interpretive error is due to the misinterpretation of seismic reflection data. The picking of stratigraphic horizons requires the researcher to interpret the geological event in the profile. That said, seismic interpretation and horizon picking are still very much manual processes (Aurnhammer and Mayoral 2004) and the uncertainty introduced by human bias has not been quantified (Bond et al. 2007). Interpretive error was minimized through the use of published references for feature interpretation and seismic facies analysis, the development of a consistent set of interpretation criteria, and the application of loop-tying and mis-tie analysis where multiple paths within the seismic grid are chosen to ensure consistency in horizon mapping. Error was also introduced during the interpretation stage where auto-correlation tools in the interpretation software lead to computer generated mis-picks. These were minimized through repeated gridding iterations and the manual correction of mis-picked horizons.

Spatial errors were introduced into the study via errors from the techniques used to gather the seismic reflection data (e.g. positioning errors), through errors in how well natural surfaces were modeled by the interpolation algorithm, and errors introduced in converting data in the "Z" domain from time to depth. For this study, all data acquisition and processing was performed by the data owners. The errors introduced at the seismic data acquisition and processing stage are generally explicitly expressed within the quality control requirements of the survey. These acquisition errors can be considered source data errors (Fisher and Tate 2006) and are independent of the interpolation method used.

For each seismic stratigraphic horizon, a continuous digital structure or elevation model (DEM) was created by applying the interpolation techniques described previously. Spatial error of interpolated surfaces is most often expressed in terms of error in the Z domain because errors in the X and Y domains will produce error in the Z domain (Fisher and Tate 2006). A standard measurement of map accuracy is the root mean squared error (RMSE) and is determined by the equation:

[Equation 1.2]
$$RMSE = \sqrt{\frac{\sum (Z_{DEM} - Z_{REF})^2}{n}}$$

where Z_{DEM} is the interpolated value, Z_{REF} is a reference measurement from another source at the same location and n is sample size, or the number of times the interpolated surface is compared with a reference measurement. If the mean error is non-zero, the RMSE is not a good description of the statistical distribution of the DEM error. Therefore, a more complete statistical description of error is to provide the mean error and the error standard deviation, or normalized root-mean squared error (Fisher and Tate 2006; Chaplot et al, 2006). Mean error (ME) is given by the equation:

[Equation 1.3]
$$ME = \frac{\sum (Z_{DEM} - Z_{REF})}{n}$$

The error standard deviation equation is similar to the RMSE equation, with the results normalized to the mean error. The equation is:

[Equation 1.4]
$$SE = \sqrt{\frac{\sum [(Z_{DEM} - Z_{REF}) - ME]^2}{n-1}}$$

Because the interpolation methods used in this study were designed to maintain trueness to the input points, the interpolated surfaces are most accurate where data are located, with the highest level of uncertainty occurring at the farthest distance from input points, i.e. the centre point between adjacent in lines and cross lines. The 1 km by 1 km cell size in the regional DEMs, however, resulted in the smoothing of features along seismic lines, a compromise that is due to the anisotropic data distribution. A comparison of the smoothed interpolated surface to the original seismic data is shown in Figure 1.7. It is clear from the example that the modeled surface is a good approximation of the actual surface in smooth areas, but does not capture the detail of features that are less than a few

km in length. It should be noted that the morphology revealed in the seismic data is in itself a smoothed representation of the actual surface because of the horizontal resolution limits of the data.

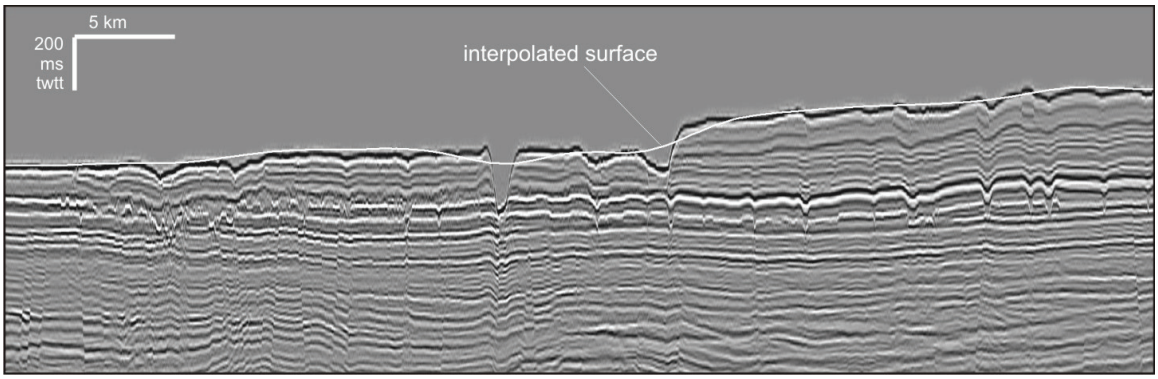

Figure 1.7 Seismic reflection profile showing the original seafloor morphology and interpolated surface. The data are courtesy ION-GXT.

In order to determine the mean error and the error standard deviation for the regional structural maps, equations 3 and 4 above were applied. Reference values from the 3D seismic data were used to compare with the regional mapping results. For an individual 1 km cell in the regional structure map, the 3D seismic data provide 2500 samples. Four locations were chosen to represent the range of possible error; a smooth and a rough location on the 3D dataset near the intersection of regional 2D lines, and a smooth and a rough location from the 3D dataset near the center location between 2D lines. The results of the analysis are shown in Figure 1.8. Three locations showed a negative mean error and one location showed a positive mean error resulting in a bulk shift of the histograms. Once the mean error was removed (by subtraction), the resultant histograms show a normal distribution around 0, with the exception of the rough area near the line intersection which is skewed towards positive values (Figure 1.8). Not surprisingly, the rough areas show greater variation about the mean, as illustrated by the shape of the data distribution with a standard deviations of 31.2 and 22.54 ms. In contrast, the smooth areas have a standard deviation of only 7.41 and 15.3 ms. The normalized RMSE is low in all cases (Equation 1.4) which essentially indicates that each cell in the regional DEM is a reasonable approximation of the average of the "real" depths within the cell. Although

this error analysis was applied to the "seafloor" horizon, and despite the fact that vertical resolution decreases with sub-surface depth, the estimation of error is likely valid for horizons in the subsurface.

Chapters 2 and 4 in the thesis apply a time to depth function to convert interpolated surfaces in the time domain to the depth domain that is based on the regression of discrete time-depth pairs from check shot and VSP data. The RMSE was calculated for the regression results to determine the error of depth estimates for the structure maps and isopach maps. Similar to Equation 2, the RMSE of the time-to-depth regression was calculated by the equation:

$$RMSE = \sqrt{\frac{\sum (Z_{REG} - Z_{OBS})^2}{n}}$$

[Equation 1.5]

where Z_{REG} represents the predicted depth from the regression result, Z_{OBS} is the observed depth from the VSP and check shot data. Comparison of the entire time-depth pair dataset (151 data points) to the predicted values from the regression resulted in an RMSE for the structure maps of 149 m.

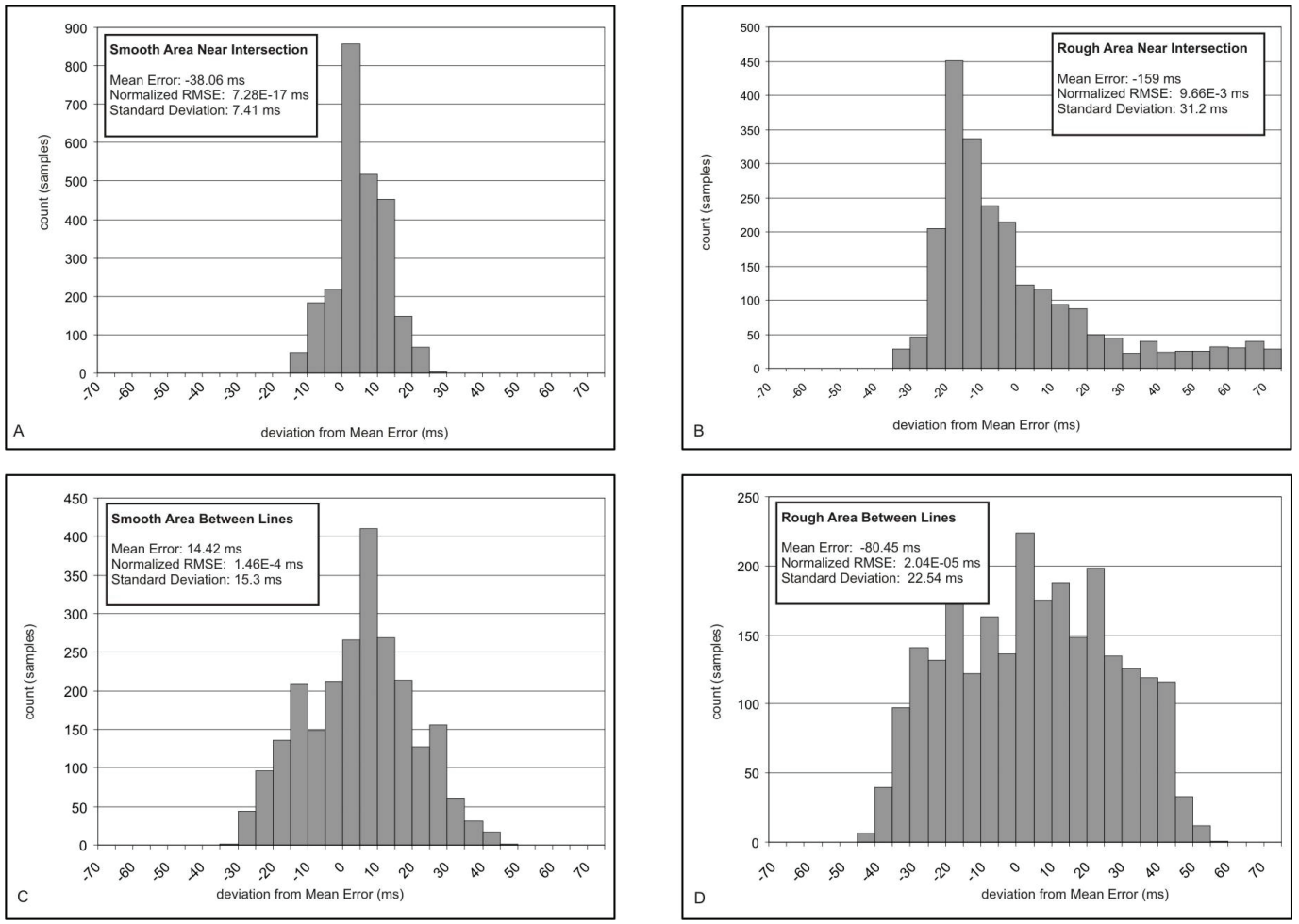

Figure 1.8- Histograms showing error analysis of interpolated surfaces. The error of a surface interpolated from regional 2D seismic reflection data was determined by comparing the interpolated results to results from a 3D seismic surface with much greater data density.

1.6 Explanation of seismic stratigraphies presented in chapters 2-6

An important aspect of this study is the development of a regional seismic stratigraphic framework for the outer Scotian margin. The manuscripts in Chapters 2 and 4 use the "standardized" framework and horizon nomenclature. Chapters 3 and 5 were written before the horizon nomenclature was finalized which resulted in a different naming scheme used in these studies. Figure 2.2 presents the relationship between the new Scotian margin framework and frameworks developed in other studies. Figure 1.9 presents the relationship between horizons discussed in Chapters 3 and 5 and the new framework.

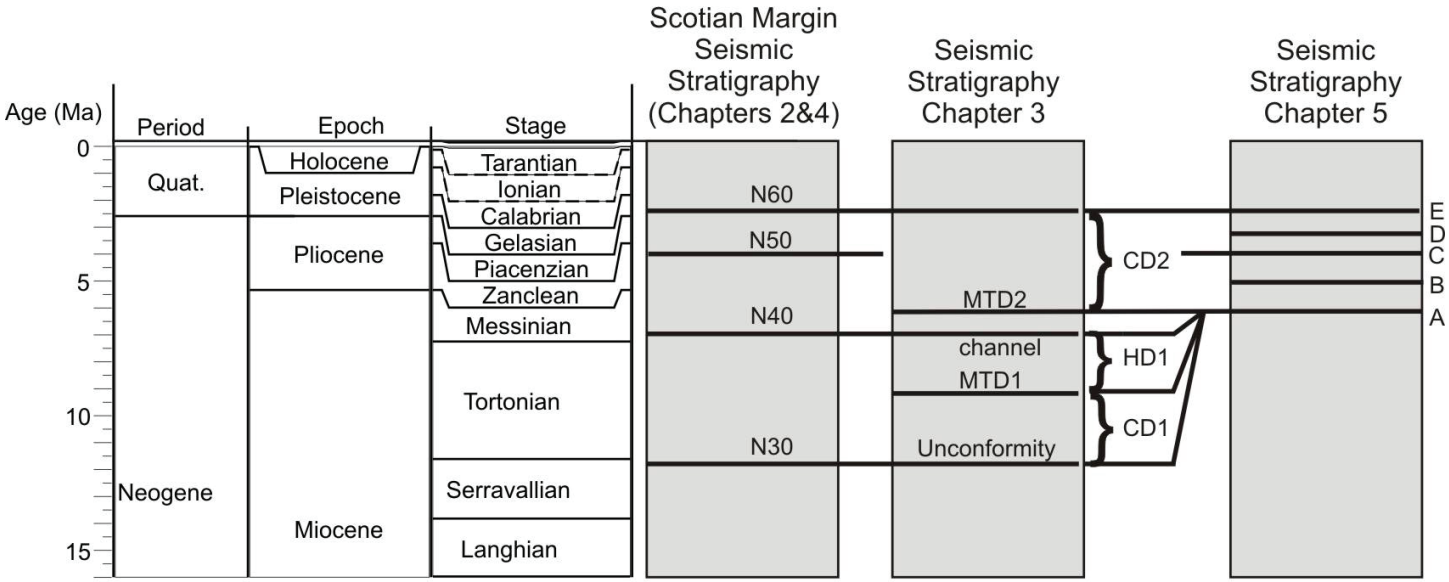

Figure 1.9 Diagram illustrating the relationship of seismic stratigraphies used in Chapters 2-5.

1.7 REFERENCES CITED IN CHAPTER 1

Aurnhammer, M., and Mayoral, R. 2004. Improving seismic horizon matching by ordinal measures. In Proceedings of the 17th International Conference on Pattern Recognition, Vol. 3, pp. 642-645.

Boggs, S. 1995. Principles of Sedimentology and Stratigraphy. Prentice-Hall, Inc., Englewood Cliffs, New Jersey.

Bond, C.E., Gibbs, A.D., Shipton, Z.K., and Jones, S. 2007. What do you think this is? "Conceptual uncertainty" in geoscience interpretation. GSA Today, v. 17. p. 4-10.

Carter, L. and McCave, I.N. 1994. Development of sediment drifts approaching an active plate margin under the SW Pacific deep western boundary current. Paleoceanography, v. 9, p. 1061-1085.

Carvajal, C., Steel, R., and Petter, A. 2009. Sediment supply: The main driver of shelf-margin growth. Earth-Science Reviews, v. 96, p. 221–248.

Chaplot, V., Darboux, F., Bourennane, H., Leguédois, S., Silvera, N., and Phachomphon, K. 2006. Accuracy of interpolation techniques for the derivation of digital elevation models in relation to landform types and data density. Geomorphology, v. 77, p. 126-141.

Chen, J. and Schuster, G.T. 1999. Resolution limits of migrated images. Geophysics, v. 64, p. 1046-1053.

Davies, R.J., Posamentier, H.W., Wood, L.J., and Cartwright, J.A. (eds.) 2007. Seismic geomorphology: applications to hydrocarbon exploration and production. Geological Society of London, Special Publications, v. 277, 274 p.

Deptuck, M.E. 2003. Post-rift geology of the Jeanne d'Arc basin, with a focus on the architecture and evolution of early Paleogene submarine fans, and insights from modern deepwater systems. PhD. Thesis, Dalhousie University. 326 p, plus appendices.

Ebinger C.A., and Tucholke, B.E. 1988. Marine Geology of the Sohm Basin, Canadian Atlantic Margin. Bulletin of American Association of Petroleum Geologists, v. 72, p. 1450-1468.

Emery, K.O., Uchupi, E., Phillips, J.D., Brown, C.O., Bunce, E.T., and Knott, S.T. 1970. Continental rise off eastern North America. AAPG Bulletin, v. 54, 44-108.

Faugères, J.-C., Mezerais, M.L., and Stow, D.A.V. 1993. Contourite drift types and their distribution in the North and South Atlantic Ocean basins. Sedimentary Geology, v. 82, p.189–203.

Faugères, J-C, Stow, D.A.V., Imbert, P., and Viana, A., 1999, Seismic features diagnostic of contourite drifts: Marine Geology, v. 162, p. 1-38.

Faugères, J.C., and Stow, A.V., 2008. Contourite drifts: nature, evolution and controls. In: Rebesco, M., Camerlenghi, A. (Eds.), Contourites. Developments in Sedimentology, v. 60, Elsevier, p. 259-288.

Fisher, P.F., and Tate, N.J. 2006. Causes and consequences of error in digital elevation models. Progress in Physical Geography, v. 30, p. 467-489.

Hansen, R.O. 1993. Interpretive gridding by anisotropic kriging. Geophysics, v. 58, p. 1491-1497.

Hernández-Molina, F.J., Llave, E., and Stow, D.A.V. 2008. Continental slope contourites. In: Rebesco, M. and Camerlenghi, A. (Eds.), Contourites. Developments in Sedimentology, v. 60, Elsevier, p. 379- 408.

Hernández-Molina, F.J., Llave, E., Stow, D.A.V., García, M., Somoza, L., Vázquez, J.T., Lobo, F., Maestro, A., Díaz del Río, V., León, R., Medialdea, T., and Gardner, J. 2006. The Contourite Depositional System of the Gulf of Cadiz: A sedimentary model related to the bottom current activity of the Mediterranean Outflow Water and the continental margin characteristics. Deep-Sea Research I, v. 53, p. 1420–1463.

Heezen, B.C., Hollister, C.D., and Ruddiman, W.F. 1966. Shaping of the continental rise by deep geostrophic contour currents. Science, v. 152, p. 502–508.

Hohbein, M., Cartwright, J. 2006. 3D seismic analysis of the West Shetland Drift system: Implications for Late Neogene palaeoceanography of the NE Atlantic. Marine Geology, v. 230, p. 1-20.

Hopfauf, V., and Spiess, V. 2001. A three-dimensional theory for the development and migration of deep sea sediment waves. Deep-Sea Research I, v. 48, p. 2497–2519.

Hughes Clarke, J.E., O'leary, D.W., and Piper, D.J.W. 1992. Western Nova Scotia continental rise: relative importance of mass wasting and deep boundary-current activity. In: Poag, C.W. and De Graciansky, P.C. (Eds.), Geologic Evolution of Atlantic Continental Rises. Van Nostrand Reinhold, New York, p. 266-281.

Jansa, L.F., Enos, P., Tucholke, B.E., Gradstein, F.M. and Sheridan, R.E. 1979. Mesozoic-Cenozoic sedimentary formations of the North American Basin; Western North Atlantic. In: Talwani M., Hay, W., and Ryan, W.B.F. (Eds.), Deep Drilling Results in the Atlantic Ocean: continental margins and paleoenvironment. American Geophysical Union Maurice Ewing Series, v. 3 , p. 1–57.

Keen, M.J. and Piper, D.J.W. 1990. Geophysical and historical perspective. In: Keen, M.J. and Williams, G.L. (Eds.), Geology of the Continental Margin of Eastern Canada. Geological Survey of Canada, Geology of Canada v. 2, p. 5–30.

Knutz, P.C., and Cartwright, J. 2003. Seismic stratigraphy of the West Shetland Drift: Implications for Late Neogene paleocirculation in the Faeroe-Shetland Gateway. Paleoceanography, v. 18, p. 1093. doi: 10.1029/2002PA000786.

Laberg, J.S., Stoker, M.S., Dahlgren, K.I.T., de Haas, H., Haflidason, H., Hjelstuen, B.O., Nielsen, T., Shannon, P.M., Vorren, T.O., Van Weering, T.C.E., Ceramicola, S. 2005. Cenozoic alongslope processes and sedimentation on the NW European Atlantic margin. Marine and Petroleum Geology, v. 22, p.1,069-1,088.

Locker, S.D., and Laine, E.P. 1992. Paleogene-Neogene depositional history of the middle U.S. Atlantic continental rise: mixed turbidite and contourite depositional systems. Marine Geology, v. 103, p. 137-164.

McCave I.N. and Tucholke B.E. 1986. Deep current controlled sedimentation in the western North Atlantic. In: Vogt P.R. and Tuchkolke B.E. (Eds.), The Geology of North America vol. M: The Western North Atlantic region. Geological Society of America. p. 451–468.

McCave, I.N., Chandler, R.C., Swift, S.A., and Tucholke, B.E. 2002. Contourites of the Nova Scotian continental rise and the HEBBLE area. Geological Society, London, Memoirs, v. 22, p. 21-38.

Miall, A.D., Balkwill, H.R. and McCracken, J. 2008. Chapter 14- The Atlantic Margin Basins of North America. In: Miall, A.D. (Ed.), Sedimentary Basins of the World. Elsevier, Volume 5- The Sedimentary Basins of the United States and Canada, p. 473-504.

Miller, K.G., Wright, J.D., Katz, M.E., Wade, B.S., Browning, J.V., Cramer, B.S., and Rosenthal, Y. 2009. Climate threshold at the Eocene-Oligocene transition: Antarctic ice sheet influence on ocean circulation, in Koeberl, C., Montanari, A., (eds.) The Late Eocene Earth—Hothouse, Icehouse, and Impacts: Geological Society of America Special Paper 452, p. 169–178, doi: 10.1130/2009.2452(11).

Mosher, D.C., Bigg, S. and LaPierre, A. 2006. 3D seismic versus multibeam sonar seafloor surface renderings for geohazard assessment: Case examples from the central Scotian Slope. The Leading Edge, v. 25, p. 1484-1494.

Mountain, G.S., Burger, R.L., Delius, H., Fulthorpe, C.S., Austin, J.A., Goldberg, D.S., Steckler, M.S., et al. 2007. The long-term stratigraphic record on continental margins. In: Nittrouer, C.A., Austin, J.A., Field, M.E., Kravitz, J.H., Syvitski, J.P.M., and Wiberg, P.L. (Eds.), Continental margin sedimentation: from sediment transport to sequence

stratigraphy. International Association of Sedimentologists Special Publication. v. 37, p. 381–458.

Mountain, G.S. and Tucholke, B.E. 1985. Mesozoic and Cenozoic Geology of the U.S. Atlantic Continental Slope and Rise. In: Poag, C.W. (Ed.), Geologic Evolution of the U.S. Atlantic Margin. Van Nostrand Reinhold. p. 293-341.

Mulder, T., Faugères, J-C, Gonthier, E. 2008. Mixed turbidite-contourite systems. In: M. Rebesco, M. and Camerlenghi, A. (Eds.), Contourites. Developments in Sedimentology, v. 60, Elsevier, p. 435-456.

Nittrouer, C.A., Austin, J.A., Field, M.E., Kravitz, J.H., Syvitski, J.P.M., and Wiberg, P.L. 2007. Writing a Rosetta stone: insights into continental-margin sedimentary processes and strata., In: Nittrouer, C.A., Austin, J.A., Field, M.E., Kravitz, J.H., Syvitski, J.P.M., and Wiberg, P.L. (Eds.), Continental margin sedimentation: from sediment transport to sequence stratigraphy. International Association of Sedimentologists Special Publication. v. 37, p. 1-48.

Nowell, A.R.M., and Hollister, C.D. (Eds.). 1985. Deep Ocean Sediment Transport – Preliminary Results of the High Energy Benthic Boundary Layer Experiment. Marine Geology, v. 66, 420 p.

Payton, C.E. (Ed.). 1977. Seismic stratigraphy- Applications to hydrocarbon exploration. AAPG Memoir 26, American Association of Petroleum Geologists, 502 p.

Pickart, R.S. 1992. Water mass components of the North Atlantic Deep Western Boundary Current. Deep-Sea Research, v. 39, p. 1553-1572.

Piper, D.J.W. 2005. Late Cenozoic evolution of the continental margin of eastern Canada. Norwegian Journal of Geology, v. 85, p. 231-244.

Poag, C.W. and Ward, L.W. 1993. Allostratigraphy of the U.S. Middle Atlantic continental margin- Characteristics, distribution, and depositional history of principal unconformity bounded Upper Cretaceous and Cenozoic sedimentary units. U.S. Geological Survey Professional Paper 1542, 81 p.

Posamentier, H.W., and Kolla, V. 2003. Seismic geomorphology and stratigraphy of depositional elements in deep-water settings. Journal of Sedimentary Research, v. 73, p. 367-388.

Posamentier, H.W., Davies, R.J., Cartwright, J.A., and Wood, L.J. 2007. Seismic geomorphology; an overview. Seismic geomorphology; applications to hydrocarbon exploration and production, Geological Society Special Publications 277, p. 1-14.

Prather, B. E. 2003. Controls on reservoir distribution, architecture and stratigraphic trapping in slope settings. Marine and Petroleum Geology, v. 20, p. 527–543.

Ramsayer, G.R. 1979. Seismic stratigraphy, a fundamental exploration tool. Offshore Technology Conference Paper OTC 3568, p. 1859-1862.

Rebesco, M., and Stow, D.A.V. 2001. Seismic Expression of Contourites and Related Deposits: A Preface. Marine Geophysical Researches, v. 22, p. 303-308.

Sangree, J.B. and Widmier, J.M. 1979. Interpretation of depositional facies from seismic data. Geophysics, v. 44, p. 131-160.

Schlee, J.S., Poag, C.W. and Hinz, K. 1985. Seismic stratigraphy of the continental slope and rise seaward of Georges Bank. In: Poag, C.W. (Ed.), Geologic evolution of the United States Atlantic margin. New York, Van Nostrand, p. 265-292.

Schmitz , W.J. and McCartney, M.S. 1993. On the North Atlantic Circulation. Reviews of Geophysics, v. 31, p. 21-39.

Shannon, P. M, Stoker, M. S., Praeg, D., van Weeringc, T.C.E., de Haasc, H., Nielsend, T., Dahlgrene, K.I.T., and Hjelstuenf, B.O. 2005. Sequence stratigraphic analysis in deep-water, underfilled NW European passive margin basins. Marine and Petroleum Geology, v. 22, p. 1185–1200.

Shaw, J., and Courtney, R.C. 2004. Digital elevation model of Atlantic Canada: Geological Survey of Canada Open File 4634.

Sheriff, R.F., 1985, Aspects of Seismic Resolution. In: Berg, O.R. and Woolverton, D.G. (Eds.), Seismic Stratigraphy II - An Integrated Approach. AAPG Memoir 39, American Association of Petroleum Geologists, p. 1-10.

Shimeld, J. 2004. A comparison of salt tectonic subprovinces beneath the Scotian Slope and Laurentian Fan. In: Post, P.J., Olson, D.L., Lyons, K.T., Palmes, S.L., Harrison, P.F., and Rosen, N. (eds.) Salt–sediment Interactions and Hydrocarbon Prospectivity: Concepts, Applications, and Case Studies for the 21st Century. 24th Annual Gulf Coast Section of the Society of Economic Paleontologists and Mineralogists Foundation Bob F. Perkins Research Conference, Houston, Texas, Dec. 5-8, 2004, p. 502-532.

Smith, R.S. and O'Connell, M.D. 2005. Interpolation and gridding of aliased geophysical data using constrained anisotropic diffusion to enhance trends. Geophysics, v. 70, V121-V127.

Steffens, G.S., Biegert, E.K., Sumner, S., and Bird, D. 2003. Quantitative bathymetric analyses of selected deepwater siliciclastic margins: receiving basin configurations for deepwater fan systems. Marine and Petroleum Geology, v. 20, p. 547-561.

Stoker, M.S., Praeg, D., Hjelstuen, B.O., Laberg, J.S., Nielsen, T., and Shannon, P.M. 2005. Neogene stratigraphy and the sedimentary and oceanographic development of the NW European Atlantic margin. Marine and Petroleum Geology, v. 22. p. 977-1005.

Stow D.A.V. and Mayall M. 2000. Deep-Water Sedimentary Systems: New Models for the 21st Century. Marine and Petroleum Geology, v. 17, p. 125-135.

Swift, S.A. 1987. Late Cretaceous-Cenozoic development of outer continental margin, southwestern Nova Scotia. AAPG Bulletin, v. 71, p. 678-701.

Tucholke, B. E. and Mountain, G.S. 1979. Seismic stratigraphy, lithostratigraphy and paleosedimentation patterns in the North American Basin. In: Talwani M., Hay, W., and Ryan, W.B.F. (Eds.), Deep Drilling Results in the Atlantic Ocean: continental margins and paleoenvironment. American Geophysical Union Maurice Ewing Series, v. 3 ,p. 58-86.

Tucholke, B. E. and Mountain, G.S. 1986. Tertiary paleoceanography of the western North Atlantic Ocean. In: Vogt, P.R. and Tucholke, B.E (Eds.), The Geology of North America, Vol. M, The Western North Atlantic Region, Geological Society of America, Boulder, CO, p. 631–650.

Uenzelmann-Neben, G. 2006. Depositional patterns at Drift 7, Antarctic Peninsula: Along-slope versus down-slope sediment transport as indicators for oceanic currents and climatic conditions. Marine Geology, v. 233, p. 49-62.

Vail, P. R., R. G. Todd, and J. B. Sangree 1977. Seismic Stratigraphy and Global Changes of Sea Level: Part 5. Chronostratigraphic Significance of Seismic Reflections. In: Payton, C.E. (Ed.), Seismic stratigraphy- Applications to hydrocarbon exploration. AAPG Memoir 26, American Association of Petroleum Geologists, p. 99 – 116.

Viana, A.R., Almeida Jr., W., Nunes, C.V., and Bulhões, E.M. 2007. The Economic importance of contourites. In: Viana, A.R., Rebesco, M. (Eds.), Economic and Palaeoceanographic Significance of Contourite Deposits. Geological Society of London Special Publication v. 276, p. 1–23.

Viana, A.R., 2008, Economic relevance of contourites. In: Rebesco, M. and Camerlenghi, A. (Eds.), Contourites. Developments in Sedimentology v. 60, Elsevier, p. 493-510.

Wade, J.A. and MacLean, B.C. 1990. The Geology of the Southeastern Margin of Canada, Part 2: Aspects of the Geology of the Scotian Basin from Recent Seismic and Well Data. In: Keen, M.J. and Williams, G.L. (Eds.), Geology of the Continental Margin of Eastern Canada. Geological Survey of Canada, Geology of Canada v. 2, p.190-238.

Wade, J. A., MacLean, B. C., and Williams, G. L. 1995. Mesozoic and Cenozoic stratigraphy, eastern Scotian Shelf: New interpretations. Canadian Journal of Earth Sciences, v. 32, p. 1462-1473.

White, R. and Simm, R. 2003. Tutorial: Good practice in well ties. First Break, v.21, p. 75-83.

Worthington, L.V., 1976: On the North Atlantic Circulation. The Johns Hopkins Oceanographic Studies, No. 6, 110 pp.

Wynn, R.B. and Masson, D.G. 2008. Sediment waves and bedforms. In: Rebesco, M. and Camerlenghi, A. (Eds.), Contourites. Developments in Sedimentology, v. 60, Elsevier, p 289-300.

Yilmaz, O. 1987. Seismic Data Processing, v. 2. Society of Exploration Geophysicists, Tulsa Oklahoma.

Chapter 2: Seismic Stratigraphic Framework and Depositional History of an Upper Cretaceous and Cenozoic Depocenter off Southwest Nova Scotia, Canada

2.1 INTRODUCTION

Regional studies of outer continental margin evolution depict the lateral or along-slope changes in margin development not apparent from narrow corridor, shelf to slope transects (e.g. Locker and Laine 1992; Poag and Ward 1993; Stoker et al. 2005). Such studies typically rely on the correlation of regionally mappable seismic stratigraphic horizons that generally correlate to impedance contrasts generated at condensed intervals, lithological boundaries, and erosional unconformities. In many cases, the sequence stratigraphic significance of horizons within a stratigraphic framework is not obvious, particularly in relatively sediment-starved or deepwater margins (Mountain and Tucholke 1985; Stoker et al. 2005; Shannon et al. 2005; Carvajal et al. 2009). The intervening seismic reflection stacking geometries and stratal relationships provide important information on the complex interactions between sediment supply, local and regional tectonics, variations in eustatic and local sea-level, oceanographic conditions, and climate change.

The continental margin offshore Nova Scotia (herein the Scotian margin) forms the northern edge of the North American Basin (Figure 2.1). South of the New England Seamounts, the geology and seismic stratigraphy of the lower continental rise and abyssal plain in the basin are well known (Emery et al. 1970; Jansa et al. 1979; Tucholke and Mountain 1979; Mountain and Tucholke 1985) and an allostratigraphic framework for the continental margin was established (Poag and Ward 1993). In contrast, the Upper Cretaceous and Cenozoic stratigraphy and geological history of the outer Scotian margin are not well known. This knowledge gap is due to a number of factors that include historically sparse seismic data coverage, widely spaced hydrocarbon exploration wells, difficulty extending the seismic stratigraphy of the North American Basin north of the New England Seamounts, and uncertainties of seismic correlation across areas highly

deformed by salt diapirism (Swift 1987; Ebinger and Tucholke 1988; Wade et al. 1995; Piper 2005; Schlee et al. 1985). Most deepwater hydrocarbon exploration wells from the margin also show substantial biostratigraphic unconformities in the Cenozoic section (Fensome et al. 2008). Together, these factors make it difficult to link the stratigraphy of the deep basin onto the continental slope and shelf.

This study seeks to understand the Late Cretaceous and Cenozoic geologic development of a North Atlantic passive margin by examination of the seismic stratigraphy of a large (~50 000 km^2) deep water depocenter located along the southwestern Scotian margin. The expanded stratigraphy within the depocenter should preserve a detailed record of margin processes during the last 70 Ma. The study examines the timing and processes that led to the formation of several deep-water seismic stratigraphic markers along the margin and compares the seismic stratigraphy to the well-studied North American Basin margin to the south. Since 1998, several high quality 2-D and 3-D seismic reflection datasets were collected on the outer Scotian margin, along with five exploration wells, vastly improving data coverage density and alleviating some of the issues related to seismic correlation experienced by earlier researchers. This study uses these new data, along with lithostratigraphic and biostratigraphic data from existing deepwater exploration wells.

Figure 2.1 A) Map of the western North Atlantic showing locations discussed in the text and the distribution of ocean drilling sites and, for the Nova Scotia margin, deepwater hydrocarbon exploration wells. B) Location map of the continental margin off Nova Scotia showing locations discussed in the text. C) Map of data used for this study and major structural elements. Regional 2D seismic reflection data shown as a grid. 3D seismic datasets are shown as white polygons and consist of the Barrington (B) and Torbrook (T) survey areas. Exploration wells used for the study are Bonnet P-23 (1), Shelburne G-29 (2), Albatross B-13 (3), Torbrook C-15 (4), Acadia K-62 (5), Shubenacadie H-100 (6), Newburn H-23 (7), Weymouth A-45 (8), Balvenie B-79 (9), and Annapolis G-24 (10).

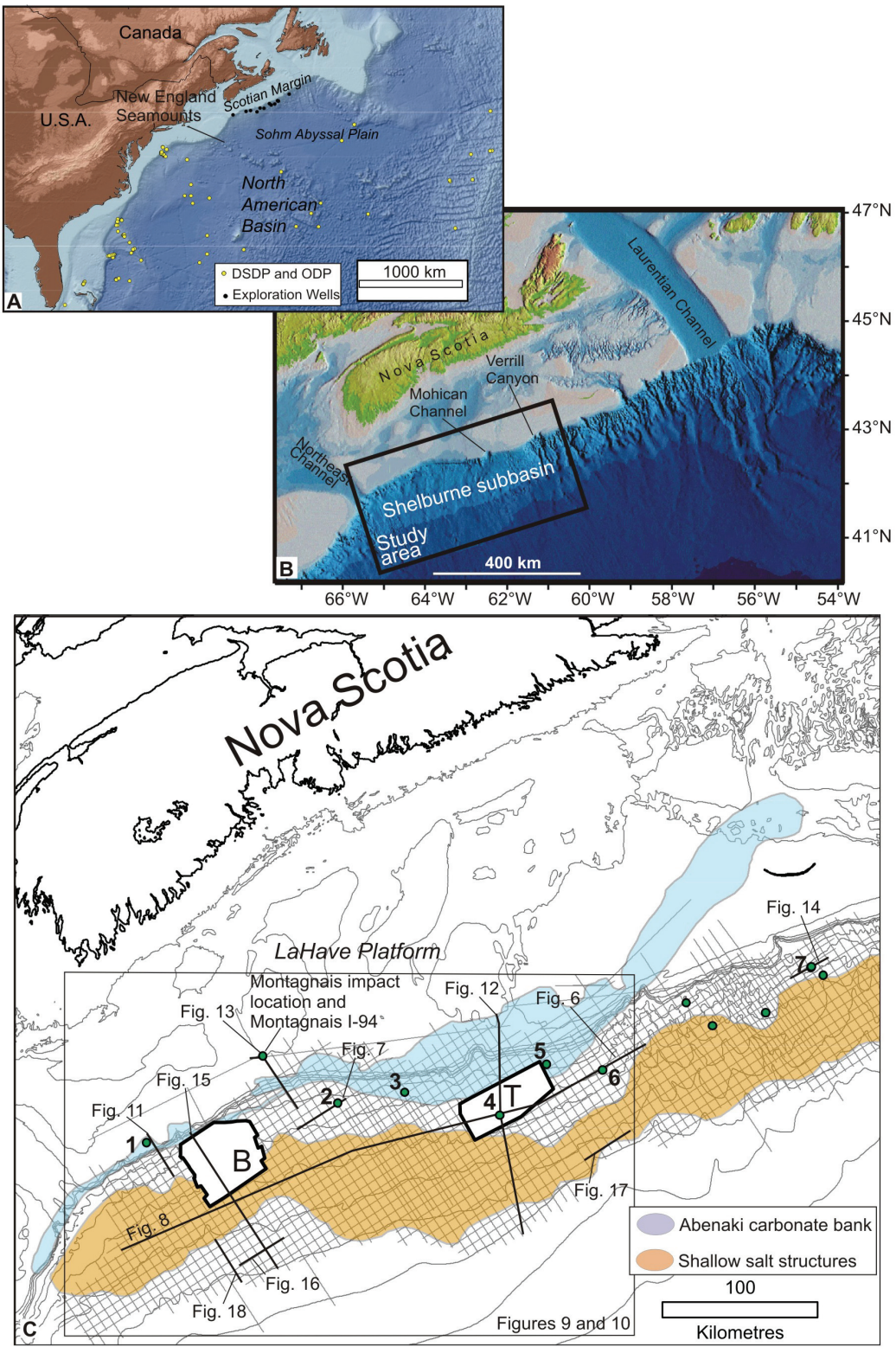
Canada
U.S.A.
New England Seamounts
Scotian Margin
Sohm Abyssal Plain
North American Basin
DSDP and ODP
Exploration Wells
1000 km
A
Laurentian Channel
Nova Scotia
Verrill Canyon
Mohican Channel
Northeast Channel
Shelburne subbasin
Study area
400 km
B
47°N
45°N
43°N
41°N
66°W
64°W
62°W
60°W
58°W
56°W
54°W
Nova Scotia
LaHave Platform
Montagnais impact location and Montagnais I-94
Fig. 12
Fig. 6
Fig. 13
Fig. 7
Fig. 15
Fig. 11
Fig. 14
Fig. 17
Fig. 8
Fig. 16
Fig. 18
1
2
3
4
5
6
7
T
B
Figures 9 and 10
Abenaki carbonate bank
Shallow salt structures
100
Kilometres
C

2.2 Study Area and Geological Setting

The Scotian margin consists of the continental shelf, slope and rise south of Nova Scotia and forms most of the northern margin of the North American Basin, a large bathymetric depression in the northwest Atlantic Ocean centered over the Bermuda Rise (Figure 2.1) (Jansa et al. 1979). The margin initiated during the Late Triassic and Early Jurassic rifting of Pangea and the opening of the central North Atlantic Ocean, which created a series of inter-connected sub-basins seaward of more stable structural elements and a major basement hinge zone (Grant et al. 1986; Wade and MacLean 1990). This study focuses on the Upper Cretaceous and Cenozoic deposits along the outer Scotian margin west of Verrill Canyon in the Shelburne subbasin where Jansa and Wade (1975) and Swift (1987) identified the existence of a thick depocenter (Figure 2.1b).

Late Cretaceous and Cenozoic depositional patterns in the study area are influenced by several important regional structural features. The Jurassic Abenaki Fm carbonate platform flanks the outer LaHave Platform and approximately coincides with the margin hinge zone in the study area (Figure 2.1c, Figure 2.2) (Wade and MacLean 1990). Along the northern margin of the Shelburne subbasin , the steep buried carbonate platform edge follows the approximate trend of the modern shelf edge. East of the Shelburne subbasin, the trend of the carbonate platform diverges northward of the modern shelf edge because of a major progradational system that advanced seaward of the carbonate platform during the Late Jurassic and Early Cretaceous (Wade and MacLean 1990). Another important feature is a 40-100 km wide belt of autochthonous and allochthonous salt structures belonging to the Triassic Argo Fm that disrupts the Mesozoic and Cenozoic stratigraphy (Wade and MacLean 1990; Shimeld 2004). The study area also spans the location of the Montagnais structure, interpreted as an Early Eocene Montagnais bolide impact (Jansa et al. 1989) (Figure 2.1c).

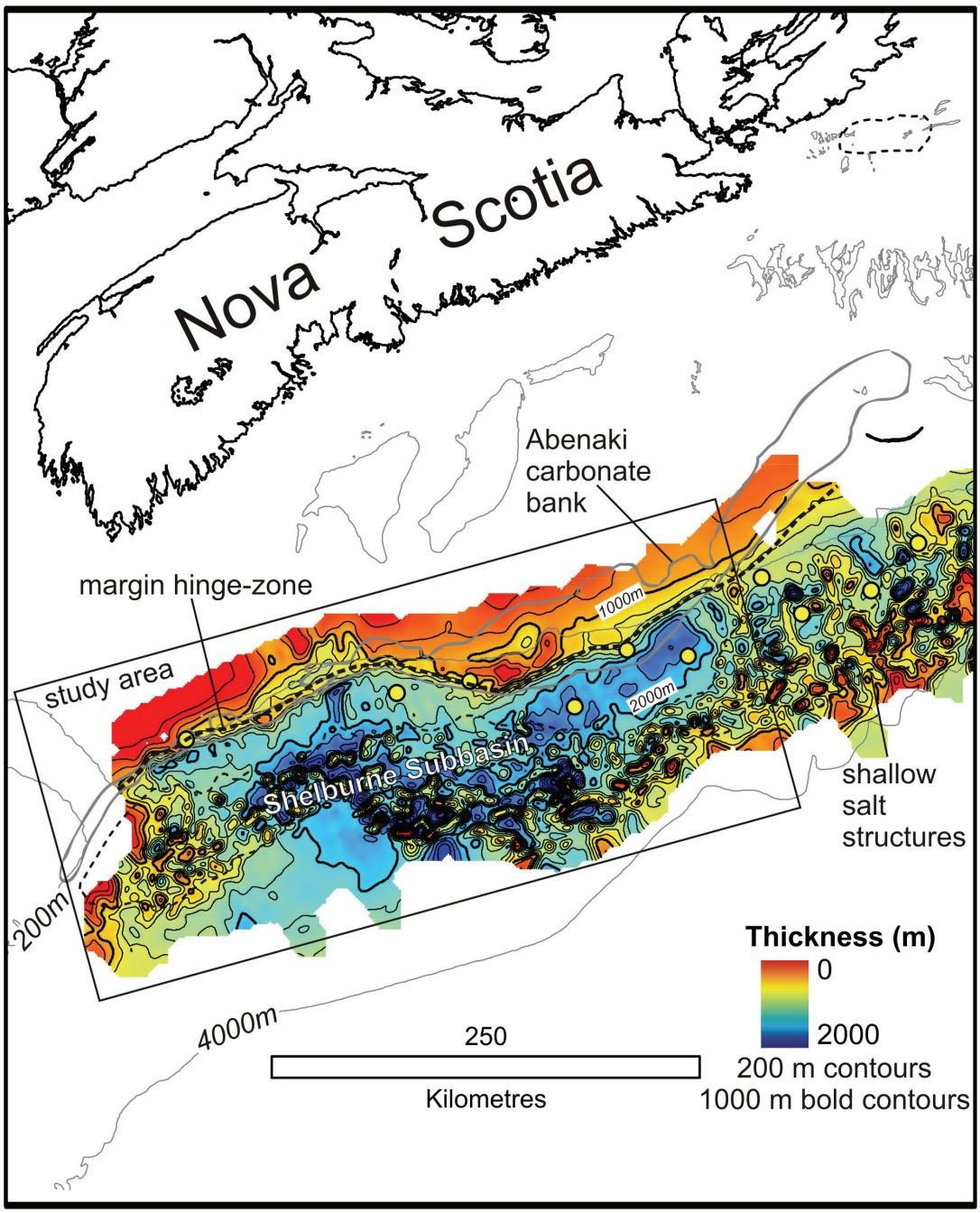

Figure 2.2 Isochore map of Upper Cretaceous and Cenozoic deposits on the outer western Scotian margin (horizons C100 to seabed). The depocenter located in the Shelburne sub-basin is the focus of this study. The location of the margin hinge-zone is indicated by the bold dashed line. The locations of explorations wells are shown as yellow circles. This map is based on seismic data courtesy of TGS-NOPEC Geophysical Company L.P.

2.2.1 Upper Cretaceous and Cenozoic Lithologic and Seismic Stratigraphies of the North American Basin and Scotian Margin

Lithostratigraphy of the North American Basin

Upper Cretaceous and Cenozoic deposits of the North American Basin south of the New England Seamounts and along the continental margin of the eastern United States have been extensively studied (e.g. Deep Sea Drilling Program (DSDP) legs 11, 43, 93, 95, Ocean Drilling Program (ODP) legs 150 and 174). Jansa et al. (1979) presented the lithostratigraphy of these deposits based on DSDP legs 11 and 43 drilling results (Figure 2.3). Upper Cretaceous to Quaternary deposits consist of the Plantagenet, Bermuda Rise, and Blake Ridge formations. The Plantagenet Fm includes Upper Cenomanian to Upper Paleocene variegated, non calcareous claystone. They are interpreted as pelagic deposits that accumulated in an oxygenated environment below the carbonate compensation depth (CCD). A relatively thin but conspicuous interval of nannofossil chalks, marls and limestones is found in the upper part of the Plantangenet Fm and has been designated the Crescent Peaks Member. The age of the Crescent Peaks Member is Middle Maastrichtian to earliest Paleocene. It is interpreted to have formed via pelagic deposition in quiescent conditions above the CCD. The overlying Bermuda Rise Fm spans Upper Paleocene to Middle Eocene sediments enriched in biogenic silica and chert. The Bermuda Rise Fm is interpreted to have accumulated in an environment where biogenic silica deposition

Figure 2.3 Stratigraphic framework. Timescale and sea-level curve are from Time Scale Creator (www.tscreator.com accessed April 15, 2011). Upper Cretaceous and Cenozoic lithostratigraphy of the North American Basin is from Jansa et al. (1979) and Scotian Shelf is from McIver et al. (1972), Jansa and Wade (1975), and Wade and MacLean (1990). Seismic stratigraphy of the North American Basin are from Tucholke and Mountain (1979) and Mountain and Tucholke (1985). Seismic stratigraphies developed for the outer Scotian margin are by Swift (1987) and Ebinger and Tucholke (1989). Note that separate stratigraphies were developed by Swift (1987) for the rise and slope. Right column shows the seismic stratigraphy developed for this study.

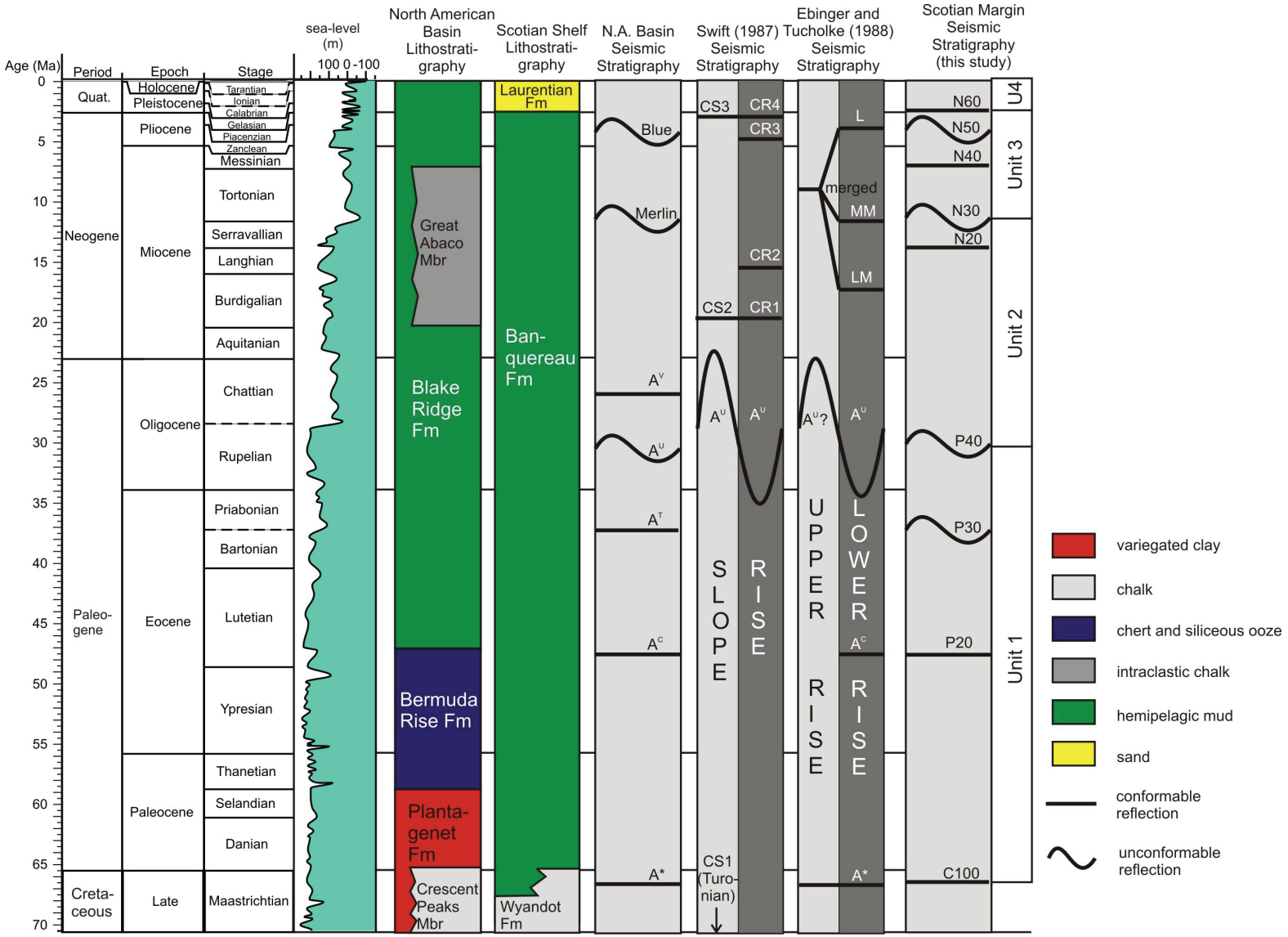
Age (Ma)
Period
Epoch
Stage
sea-level (m)
100 0 -100
North American Basin Lithostrati-graphy
Scotian Shelf Lithostrati-graphy
N.A. Basin Seismic Stratigraphy
Swift (1987) Seismic Stratigraphy
Ebinger and Tucholke (1988) Seismic Stratigraphy
Scotian Margin Seismic Stratigraphy (this study)
Quat.
Neogene
Paleo-gene
Creta-ceous
Holocene
Pleistocene
Pliocene
Miocene
Oligocene
Eocene
Paleocene
Late
Tarantian
Ionian
Calabrian
Gelasian
Piacenzian
Zanclean
Messinian
Tortonian
Serravallian
Langhian
Burdigalian
Aquitanian
Chattian
Rupelian
Priabonian
Bartonian
Lutetian
Ypresian
Thanetian
Selandian
Danian
Maastrichtian
Great Abaco Mbr
Blake Ridge Fm
Bermuda Rise Fm
Planta-genet Fm
Crescent Peaks Mbr
Laurentian Fm
Ban-quereau Fm
Wyandot Fm
Blue
Merlin
CS3
CS2
CS1 (Turo-nian)
CR4
CR3
CR2
CR1
SLOPE
RISE
merged
L
MM
LM
UPPER RISE
LOWER RISE
N60
N50
N40
N30
N20
P40
P30
P20
C100
U4
Unit 3
Unit 2
Unit 1
variegated clay
chalk
chert and siliceous ooze
intraclastic chalk
hemipelagic mud
sand
conformable reflection
unconformable reflection

predominated over biogenic carbonate in the deep basin below the CCD, or where biogenic silica contributed significantly to deposits above the CCD. The Blake Ridge Fm spans Middle Eocene and younger sediments. It is a widespread, greenish-grey and brown hemipelagic mud interpreted to have been deposited in an environment very similar to what currently prevails in the Northwest Atlantic. Much of the formation was deposited directly from turbidity currents and reworked by bottom currents. Within the Blake Ridge Fm, a locally restricted, massive interval of intraclastic chalk is designated the Great Abaco Member. The Great Abaco Member is Early to Middle Miocene age and is interpreted to be a mass transport complex, possibly sourced from the Blake Plateau.

Seismic stratigraphy of the North American Basin

The seismic stratigraphy of the North American Basin was presented by Tucholke (1979) and Tucholke and Mountain (1979) and has been refined by subsequent researchers (e.g. Mountain and Tucholke 1985; Tucholke and Mountain 1986; Poag and Mountain 1987; Ebinger and Tucholke 1988) (Figure 2.2). A series of prominent Upper Cretaceous and Cenozoic seismic reflections are recognized on most profiles in the North American Basin, and these reflections were correlated to various ocean drilling sites. Horizon A* correlates to the Crescent Peaks Mbr of the Plantagenet Fm, a marly nannofossil rich chalk. Its age is upper Maastrichtian. Above A*, the Horizon-A complex is a series of prominent reflections that range in age from Eocene to Oligocene (Tucholke 1979). Early studies often mapped the complex as a single reflection horizon, for example Emery et al. (1970), but ocean drilling and improved quality seismic data show that the Eocene to Oligocene interval consists of at least four discrete reflection horizons. Horizon A^C is in most places the highest amplitude reflection within the complex and correlates to high impedance contrasts in the Bermuda Rise Fm, with strong reflectivity associated with the Middle Eocene cherts of this formation. Horizon A^T correlates with the top of a turbidite interval within the Blake Ridge Fm. Its age is Middle to Upper Eocene and it is attributed to widespread input of bioclastic and terrigenous turbidites into the basin. Horizon A^U is a basin-wide erosional unconformity attributed to erosion by abyssal currents. Its age is variable and in many areas represents a hiatus from Upper Eocene to Lower Miocene. Horizon A^V correlates to an apron of volcanoclastic turbidites deposited around Bermuda.

The age of the horizon is Upper Oligocene and is attributed to subaerial weathering of the Bermuda pedestal which emerged above sealevel by Middle Eocene time.

Various Neogene seismic reflection unconformities have been widely referenced in the literature (e.g. Mountain and Tucholke 1985; Tucholke and Mountain 1986; Swift 1987; Ebinger and Tucholke 1988; Locker and Laine 1992). These are horizon X/Unconformity/LM of Lower to Middle Miocene age, horizon Merlin/MM of Middle Miocene age, and horizon Blue/L of Pliocene age. Apart from the Horizon-A complex, horizons Merlin and Blue (Figure 2.3) are most widely cited in the literature and are interpreted to represent margin erosion due to strengthened abyssal currents (Mountain and Tuckolke 1985).

Lithostratigraphy of the Scotian Margin

Little was known about the Mesozoic and Cenozoic geology of the Scotian margin prior to drilling of the Sable Island C-67 exploration well by Mobil Oil Co. in 1967 (McIver 1972; Fensome et al. 2008). The Mesozoic and Cenozoic deposits of the margin are divided into thirteen formations that represent the syn-rift and post rift depositional history (McIver 1972; Jansa and Wade 1975; Wade and MacLean 1990). These divisions are primarily based on data from hydrocarbon exploration wells below the modern Scotian Shelf. Of the thirteen formations, Upper Cretaceous to Cenozoic deposits include the Wyandot (Upper Cretaceous), Banquereau (Upper Cretaceous to Lower-Mid Pleistocene) and Laurentian formations (Lower-Mid Pleistocene to recent) (Figure 2.3).

The Wyandot Fm consists of Upper Cretaceous chalks and lesser marls and calcareous mudstones, and is considered equivalent to the Crescent Peaks Member of the Plantagenet Fm. The formation reaches 400 m thickness near the shelf edge and has an average thickness of 135 m. The Banquereau Fm consists of Upper Cretaceous to Pliocene mudstone with lesser sandstones and thin chalk beds. Hardy (1975) proposed a four unit informal division of the Banquereau Fm, however these divisions have rarely been adopted because of difficulty distinguishing the units on seismic data and in regional correlation (Wade and MacLean 1990; Fensome et al. 2008). A thin, Lower

Eocene chalk is regionally identifiable on seismic reflection data over much of the outer shelf and slope (Fensome et al. 2008). Above the Eocene chalk, the Banquereau Formation becomes increasingly sandy. The Banquereau Fm reaches 1500 m thickness in some wells and thins to zero thickness beneath the modern middle shelf. Quaternary deposits on the Scotian Shelf are assigned to the Laurentian Fm and consist of glacial till and proglacial sediments. The Laurentian Fm reaches a maximum thickness of more than 1200 m where it has prograded along the outer shelf.

The present study is focused on the distal equivalents of the Wyandot, Banquereau, and Laurentian Formations preserved below the modern western Scotian Slope and Rise. Due to a paucity of data, formations in this area have not been formalized and no detailed lithostratigraphic summary exists. Samples show that the interval is mud-dominated, but like the shelf, has a general coarsening up pattern of deposition. Upper Cretaceous, Paleocene and Lower Eocene chalks, similar age to those on the shelf, are recognized in a number of wells (Fensome et al. 2008).

Seismic stratigraphy of the Scotian margin

Previous authors attempted to correlate the North American Basin seismic stratigraphy onto the Scotian margin (Jansa and Wade 1975; Parsons 1975; Jansa et al. 1979; Uchupi and Austin 1979; Swift et al. 1986; Swift 1987; Ebinger and Tucholke 1988; Wade and MacLean 1990; Wade et al. 1995), however no standardized seismic reflection nomenclature exists for the Upper Cretaceous and Cenozoic succession. In the deepwater Scotian Basin, Jansa and Wade (1975) tentatively correlated prominent seismic reflections to oceanic horizon A (Eocene-Oligocene) (Emery et al. 1970) and a base-Quaternary reflection to produce a regional isopach map of the approximate distal equivalent of the Banquereau Fm. This map is the only regional published map of Banquereau Fm thickness for the deepwater margin off Nova Scotia. Swift et al. (1986) provided the first direct seismic stratigraphic correlation of the North American Basin stratigraphy across the New England Seamounts, however only horizons A* and A^U were correlated with confidence onto the Sohm Abyssal Plain.

The most detailed published studies of the Upper Cretaceous and Cenozoic seismic stratigraphy of the continental slope and rise off Nova Scotia are by Swift (1987), Piper et al. (1987), Ebinger and Tulcholke (1988), MacLean and Wade (1993), and Wade et al. (1995). All these studies report a number of seismic unconformities above horizon A^U, but because of no direct seismic tie, the studies developed Neogene seismic stratigraphies independent from the framework utilized along the U.S. margin (Figure 2.3). Deepwater unconformities were interpreted to be produced by bottom current erosion of the continental rise and abyssal plain with inferred ages of Oligocene, Lower Miocene, Middle Miocene, and Pliocene. Swift (1987) developed separate nomenclature for seismic horizons seaward and landward of salt structures. Ebinger and Tucholke (1988) found that the three regional Neogene unconformities that were mapped on the continental rise merged to form a single unconformity below the continental slope (Figure 2.3). Wade et al. (1995) identified discrepancies in the identification of horizons A^U and A^C on the rise by Ebinger and Tucholke (1988). Wade et al. (1995) also discussed the diachroneity of a middle Cenozoic unconformity below the eastern Scotian Slope near the Tantallon M-41 well, suggesting that the time gap represented by the unconformity decreased seaward from the well.

2.3 METHODS

2D and 3D multichannel seismic reflection data were interpreted for this study and integrated with biostratigraphic and geological information from 10 exploration wells (Figure 2.1c). A regional grid of 80 to 106 fold 2D seismic reflection profiles was used to correlate seismic horizons and interpret regional depositional patterns and structures. 2D seismic reflection data were acquired by TGS-Nopec Geophysical Company in 1998 and 1999, with a line spacing of 6 km in the strike direction and 3 to 6 km in the dip direction. Hydrophone streamer length was 6 to 8 km and the acoustic source was a 130 L tuned airgun array. Long 2D seismic lines collected by ION-GXT supplement the 2D grid and aided in regional correlation.

Two large 3D seismic surveys were used to examine in detail the seismic geomorphology. The 3D seismic volumes, termed the Torbrook and Barrington 3D survey areas, were acquired in 2000 and 2001 for EnCana Corporation (then Pan Canadian). The Torbrook survey covers an area of approximately 1560 km^2. Data were recorded by six 6000 m long hydrophone streamers, each with 240 channels. Channel separation was 25 m and bin size was 12.5 m x 25 m. The acoustic source was a 62 *l* tuned airgun array generating a frequency bandwidth of 3-180 Hz. The Barrington survey covers an area of approximately 1790 km^2. Data were recorded by six 6000 m long hydrophone streamers, each with 240 channels. Channel separation was 25 m and bin spacing was 12.5 m x 37.5 m. The acoustic source was a 62 *l* tuned airgun array generating a frequency bandwidth of 3-180 Hz. Processing of both the 2D and 3D datasets was conducted by the data owners prior to this study.

Seismic reflection data were interpreted using SeismicMicro Technologies Kingdom Suite™ and Schlumberger GeoFrame™ software packages. For the 3D seismic dataset, reflection horizons were mapped and gridded to produce continuous surfaces with a grid cell size of 25 m. Seismic reflection travel time, amplitude, and geometric attributes were used to interpret the seismic geomorphology. For the 2D seismic dataset, reflection horizons were mapped and gridded to produce continuous surfaces with a grid cell size of 1000 m. Plan view dimensions of morphological features are given in SI units. Two-way travel time (TWTT) was converted to depth and thickness in metres for the seismic structure and isochore maps. To convert TWTT to depth, checkshot and VSP derived time-depth pairs were compiled for all deepwater wells in the study area for the upper Cretaceous and Cenozoic interval (i.e. the interval between the seafloor to C100 reflections discussed further below). The data were normalized to time and depth below seafloor. Comparison of the normalized data revealed a systematic relationship between time and depth in the study area (Figure 2.4). This relationship was modeled by power regression given by the equation:

[Equation 2.1] $\text{Depth} = 0.5316*(\text{two-way travel time})^{1.0731}$

The model regression resulted in an R-squared value of 0.97 for a sample size of 151. Additionally, "percent residual thickness" maps were generated by dividing the thickness of a particular seismic stratigraphic unit by the total thickness of the Upper Cretaceous and Cenozoic succession. The "percent residual thickness" maps provide important information about how much a specific seismic stratigraphic unit contributes to the total preserved succession.

Geological sample control for the study is provided by samples and well logs from six hydrocarbon exploration wells within the studied depocenter and four deepwater wells from east of the depocenter where seismic continuity allowed correlation. The wells outside the depocenter provide additional, and in some cases superior, sample and age control for the Paleogene interval (Figure 2.1, Table 2.1). Five of the ten wells examined were drilled since 2000 and were not available for previous studies. Despite the new wells, sample control is limited for the Late Cretaceous and Cenozoic interval. No conventional cores exist for the Neogene, and most of the Upper Pliocene and Quaternary succession is entirely unsampled. The majority of the geological information is provided by cuttings and sidewall core sample descriptions in well history reports, supplemented by borehole logs and inferences from deep sea drilling results south of the study area. Cutting samples were typically collected over 5 m intervals, while sidewall core sample spacing was less frequent and more variable. Synthetic seismograms were generated for each well in the study area for correlation of well data to seismic reflection data. Biostratigraphic information is from published reports (Table 2.1). The only well that provided anomalous biostratigraphic results for the seismic stratigraphy was Acadia K-62. In this well, foraminifera were used for the biostratigraphy (Thomas 2001), which do not provide the same level of accuracy as the palynology results from other wells along the Scotian margin (Rob Fensome, pers. comm., 2010).

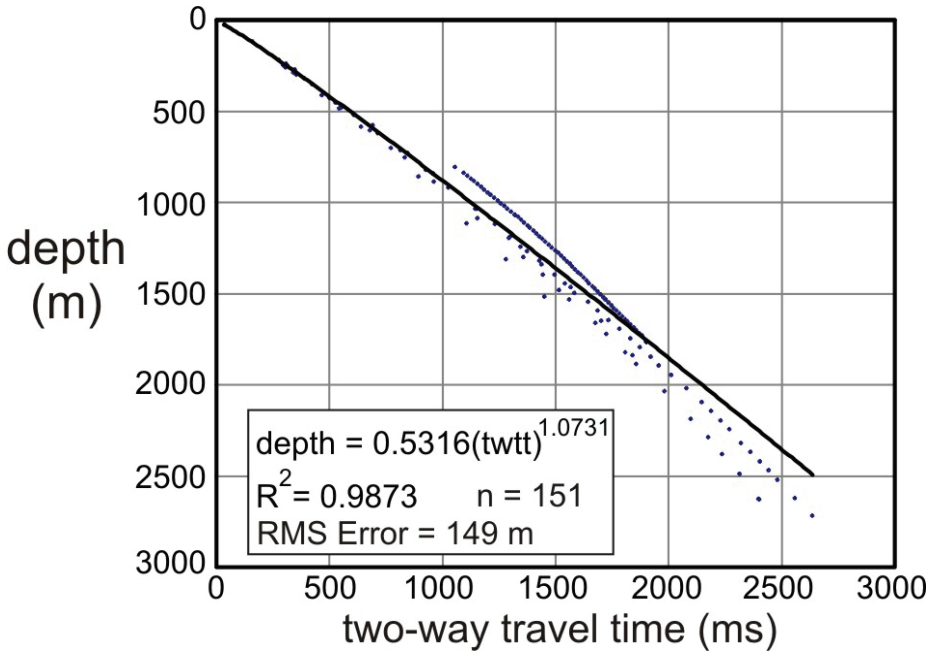

Figure 2.4 Velocity model used for converting structure and isochore maps from time to depth. All available checkshot data for the Upper Cretaceous to seafloor succession in the depocenter were normalized to two-way travel time (twtt) and depth (m) below seabed and an exponential fit was generated using a nonlinear least squares algorithm. Data used for the model are presented in Appendix I.

2.4 RESULTS

As part of this study, reflection C100 (discussed below in detail) and the seafloor reflection were mapped to produce an isochore map of the Upper Cretaceous to Present sediment thickness along the outer Scotian margin (Figure 2.2). The preliminary mapping results confirmed the existence of a 50 000 km^2 depocenter in the Shelburne sub-basin first identified by Jansa and Wade (1975) and then by Swift (1987). The depocenter is located between Northeast Channel and Verrill Canyon, seaward of the Abenaki carbonate platform and the margin hinge zone. This depocenter is the focus of this study and its detailed seismic stratigraphy is presented below.

2.4.1 Seismic stratigraphic framework

Seismic stratigraphic horizons mapped in this study are shown in Figure 2.3. Details about the seismic reflection character, intersection depth at exploration wells in the study area, as well as the lithology and biostratigraphic age determinations at individual wells are summarized in Table 2.1, Table 2.2 and Figure 2.5. Regionally significant horizons were identified on the basis of several criteria as described in Payton (1977), Sangree and Widmier (1979) and Ramsayer (1979). Each horizon marks significant changes in acoustic facies and reflection configuration above and below. Reflections that have higher amplitude than overlying and underlying reflections and were regionally identifiable were also selected. Finally, reflections that form prominent bounding discontinuities were incorporated into the framework.

It is difficult to correlate with a high level of confidence every horizon in the seismic stratigraphic framework to every well in the study area. This difficulty is due to the truncation of reflections near well locations, uncertainties in seismic correlation in areas of salt deformation, and the fact that most intervals become condensed below the modern middle to upper slope. Additionally, some wells do not sample the Neogene and

Paleogene interval. Nevertheless, consistent results among multiple wells increase the level of confidence in the age and lithology results for the framework. The best lithological and biostratigraphic control for the framework is at the Shubenacadie H-100 (Figure 2.6) and Shelburne G-29 wells (Figure 2.7). Both wells are located in the thicker part of the succession in the depocenter, and both wells have new biostratigraphic interpretations (Fensome et al. 2008).

Table 2.1- Explanation of reflection character for seismic stratigraphic framework and correlation to exploration wells in the study. Well intersection depth (measured depth below rotary table), lithology, and biostratigraphic age are provided. SWC refers to sidewall core sample. Synthetic seismograms and logs for each well are shown in Appendix II.

Seismic Horizon	Predominant Nature of Reflection Termination		Typical Reflection Coeffecient	Bonnet P-23	Shelburne G-29	Albatross B-13	Torbrook C-15	Acadia K-62
	Underlying	Overlying						
Seafloor (Top Unit 4)	Erosional truncation along mid to upper slope. Apparent truncation along lower slope and rise.	None.	High positive	133.5 m	1153 m	1341 m	1674 m	866 m
N60 (Top Unit 3)	Concordant. Erosional truncation at localized channels. Onlaps N30 below the middle slope	Downlap along upper slope; concordant elsewhere.	Moderate positive	N/A	1686 m Lith: Fine sandstone in swc at 1644. Age: Piacensian.	1720 m Not sampled	1991 m Not sampled	1434 m Lith: Light grey claystone with minor silt and sand. Cuttings. Age: Late Miocene/Early Pliocene
N50	Erosional truncation in the east, concordant in the west. Onlaps N30 below the middle slope.	Onlap.	High positive	N/A	1834 m Lith: Fine sandstone at 1850-1890 m in cuttings. Age: Zanclean	1786 m Not sampled	2364 m Not sampled	1848 m Lith: Light grey to brown-grey claystone, minor silt. SWC and cuttings. Age: Late Miocene
N40	Concordant; Erosional truncation at localized channels. Onlaps N30 below the middle slope.	Concordant; onlap in channels	High to moderate positive	N/A	2192 m Lith: Fine sandstone in swc at 2195m. Age: Late Miocene	1952 m Lith: Brownish grey claystone. Cuttings. Age: Late Miocene.	3157 m Lith: Brown siltstone with occasional sand grains. Cuttings and SWC at 3129 m. Age: N/A	2261 m Lith: Medium brown siltstone (SWC). Age: Middle Eocene
N30 (Top Unit 2)	Erosional truncation. Offset and hummocky reflections below.	Onlap below the middle slope. Concordant below the lower slope and rise.	Moderate to high positive; High negative in west	526 m. Lith: Within an interval of sandstone. Age: Late Miocene.	2315 m Merged with N20, P40, and P30. Lith: Fine dark sandstone, scattered chert grains. Age: Late Miocene to Bartonian Unc.	2020 m Merged with N20 and P40. Lith: Brown gray claystone with occasional quartz and chert granules. Age: Correlates to Late Mocene to Middle Eocene unconformity.	3341 m Lith: Dark grey claystone. Age: N/A	2297 m. Lith: Claystone, chalky. Cuttings. Age: Middle Eocene.
N20	Concordant; local erosional truncation forming channels. Offset and hummocky reflections below.	Onlap.	Low to moderate positive	526 m Lith: Very fine grained sandstone. Age: Late Miocene.	2315 m Merged with N30, P40, and P30. Lith: Fine dark sandstone, scattered chert grains. Age: Late Miocene to Bartonian Unc.	2020 m Merged with N30 and P40. Lith: Brown gray claystone with occasional quartz and chert granules. Age: Correlates to Late Mocene to Middle Eocene unconformity.	3402 m Lith: Dark grey claystone. Age: N/A	2326 m. Lith: Chalky claystone or marlstone. Cuttings and SWC. Age: Middle Eocene.

Seismic Horizon	Predominant Nature of Reflection Termination		Typical Reflection Coeffecient	Bonnet P-23	Shelburne G-29	Albatross B-13	Torbrook C-15	Acadia K-62
	Underlying	**Overlying**						
P40 (Top Unit 1)	Concordant in interfluves; erosional truncation on ridge crests and below the lower slope and rise.	Onlap.	Low to moderate positive	1680 m Lith: Shale with dolomite fragments. Age: Early Oligocene	2315 m Merged with N30, N20, and P30. Lith: Fine dark sandstone, scattered chert grains. Age: Late Miocene to Bartonian Unc.	2025 m Merged with N30 and N20. Lith: Brown gray claystone with occasional quartz and chert granules. Age: Correlates to Late Miocene to Middle Eocene unconformity.	Below well penetration	2353 m. Lith: Chalky claystone or marlstone. Cuttings and SWC. Age: Early Eocene
P30	Erosional truncation.	Drape.	Low positive	N/A	2315 m Merged with N30, N20, and P40. Lith: Fine dark sandstone, scattered chert grains. Age: Late Miocene to Bartonian Unc.	2121 m Lith: Light grey to brownish grey claystone. Age: Middle Eocene	Below well penetration	2386 m. Lith: Light green to medium brown marlstone. SWC. Age: Early Eocene.
P20	Erosional truncation (apparent truncation)	Concordant to erosional truncation.	High positive	N/A	2440 m Lith: Claystone, trace chalky in cuttings. Age: Lutetian.	2327 m Lith: Cream to light grey limestone. Age: Early Eocene.	Below well penetration	2471 m. Lith: Calcareous mudstone. Age: Late Paleocene
C100 (Base of Unit 1)	Erosional truncation (apparent truncation)	Concordant to erosional truncation.	Moderate to high positive	N/A	3099 m Lith: Light grey marlstone. SWC. Age: Campanian. Near base of Wyandot.	2414 m Lith: Light grey Limestone. Age: Maastrichtian	Below well penetration	2620 m. Lith: Argillaceous Limestone. SWC. Near base of Wyandot Fm. Age: Maastrichtian.
		References	**lithology**	Steeves 1984	Steeves 1985b	Steeves 1985a	EnCana 2003	Lewis and Pandachuck 1978
			Biostrat-igraphy	Bujak Davies Group 1988a	Fensome et al. 2008	Bujak Davies Group 1988b	N/A	Thomas 2001
			Notes on well	Difficult to correlate Paleogene interval across carbonate bank edge. Thick Miocene interval.	Good age control. Difficult to correlate P20 and C100 to well location.	Position at carbonate bank edge makes it difficult to correlate Upper Cretaceous and Paleogene succession.	No biostratigraphy.	Position at carbonate bank edge makes it difficult to correlate Upper Cretaceous and Paleogene succession. Foraminifera biostratigraphy differs from palynology results from other wells.

Seismic Horizon	Predominant Nature of Reflection Termination		Typical Reflection Coeffecient	Shubenacadie H-100	Newburn H-23	Weymouth A-45	Balvenie B-79	Annapolis G-24
	Underlying	Overlying						
Seafloor (Top Unit 4)	Erosional truncation along mid to upper slope. Apparent truncation along lower slope and rise.	None.	High positive	1476 m	977 m	1690 m	1803 m	1678 m
N60 (Top Unit 3)	Concordant. Erosional truncation at localized channels. Onlaps N30 below the middle slope	Downlap along upper slope; concordant elsewhere.	Moderate positive	1966 m Not sampled	1635 m	N/A	2370 m Not Sampled	N/A
N50	Erosional truncation in the east, concordant in the west. Onlaps N30 below the middle slope.	Onlap.	High positive	2125 m Not sampled	N/A	N/A	N/A	N/A
N40	Concordant; Erosional truncation at localized channels. Onlaps N30 below the middle slope.	Concordant; onlap in channels	High to moderate positive	2657 m Lith: 30 m thick v. fine sand. SWC. Age: Messinian	N/A	N/A	N/A	N/A
N30 (Top Unit 2)	Erosional truncation. Offset and hummocky reflections below.	Onlap below the middle slope. Concordant below the lower slope and rise.	Moderate to high positive; High negative in west	2742 m Lith: Within interval of brown-grey silty mud. SWC. Age: Tortonian	1890 m Lith: First sample at 1944 m (SWC) greenish grey claystone. Age: Mid-Late Miocene	N/A	2970 m Lith: In interval of light grey to greenish grey claystone. Cuttings. Age: Messinian	N/A
N20	Concordant; local erosional truncation forming channels. Offset and hummocky reflections below.	Onlap.	Low to moderate positive	2889 m Lith: Within interval of brown-grey silty mud. SWC Age: Between Serravallian and Tortonian picks	N/A	N/A	N/A	N/A

Seismic Horizon	Predominant Nature of Reflection Termination		Typical Reflection Coeffecient	Shubenacadie H-100	Newburn H-23	Weymouth A-45	Balvenie B-79	Annapolis G-24
	Underlying	Overlying						
P40 (Top Unit 1)	Concordant in interfluves; erosional truncation on ridge crests and below the lower slope and rise.	Onlap.	Low to moderate positive	3068 m Merged with P30. Lith: Light grey mudstone. SWC. Age: Correlates to Serravallian-Langhian to Bartonian-Priabonian unconformity.	2519 m Lith: Brown-grey firm claystone. (SWC at 2497m) Age: At Late Eocene/Early Miocene unconformity.	2740 m Lith: Dark grey Claystone	3099 m Lith: In interval of medium grey claystone. Cuttings. Age: Priabonian	2678 m Lith: Brown grey claystone Age: Rupelian
P30	Erosional truncation.	Drape.	Low positive	3083 m Merged with P40. Lith: Light grey mudstone. SWC Age: Correlates to Serravallian-Langhian to Bartonian-Priabonian unconformity.	N/A	N/A	3220 m Lith: Near transition between dark grey and light grey (more calcareous) claystone. Age: Priabonian-Lutetian boundary.	3062 m Lith: Increasingly calcareous claystone Age: Priabonian
P20	Erosional truncation (apparent truncation)	Concordant to erosional truncation.	High positive	3333 m Lith: Chalk. SWC. Age: Lutetian	N/A	N/A	3445 m Lith: Limestone Age: Ypresian.	3279 m Lith: Marlstone Age: Lutetian
C100 (Base of Unit 1)	Erosional truncation (apparent truncation)	Concordant to erosional truncation.	Moderate to high positive	3777 m Lith: Chalk. SWC Near base of Wyandot Fm. Age. Maastrictian.	2820 m Lith: Light grey-green marlstone (SWC at 2815 m) Age: Early Maastrichtian/Late Campanian.	2850 m Lith: Brecciated claystone and marlstone.	3603 m Lith: Interval of interbedded claystone, marlstone, and minor sandstone. Age: Late Maastrichtian	3399 m Lith: Marlstone and limestone Age: Selandian
		References	**lithology**	Shell Canada Resources Ltd. 1983	Chevron et al. 2002	EnCana 2003	Imperial Oil Resources Ventures Limited 2003	Archibald 2003
			Biostrat-igraphy	Fensome et al. 2008	Crux and Shaw 2002	N/A	Robertson Research 2004	Robertson Research 2004
			Notes on well	Good age control. Oligocene to Middle Miocene interval absent.	Difficult to correlate several horizons to this well.	Position in area highly deformed by salt makes it difficult to correlate to this well. No biostratigraphy for studied interval.	Position at edge of large late Paleogene canyon makes it difficult to correlate P40.	Good age and lithological control for the Paleogene succession.

Table 2.2 Description and examples of seismic facies for seismic stratigraphic units.

Seismic Stratigraphic Units	Seismic facies	Example	Interval Description
Unit 4- N60 to Seafloor	Chaotic, medium to high amplitude, lenticular (depression-filling)		N60- Seafloor: Gravity flow predominance and widespread canyons.
	Sub-parallel to concordant, medium to high amplitude	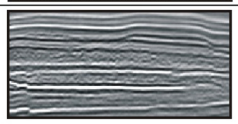	
Unit 3- N30 to N60	Wavy, medium to low amplitude	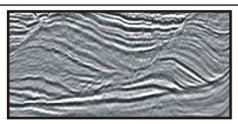	N40-N60: Regional sediment drift development. Giant sediment wave growth in the SW. Megaslumps appear to be most common in this interval. N30-N40: Local sediment drift development, mass transport deposits, and channels.
	Divergent to concordant, medium to low amplitude	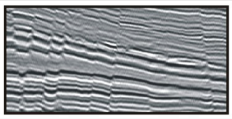	
Unit 2- P40 to N30	Offset, concordant, medium to high amplitude		N30 often erodes down to N20 or deeper along the middle slope. Local sediment drift development. P40-N20: Interval not represented in most deepwater wells from the margin, but in most cases thickens significantly away from wells. Delta progradation on the shelf and depocenter development on the slope in the central study area. Channel development in many areas. Highly faulted in the west where not associated with down-slope processes.
	Divergent to chaotic, medium to high amplitude	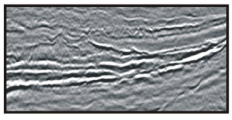	
Unit 1- C100 to P40	Drape, concordant, low amplitude, or reflection free	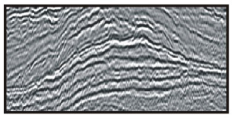	P30-P40: Distinct, acoustically transparent interval that drapes the top of the Eocene gullied surface. Where sampled, contains less chalk and limestone than underlying strata. C100-P30: Complicated interval containing multiple unconformities. In places P30 erodes down to C100 or deeper. Top of interval appears as distinct gullied or canyon surface where mapped. Where sampled, the interval consists of chalks and marls with lesser mudstones.
	Mounded with sub-parallel and truncated internal reflections, medium to high amplitude	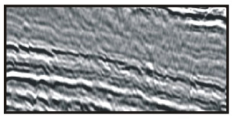	

2.4.2 Seismic Stratigraphy

Four depositional units representing significant changes in acoustic facies and reflection configuration are evident from regional mapping results. (Figure 2.3, Table 2.1, Table 2.2).

Unit 1- Horizons C100- P40 (Upper Cretaceous to Lower Oligocene)

Unit 1 is bound by C100 at its base and P40 at its top and includes P20 and P30. Unit 1 is more reflective than underlying and overlying intervals (Figures 2.6-2.8). The interval locally exceeds 600 m thickness in the study area (Figure 2.9a), but generally accounts for less than 20% of the total residual thickness of the Upper Cretaceous and Cenozoic succession. In general, Unit 1 exhibits a mounded geometry on strike oriented profiles and becomes less reflective towards its top. This mounded appearance is most apparent seaward of the Jurassic carbonate platform and the edge of the underlying margin hinge zone. This external seismic geometry is imposed at least in part by erosion revealed as multiple internal unconformities described in more detail below (Figure 2.8). The interval locally appears thick within areas of abundant salt diapirs, although seismic correlation within the diapir province is tenuous.

Horizon C100 is a strong positive reflection that marks the base of Unit 1. In the Shubenacadie H-100 and Shelburne G-29 wells, C100 correlates with a strong reflection within an interval of chalk and limestone assigned to the distal Wyandot Fm equivalent (Table 2.1). In some locations, for example in the vicinity of the Shubenacadie H-100 well, the presence of strong reflection couplets causes uncertainty about how to correlate the C100 marker (Figure 2.6). These prominent reflection couplets probably indicate

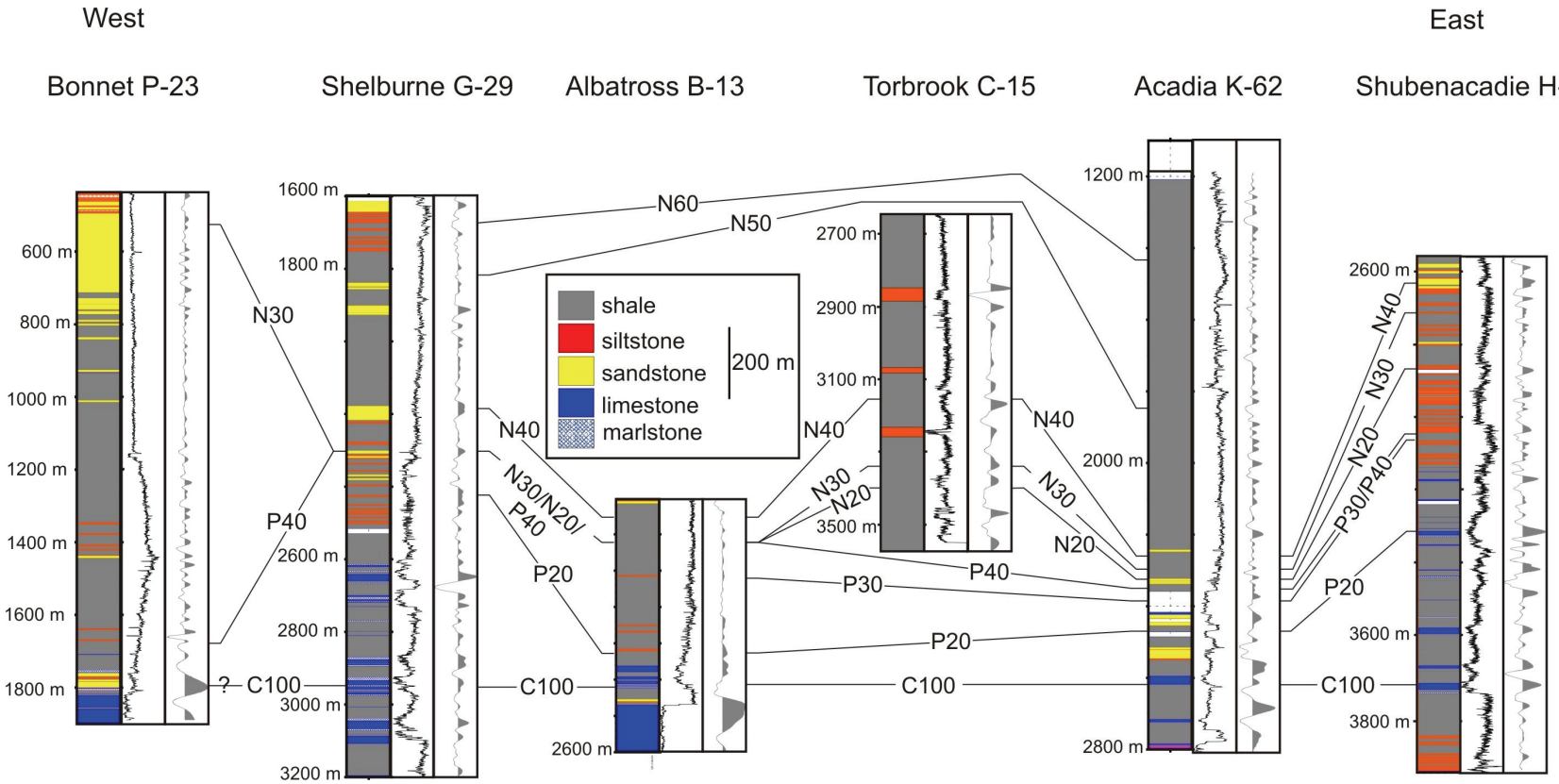

Figure 2.5 Cross-section through wells in the study area showing lithology, gamma ray log, synthetic seismogram, and intersection of the seismic stratigraphic framework. See Table 2.1, Table 2.3 for precise intersection depths, biostratigraphic, and lihologic information and references. Datum is the C100 reflection. Well locations shown in Figure 2.1c. Synthetic seismograms and logs for each well are shown in Appendix II.

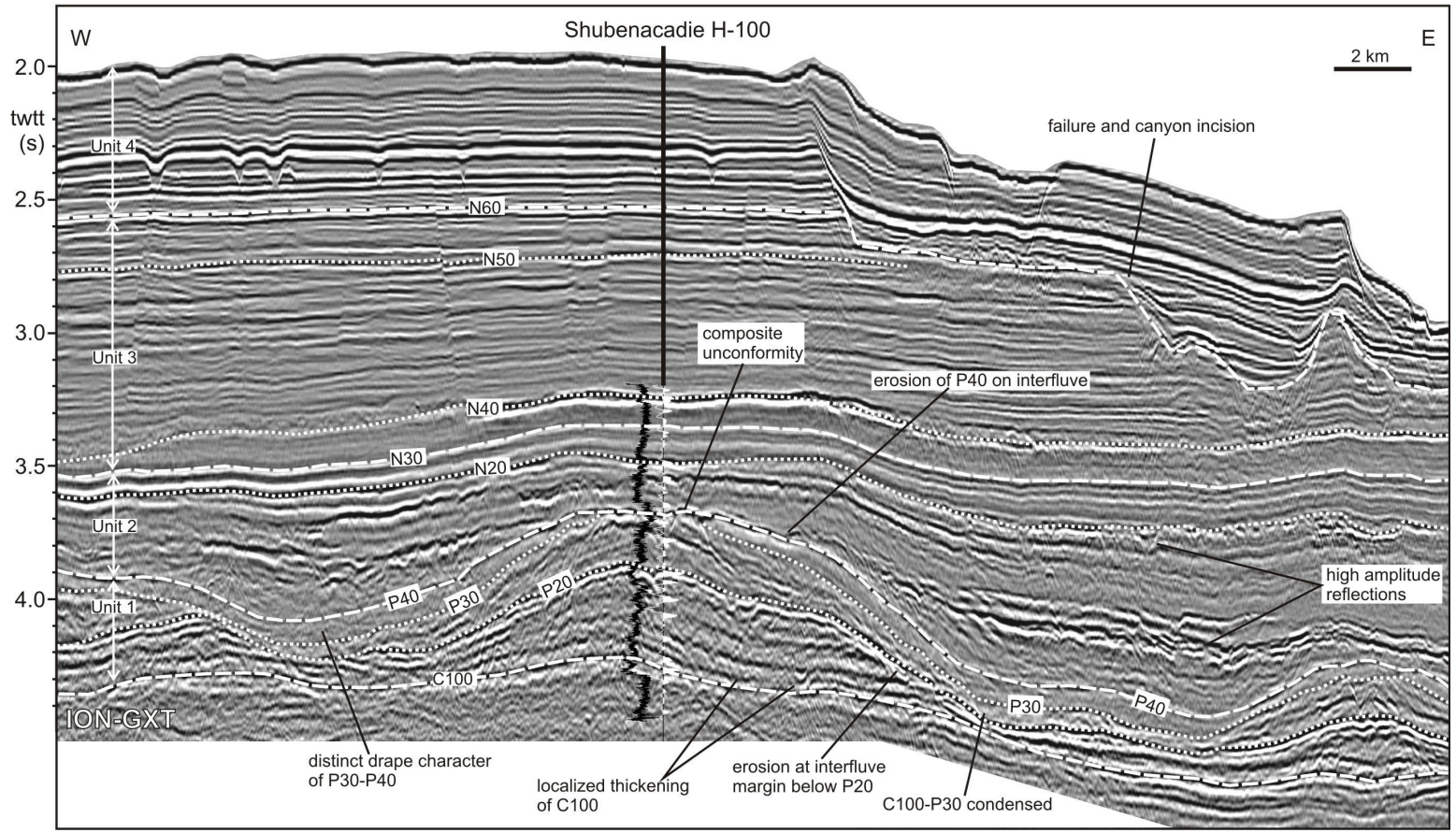

Figure 2.6- Seismic reflection profile through the Shubenacadie H-100 well showing seismic stratigraphic framework and seismic reflection character. The gamma ray log and synthetic seismogram are also shown for reference to Figure 2.5. Figure location is shown in Figure 2.1c. Data are courtesy of ION-GXT.

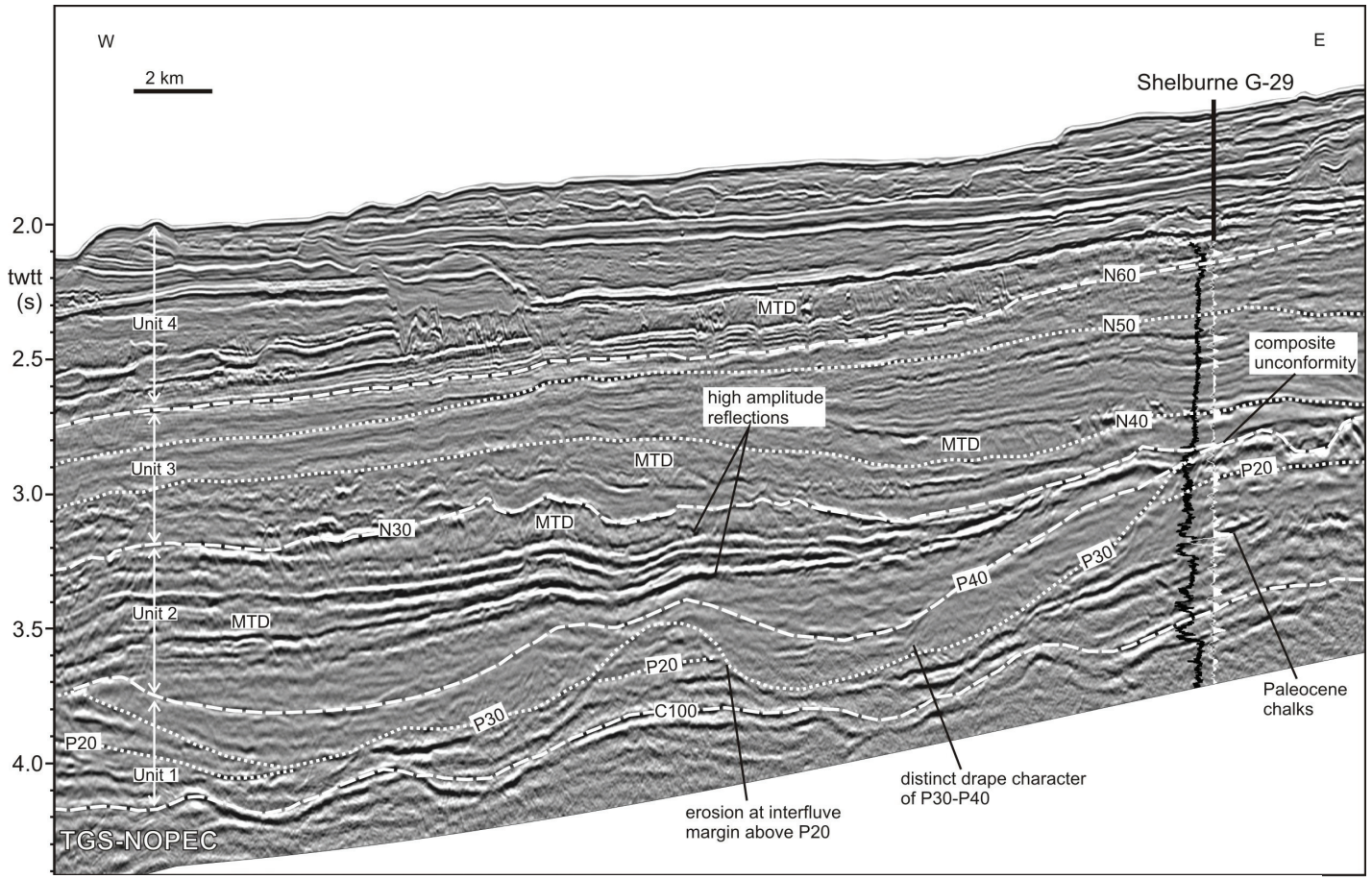

Figure 2.7 Seismic reflection profile through the Shelburne G-29 well showing seismic stratigraphic framework and seismic reflection character. The gamma ray log and synthetic seismogram are also shown for reference to Figure 2.5. Figure location is shown in Figure 2.1c. Data are courtesy of TGS-NOPEC Geophysical Company L.P.

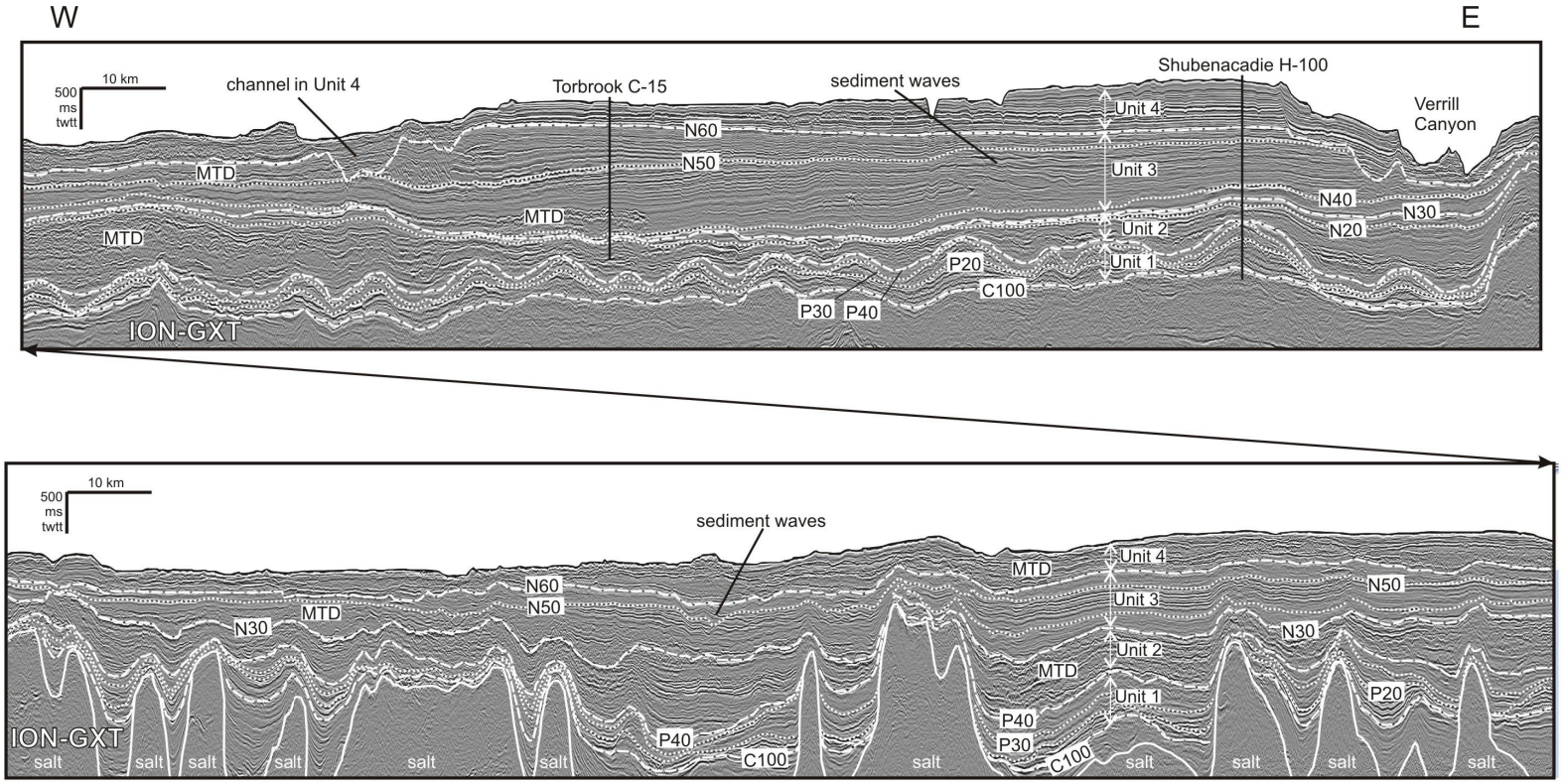

Figure 2.8 Regional, strike-oriented seismic reflection profile through the study area. Figure location is shown in Figure 2.1c. Data are courtesy of ION-GXT.

localized thickness variations within the highly reflective succession of chalks and marlstones (Table 2.1, Figure 2.5). Where these couplets exists, the most continuous strong reflection of the series was mapped, which in most cases is the lowermost reflection. In fact the C100 reflection is likely diachronous since the age of the distal Wyandot Fm equivalent in some wells spans only the Maastrichtian (e.g. at Shubenacadie H-100) while at other wells it spans the Campanian and Maastrichtian (e.g. at Shelburne G-29) (Fensome et al. 2008).

The structure map of C100 (Figure 2.10a) shows a gently dipping and undulating lower slope seaward of the carbonate bank. The morphological character of salt diapir sub-provinces I and II of Shimeld (2004) and the seaward limit of shallow salt structures are apparent. Seismic correlation of C100 is problematic below the upper slope and outer shelf. There are relatively few locations where seismic continuity allows the direct correlation of C100 from the slope onto the shelf. On most seismic reflection profiles that cross the buried paleo-slope, C100 is truncated by regional escarpments and failure or décollement surfaces. Therefore, the apparent steepness of the upper slope on the C100 structure map does not represent the bathymetric character at time of deposition, but rather represents subsequent erosion of the C100 surface later in the Paleogene. For example, near the Bonnet P-23 well a prominent erosional surface, interpreted to represent an escarpment up to 300 m high, is buried just landward of the well (Figure 2.11). Biostratigraphic data at the well suggest that Middle Eocene sediments directly overlie Aptian to Cenomanian sediments, with much of the Upper Cretaceous and Paleocene section missing (Bujak Davies Group 1988a). In such areas, C100 was mapped as a continuous surface from the slope, across the scarp face, and correlated onto the shelf with a prominent reflection that probably represents the Wyandot Fm or the stratigraphic level of erosion of the Wyandot Fm. Below the upper slope near the Acadia K-62 well, the interval above C100 is deformed, with discrete tilted blocks apparent in dip-oriented seismic reflection profiles (Figure 2.12). Here, C100 was mapped as an erosional surface interpreted to represent a décollement surface at the base of the deformed interval. In the area of the Montagnais structure (Figure 2.1c), C100 was mapped as a prominent erosional surface and underlies the zone of chaotic seismic facies interpreted to represent

the impact breccia (Figure 2.13). Due to poor seismic imaging beneath this chaotic zone, C100 was not mappable below much of the impact breccia (Figure 2.10a).

The next youngest horizon above C100 is P20. P20 is a prominent positive-amplitude reflection found within a highly-reflective interval of converging and diverging reflections between C100 and P30, giving the interval an overall mounded appearance (Figures 2.6-2.8). In most wells, the age of P20 is Ypresian to Lutetian and the lithology is chalk, limestone, or calcareous mudstone (Table 2.1). The structure map of P20 shows that the mounds are elongate in the downslope direction and are interpreted to be erosional gullies with intervening ridges (Figure 2.10b). They are most prominent just seaward of the buried carbonate bank edge. Similar to C100, P20 exhibits localized thickness variations which are especially apparent in interfluves

Figure 2.9 Isochore and percent residual thickness maps of seismic stratigraphic units 1-4. A) Unit 1 deposits are preserved in the interfluves between pervasive erosional gullies, and seaward of shallow salt structures in the southwest. In general, Unit 1 represents less than 20% of the total preserved Upper Cretaceous to Present succession. B) Unit 2 deposits are preserved immediately seaward of the Abenaki carbonate bank and margin hinge zone in the western part of the study area where they represent more than 60% of the total preserved succession. A broad zone of erosion and non-deposition is apparent below the middle slope between the Shelburne G-29 and Shubenacadie H-100 wells. Unit 2 deposits thicken seaward from this zone of non-deposition. C) Unit 3 deposits are preserved in a wedge, elongate along-slope. Unit 3 is thicker in the east where it is more than 1400 m thick and represents more than 60% of the total preserved succession. D) Unit 4 deposits are focused along the upper slope. Dashed polygons represent 3D survey areas. The maps are based on seismic data courtesy of TGS-NOPEC Geophysical Company L.P.

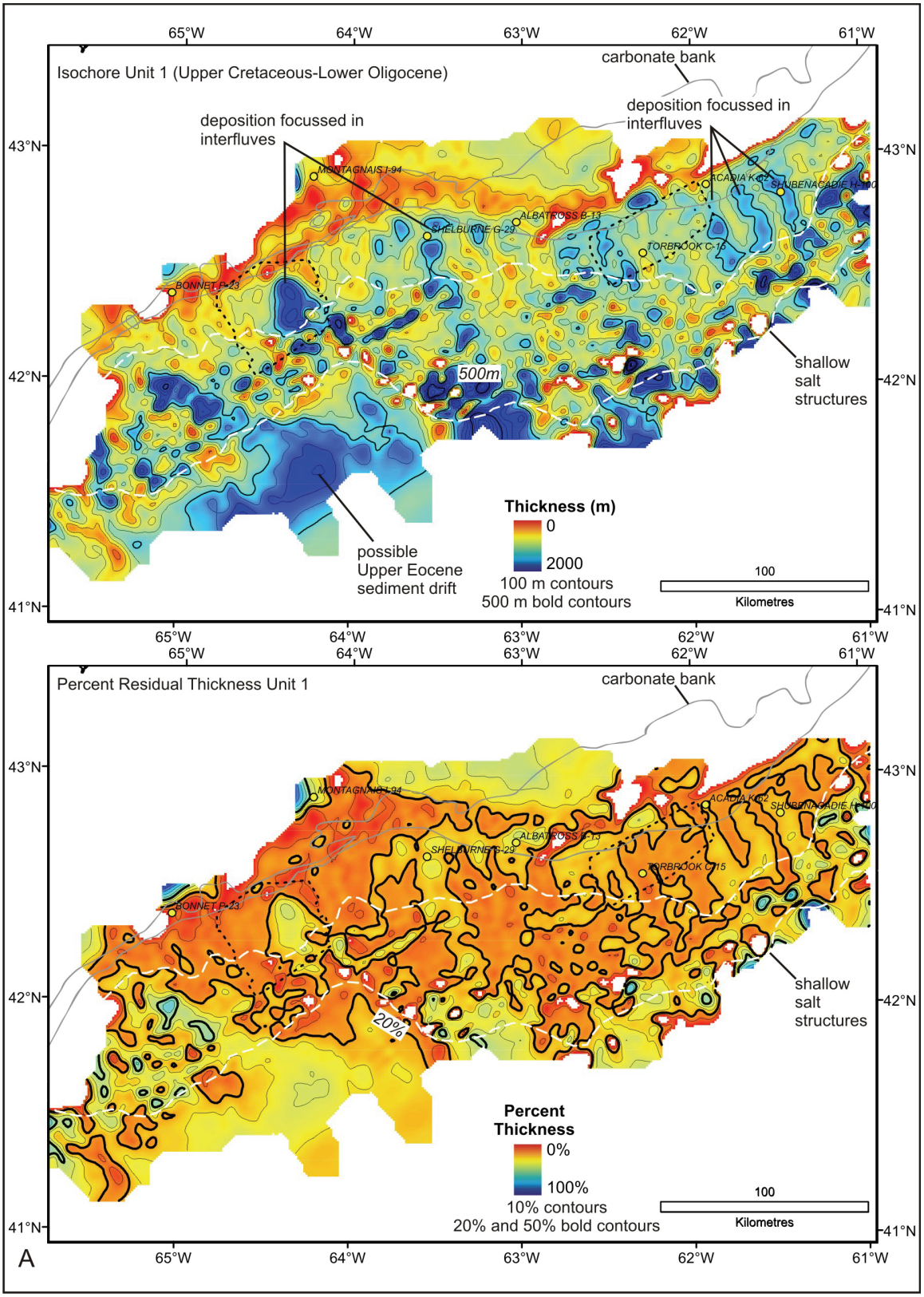
Isochore Unit 1 (Upper Cretaceous-Lower Oligocene)
carbonate bank
deposition focussed in interfluves
deposition focussed in interfluves
MONTAGNAIS I-94
SHELBURNE G-29
ALBATROSS B-13
TORBROOK C-15
BONNET P-23
500m
shallow salt structures
possible Upper Eocene sediment drift
Thickness (m)
0
2000
100 m contours
500 m bold contours
100
Kilometres
Percent Residual Thickness Unit 1
carbonate bank
20%
shallow salt structures
Percent Thickness
0%
100%
10% contours
20% and 50% bold contours
100
Kilometres
65°W
64°W
63°W
62°W
61°W
43°N
42°N
41°N
A

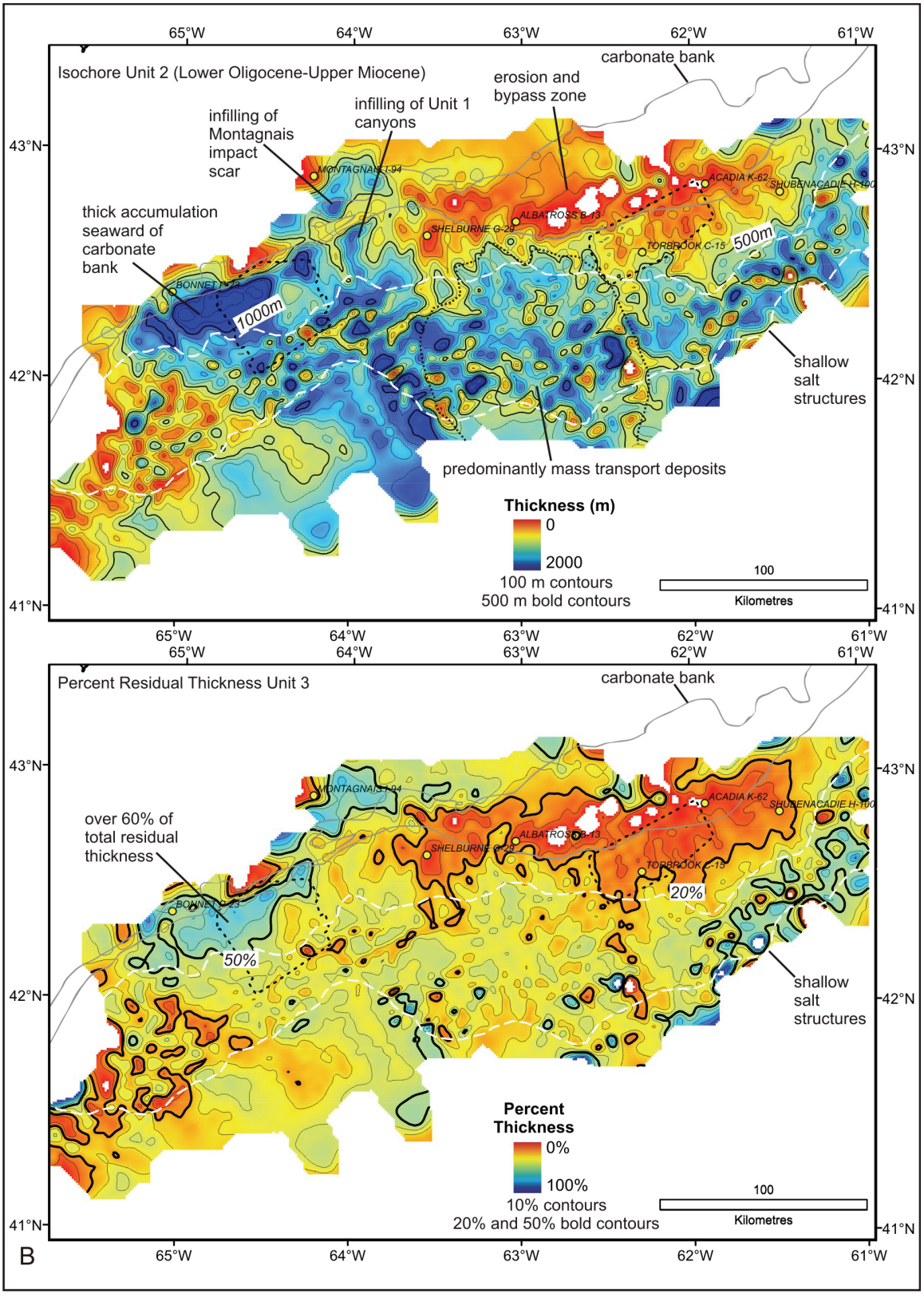
Isochore Unit 2 (Lower Oligocene-Upper Miocene)
carbonate bank
erosion and bypass zone
infilling of Montagnais impact scar
infilling of Unit 1 canyons
thick accumulation seaward of carbonate bank
MONTAGNAIS I-94
ACADIA K-62
SHUBENACADIE H-100
ALBATROSS B-13
SHELBURNE G-29
TORBROOK C-15
BONNET P-23
500m
1000m
shallow salt structures
predominantly mass transport deposits
Thickness (m)
0
2000
100 m contours
500 m bold contours
100
Kilometres
65°W
64°W
63°W
62°W
61°W
43°N
42°N
41°N
Percent Residual Thickness Unit 3
carbonate bank
over 60% of total residual thickness
MONTAGNAIS I-94
ACADIA K-62
SHUBENACADIE H-100
ALBATROSS B-13
SHELBURNE G-29
TORBROOK C-15
BONNET P-23
20%
50%
shallow salt structures
Percent Thickness
0%
100%
10% contours
20% and 50% bold contours
100
Kilometres
B

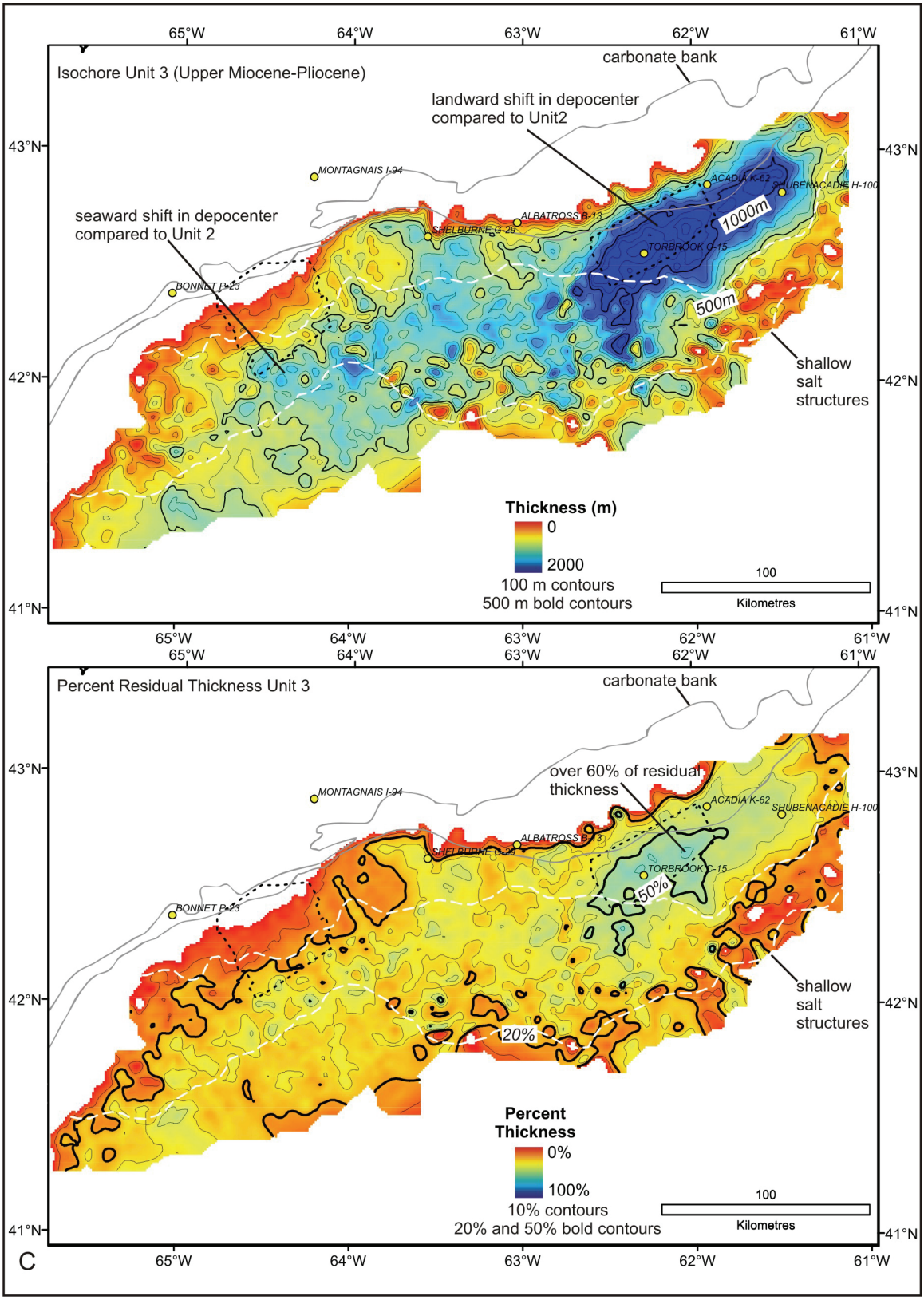
Isochore Unit 3 (Upper Miocene-Pliocene)
carbonate bank
landward shift in depocenter compared to Unit2
seaward shift in depocenter compared to Unit 2
MONTAGNAIS I-94
ACADIA K-62
SHUBENACADIE H-100
ALBATROSS B-13
SHELBURNE G-29
TORBROOK C-15
BONNET P-23
1000m
500m
shallow salt structures
Thickness (m)
0
2000
100 m contours
500 m bold contours
100
Kilometres
65°W
64°W
63°W
62°W
61°W
43°N
42°N
41°N
Percent Residual Thickness Unit 3
carbonate bank
over 60% of residual thickness
50%
20%
shallow salt structures
Percent Thickness
0%
100%
10% contours
20% and 50% bold contours
C

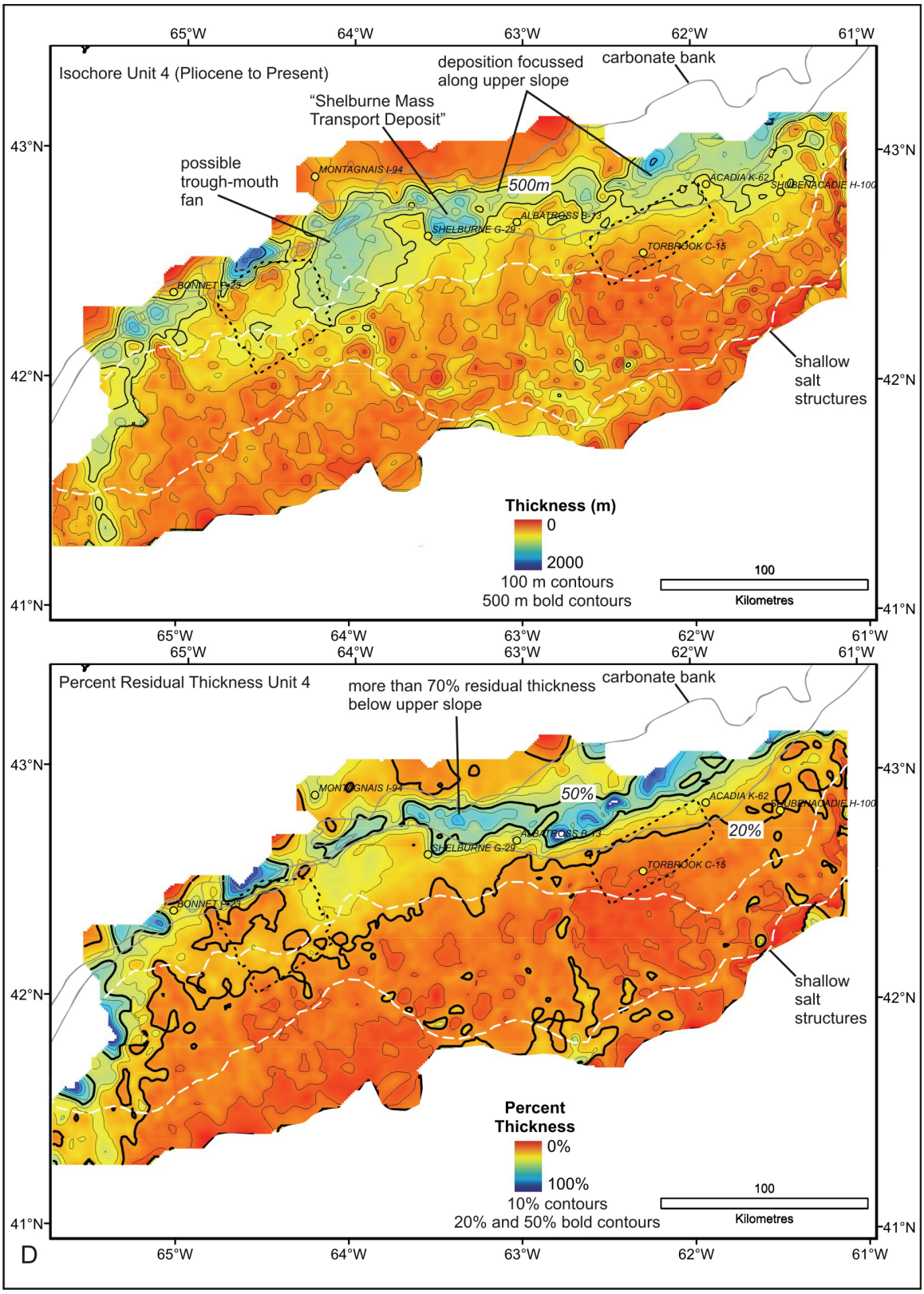
Isochore Unit 4 (Pliocene to Present)
deposition focussed along upper slope
carbonate bank
"Shelburne Mass Transport Deposit"
possible trough-mouth fan
MONTAGNAIS I-94
500m
ACADIA K-62
SHUBENACADIE H-100
ALBATROSS B-13
SHELBURNE G-29
TORBROOK C-15
BONNET P-23
shallow salt structures
Thickness (m)
0
2000
100 m contours
500 m bold contours
100
Kilometres
65°W
64°W
63°W
62°W
61°W
43°N
42°N
41°N
Percent Residual Thickness Unit 4
more than 70% residual thickness below upper slope
50%
20%
Percent Thickness
0%
100%
10% contours
20% and 50% bold contours
D

between gullies, while in some gullies the entire C100-P30 interval condenses to one or two reflections (Figure 2.6). Therefore, systematic correlation of P20 across interfluves is difficult in the area of prominent gullies between the margin hinge zone and the zone of shallow salt structures (Figure 2.10b). At the margins of interfluves, reflections immediately underlying P20 appear truncated (Figure 2.6), and it is interpreted that the chalk or limestone interval that causes the P20 reflection drapes a prominent erosional surface. It is possible that in some areas, the reflection mapped as P20 actually corresponds to Upper Paleocene or Ypresian chalks, for example those sampled by the Shelburne G-29 well (Figure 2.5, 2.7) (Fensome et al. 2008). Along the steep carbonate bank seaward of the Montagnais impact site and further west, P20 and C100 were mapped as the same reflection because the interval is condensed in this area (Figure 2.11). In the area of the Montagnais impact, P20 is tentatively mapped as the failure escarpment and as the top of the Montagnais impact breccia because the breccia appears to be overlain by P30 (discussed below). This interpretation is supported by K/Ar and $^{39}Ar/^{40}Ar$ dating results of 51 Ma for the basal melt rock formed through the impact (Jansa et al. 1989) which is within the range of the Lower Eocene age assigned to P20 (Table 2.1).

Above P20, P30 is a moderate to weak positive amplitude reflection that truncates underlying reflections and marks the top of the high amplitude mounded interval above C100 (Figures 2.6-2.8). At most wells in the study area, P30 merges with other unconformities to form a composite, Middle or Late Eocene to Middle or Late Miocene unconformity (Figures 2.5-2.7). The best age and lithological control for P30 is found east of the study area at the Annapolis G-24 well where it correlates to an erosional surface in Priabonian sediments that separates more calcareous claystone below from less calcareous claystone above (Figure 2.14) (Archibald 2003; Robertson Research International Ltd 2004). In many cases, P30 mimics the morphology of P20, and converges towards P20 along the axes of gullies originally eroded below the P20 marker. Therefore, P30 is interpreted to represent a predominantly erosional surface, formed in the Priabonian, and marks the final period of canyon and gully formation before these features were largely filled on the continental slope.

Figure 2.10- Structure maps for selected horizons in the seismic stratigraphic framework. A) Horizon C100 shows the structure of shallow buried salt structures and an escarpment/decollement along the upper slope. B) The structure of P20 is dominated by pervasive gullies between the carbonate bank edge and shallow salt structures. The insets show the detailed structure of the gullied relief from 3D seismic data. In the area of the Montagnais bolide impact, a circular failure escarpment and central uplift in the crater are apparent. C) The structure of P40 appears similar to P20 because the reflection drapes the underlying gullied relief. Seaward of salt structures in the southwest, there is evidence for along-slope erosion by bottom currents. D) The structure of N30 shows the development of a broad terrace in the east formed by bottom current erosion, and the development of a steep ramp in the west formed by mass wasting. The gullied relief of the underlying succession is no longer apparent. E) The structure of N60 reveals a large, southwest-trending ridge in the east, and a broad terrace formed by the build up of giant sediment waves in the west. A channel in the overlying Unit 4 is deflected westward by the ridge. F) The structure of the seafloor shows a relatively steep upper slope in the west and Verrill Canyon in the east. Maps are based on seismic data courtesy of TGS-NOPEC Geophysical Company L.P.

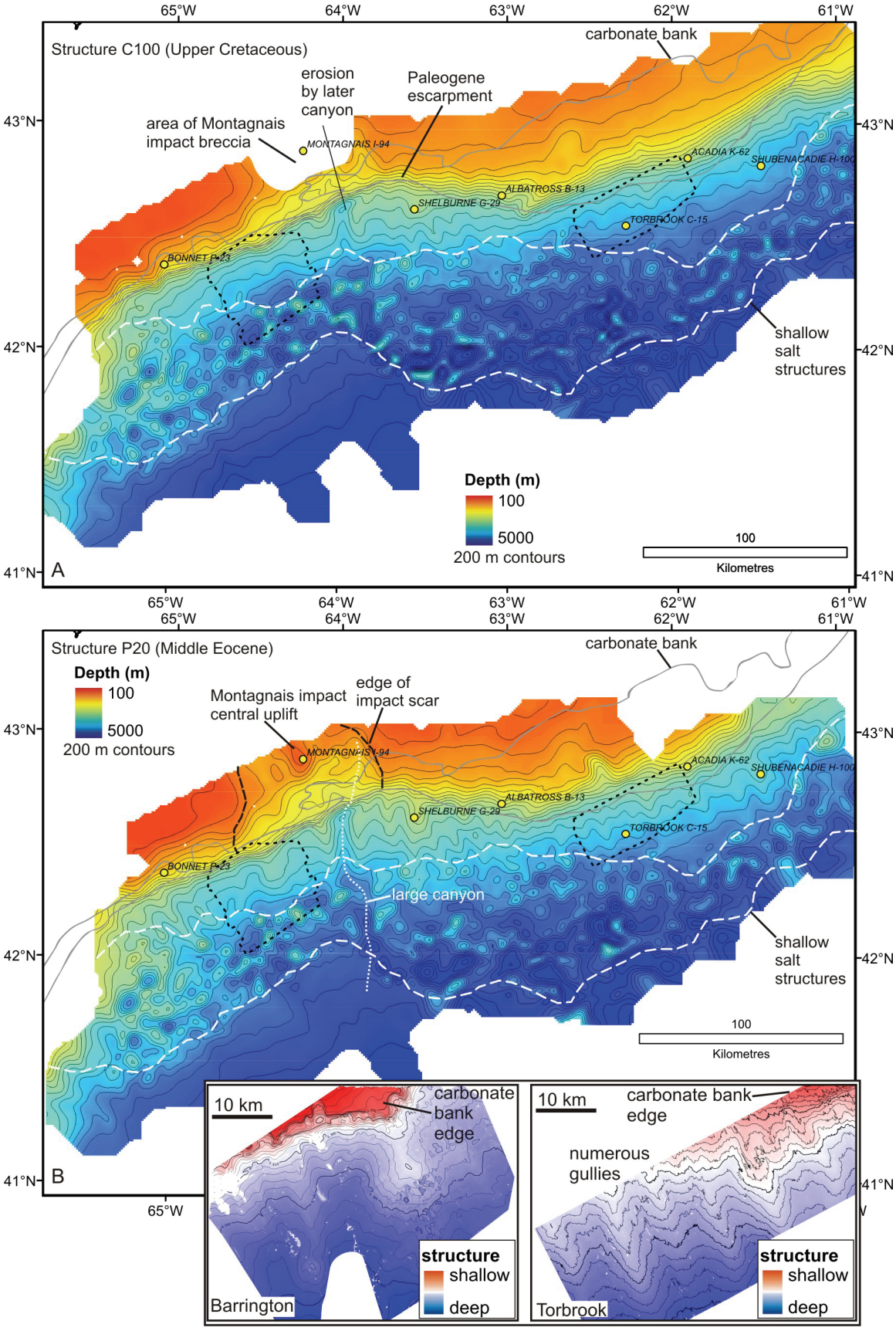
65°W
64°W
63°W
62°W
61°W
Structure C100 (Upper Cretaceous)
carbonate bank
erosion by later canyon
Paleogene escarpment
area of Montagnais impact breccia
MONTAGNAIS I-94
ACADIA K-62
SHUBENACADIE H-100
ALBATROSS B-13
SHELBURNE G-29
TORBROOK C-15
BONNET P-23
shallow salt structures
43°N
42°N
41°N
Depth (m)
100
5000
200 m contours
100
Kilometres
A
Structure P20 (Middle Eocene)
Depth (m)
100
5000
200 m contours
carbonate bank
Montagnais impact central uplift
edge of impact scar
large canyon
shallow salt structures
B
10 km
carbonate bank edge
structure
shallow
deep
Barrington
numerous gullies
Torbrook

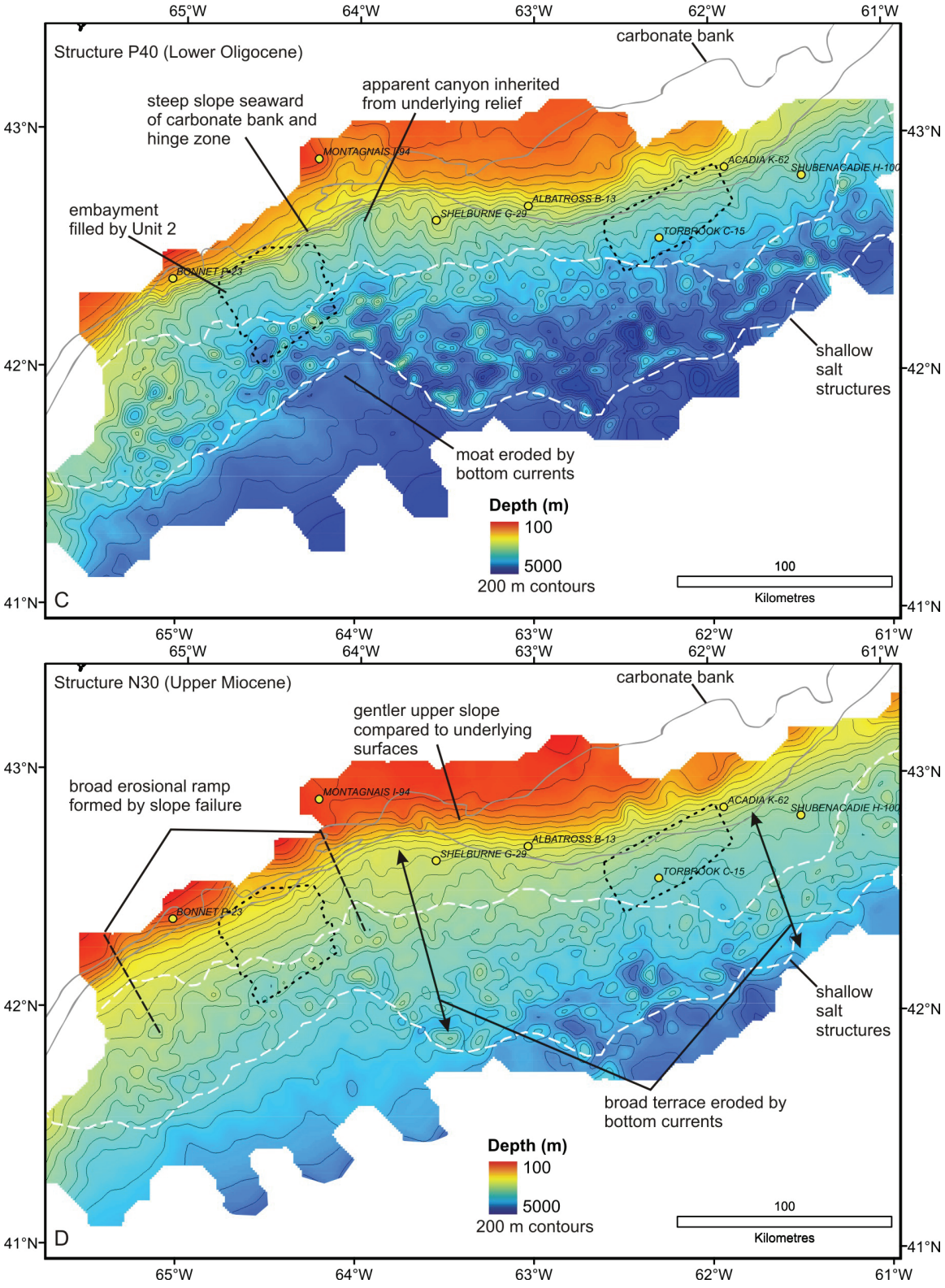
65°W
64°W
63°W
62°W
61°W
Structure P40 (Lower Oligocene)
carbonate bank
apparent canyon inherited from underlying relief
steep slope seaward of carbonate bank and hinge zone
embayment filled by Unit 2
MONTAGNAIS I-94
ACADIA K-62
SHUBENACADIE H-100
ALBATROSS B-13
SHELBURNE G-29
TORBROOK C-15
BONNET P-23
shallow salt structures
moat eroded by bottom currents
Depth (m)
100
5000
200 m contours
100
Kilometres
C
43°N
42°N
41°N
Structure N30 (Upper Miocene)
carbonate bank
gentler upper slope compared to underlying surfaces
broad erosional ramp formed by slope failure
shallow salt structures
broad terrace eroded by bottom currents
D

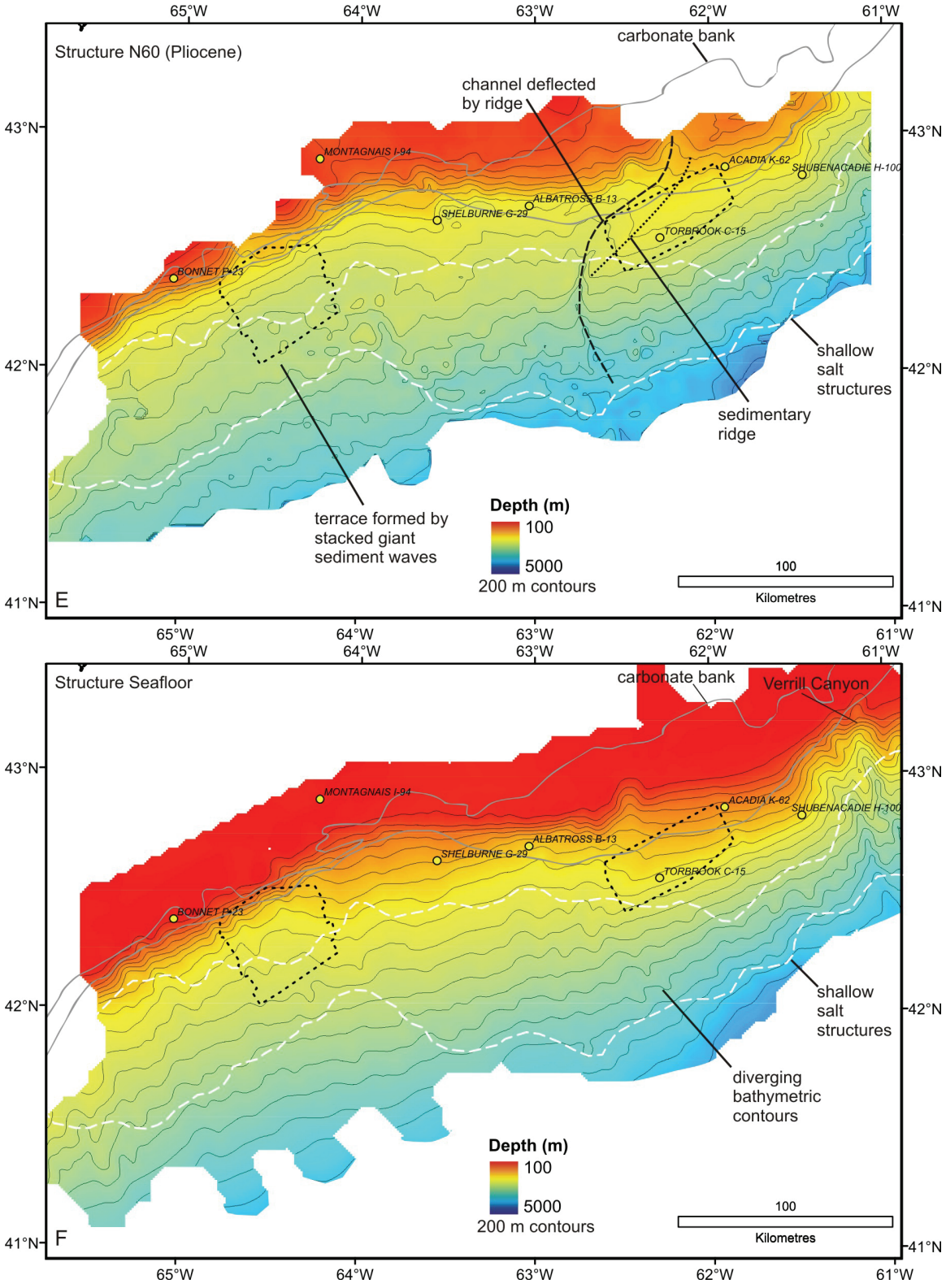
Structure N60 (Pliocene)
carbonate bank
channel deflected by ridge
MONTAGNAIS I-94
ACADIA K-62
SHUBENACADIE H-100
ALBATROSS B-13
SHELBURNE G-29
TORBROOK C-15
BONNET P-23
shallow salt structures
sedimentary ridge
terrace formed by stacked giant sediment waves
Depth (m)
100
5000
200 m contours
100
Kilometres
E
Structure Seafloor
carbonate bank
Verrill Canyon
shallow salt structures
diverging bathymetric contours
F
65°W
64°W
63°W
62°W
61°W
43°N
42°N
41°N

P40 overlies P30 and marks the top of Unit 1 and the base of Unit 2. P30 to P40 is a distinct, acoustically transparent interval that drapes or mimics horizon P30, the last erosion surface that gives the gullied appearance to Unit 1. The interval marks a change in acoustic facies compared to the more reflective C100 to P30 interval below, and its thickness varies little within gullies; however, in many cases the interval is completely eroded on the crests of interfluves (Figures 2.6-2.8). Data from wells suggests the interval consists of Priabonian mudstone (Table 2.1, Table 2.2). The top of the acoustically transparent interval is defined by P40 which marks an upward change in reflection configuration to higher amplitude, onlapping or divergent and highly faulted reflections (Figure 2.8). Seaward of salt structures in the southwest part of the study area, the P30-P40 interval is thick and shows faint, wavy internal reflectivity (Figures 2.15-2.16). This increased thickness is apparent on the isochore map for Unit 1 (Figure 2.9a), and possibly represents an Upper Eocene sediment drift.

Unit 2- Horizons P40- N30 (Lower Oligocene to Upper Miocene)

The dominant acoustic facies of Unit 2 is hummocky and offset reflections that appear due to the presence of pervasive, high density, small offset faults, similar to those described as polygonal faults by Cartwright and Dewhurst (1998). The faults are most apparent where they cut parallel and concordant reflections, for example seaward of the Shubenacadie H-100 well (Figure 2.17). Unit 2 is bound by reflections P40 at its base and N30 at its top and includes N20. The interval locally exceeds 800 m thickness in the vicinity of the Barrington 3D survey area (Figure 2.9b). Unit 2 represents more than 20% of the total residual thickness of the Upper Cretaceous and Cenozoic succession over most of the study area, and more than 50% of the residual thickness seaward of the Montagnais I-94 and Bonnet P-23 wells. At the base of Unit 2, P40 separates acoustically transparent reflections below (at the top of Unit 1) from higher amplitude, onlapping and divergent, faulted reflections above. Below much of the middle and upper slope, P40 merges with underlying and overlying unconformities, forming part of a composite

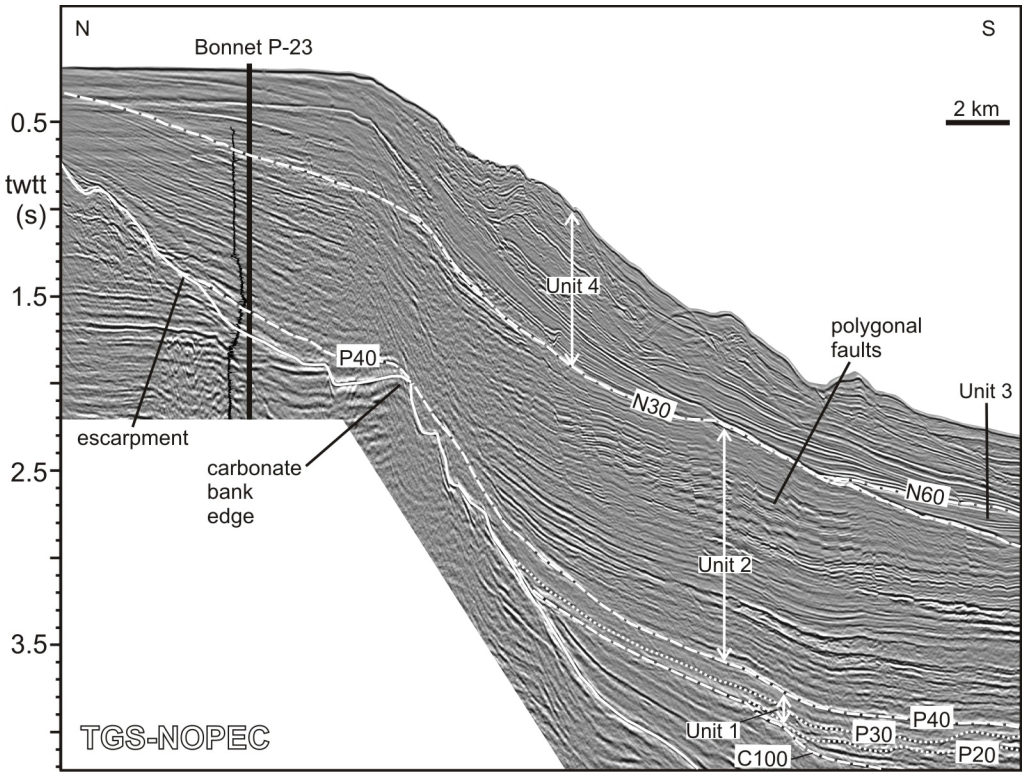

Figure 2.11 Seismic reflection profile across the upper slope and the Bonnet P-23 well. A large escarpment formed landward of the well, likely during the Paleogene, may be related to the Montagnais bolide impact. Line location is shown in Figure 2.1c. The gamma ray log is also shown for reference to Figure 2.5. Data are courtesy of TGS-NOPEC Geophysical Company L.P.

Eocene-Miocene unconformity (Figure 2.5, Table 2.1, Table 2.2). The seismic geomorphology of horizon P40 appears similar to P20, with several prominent gullies seaward of the carbonate bank (Figure 2.10c). In most cases, the gullied morphology of P40 is inherited from the underlying Unit 1. Between interfluves, there is little evidence of channel incision or gully formation on the P40 surface. On the tops of most interfluves, for example at the Shubenacadie H-100 and Shelburne G-29 wells (Figures 2.6-2.7), P40 is eroded by events that occurred later in the Oligocene and Miocene. The only location that the P40 reflection appears eroded is on the seaward side of salt diapirs in the southwest part of the study area. In this area, P40 erodes into the Priabonian interval, and the erosion is likely due to along-slope bottom currents (Figures 2.10c, 2.18).

N20 marks the top of the highly faulted interval above P40 and is also coincident with channel development locally (Figure 2.17). Over much of the study area, particularly below the middle to upper slope, N20 is eroded by N30. However, N20 is easily discernible from N30 in the area seaward of the Torbrook C-15 to Shubenacadie H-100 wells.

Above N20, N30 marks the top of Unit 2. The N30 horizon is a distinct erosional unconformity recognized over most of the study area. Below the middle slope, N30 erodes down to N20 or deeper. N30 forms a marine onlap surface over much of the study area and, in combination with N20, marks the top of the highly faulted and shingled seismic interval that makes up Unit 2. Seaward of the carbonate bank, the geomorphology of N30 differs significantly from P40, with few gullies and an overall smoother appearance (Figure 2.10d). East of the Albatross B-13 well, the erosional nature of N30 is apparent, with clear truncation of underlying reflections (Figure 2.12). In this part of the study area, N30 forms a 70 km wide terrace between the margin hinge zone and the seaward extent of salt diapirs (Figures 2.10d, 2.12). This terrace was recognized by Swift (1987) and was attributed by prolonged erosion and non-deposition related to a pulse in bottom current intensity in the late Middle Miocene. Seaward of the Shelburne G-29 well, N30 appears less erosional, separating chaotic reflections below from

concordant reflections above (Figure 2.8). West of the Shelburne G-29, N30 is a composite unconformity formed by a number of erosional processes, beginning with bottom current erosion followed by widespread mass wasting and channel incision which reworked the surface into the Late Miocene, creating a prominent angular unconformity (Campbell and Mosher 2010) (Figure 2.15).

Below the continental slope, Unit 2 is absent or thin in most deepwater wells in the study area (Figure 2.5). On the isochore map for the interval (Figure 2.9b), a broad upper slope area, coincident with the location of several deepwater exploration wells, is interpreted as a zone of bypass, erosion, or non-deposition. Unit 2 is thickest where it fills depressions inherited from canyons and gullies that formed during the development of Unit 1. The pervasive faults that are diagnostic of Unit 2 cut several other acoustic facies that provide information about the original mode of deposition. The most common acoustic facies for Unit 2 is moderate amplitude, concordant reflections. This facies is interpreted to represent hemipelagic sedimentation (Figure 2.17). There is also evidence for gravity flow input during development of Unit 2. At the base of the succession seaward of the hinge zone, moderate amplitude, lenticular to sub-parallel reflections mark the transition from the transparent Priabonian interval at the top of Unit 1, to ponding of sediment within the inherited gullied morphology. Two intervals of high amplitude, lenticular to sub-parallel reflection packages with channels are recognized in the succession; a lower interval that occurs near the base of the succession, and an upper interval at approximately the same stratigraphic level as N20 (Figure 2.6). The channels are imaged in the Torbrook 3D dataset (Figure 2.19). This facies is interpreted to represent periods of downslope sediment transport, likely attributable to turbidity currents. Most of Unit 2 in the central part of the study area, between the Torbrook C-15 and Shelburne G-29 wells, consists of moderate amplitude, lenticular, chaotic to transparent reflection packages. This facies is interpreted as mass-transport deposits. In the western part of the study area, moderate amplitude, sigmoidal reflections are present over small areas and are interpreted to represent small sediment drifts (Figure 2.15).

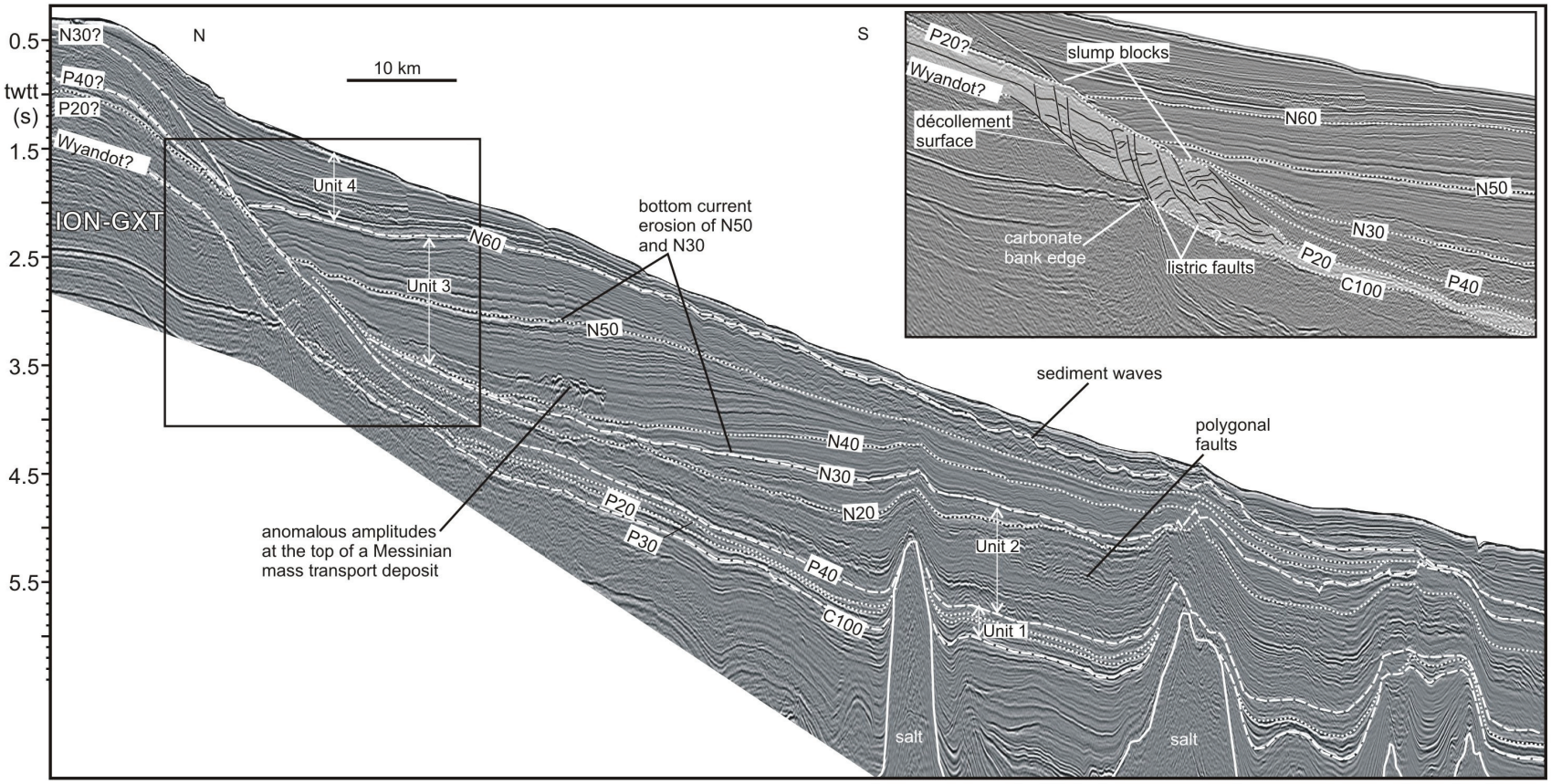

Figure 2.12- Regional dip-oriented seismic reflection profile in the eastern part of the study area showing the seismic stratigraphic framework. Truncation of underlying reflections is apparent below N30, and several reflections converge near the edge of the carbonate bank and hinge zone. Unit 3 has a distinct wedge-shape, thinning landward and basinward. Line location is shown in Figure 2.1c. Data are courtesy of ION-GXT.

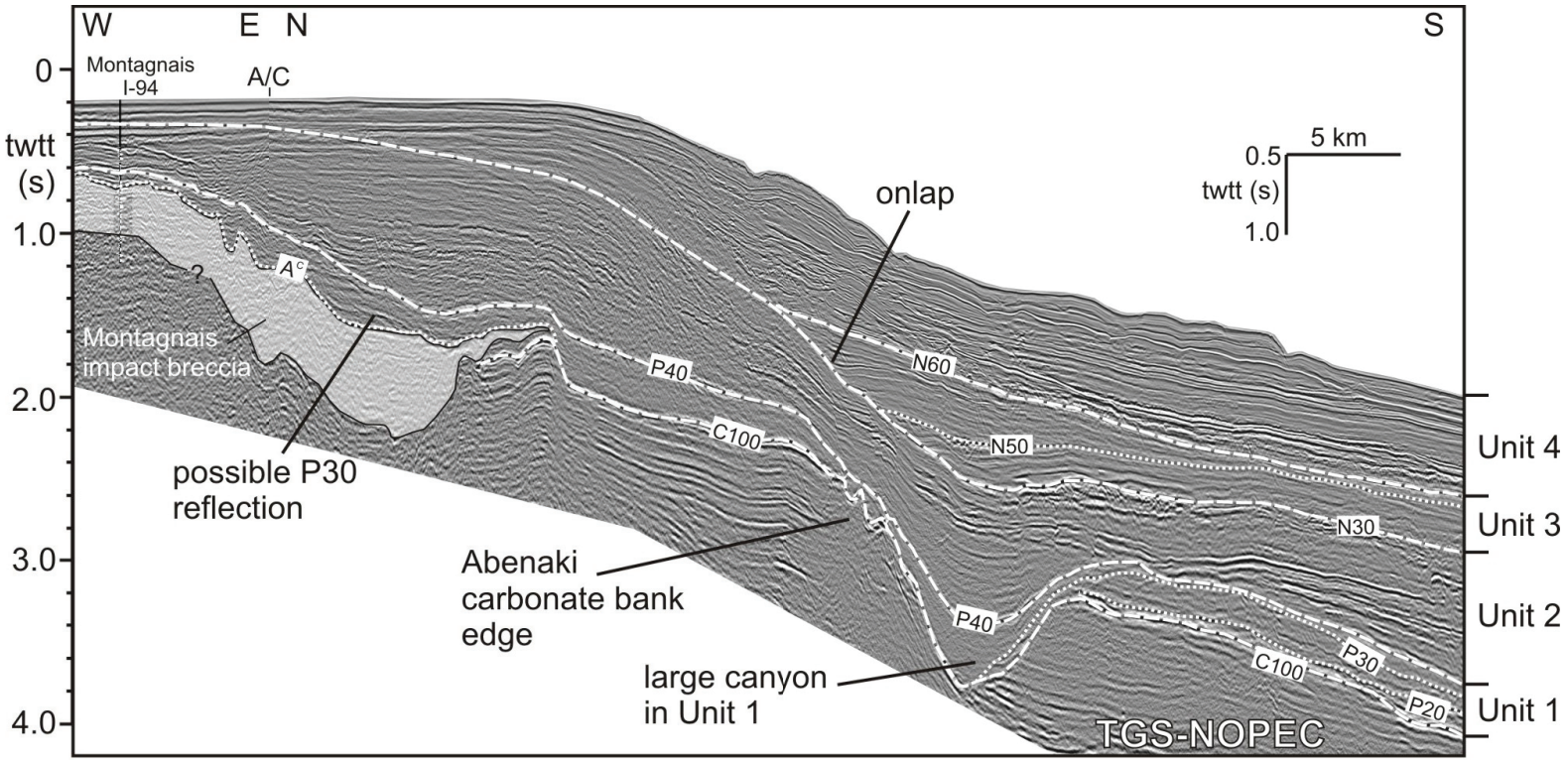

Figure 2.13- Seismic reflection profile across the upper slope near the Montagnais bolide impact site. The distinct, acoustically transparent P30-P40 interval appears to drape the impact breccia. This profile obliquely cuts a major Paleogene canyon. Line location is shown in Figure 2.1c. Data are courtesy of TGS-NOPEC Geophysical Company L.P.

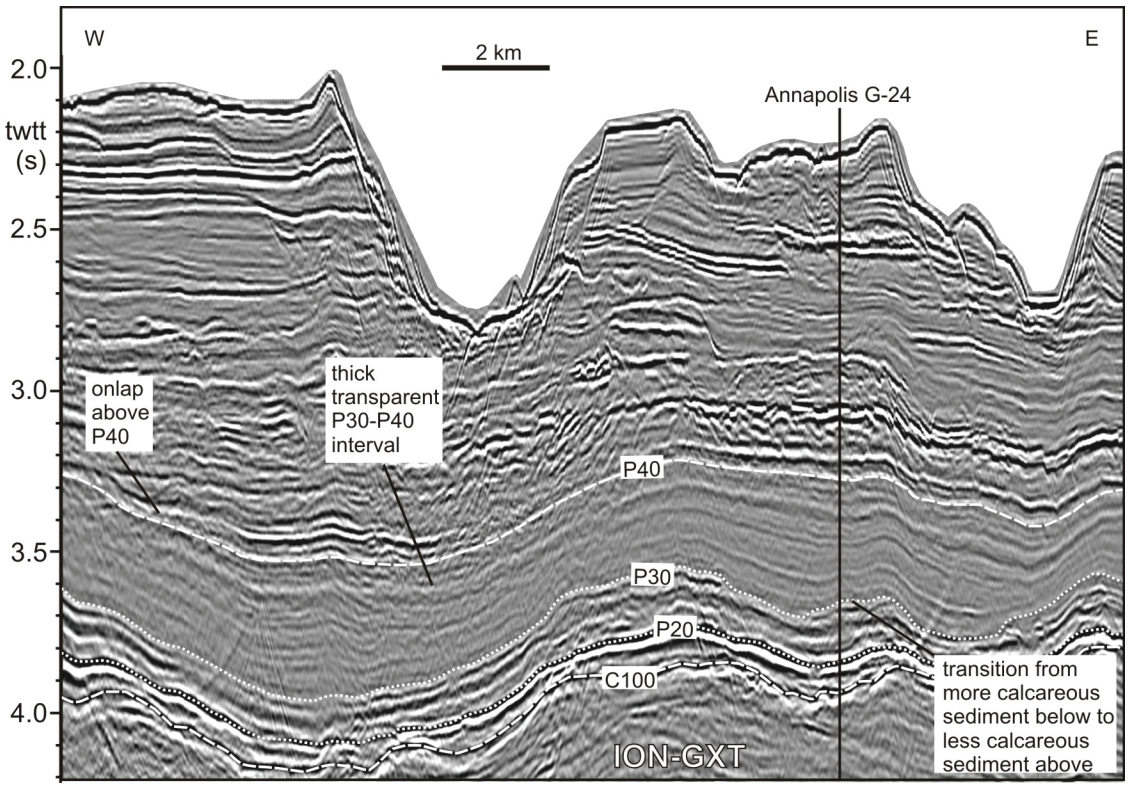

Figure 2.14- Seismic reflection profile across the Annapolis G-24 well showing the seismic stratigraphic framework. Line location is shown in Figure 2.1c. Data are courtesy of ION-GXT.

Unit 3- Horizons N30- N60 (Upper Miocene to Pliocene)

The dominant acoustic facies of Unit 3 is wavy to divergent, medium to low amplitude reflections. Polygonal faulting is common in the interval, but is not as prominent as in the underlying Unit 2. Unit 3 is bound by N30 at its base and N60 at its top and includes N40 and N50. The unit forms a thick sedimentary wedge that thins both landward and basinward, exceeding 1300 m thickness near the Torbrook C-15 well (Figure 2.9c). Unit 3 represents more than 20% of the residual Upper Cretaceous to Cenozoic succession over most of the study area, and more than 50% in the eastern part of the study area. Seismic correlation of Unit 3 onto the continental shelf is difficult because it thins to a single reflection below the upper slope. The isochore map for the interval shows that it is elongated along slope and is thickest in the eastern part of the study area where it overlies the erosional terrace formed by N30 (Figures 2.9c, 2.12). Widespread erosion during development of the overlying Unit 4 removed much of Unit 3 east of the Shubenacadie H-100 well and is responsible for the seemingly abrupt eastern edge of Unit 3 near Verrill Canyon (Figures 2.6, 2.8).

Between the basal N30 unconformity of Unit 3 and the overlying N40, there is typically an interval of concordant to wavy reflections interpreted to represent hemipelagic or bottom current deposits (Figure 2.17), or an interval of incoherent and chaotic reflections interpreted to represent mass transport deposits (MTDs). N40 is recognized over much of the study area seaward of the carbonate bank. Reflection strength of N40 is strong in the vicinity of the Shubenacadie H-100 and Shelburne G-29 wells (Figures 2.6-2.7). At the Shubenacadie H-100 well, N40 corresponds to a 30 m thick interval of Messinian very fine sand in an otherwise mud-dominated succession (Shell et al. 1983; Fensome et al. 2008). Similarly, at the Shelburne G-29 well, N40 corresponds to a 30 m thick interval of Upper Miocene very fine sand (Steeves 1985b; Fensome et al. 2008). At other wells in the study area, N40 corresponds to brown siltstone and claystone with occasional sand grains (Table 2.1, Table 2.2). In the Torbrook 3D survey area, N40 appears as a widespread high amplitude anomaly, however there are no discernible indicators of down slope depositional elements such as channels. In the Barrington survey area, a large channel, approximately 3 km wide and 100-200 m deep (Figure 2.20), correlates to

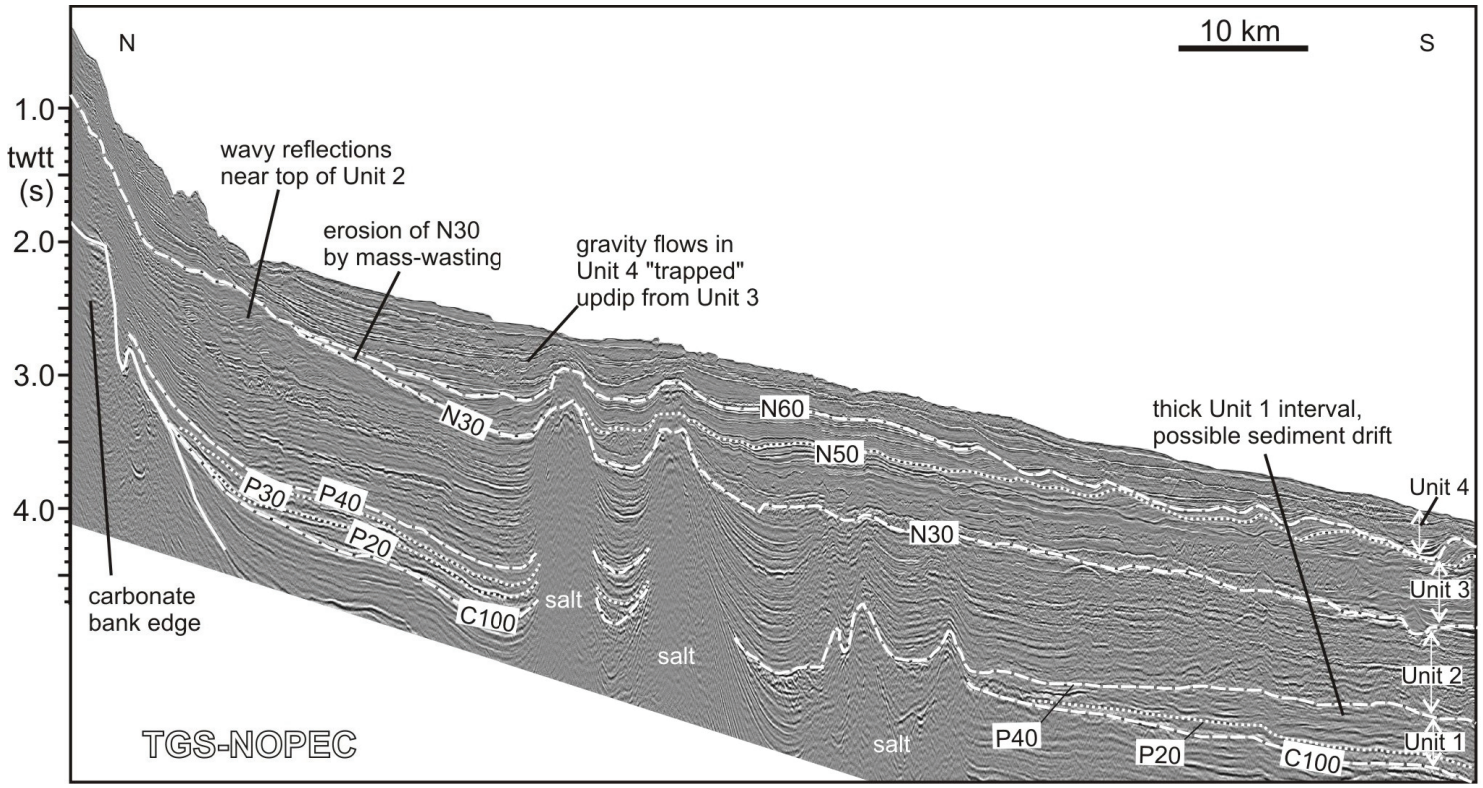

Figure 2.15- Regional dip-oriented seismic reflection profile in the western part of the study area showing the seismic stratigraphic framework. Paleogene reflections merge and onlap the seaward flank of the carbonate bank, and Neogene reflections merge and onlap N30. N30 truncates underlying reflections below the middle slope and was reworked by mass wasting. Giant sediment waves overlie mass transport deposits in Unit 3. Line location is shown in Figure 2.1c. Data are courtesy of TGS-NOPEC Geophysical Company L.P.

approximately the same stratigraphic level as N40. Seismic amplitudes on the channel floor resemble a series of stacked and offset sinuous channels.

Zones of chaotic and incoherent reflections, interpreted to represent MTDs, are common immediately above N40. In the western part of the study area, a very large MTD covers an area of 10 500 km^2 and represents ~680 km^3 of failed sediment (Figure 2.18) (MTD2 in Campbell and Mosher 2010). This single deposit affected approximately 20% of the study area and reworked the N30 erosional surface. In the eastern part of the study area, a MTD eroded down to the level of N40 and is mappable from east of the Shubenacadie H-100 well to seaward of the Albatross B-13 well. In the Torbrook 3D survey area, this MTD, one of the exploration targets for the Torbrook C-15 well (EnCana 2002), has strong seismic amplitudes present at its upper surface (Figures 2.8, 2.12). Correlations of the MTDs to wells in the study area provide a Messinian age.

Above the Messinian MTDs, an interval of concordant to wavy reflections makes up most of the remainder of Unit 3. Near the Torbrook C-15 well, this interval is more than 1000 m thick and thins towards the west, mimicking the depositional pattern of the entire succession. Southwest of the Shelburne G-29 well, a region of sigmoidal to wavy reflections, stratigraphically equivalent to concordant reflections to the east, covers an area of approximately 20 000 km^2 (Figure 2.10e, Figure 2.15). Campbell and Deptuck (In Press) interpreted the interval as a field of giant sediment waves (Stow et al. 2009), similar to deepwater antidunal features described by a number of authors (e.g. Fox et al. 1968; Rona 1969; Blumsack and Weatherly 1989; Flood 1988). The bedforms have wavelengths of approximately 5 km and wave amplitudes up to 150 m (Figure 2.20). Bedform migration direction is typically towards the east and up-slope. Stacked packages of sediment wave sequences exceed 500 m thickness. Seaward of the Torbrook C-15 well, sediment waves are recognized within this interval (Figure 2.12) and are likely the same bedforms reported by Swift (1987). Horizon N50 is a prominent reflection within the interval of concordant to wavy reflection and is correlatable over a large area. In the eastern part of the study area, N50 is a gently undulating surface that appears erosional,

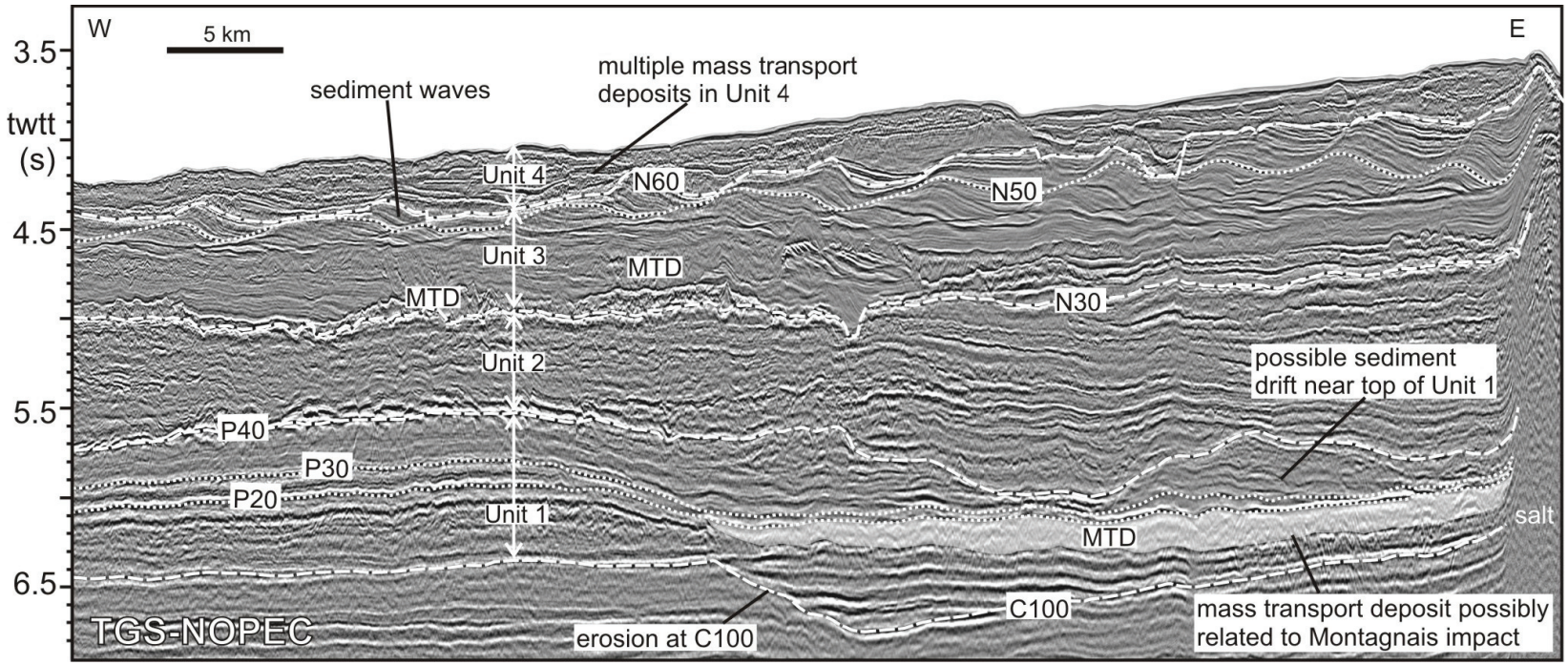

Figure 2.16 Seismic reflection profile from the southwest part of the study area showing the seismic stratigraphic framework and seismic reflection character seaward of salt structures. A MTD between C100 and P20 is possibly related to the Montagnais bolide impact. Unit 2 appears chaotic and faulted. Unit 3 is dominated by giant sediment waves and mass transport deposits. Mass transport deposits in Unit 4 fill sediment wave troughs. Line location is shown in Figure 2.1c. Data are courtesy of TGS-NOPEC Geophysical Company L.P.

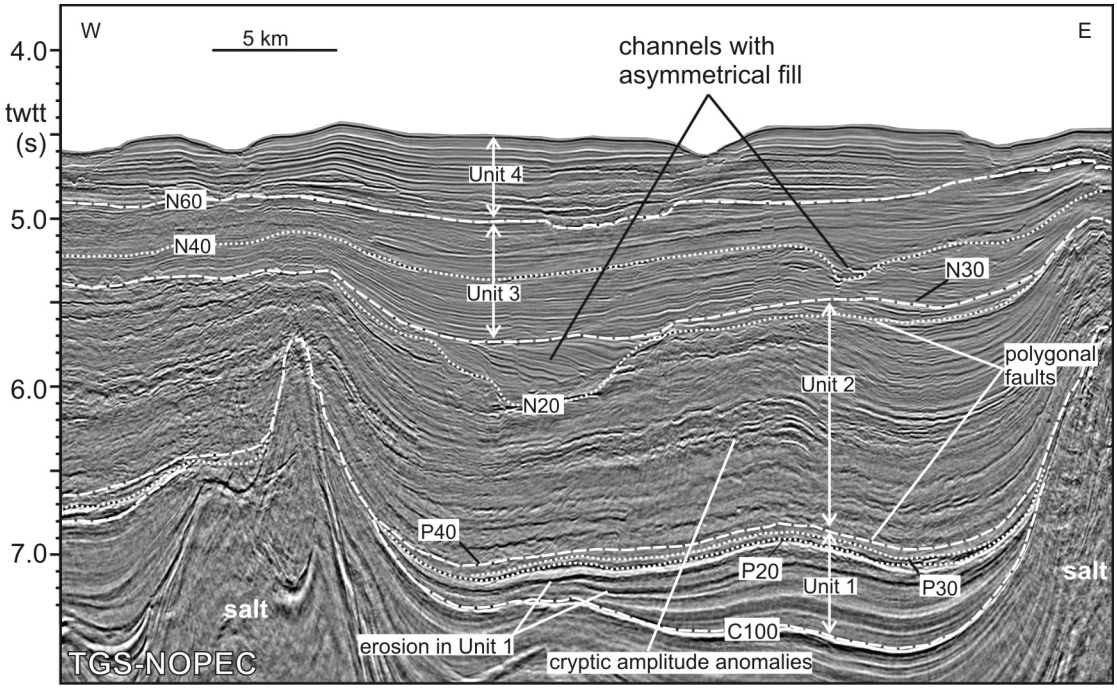

Figure 2.17 Seismic reflection profile from the southeast part of the depocenter showing the seismic stratigraphic framework and reflection characteristics. Multiple erosion surfaces are apparent in Unit 1, as well as the faulted character that is typical of Unit 2. Most Neogene channels exhibit asymmetrical infill. Line location is shown in Figure 2.1c. Data are courtesy of TGS-NOPEC Geophysical Company L.P.

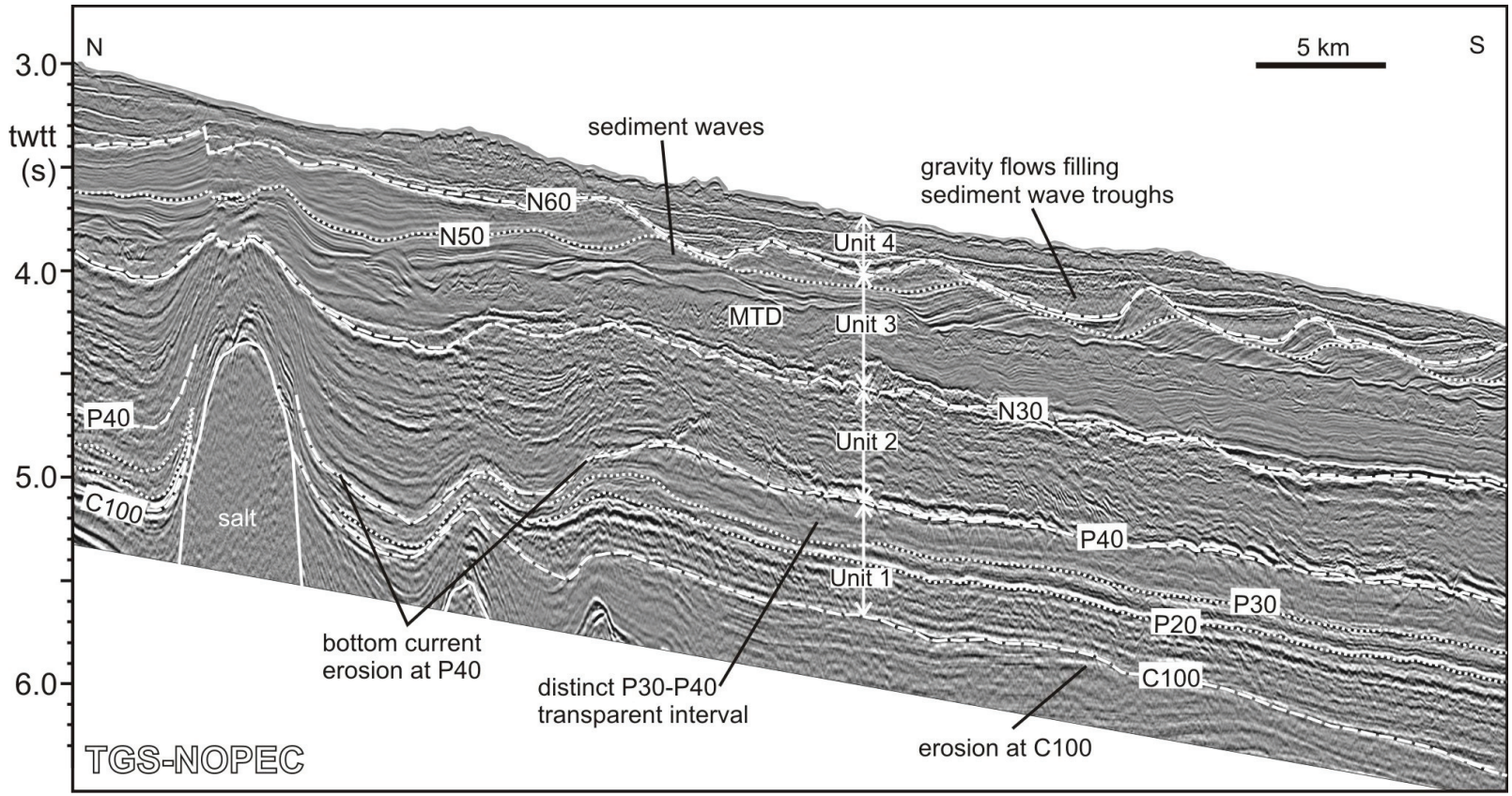

Figure 2.18 Seismic reflection profile from the southwest part of the study area showing the seismic stratigraphic framework and seismic reflection character seaward of salt structures. Erosion at P40 is interpreted to be the result of bottom current activity. Giant sediment waves appear to migrate up-slope and gravity flows in Unit 4 fill sediment wave troughs. Line location is shown in Figure 2.1c. Data are courtesy of TGS-NOPEC Geophysical Company L.P.

truncating underlying reflections (Figures 8, 12). In the western part of the study area, N50 is a prominent reflection within the sediment wave interval. Detailed mapping of N50 in the Barrington 3D dataset shows the morphology of the sediment waves (Figure 2.20). Biostratigraphic data from the Shelburne G-29 well indicate a Zanclean age for N50 (Table 2).

The upper boundary of Unit 3 is N60. The age of N60 is Piacenzian (Table 2). Over most of the study area, N60 onlaps N30, and merges with other reflections below the upper slope, making correlation of the equivalent surface difficult below the shelf (Figures 2.12, 2.15). N60 is a moderate-strength positive amplitude reflection that marks the transition from moderate to low amplitude, parallel to wavy reflections below to high amplitude, divergent and chaotic reflections above (Figures 2.6-2.7). The structure map of N60 shows that the surface is relatively smooth compared to the extensive gullied relief apparent in underlying units (Figure 2.10e). East of the Albatross well, a broad, southwest trending subtle ridge is apparent. The surface forms a terrace landward of the Torbrook and Shubenacadie wells, whereas seaward it forms a gently dipping slope. The ridge appears morphologically similar to the Chesapeake drift on the U.S. Atlantic margin (Twichell et al. 2009). West of the Shelburne G-29 well, N60 marks the top of a 50 km wide terrace, immediately seaward of the buried carbonate bank and hinge zone, formed by the buildup of giant sediment waves in Unit 3 above the N30 unconformity (Figures 2.10e, 2.15) (Campbell and Deptuck In Press).

Unit 4- N60 to Seafloor (Piacenzian to Present)

Unit 4 is bound by N60 at the base and the seafloor at the top. It exceeds 700 m thickness and is mainly confined to the area below the present upper to middle slope where it makes up more than 20% of the residual thickness of the Late Cretaceous to Cenozoic succession (Figure 2.9d). In general, the interval has higher seismic amplitude compared to the underlying Unit 3. MTDs, canyons, and multiple unconformities are also common in Unit 4. Seaward of the buried carbonate bank and margin hinge zone, Unit 4 is thickest where it overlies terraces that formed on the basal N60 surface. The morphology of

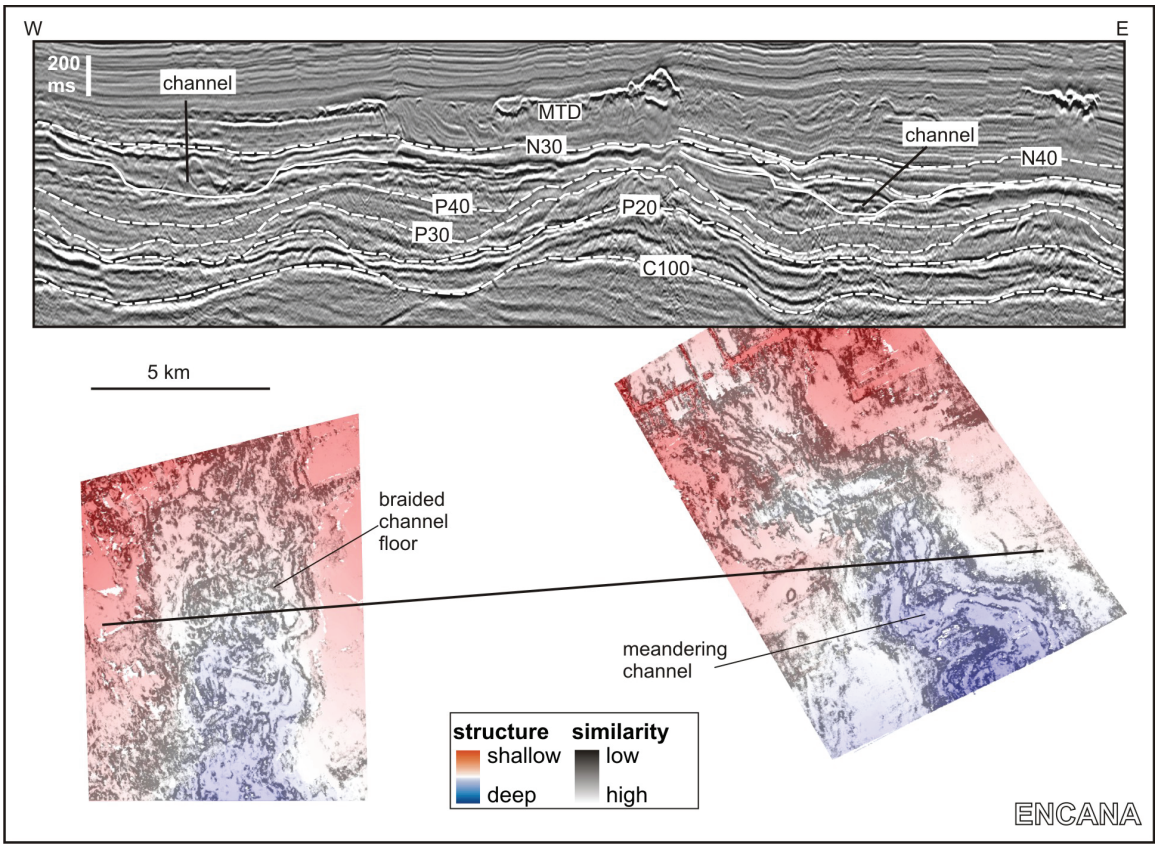

Figure 2.19 Seismic reflection profile and seismic geomorphology of large channels developed in Unit 2 in the Torbrook 3D survey area. Seismic geomorphology is shown as structure draped over similarity. Unit 2 is condensed in this area. Location of the Torbrook 3D dataset is shown in Figure 2.1c. Data are courtesy of EnCana Corp.

Figure 2.20 Seismic reflection profile and seismic geomorphology of sediment waves, channels, and polygonal faults in the Barrington 3D dataset. A) Seismic reflection profile showing sediment waves and a large channel developed above the N30 unconformity. The sediment waves developed southwest of a large escarpment. Polygonal faults, typical of Unit 2, are present below N30 and shown in Part D. B) Shaded relief image showing the geomorphology of sediment waves developed on horizon N50. The largest waves are developed southwest of seafloor obstacles, such as shallow salt diapirs and escarpments. C) Seismic geomorphology of the large channel shown in Part A displayed as reflection amplitude draped over similarity. Seismic amplitudes reveal a braided morphology in the channel thalweg. D) Similarity map of a horizon slice through Unit 2. The dark lines delineate the edges of small-offset faults (polygonal faults) typical of the unit. The vertical position of the horizon slice is shown in Part A. Location of the Barrington 3D dataset is shown in Figure 2.1c. Data are courtesy of EnCana Corp.

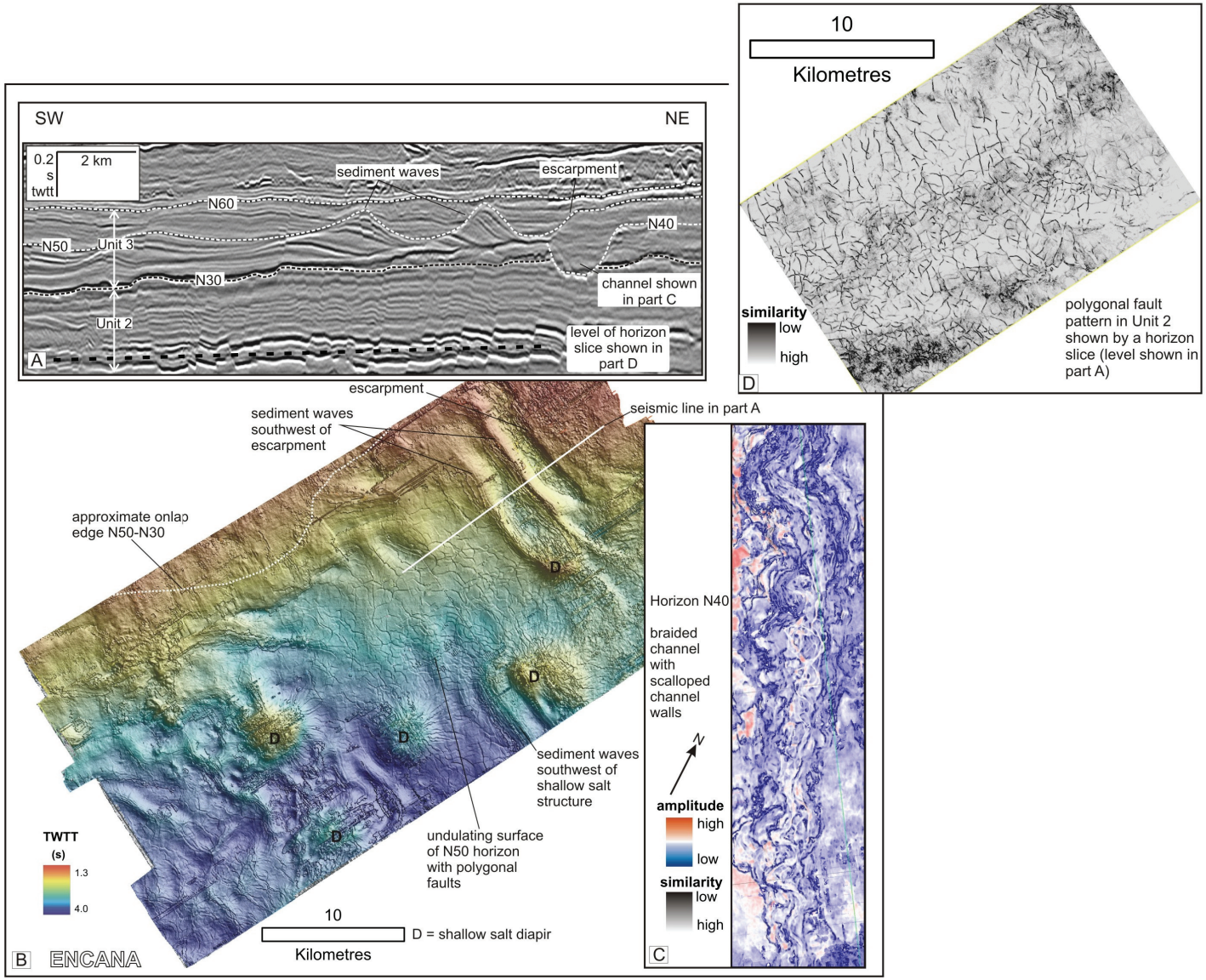
SW
NE
0.2 s twtt
2 km
sediment waves
escarpment
N60
N40
N50
Unit 3
N30
channel shown in part C
Unit 2
level of horizon slice shown in part D
A
10
Kilometres
similarity
low
high
polygonal fault pattern in Unit 2 shown by a horizon slice (level shown in part A)
D
escarpment
sediment waves southwest of escarpment
seismic line in part A
approximate onlap edge N50-N30
Horizon N40
braided channel with scalloped channel walls
N
amplitude
high
low
similarity
low
high
C
sediment waves southwest of shallow salt structure
undulating surface of N50 horizon with polygonal faults
TWTT (s)
1.3
4.0
10
Kilometres
D = shallow salt diapir
B
ENCANA

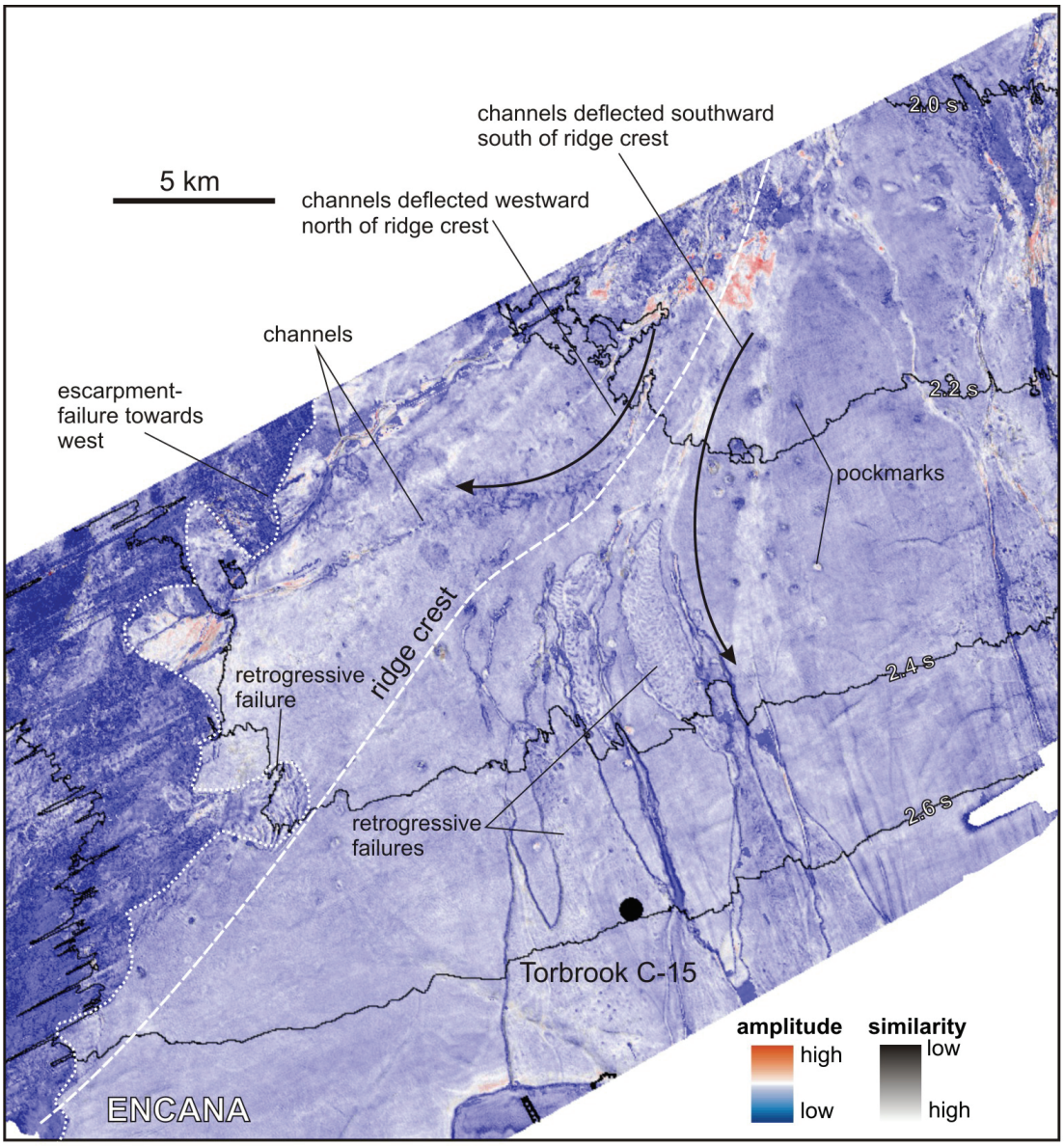

Figure 2.21- Seismic geomorphology of N60 in the Torbrook 3D area displayed as reflection amplitude draped over similarity. The area spans the large, southwest trending ridge shown in Figure 2.10e. The surface shows evidence of gravity flows in the form of channels and mass transport deposits, as well as fluid flow in the form of pockmarks. Channels and mass transport deposits north of the ridge crest are deflected to the southwest. Location of the Torbrook 3D dataset is shown in Figure 2.1c. Data are courtesy of EnCana Corp.

sediment drifts in the southwest part of the study area, formed during development of Unit 3, trapped subsequent gravity flows in Unit 4 (Figure 2.15) (Campbell and Deptuck In Press). A similar phenomenon appears to have occurred landward of the Torbrook C-15 well where gravity flows and channels were deflected westward by the pre-existing morphology of the underlying sediment drift. This deflection is apparent on the regional structure map (Figure 2.10e). In the Torbrook 3D area, the morphological map of N60 reveals westward channel deflection on the landward side of the ridge in the underlying Unit 3 (Figure 2.21). Between the Shelburne G-29 and Albatross B-13 wells, a small depocenter is the expression of the Late Pliocene or Early Pleistocene "Shelburne mass transport deposit" (Shimeld et al. 2003; Mosher et al. 2010). Seaward of the Montagnais I-94 well, the fan-shaped plan-view morphology of a small depocenter appears similar to the morphology described for trough mouth fans (Vorren and Laberg 1997) recognized elsewhere along the eastern Canadian margin (Piper and Normark 2009). East of the Shubenacadie H-100 well, substantial erosion during the development of Unit 4 resulted in the removal of much of the underlying Unit 3. The erosion marks the western edge of the ubiquitous Quaternary canyons that dominate the seabed of the modern Scotian margin east of Verrill Canyon (Figure 2.1, 2.10f) (Mosher et al. 2004).

2.5 Discussion

2.5.1 Relationship between seismic stratigraphy of the Scotian margin and North American Basin south of the New England Seamounts

C100 and A*

South of the study area in the North American Basin, the A* horizon correlates with the Crescent Peaks Mbr of the Plantegenet Fm, a marly nannofossil rich chalk (Tucholke and Mountain 1979). The Wyandot Fm is thought to be equivalent to the Crescent Peaks Mbr (Jansa et al. 1979) and the resulting correlation of the C100 horizon to prominent reflections within the Wyandot Fm below the outer Scotian margin supports that interpretation (Table 2.1). Therefore, in the study area C100 is approximately A*.

P20 and A^C

Horizon P20 is approximately age-equivalent to A^C in the North American Basin. In the basin, A^C correlates to the top of a Middle Eocene cherty turbidite interval and marks the top of the Bermuda Rise Fm (Mountain and Tucholke 1985). Swift et al. (1986) and Ebinger and Tucholke (1988) correlated A^C across the New England Seamounts onto the Sohm Abyssal Plain. Ebinger and Tucholke (1988) interpreted that A^C was eroded by an unconformity likely equivalent to A^U (Lower Oligocene) on the central Scotian Rise and Slope. There is no recognition of siliceous chert from samples at P20 at Shubenacadie H-100, however chert fragments are described in cuttings and sidewall core samples from Ypresian and Lutetian sediment from Shelburne G-29 (chert fragments in a sidewall core at 2580.5 m, quartz and chert grains in cuttings from 2525 m to 2590 m) (Fensome et al., 2008; Steeves 1985b). In general, though, P20 correlates to chalk and limestone rich intervals that drape erosion surfaces where intersected by wells. Apart from a similar age, there is no obvious direct link between P20 and A^C.

P30 and A^T

Horizon P30 is approximately age-equivalent to horizon A^T in the North American Basin. In the basin, horizon A^T correlates with the top of a turbidite interval within the Blake Ridge Fm. Its age is Middle to Upper Eocene and is interpreted to mark the end of widespread terrigenous input into the basin (Tucholke and Mountain 1979). Horizon P30 represents the end of widespread slope erosion in the Late Eocene. This slope erosion was possibly a consequence of the turbidity currents that contributed to the turbidite deposition below A^T.

P40 and A^U

In the North American Basin, a widespread unconformity interpreted to be formed by bottom current erosion during the Early Oligocene is designated A^U (Tucholke and Mountain 1979; Mountain and Tucholke 1985). In the southwest part of the study area, the P40 reflection appears erosional on the seaward side of salt diapirs. P40 erodes into

the Priabonian interval, and the erosion is likely due to along-slope bottom currents. Ebinger and Tucholke (1988) recognized similar abyssal erosion east of the study area and equated the erosion surface to horizon A^U. In this study, in the area seaward of shallow salt structures P40 is interpreted to be equivalent to A^U. Further landward and upslope, where P40 marks a transition to onlapping and infilling of Eocene gullies, erosion by bottom currents is not apparent.

N30 and Merlin

On the U.S. Atlantic margin, the Merlin horizon is an important regional seismic marker and erosional unconformity that correlates with the top of a widespread hummocky and shingled unit below the continental rise. The unconformity is attributed to a pulse of strengthened abyssal current circulation in the late Middle Miocene (Mountain and Tucholke 1985). In the study area, N30 is a lower Upper Miocene erosional unconformity that marks the top of a widespread hummocky and faulted unit, and is interpreted to be equivalent to Merlin.

N50 and Blue

On the U.S. Atlantic margin, horizon Blue is attributed to a pulse of bottom current intensification that occurred at around 3 Ma (Mountain and Tucholke 1985; Tucholke and Mountain 1986). Horizon N50 possibly represents the same bottom current pulse on the Scotian margin.

2.5.2 Depositional patterns

Regional mapping has identified a large Upper Cretaceous to Cenozoic depocenter along the outer continental margin off Nova Scotia. There is a strong spatial relationship between the depocenter and pre-existing structural elements. Most of the depocenter is confined between the seaward edge of the Abenaki carbonate bank to the north, and a zone of shallow salt structures to the south (Figure 2.2). Extensive periods of erosion along the outer shelf and upper slope removed evidence of whether the shelf break migrated beyond the carbonate bank edge during the Cenozoic (Figure 2.10). Within the

depocenter, four main phases of deposition with distinct styles are recognized at different time periods: Late Cretaceous to Late Eocene, Oligocene to Middle Miocene, Late Miocene to Pliocene, and Late Pliocene to present.

Figure 2.22 presents a series of cartoons that depict the interpreted sequence of the main down-slope and along-slope events that led to the observed seismic stratigraphic framework preserved in the study area. Upper Cretaceous to Upper Eocene deposits of Unit 1 are focused mainly in elongate, down-slope oriented ridges (Figures 2.8, 2.9a). These ridges were exploration targets at the Shubenacadie H-100 and Shelburne G-29 wells (Shell 1983; Petro Canada 1985) and were previously interpreted as turbidite fans prior to drilling, and later as chalky fans by Swift (1987). Results from this study reveal that these ridges are clearly erosional features and form remnant interfluves between gullies that developed during the Late Cretaceous and Paleogene. In locations where ridges are thick, the seismic stratigraphy records several unconformities that are locally mappable, suggesting that repeated slope erosion events occurred throughout the Late Cretaceous to Eocene interspersed with periods of hemipelagic and occasionally carbonate-rich deposition. It is difficult to determine how much erosion at a given stratigraphic level contributed to the overall mounded appearance of the interval, however it appears that the last major period of erosion occurred in the late Bartonian or early Priabonian (correlating to the P30 horizon) because a distinct, acoustically transparent unit drapes the erosion surface over much of the study area after this time (Figures 2.6-2.8). The seismic reflection configuration of the Upper Cretaceous to Upper Eocene interval below the slope appears remarkably similar to the equivalent-age interval on the U.S. Atlantic margin, described as “ribbed” by Poag and Mountain (1987), and also interpreted to represent extensive erosional channels (Mountain 1987).

Most of the deposits within the depocenter are Oligocene to Upper Pliocene age and belong to Units 2 and 3 (Figure 2.9b-2.9c). Results from exploration drilling on the Scotian Slope suggest that Oligocene to Middle Miocene sediments are thin or absent across the deepwater margin (Fensome et al. 2008). Piper et al. (2005) reported a similar absence of sediments of this age east of the study area on St. Pierre Slope (southwest

Grand Banks of Newfoundland). The distribution of Unit 2, however, shows that thick accumulations of Oligocene to Middle Miocene sediments are likely present throughout the study area, but are not well-sampled by exploration drilling (Figure 2.5). A broad middle slope zone of erosion and non-deposition, coinciding with the location of many of the exploration wells seaward of the margin hinge zone, is interpreted from the sediment distribution of the Oligocene to Middle Miocene interval (Figure 2.9b). The Late Eocene to Oligocene transition marks a significant change in seismic reflection architecture in the study area. In the Priabonian, pelagic or hemipelagic sediments draped the seafloor after a prolonged period of gully development. Beginning in the Early Oligocene, sedimentation style changed, with onlapping and infilling of depressions associated with the underlying gullied interval, followed by erosion into the draped Priabonian unit on the ridge tops later in the Oligocene and Miocene. Large channels developed in this interval in the eastern part of the study area (Figure 2.19), along with thick MTDs seaward of the Albatross B-13 and Shelburne G-29 wells. These findings suggest that gravity flow processes were active throughout development of the Oligocene to Middle Miocene succession and were likely a factor in creating the broad zone of non-deposition. Most large channels extend beyond the seaward limit of the study area. Later in the Miocene, bottom current processes seemed more important in eroding the seabed and preventing deposition below the middle slope, except in the western part of the study area where N30 forms an angular unconformity formed by regional slope failure (Campbell and Mosher 2010).

One of the characteristic features of Oligocene to Middle Miocene deposits of Unit 2 is the development of high density, small offset faults (Figures 2.17, 2.20). The faults have a polygonal shape in planview with significant subsets of the fault population confined to discrete layers (e.g. Figure 2.20b, d). These faults are interpreted to be similar to the polygonal fault systems that are recognized globally and described by Cartwright and Dewhurst (1998). Polygonal faulting is also observed in parts of Unit 1 and Unit 3, but faults are not as well developed or widespread. A similar interval of high density, small offset faults appears to characterize the Oligocene to Middle Miocene succession on the U.S. Atlantic continental margin, although 3D seismic data are not available to

investigate the planview geometry. Mountain and Tucholke (1985) originally described the interval as shingled and cryptically prograding, attributing the seismic facies to bottom-current controlled deposition. Later, Poag and Mountain (1987) proposed that the shingled reflections were faults due to sediment accumulation above a fractured and jointed Eocene chalk interval. Polygonal fault systems are recognized below the central Scotian Shelf in the Wyandot Fm and an Eocene chalk unit, and are attributed to syneresis processes (Hansen et al. 2004). Several recent papers describe mechanisms besides syneresis for polygonal fault formation, including differential compaction over irregular topography imposed by diagenetic boundaries and inherited relief (e.g. Davies et al. 2009; Ireland et al. 2010). Another possible explanation for faulting in the Oligocene to Middle Miocene succession in the study area, besides the physical compaction of fine grained sediment, is volume change due to silica digenesis and the conversion from opal-A to opal-CT, for example as described by Neagu et al (2010) for the North Sea. The conversion of opal-A to opal-CT can result in a 500% reduction in pore volume in silica rich sediments (Hurd et al. 1981). Thomas (2005) described a high abundance of radiolarians in Early Miocene sediments from the Wenonah J-75 well east of the study area and biogenic silica rich sediments are common in the Early to Middle Miocene sediments on the U.S. Atlantic margin (Haggerty et al. 1987; Vecsie and Hoppie 1996). In several locations in the study area, laterally continuous seismic amplitude anomalies in Unit 2 possibly indicate diagentic boundaries and potentially provide evidence for silica conversion (Figure 2.17)

The Upper Miocene to Upper Pliocene succession of Unit 3, again, marks a distinct change in depositional style on the margin. The major unconformity N30 divides the distinctly faulted Oligocene to Middle Miocene deposits below from less faulted deposits above. The Unit 3 succession represents more than 50% of the total thickness of the residual Upper Cretaceous and Cenozoic section in the eastern part of the study area (Figure 2.9c). East of the Shelburne G-29 well, N30 forms a broad, relatively flat terrace that coincides with a landward shift in the depocenter above the unconformity between Units 2 and 3 (Figures 2.9b, 2.9c, 2.12). West of the Shelburne G-29 well, N30 is a steeply dipping angular unconformity and a basinward shift in deposition between Units

2 and 3 is apparent. In this area, a sediment drift developed above the lower part of the unconformity and gravity flows likely by-passed the steeper landward part of the unconformity (Figure 2.9b, 2.9c, 2.15) (Campbell and Mosher 2010; Campbell and Deptuck In Press). Previous studies suggested that sediment drifts did not exist off Nova Scotia (McCave and Tucholke 1986), or were of limited geographical extent confined to Pliocene sediment waves on the continental rise (Swift 1987; McCave et al. 2002). The current study shows that sediment drifts are a common feature in Unit 3. A large separated drift (Faugères et al. 1999) developed in the Late Miocene and Pliocene, similar in age and morphology to the Chesapeake Drift on the U.S. margin. Giant mud waves developed at the same time in the western part of the study area. Although a distinct period of channel development occurred in the Messinian (Figure 2.20), sediment drifts along with abundant and large MTDs are the main contributors to the overall depositional pattern in Unit 3.

The Late Pliocene to present succession of Unit 4 marks the transition from primarily along-slope processes back to gravity flow predominance that led to the current morphology of the outer Scotian margin. The modern bathymetry of the Scotian Slope has two morphological zones; an area of widespread Quaternary canyons east of Verrill Canyon and an area of subdued bathymetry and minor canyons west of Verrill Canyon (Figures 2.1b, 2.10f) (Mosher et al. 2004). In the west, the bathymetry shows a seaward diversion of contours between Verrill Canyon and the slope off Georges Bank (Figure 2.10f). Several authors provided explanations for the unique morphology along the western margin. Jansa and Wade (1975) suggested that this change in seafloor topography was due to the development of a large fan seaward of a major growth fault and carbonate bank edge. Uchupi and Swift (1991) suggested that low subsidence along this part of the margin prevented the incision of deep canyons; the low subsidence combined with glacial plume deposition instead of turbidity current deposition resulted in the unique morphology. Hughes-Clarke et al. (1992) attributed the low physiographic relief of the outer western Scotian margin to late Cenozoic faulting and sediment input during Pleistocene glaciations and was not a product of current-controlled sedimentation. The results from this study suggests that gravity flow-dominated Quaternary depositional

processes were effective at healing the sediment drift morphology of the underlying succession, resulting in the smoothing of bathymetric steps constructed during drift development. Therefore, sediment drift development on the lower slope and upper rise during the Late Miocene and Pliocene, followed by back-filling by Quaternary sediments below the slope, was sufficient to create the observed bathymetry.

Figure 2.22- A series of cartoons that depict the main along-slope and down-slope events that led to the observed seismic stratigraphy in the study area. The phases are lettered sequentially from A to S. Each cartoon shows a typical dip and strike profile from the eastern part of the depocenter. The colours correlate to the four seismic stratigraphic units.

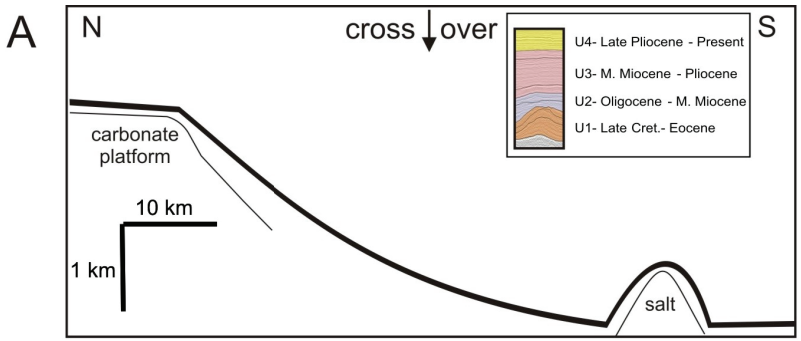

Unit 1- Upper Cretaceous to Upper Eocene

C100 -Chalk deposition above an erosional surface (Wyandot eq. or A*).

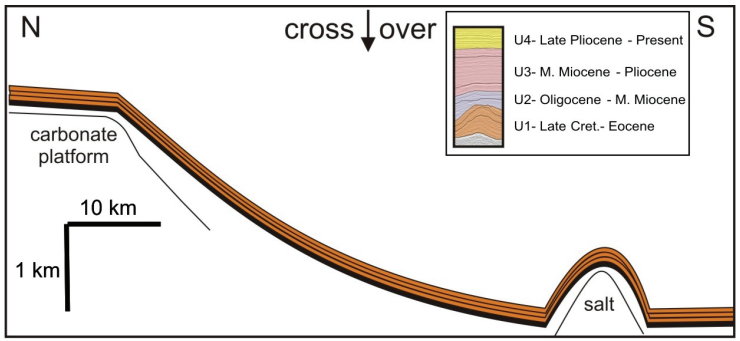

Unit 1- Upper Cretaceous to Upper Eocene

Repeated periods of erosion and pelagic/hemipelagic sedimentation.

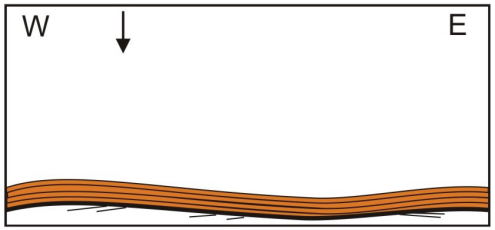

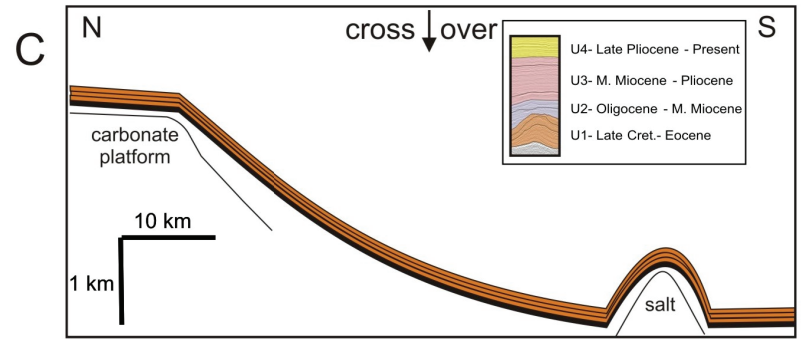

Unit 1- Upper Cretaceous to Upper Eocene

Repeated periods of erosion and pelagic/hemipelagic sedimentation.

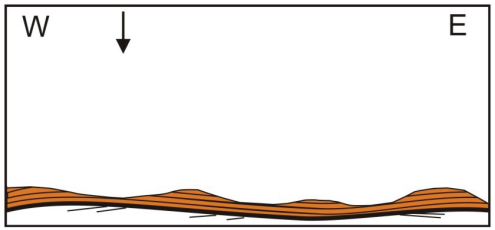

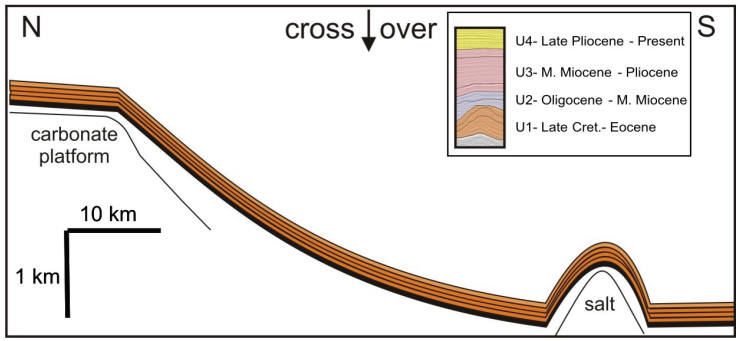

Unit 1- Upper Cretaceous to Upper Eocene

Repeated periods of erosion and pelagic/hemipelagic sedimentation.

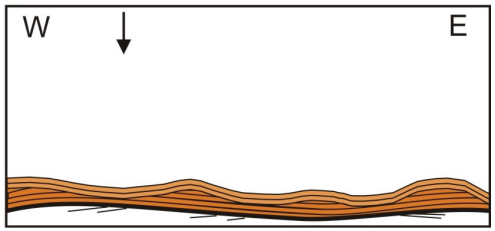

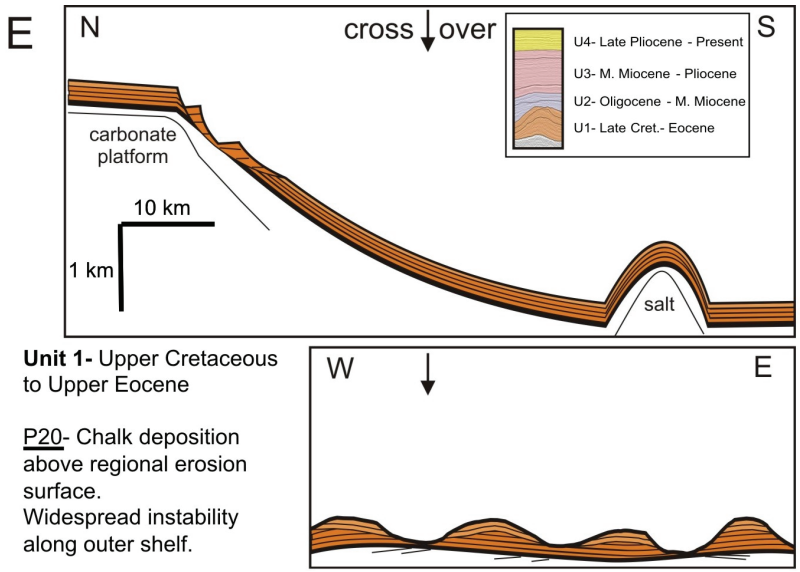

Unit 1- Upper Cretaceous to Upper Eocene

P20- Chalk deposition above regional erosion surface.
Widespread instability along outer shelf.

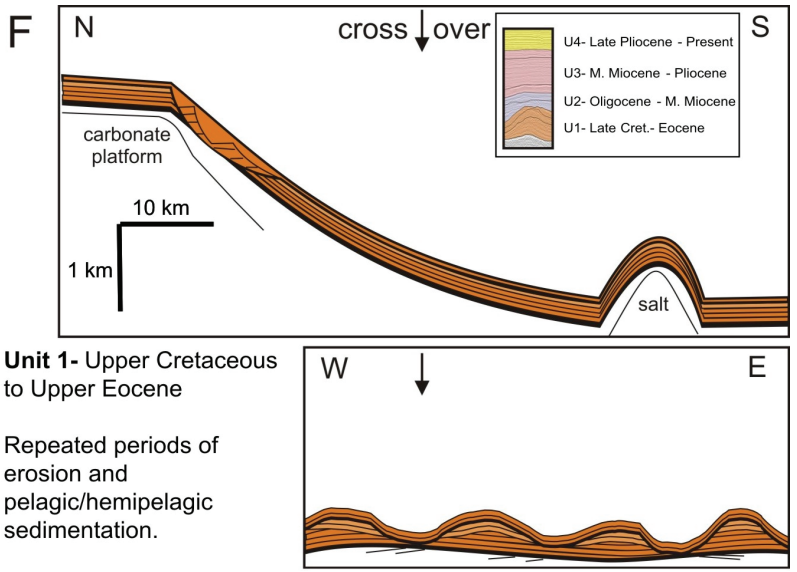

Unit 1- Upper Cretaceous to Upper Eocene

Repeated periods of erosion and pelagic/hemipelagic sedimentation.

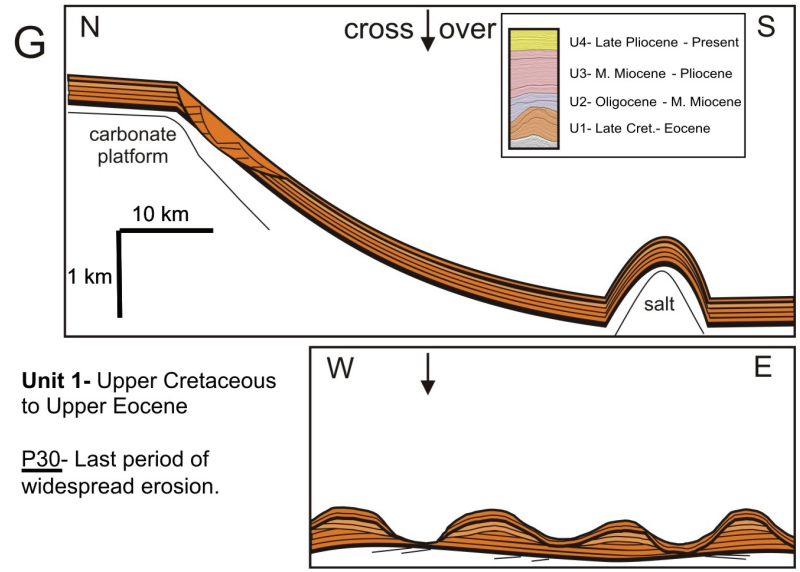

Unit 1- Upper Cretaceous to Upper Eocene

P30- Last period of widespread erosion.

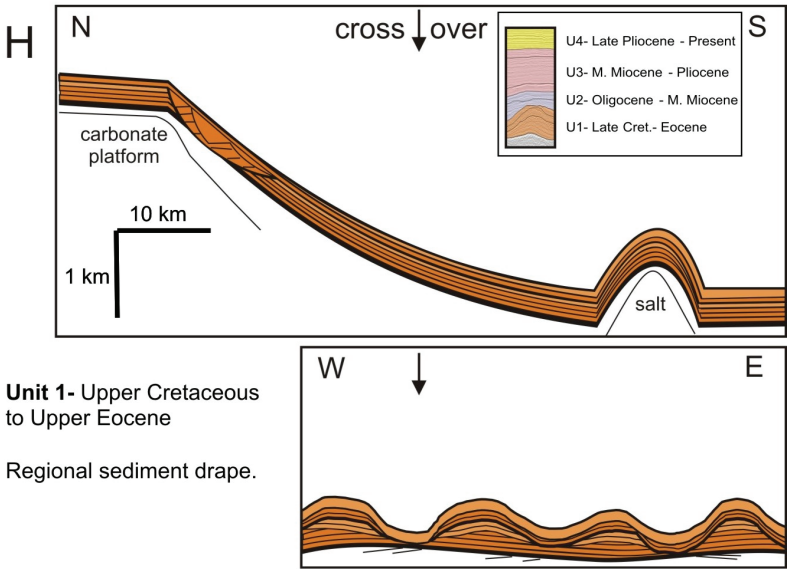

Unit 1- Upper Cretaceous to Upper Eocene

Regional sediment drape.

I

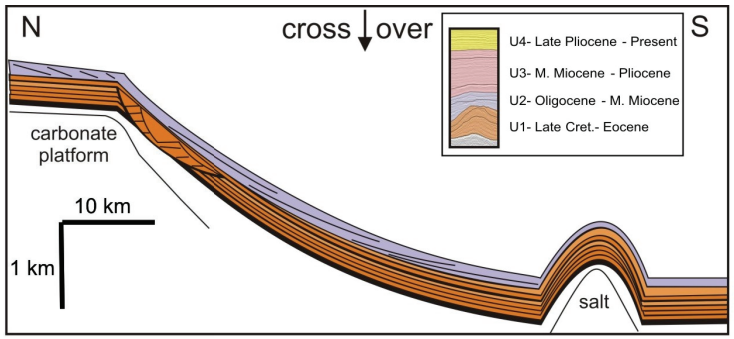

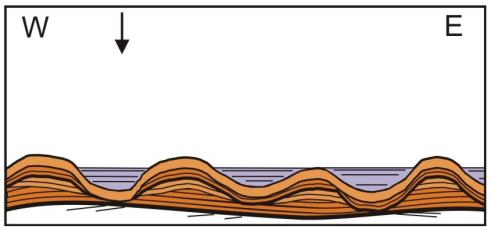

Unit 2- Lower Oligocene to Mid-Upper Miocene

P40- Marks transition from regional drape to onlap and infilling of gullies.

J

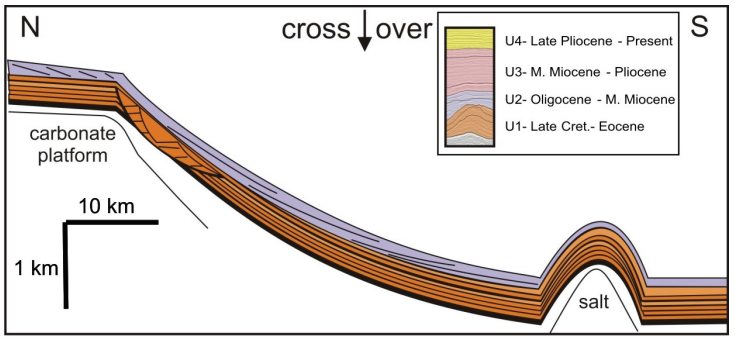

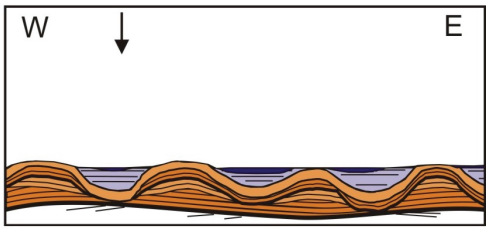

Unit 2- Lower Oligocene to Mid-Upper Miocene

Erosion of the tops of Unit 1 ridges and local channel development in the Oligocene.

K

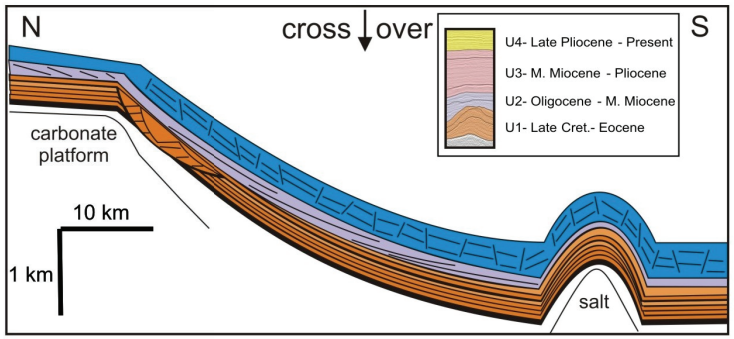

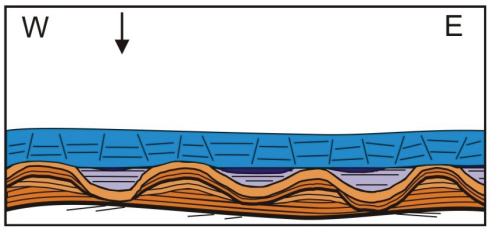

Unit 2- Lower Oligocene to Mid-Upper Miocene

Widespread, small offset faults (polygonal faults). Evidence for mass transport, sediment drifts, and hemipelagic sedimentation.

L

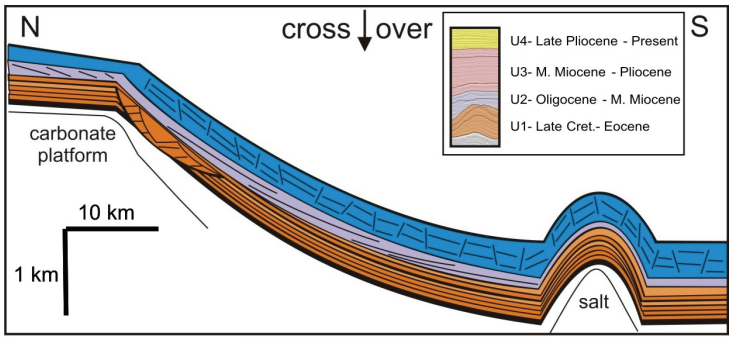

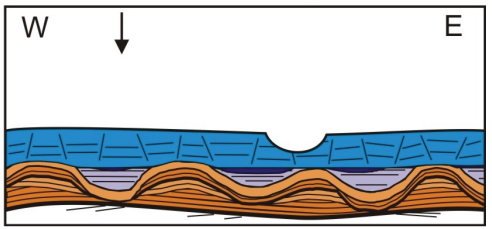

Unit 2- Lower Oligocene to Mid-Upper Miocene

N20- Marks top of faulted interval. Local channel incision.

M

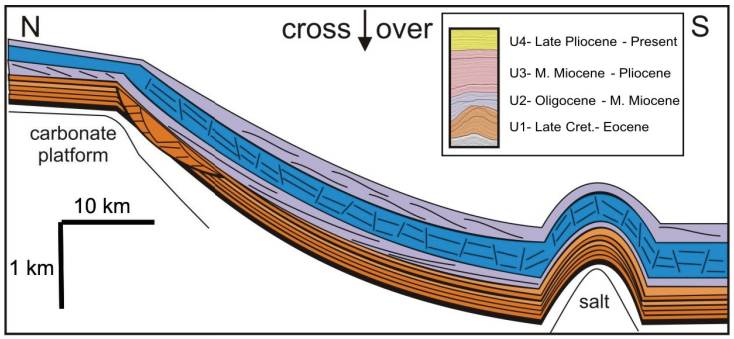

Unit 2- Lower Oligocene to Mid-Upper Miocene

Evidence for sediment drifts and mass transport.

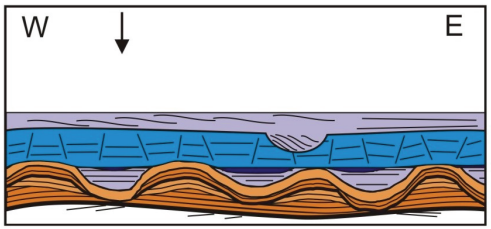

N

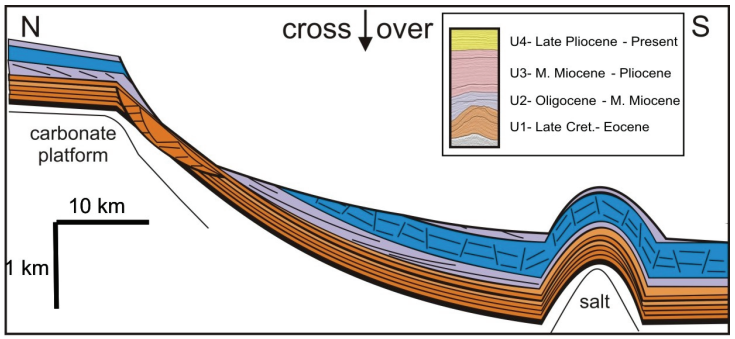

Unit 2- Lower Oligocene to Mid-Upper Miocene

N30- Regional unconformity formed by bottom current erosion, mass wasting and slope bypass.

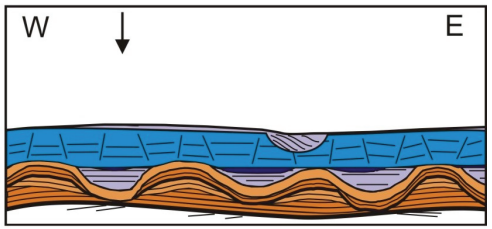

O

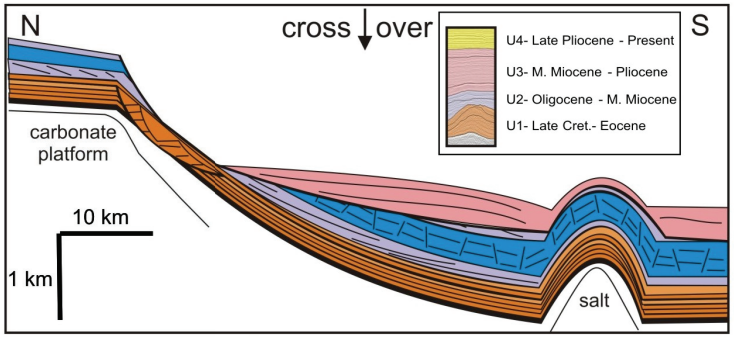

Unit 3- Mid-Upper Miocene to Pliocene

Regional sediment drift development and mass wasting.

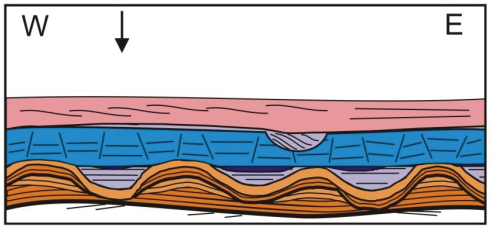

P

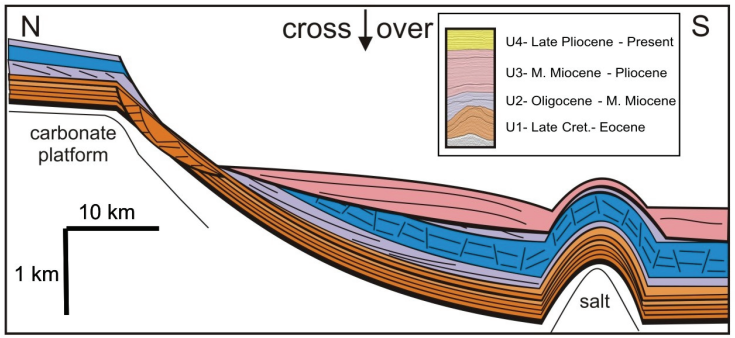

Unit 3- Mid-Upper Miocene to Pliocene

N40- Local channel development. Fine sand deposition.

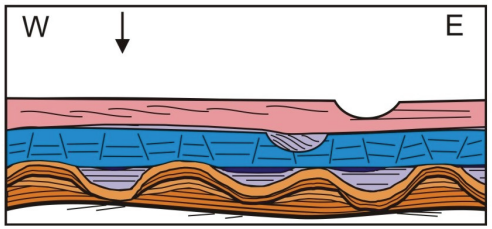

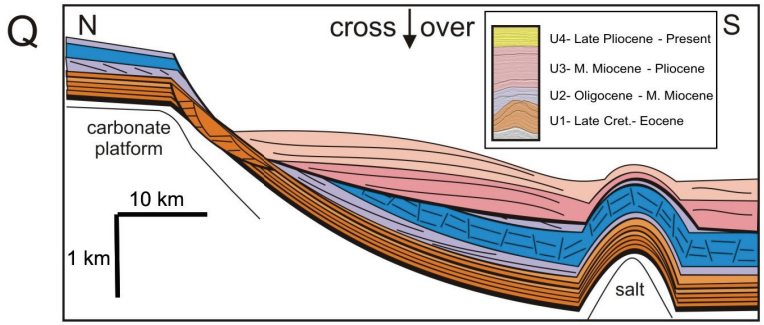

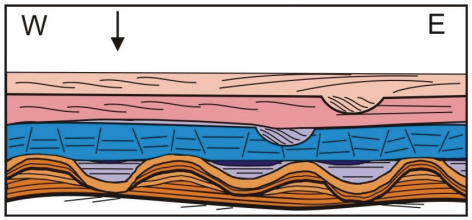

Unit 3- Mid-Upper Miocene to Pliocene

Regional sediment drift development and mass wasting.

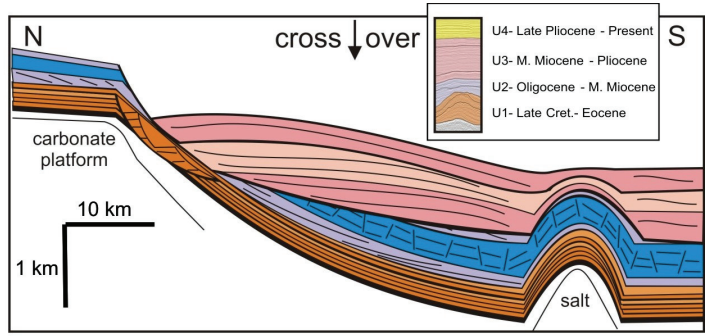

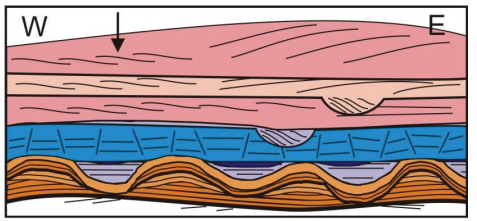

Unit 3- Mid-Upper Miocene to Pliocene

N50- Erosion by bottom currents and enhanced bedform development.

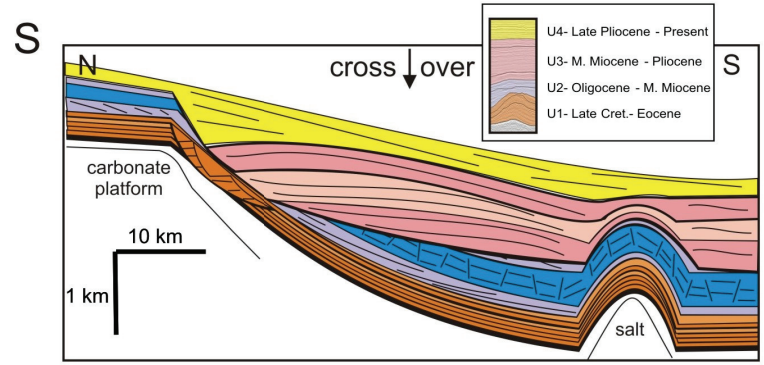

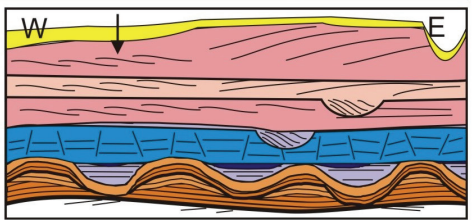

Unit 4- Upper Pliocene to present

N60- Top of sediment drifts, eroded in many areas by Quaternary processes.

2.5.3 Slope instability in the Upper Cretaceous to Eocene interval and relationship to the Montagnais impact

The Montagnais bolide impact occurred 51 million years ago (Ypresian) (Bottomley and York 1988) and the impact structure is located below the outer continental shelf within the study area (Jansa and Pe-Piper 1987) (Figure 2.9b). The most obvious geological effects of the impact were the development of a crater, central uplift, and partial circular failure scar below the shelf where the force of the impact deeply excavated the seabed (Figure 2.10b). The geological effects away from the Montagnais impact site on the continental slope and rise are less obvious. On the U.S. margin, Poag and Ward (1993) proposed that some of the erosion that occurred in the Paleogene section below the slope was due to direct and indirect processes related to the Late Eocene Chesapeake Bay bolide impact on the U.S. Atlantic shelf. On the Scotian margin, Unit 1 demonstrates widespread evidence of slope erosion, manifested in the ubiquitous canyons both in the study area and further east (e.g. Parson 1975; Brake 2009). In some locations, these canyons erode deeply into the underlying Cretaceous deposits (Figure 2.12). Dypvik and Jansa (2003) interpreted a slump wedge of Late Cretaceous sediment seaward of the Montagnais impact crater on old multichannel seismic data and tentatively attributed the feature to slope failure due to the impact. Detailed mapping in this study shows that the slump interpreted by Dypvik and Jansa (2003) is actually the wall of a large Paleocene or Eocene canyon cut obliquely by the seismic line shown in their study (Figures 2.10b, 2.13). The large canyon appears to lead directly from the eastern part of the circular scarp, deviates towards the west near the buried carbonate bank edge, then continues seaward down slope. The first deposits clearly imaged in seismic data that fill the canyon and onlap the impact breccia correlate to the distinct, acoustically transparent Priabonian unit above P30, which is at least 14 Ma younger than the impact (Figure 2.13). It is possible that some of the canyon erosion was related to the impact, and that reworking or flushing of the canyon happened throughout the Eocene. It is also possible that seismic data do not adequately image Lower and Middle Eocene deposits that overlie the impact breccia; up to 100 m of Lower and Middle Eocene sediments are found above the impact deposits at the Montagnais I-94 well (Jansa et al. 1989). The fact that the largest Eocene Canyon in the study area shows such a strong spatial relationship with the Montagnais

structure suggests that canyon erosion processes were at least enhanced by the bolide impact.

East and west of the Montagnais impact, evidence of slope instability is apparent throughout most of Unit 1 below the outer shelf and upper slope, above the buried carbonate bank and margin hinge zone. Here, a large fault scarp or listric fault follows the trend of the outer carbonate bank edge. Jansa and Wade (1975) originally recognized the feature, interpreting the structure as a regional hinge-line or growth fault. The current study shows that the feature primarily affects the Upper Cretaceous to Upper Eocene succession. In the east, between the Albatross B-13 and Acadia K-62 wells, the scarp forms a listric fault or décollement and the entire C100 to P30 interval consists of tilted and rotated blocks bound by listric faults that sole out near the C100 marker and propagate up to the P30 marker (Figure 2.12). The continuity within individual blocks suggests that the slumping occurred at approximately the time of the formation of P30, although failure may have started earlier in the Paleogene and was a continuous processes. In the west, the fault forms an escarpment, for example near the Bonnet P-23 well where there is clear truncation at the scarp face and evacuation of material seaward of the fault (Figure 2.11). Biostratigraphic data at the Bonnet P-23 well provides some age control for the escarpment. Middle Eocene sediments overlie Lower Cretaceous sediments where the well intersects the escarpment (Figure 2.11) (Bujak Davies Group 1988), and it is therefore possible that the last major erosion event along the escarpment is related to the Montagnais impact. Assuming dating of the impact by previous researchers is correct, and that absolute ages imposed by the biostratigraphic data and radiometric methods agree, evidence of the bolide impact should be found near the same stratigraphic level as P20 and above C100. Seaward of the impact structure and the large canyon, seismic data reveal a MTD that is immediately below P30 and above C100 (Figure 2.16) which may be a more likely candidate for an impact-related, mass-wasting deposit.

2.5.4 Unconformity formation

The large number of boreholes along the U.S. Atlantic continental margin allowed Poag and Ward (1993) to develop an allostratigraphic framework that encompassed deposits from the coastal plain to the continental rise. Poag and Ward (1993) described at length the various processes that possibly lead to unconformity formation on the continental margin, from the obvious effects of sea-level change on the continental shelf, to more exotic phenomenon in deep water, such as erosion by internal waves at density boundaries. They concluded, however, that below the continental slope and upper rise of the U.S. Atlantic margin, gravity flow processes were the dominant factor in unconformity formation.

In the study area, some of the reflections that make up the seismic stratigraphic framework are not clear unconformites at the resolution of the seismic data; for example, N60 marks a change in acoustic facies that is regionally recognizable, but does not necessarily represent erosion or a hiatus. Similarly, N20 locally coincides with a channel erosion surface, but for the most part separates faulted reflections below from less faulted reflections above. Horizons C100 and P20 correlate to lithologic boundaries, with carbonate-rich intervals attributed to generating the requisite impedance contrast to create a regionally mappable reflection. In both cases, the carbonate-rich intervals were likely deposited during quiescent oceanographic conditions, possibly correlating to a sea level highstand and perhaps represent deepening of the CCD. For both C100 and P20, erosion is apparent immediately below the reflection surface, implying that carbonate rich sediments drape erosion surfaces and were the first deposits preserved above widespread erosion events. In such cases, although the reflection represents what is likely a conformable interval, the seismic geomorphology of the horizon reflects the underlying erosional surface. Conversely, the formation of P30 is attributed to erosion by down slope processes. The increased reflectivity below P30 that makes the surface distinct in seismic data is attributed to an increase in carbonate-rich sediments, and therefore also coincides with a subtle lithological boundary.

In Units 2 and 3, unconformity formation appears to be caused by processes related to both down-slope gravity flows and along-slope bottom currents. Over much of the western North Atlantic, pulses of increased bottom current intensity are recognized along the North American Basin margins, forming erosional unconformities A^U in the Early Oligocene, Merlin in the Middle Miocene, and Blue in the Pliocene (Mountain and Tucholke 1985; Tucholke and Mountain 1986). P40 has a bottom current eroded appearance on the seaward side of salt structures, with development of possible erosional moats, and is considered equivalent to horizon A^U (Figures 2.10c, 2.16). Further landward, P40 forms a subtle marine onlap surface and along-slope erosion is less apparent. Although it is possible that along-slope currents contributed to the preferential erosion of Priabonian sediments on ridge crests in the Early Oligocene, it is more likely that down-slope erosion later in the Oligocene and Miocene eroded the Priabonian interval. Miller et al. (1985) recognized that on the U.S. Atlantic margin, bottom current erosion occurred in the Early Oligocene (Horizon A^U) before a middle Oligocene sea level lowstand led to gravity flow erosion of the margin. The N30 unconformity is one of the most distinct seismic stratigraphic horizons on the Scotian margin. In the western part of the study area, Campbell and Mosher (2010) investigated in detail the seismic geomorphology and erosion history of the N30 unconformity and proposed that erosion initially occurred under the influence of a southwest flowing bottom current, followed by repeated reworking of the unconformity by gravity flow processes. Swift (1987) proposed that bottom currents alone eroded N30 (horizon CS2 in Swift 1987) in the eastern part of the study area. Our data support Swift's interpretation in some locations, however, in areas below the middle slope where Unit 2 thins landward, several unconformities merge making it difficult to discern N30 from other horizons (Figure 2.12). Horizon N40 is correlated with local high amplitude seismic anomalies, very fine sand deposition, and channel erosion during a time when sediment drift development was active along the western North Atlantic (Tucholke and Mountain 1986). In many cases, Late Miocene channels are filled asymmetrically (Figure 2.17), from west to east, suggesting that channel fill was influenced by an east to west flowing bottom current following processes described by Faugères et al (1999) and Hopfauf and Speiss (2001). It is also possible that winnowing of fine sediment by bottom currents may account for some of the sandiness

associated with N40. Therefore, the formation of horizons P40, N30, and N40 in the study area is attributed to both along-slope and down-slope processes. In contrast, the N50 horizon shows no evidence of down-slope erosion (e.g. channels, escarpments, etc) and all erosion appears to be the result of along-slope processes.

What is clear from this study is that unconformities along the margin form through a variety of complex processes. The specific processes that lead to margin erosion become less obvious moving from the lower continental rise to the slope as unconformities merge, preserving only evidence of the most recent erosion event. Age control suggests that unconformity formation occurred at similar periods throughout the Late Cretaceous and Cenozoic between the study area and the U.S. Atlantic margin to the south, and a generally comparable depositional architecture is observed. For example, the same broad divisions of Upper Cretaceous and Cenozoic deposits resulting from this study were arrived at by Mountain and Tucholke (1985), Poag and Mountain (1987), and Locker and Laine (1993) for the U.S. margin. This is an important result that implies that regional, basin-scale processes dominate over local processes.

2.6 Conclusions

1. A large (~50 000 km^2) Late Cretaceous to Cenozoic deepwater depocenter is located along the outer continental margin southwest of Nova Scotia in the Shelburne sub-basin. Pre-existing structural features, namely the Abenaki carbonate bank and underlying margin hinge zone as well as shallow salt structures, exerted considerable control over depositional patterns during the development of the depocenter.

2. The geological history of the depocenter is broadly divided into four phases. The first phase spanned the Late Cretaceous to Late Eocene and resulted in widespread and repeated periods of gully erosion interspersed with periods of hemipelagic and carbonate-rich sedimentation. A widespread zone of instability along the trend of the buried carbonate bank and coincident with the margin's hinge zone is recognized within this interval, expressed as a series of tightly spaced faults that sole out and show detachment

along Upper Cretaceous chalk dominated intervals. The relationship between slope instability features and the Montagnais impact is not clear. It does seem likely, however, that the largest canyons in the study area, which formed directly downslope from the impact site, formed in response to the bolide impact. The second phase spanned the Oligocene to Middle Miocene and resulted in erosion and deposition by gravity flows and reworking of sediments by bottom currents. A broad zone of erosion or non-deposition below the middle slope, attributed to both down-slope and along-slope erosion processes, explains the paucity of Oligocene to Middle Miocene sediments in exploration wells in the study area. The third phase spanned the Late Miocene to Late Pliocene, during which time bottom current controlled deposition dominated. Stacked sequences of giant sediment waves and a coeval large separated drift represent more than 50% of the total preserved Upper Cretaceous to present sedimentary succession along the slope. The final phase spanned the Late Pliocene to present and marked a return to gravity flow predominance and deposition was focused below the upper slope.

3. The broad seismic stratigraphic divisions and depositional architecture in the study area are shared with the U.S. Atlantic margin to the south. Biostratigraphy and seismic geomorphology suggest that unconformities formed at similar periods and by similar processes throughout the Late Cretaceous and Cenozoic. This is an important result that implies that regional, basin-scale processes dominate over local processes.

2.7 Acknowledgements.

The authors would like to express appreciation to EnCana Corp., TGS-Nopec Geophysical Co. L.P., and ION-GXT for data access.

2.8 REFERENCES CITED IN CHAPTER 2

Archibald, M. 2003. Geological report for mMarathon Canada Ltd. Annapolis G-24 exploration well. 95 p.

Blumsack, S.L. and Weatherly, G.L. 1989. Observations of the nearby flow and a model for the growth of mudwaves. Deep Sea Reseach Part A. v. 36, p. 1327-1339.

Bottomley, R. and York D. 1988. Age measurement of the submarine mMontagnais impact crater. Geophysical Research Letters, v. 15, p. 1409-1412.

Brake, V.I. 2009. Evolution of an Oligocene Canyon System on the Eastern Scotian Margin. Unpublished M.Sc. Thesis, Dalhousie University, Halifaxm Nova Scotia, Canada.

Bujak Davies Group 1988a. Palynological Analysis of the Interval 440-3950 M, Bonnet P-13, Scotian Shelf. Geological Survey of Canada Open File 1858, 19 p.

Bujak Davies Group 1988ab. Palynological Analysis of the Interval 1875-4045 M, Albatross B-13, Scotian Shelf. GSC Open File 1857, 13 p

Campbell, D.C. and Deptuck, M.E. In Press. Alternating bottom current dominated and gravity flow dominated deposition in a lower slope and rise setting- Insights from the seismic geomorphology of the western Scotian margin, Eastern Canada. SEPM special publication.

Campbell, D.C. and Mosher, D.C. 2010. Middle to Late Miocene slope failure and the generation of a regional unconformity beneath the western Scotian Slope, eastern Canada. Submarine Mass Movements and Their Consequences, Advances in Natural and Technological Hazards Research, v. 28, p. 645-655.

Cartwright, J.A. and Dewhurst, D.N. 1998. Layer-bound compaction faults in fine-grained sediments. Geological Society of America Bulletin, v. 110, p 1242-1257.

Carvajal, C., Steel, R., and Petter, A.. 2009. Sediment supply: The main driver of shelf-margin growth. Earth-Science Reviews, v. 96, p. 221–248.

Chevron et al. 2002. Well history report for Chevron et al. Newburn H-23. 486 p.

Crux, J.A. and Shaw, D. 2002. Biostratigraphy of the Chevron et al. Newburn H-23 well, offshore Nova Scotia. 37 p.

Davies, R.J., Ireland, M.T., amnd Cartwright, J.A. 2009. Differential compaction due to the irregular topology of a diagenetic reaction boundary: a new mechanism for the formation of polygonal faults. Basin Research, v. 21, p 354-359.

Dypvik, H. and Jansa, L.F. 2003. Sedimentary signatures and processes during marine bolide impacts: a review. Sedimentary Geology, v. 161, p. 309-337.

Ebinger C.A., and Tucholke, B.E., 1988, Marine Geology of the Sohm Basin, Canadian Atlantic Margin: Bulletin of American Association of Petroleum Geologists, v. 72, p. 1450-1468.

Emery, K.O., Uchupi, E., Phillips, J.D., Brown, C.O., Bunce, E.T., and Knott, S.T. 1970. Continental rise off eastern North America. AAPG Bulletin, v. 54, p. 44-108.

EnCana 2003a. Well history report, EnCana Torbrook C-15 volume 2. 129 p.

EnCana 2003b. Well history report, EnCana Weymouth A-45 volume 2. 189 p.

Faugères, J-C, Stow, D.A.V., Imbert, P., and Viana, A. 1999. Seismic features diagnostic of contourite drifts. Marine Geology, v. 162, p. 1-38.

Fensome, R.A., Crux, J.A., Gard, I.G., MacRae, R.A., Williams, G.L., Thomas, F.C., Fiorini, F., and Wach, G., 2008, The last 100 million years on the Scotian Margin, offshore eastern Canada: an event-stratigraphic scheme emphasizing biostratigraphic data: Atlantic Geology, v. 44, p. 93-126.

Flood, R.D., 1988, A lee wave model for deep-sea mudwave activity: Deep-Sea Research, v 35, p. 973-983.

Fox, P.J., Heezen, B.C., and Harian, A.M. 1968. Abyssal anti-dunes. Nature, v. 220, p.470-472.

Gradstein F.M., Jansa L.F., Srivastava S.P., Williamson M.A., Bonham Carter G., and Stam B. 1990. Aspects of North Atlantic paleoceanography. In Geology of the continental margin off eastern Canada. Edited by M.J. Keen and G.L. Williams. Geological Survey of Canada, Geology of Canada no. 2, p. 351-389.

Haggerty, J., Sarti, M., von Rad, U., Ogg, J.G., and Dunnet, D.A. 1987. Late Aptian to Recent sedimentological history of the lower continental rise off New Jersey, Deep Sea Drilling Project Site 603. Initial Reports Deep Sea Drilling Project, v. 93, p. l285-l304.

Hansen, D.M., Shimeld, J.W., Williamson, M.A., and Lykke-Andersen, H. 2004. Development of a major polygonal fault system in Upper Cretaceous chalk and Cenozoic mudrocks of the Sable Subbasin, Canadian Atlantic margin. Marine and Petroleum Geology, v. 21, p. 1205-1219.

Hardy, I.A. 1975. Lithostratigraphy of the Banquereau Formation of the Scotian Shelf. In Offshore geology of eastern Canada. Edited by W.J.M. van der Linden and J.A. Wade, Geological Survey of Canada Paper 74-30, pp. 163–174.

Hopfauf, V., and Spiess, V., 2001, A three-dimensional theory for the development and migration of deep sea sediment waves: Deep-Sea Research I, v. 48, p. 2497–2519.

Hughes Clarke, J.E., O'Lleary, D.W., and Piper, D.J.W. 1992. Western Nova Scotia continental rise: relative importance of mass wasting and deep boundary-current activity. In: Poag, C.W., De Graciansky, P.C. (Eds.) Geologic Evolution of Atlantic Continental Rises. Van Nostrand Reinhold, New York, p. 266-281.

Hurd, D.C., Pankratz, H.S., Asper, V., Fugate, J., and Morrow, H. 1981. Changes in the physical and chemical properties of biogenic silica from the central equatorial Pacific: Part III, Specific pore volume, mean pore size, and skeletal ultrastructure of acid cleaned samples. American Journal of Science, v. 281, p. 833-895.

Imperial Oil Resources Ventures Ltd. 2003. Vol. 2 well history report, IORVL et al. Balvenie B-79 offshore nova Scotia. 229 p.

Ireland, M.T., Goulty, N.R., and Davies, R.J. 2010. Influence of stratigraphic setting and simple shear on layer-bound compaction faults offshore Mauritania. Journal of Structural Geology, v. 33, p. 487-499.

Jansa, L.F. and Pe-Piper, G. 1987. Identification of an underwater extraterrestrial impact crater. Nature, v. 327, p. 612- 614.

Jansa, L. F., and Wade, J. A. 1975. Geology of the continental margin off Nova Scotia and Newfoundland: Geological Survey of Canada Paper 74-30, Offshore geology of eastern Canada, v. 2: p. 51-105.

Jansa, L.F., Pe-Piper, G., Robertson, P.B., and Friedenreich, O. 1989. Montagnais: A submarine impact structure on the Scotian Shelf, eastern Canada. Geological Society of America Bulletin, v. 101, p. 450-463.

Jansa, L.F., Enos, P., Tucholke, B.E., Gradstein, F.M. and Sheridan, R.E. 1979. Mesozoic-Cenozoic sedimentary formations of the North American Basin: Western North Atlantic. In Deep Drilling Results in the Atlantic Ocean: continental margins and paleoenvironment, Edited by M. Talwani, W. Hay and W.B.F. Ryan, American Geophysical Union Maurice Ewing Series, v. 3 , p. 1–57.

Lewis, D.G. and Pandachuck, P.N. 1978. Well history report, Chevron PEX Shell Acadia A K-62 well. 87 p.

Locker, S.D., and Laine, E.P., 1992, Paleogene-Neogene depositional history of the middle U.S. Atlantic continental rise: mixed turbidite and contourite depositional systems: Marine Geology, v. 103, p. 137-164.

MacLean, B.C. and Wade, J.A. 1993. Seismic markers and stratigraphic picks in Scotian Basin wells. Atlantic Geoscience Center, Geological Survey of Canada, 276 p.

McCave I.N. and Tucholke B.E. 1986. Deep current controlled sedimentation in the western North Atlantic. in: The geology of North America vol. M: The western North Atlantic region. Vogt P.R. & Tuchkolke B.E. (eds.). Geological Society of America. p. 451–468.

McCave, I.N., Chandler, R.C., Swift, S.A., and Tucholke, B.E. 2002. Contourites of the Nova Scotian continental rise and the HEBBLE area. Geological Society, London, Memoirs, v. 22, p. 21-38.

McIver, N. L. 1972. Cenozoic and Mesozoic stratigraphy of the Nova Scotia Shelf. Canadian Journal of Earth Sciences, v. 9, p. 54-70.

Miller, K.G., Mountain, G.S., and Tucholke, B.E. 1985. Oligocene glacio–eustasy and erosion on the margins of the North Atlantic. Geology, v. 13, p. 10-13.

Mosher, D.C., Piper, D.J.W., Campbell, D.C., and Jenner, K.A., 2004, Near-surface geology and sediment-failure geohazards of the central Scotian Slope: American Association of Petroleum Geologists Bulletin, v. 88, p. 703-723.

Mosher, D.C., Louden, K., LeBlanc, C., Shimeld, J.W., and Osadetz, K.G. 2005. Gas Hydrates Offshore Eastern Canada: Fuel for the Future? Offshore Technology Conference paper 17588. In: Offshore Technology Conference.
Houston, Tx. 2-5 May 2005.

Mountain, G.S. 1987. Cenozoic Margin Construction and Destruction Offshore New Jersey. in: C.Ross and D. Haman (eds.), Cushman Foundation for Foraminiferal Research, Special Publication. 24, p. 57-83.

Mountain, G.S. and Tucholke, B.E. 1985. Mesozoic and Cenozoic Geology of the U.S. Atlantic Continental Slope and Rise. in: Geologic Evolution of the U.S. Atlantic Margin. C.W. Poag (ed.). Van Nostrand Reinhold. p. 293-341.

Neagu, R.C., Cartwright, J., Davies, R., and Jensen, L. 2010. Fossilisation of a silica diagenesis reaction front on the mid-Norwegian margin, Marine and Petroleum Geology, v. 27, p. 2141-2155.

Parsons, M. G., 1975, The geology of the Laurentian Fan and the Scotia Rise, in C. J. Yorath, E. R. Parker, and D. J. Glass, eds., Canada's continental margins and offshore petroleum exploration: Canadian Society of Petroleum Geologists Memoir 4, p. 155-167.

Payton, C.E. (Ed.). 1977. Seismic stratigraphy- Applications to hydrocarbon exploration. AAPG Memoir 26, American Association of Petroleum Geologists, 502 p.

Piper, D.J.W. 2005. Late Cenozoic evolution of the continental margin of eastern Canada. Norwegian Journal of Geology, v. 85, p. 231-244.

Piper D.J.W., Normark W.R., and Sparkes 1987. Late Cenozoic stratigraphy of the central Scotian Slope, Eastern Canada. Canadian Bulletin of Petroleum Geology, v. 35, p. 1-11.

Piper, D.J.W., MacDOnald, A.W.A., Ingram, S., Williams, G.L. and McCall, C. 2005. Late Cenozoic architecture of the St. Pierre Slope. Canadian Journal of Earth Sciences, v. 42, p. 1987-2000.

Piper, D.J.W. and Normark, W.R. 2009. Processes that initiate turbidity currents and their influence on turbidites: A marine geology perspective: Journal of Sedimentary Research, v. 79, p. 347-362.

Poag, C.W. and Mountain, G.S. 1987. Late Cretaceous and Cenozoic evolution of the New Jersey Continental Slope and Upper Rise; An integration of borehole data with seismic reflection profiles. in Poag. C.W., Watts. A.B. and others, Initial reports of the Deep Sea Drilling Project. v. 95, p. 673-724.

Poag, C.W. and Ward, L.W. 1993. Allostratigraphy of the U.S. Middle Atlantic continental margin- Characteristics, distribution, and depositional history of principal unconformity bounded Upper Cretaceous and Cenozoic sedimentary units. U.S. Geological Survey Professional Paper 1542, 81 p.

Ramsayer, G.R. 1979. Seismic stratigraphy, a fundamental exploration tool. Offshore Technology Conference Paper OTC 3568, p. 1859-1862.

Robertson Research. 2004. Nova Scotia Shelf: Biostratigraphic and Sequence Stratigraphic Correlation of the Early Cretaceous Strata in Seven Wells - Report No.6620/Ib. Canada-Nova Scotia Offshore Petroleum Board File SR(E) 2004-1, 47 p.

Rona, P.A. 1969. Linear “lower continental rise hills” off Cape Hatteras. Journal of Sedimentary Petrology, v. 39, p. 1132-1141.

Sangree, J.B. and Widmier, J.M. 1979. Interpretation of depositional facies from seismic data. Geophysics, v. 44, p. 131-160.

Schlee, J.S., Poag, C.W. and Hinz, K. 1985. Seismic stratigraphy of the continental slope and rise seaward of Georges Bank. in C.W. Poag, ed., Geologic evolution of the United States Atlantic margin: New York, Van Nostrand, p. 265-292.

Shannon, P. M, Stoker, M. S., Praeg, D., van Weeringc, T.C.E., de Haasc, H., Nielsend, T., Dahlgrene, K.I.T., and Hjelstuenf, B.O. 2005. Sequence stratigraphic analysis in deep-water, underfilled NW European passive margin basins. Marine and Petroleum Geology, v. 22, p. 1185–1200.

Shell Canada Reources Limited. 1983. Well history report Shell et al. Shubenacadie H-100. 115 p.

Shimeld, J., 2004, A comparison of salt tectonic subprovinces beneath the Scotian Slope and Laurentian Fan, *in* Post, P.J., Olson, D.L., Lyons, K.T., Palmes, S.L., Harrison, P.F., and Rosen, N., eds., Salt–sediment Interactions and Hydrocarbon Prospectivity: Concepts, Applications, and Case Studies for the 21st Century. 24th Annual Gulf Coast Section of the Society of Economic Paleontologists and Mineralogists Foundation Bob F. Perkins Research Conference, Houston, Texas, Dec. 5-8, 2004, p. 502-532.

Shimeld, J.W., Warren, S.N., Mosher, D.C., and MacRae, R.A. 2003. Tertiary-aged megaslumps under the Scotian Slope, south of the Lahave Platform, offshore Nova Scotia (abs.). Geological Society of America, Northeastern Section Conference, Halifax, April, 2003, Program with Abstracts v. 35, no. 3.

Steeves, G.B. 1984. Well history report Petro-Canada et al. Bonnet P-23. 198 p.

Steeves, G.B. 1985a. Well history report Petro-Canada et al. Albatross B-13. 143 p.

Steeves, G.B. 1985b. Well history report Petro-Canada et al. Shelburne G-29. 116 p.

Stoker, M.S., Praeg, D., Hjelstuen, B.O., Laberg, J.S., Nielsen, T., and Shannon, P.M. 2005. Neogene stratigraphy and the sedimentary and oceanographic development of the NW European Atlantic margin. Marine and Petroleum Geology, v. 22. p. 977-1005.

Stow, D.A.V., Hernández-Molina, F.J., Llave, E., Sayago-Gil, M., Díaz del Río, V., and Branson, A. 2009. Bedform-velocity matrix: The estimation of bottom current velocity from bedform observations. Geology, v. 37, p. 327-330.

Swift, S.A., Ebinger, C.J., and Tucholke, B.E., 1986, Seismic stratigraphic correlations across the New England Seamounts, western North Atlantic Ocean: Geology, v. 14, p. 346-349.

Swift, S.A., 1987, Late Cretaceous-Cenozoic development of outer continental margin, southwestern Nova Scotia: Bulletin of American Association of Petroleum Geologists, v. 71, p. 678-701.

Thomas, F.C. 2001. Cenozoic micropaleontology of three wells, Scotian Shelf and Slope. Geological Survey of Canada Open File 4014, 42 p.

Thomas, F.C., 2005, Oligocene benthic foraminifera from the Paleogene Wenonah Canyon, Scotian Shelf- normal versus canyon assemblages: Atlantic Geology, v. 41, p 1-16.

Tucholke, B.E., 1979, Relationships between acoustic stratigraphy and lithostratigraphy in the western North Atlantic basin, in Tucholke, B.E., Vogt, P.R., and others, Initial reports of the Deep Sea Drilling Project, v. 43, p. 827-846.

Tucholke, B. E., and Mountain, G.S. 1979. Seismic stratigraphy, lithostratigraphy and paleosedimentation patterns in the North American Basin, Edited by M. Talwani, W. Hay, and W. B. F. Ryan, Deep Drilling Results in the Atlantic Ocean: continental margins and paleoenvironment, American Geophysical Union Maurice Ewing Series, 3: 58-86.

Tucholke, B. E., and Mountain, G.S. 1986. Tertiary paleoceanography of the western North Atlantic Ocean. In The Geology of North America, Vol. M, The Western North Atlantic Region (ch. 38), Edited by Vogt, P.R. and Tucholke, B.E., Geological Society of America, Boulder, CO, p. 631–650.

Twichell, D.C., Chaytor, J.D., ten Brink, U.S., and Buczkowski, B. 2009. Morphology of late Quaternary submarine landslides along the U.S. Atlantic continental margin. Marine Geology, v. 264, p. 4-15.

Uchupi, E., and Austin, J.A. 1979. The geological history of the passive margin off New England and the Canadian Maritime provinces. Tectonophysics, v. 59, p. 53-69.

Uchupi, E. and Swift, S. A. 1991. Plio-Pleistocene slope construction off western Nova Scotia, Canada. Cuadernos de Geologia Iberica, Special Issue no. 15, p.15-35.

Vecsie. A. and Hoppie, B.W. 1996. Sequence stratigraphy and diagenesis of the Miocene-Oligocene below the New Jersey continental slope: Implications of physical properties and mineralogical variations. Proceedings of the Ocean Drilling Program, Scientific Results, v. 150, p. 361- 376.

Vorren, T.O. and Laberg, J.S. 1997. Trough mouth fans- Palaeoclimate and ice-sheet monitors. Quaternary Science Reviews, v. 16, p. 865-881.

Wade, J.A. and MacLean, B.C. 1990. The Geology of the Southeastern Margin of Canada, Part 2: Aspects of the Geology of the Scotian Basin from Recent Seismic and Well Data. In Geology of the continental margin off eastern Canada. Edited by M.J. Keen and G.L. Williams. Geological Survey of Canada, Geology of Canada no. 2, p.190-238.

Wade, J. A., MacLean, B. C., and Williams, G. L. 1995. Mesozoic and Cenozoic stratigraphy, eastern Scotian Shelf: New interpretations. Canadian Journal of Earth Sciences, v. 32, p. 1462-1473.

Wise, S.W. and van Hinte, J.E. 1987. Mesozoic-Cenozoic depositional environments revealed by Deep Sea Drilling Project Leg 93 Drilling on the continental rise off the eastern United States: cruise summary, In: Initial Reports of the Deep Sea Drilling Project, v. 93, p. 1367-1423.

Chapter 3: Middle to Late Miocene Slope Failure and the Generation of a Regional Unconformity Beneath the Western Scotian Slope, Eastern Canada*

3.1 Introduction

Deepwater erosional unconformities are attributed to either down-slope or along-slope processes. Down-slope processes include the spectrum of gravity-driven flows associated with sediment transport into deeper parts of a basin that lead to the formation of failure scars, gullies, channels and canyons (Stow and Mayall, 2000). Along-slope erosion processes are associated with bottom-current activity when current velocities exceed the threshold of deposition and form erosional terraces, abraded surfaces, contourite channels, moats and furrows (Hernández-Molina et al., 2008). Determination of the processes that formed such erosional surfaces, whether predominantly down-slope, along-slope, or mixed, has implications for understanding controls on margin evolution, paleoceanography, and sequence stratigraphy.

The global greenhouse to icehouse transition that occurred during the middle Cenozoic (Late Eocene to Middle Miocene) marked a major shift in the geological and oceanographic conditions in the northwest Atlantic Ocean (Miller et al., 2009). During this transition, strong contour currents developed (Tucholke and Mountain, 1986) and sediment input to the North American Basin increased (Poag and Ward, 1993). These events were coeval with the development of regional unconformities within the basin and along the basin margins (Ebinger and Tucholke, 1988; Locker and Laine, 1992). In many cases, the relationship between unconformities on the continental rise and slope is unclear. Seismic reflection data from the southwestern Scotian Slope and Rise reveal a previously undocumented, widespread erosional unconformity overlain by large-scale mass-transport deposits (MTDs). Recent studies have shown that the basal surfaces of submarine mass movements can severely erode underlying strata through processes such

as basal shear and erosion by rafted, intact blocks (Frey-Martínez et al., 2006; Gee et al., 2005). The purpose of this paper is to describe the seismic geomorphology of the erosion surface and determine the relative importance of submarine mass-movement in its formation.

3.2 Study area and geological setting

The study area is the continental slope and rise off southwestern Nova Scotia, Canada (Figure 3.1). The passive Scotian margin is part of the Scotian basin, a 1200 km long basin offshore Nova Scotia that formed during Late Triassic and Early Jurassic rifting of Pangea and the opening of the Atlantic Ocean (Wade and MacLean, 1990). Syn-rift evaporites (Argo Fm) were deposited throughout the basin forming a significant salt province (Shimeld 2004). A major carbonate bank (Abenaki Fm) developed in the Jurassic, the steep buried edge of which trends sub-parallel to the modern shelf break (Figs. 1- 2). Cenozoic age deposits in the basin are assigned to the Banquereau (Late Cretaceous to Pliocene) and Laurentian (Pleistocene to Recent) formations (Jansa and Wade, 1975). Apart from Quaternary deposits, little is known about the Cenozoic history of the outer Scotian margin (Piper, 2005). Most studies have focused on the central Scotian shelf and upper slope area where the density of hydrocarbon wells and seismic reflection coverage is greatest (e.g. Wade et al., 1995; Fensome et al., 2008). These studies show that localized progradation of depositional lobes and progressively deeper canyon incision on the upper slope during periods of relative sea-level lowstands dominated sedimentation in the area during the Cenozoic. On the lower continental slope and rise east of the study area, Swift (1987) and Ebinger and Tulcholke (1988) reported a number of erosional unconformities in seismic reflection data and suggested a bottom current origin with inferred ages of Oligocene, Lower Miocene, Middle Miocene, and Pliocene.

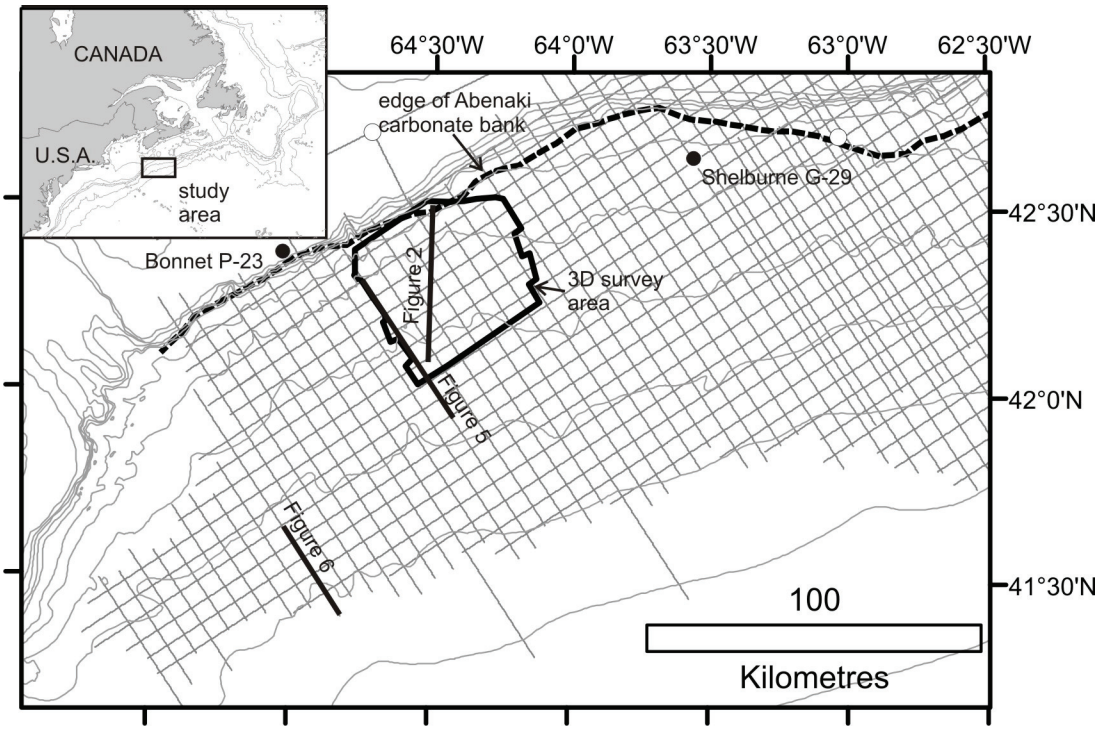

Figure 3.1 Map of the study area showing locations of 3D and 2D seismic reflection data, hydrocarbon exploration wells used for age control, and figure locations. The edge of the buried Abenaki carbonate bank is shown by a dashed line.

3.3 METHODS

This study uses 2D and 3D marine multichannel seismic reflection data, along with biostratigraphic information from hydrocarbon exploration wells (Figure 3.1). Recent biostratigraphic analysis on the Shelburne G-29 well (Fensome et al. 2008) and biostratigraphic data from the Bonnet P-23 well (Bujak Davies Group, 1988) provide age control.

The 2D seismic reflection dataset used in this study is a regional grid acquired by TGS-Nopec Geophysical Company in 1998 and 1999 (Shimeld 2004). Line spacing is 8 km in the strike orientation and 4 to 8 km in the dip orientation. Hydrophone streamer length was 6 to 8 km. The acoustic source for the surveys was a 130 L tuned airgun array and

the data are 80 to 106 fold. The 3D seismic reflection dataset was acquired in 2001 for EnCana Corporation (Mosher and Campbell, 2011). The survey covered an area of approximately 1790 km^2, termed the Barrington exploration block. The survey consisted of 98 lines spaced 450 m apart. Each sailing line consisted of eight hydrophone streamers 6000 m long with 240 channels per streamer. Channel separation was 25 m. The acoustic source was a 62 L tuned airgun array generating a peak frequency of 70 Hz and a bandwidth of 5 – 100 Hz, implying about 5.5 m vertical resolution. Bin spacing is 12.5 m by 12.5 m. Processing of both datasets was conducted by the data owner prior to this study. For the purpose of this study, the authors were given access to the upper 2 s two-way travel time (twtt) below the seafloor of the 3D seismic dataset. Seismic reflection data were interpreted in Seismic Micro Technologies Kingdom Suite and Schlumberger GeoFrame software packages. For the 3D seismic dataset, reflection horizons were mapped and interpolated to produce continuous surfaces. Seismic reflection structure, amplitude, and dip of maximum similarity attributes were used to interpret the seismic geomorphology. The dip of maximum similarity is a geometric attribute computed by first determining semblance of adjacent traces over a sliding time window and range of dips, and then extracting the dip of maximum semblance within the time window. It is useful for identifying structural discontinuities. The 2D seismic reflection data were used to map the extent of depositional elements, interpret regional structure, and to correlate events to the Shelburne G-29 and Bonnet P-23 wells. For estimates of volume and other dimensions, two-way travel time was converted to depth using a sound velocity of 2000 m/s based on velocity data from the Shelburne G-29 well.

3.4 Results

One of the most striking features in the study area is a widespread, non-conformable reflection that is recognized below the modern slope and rise (Fig 3.2). The horizon truncates underlying seismic reflections in several places, while overlying reflections onlap the surface. Over much of the study area, the horizon is the product of multiple erosion events, formed where horizons coalesce to form a single surface at the resolution

of the seismic data. Laterally and basinward, the coalesced reflections separate and diverge, and it is possible to infer processes that were active during formation of the unconformity. The following sections describe the seismic reflection character and estimated age of the unconformity and the onlapping deposits.

3.4.1 Seismic reflection character of the unconformity

On seismic reflection profiles, the unconformity appears as a strong, negative reflection (Figure 3.2). Shelfward, the erosional surface becomes conformable and its erosional nature is less apparent. Laterally and basinward, the erosional nature of the unconformity is recognized as far west and south as the data extent, and at least as far east as the Shelburne G-29 well. The regional geomorphology of the unconformable surface is shown in Figure 3.3. The surface dips steeply to the south seaward of the edge of the Abenaki carbonate bank. Downslope, a second regional change in gradient occurs at the southern edge of the Scotian Slope salt province (Shimeld 2004). Here, a major arcuate escarpment marks the northern edge of a buried submarine embayment. A series of broad gullies incise the surface and lead to the embayment.

Maps of 3D time-structure overlain with dip of maximum similarity show evidence of pronounced down-slope erosion (Figure 3.4). In the southwestern corner of the 3D dataset, a long arcuate escarpment more than 220 m high corresponds to the northern edge of the submarine embayment. Down-dip of the escarpment, the surface relief is slightly mounded and there are no lineations to indicate flow direction. Immediately north and east of the escarpment, long, linear grooves oriented down-dip characterize much of the unconformity. The grooves are up to 14 km long, 400 m wide, and 30 m deep. In the 3D data area, five domal structures are present on the unconformity and are the sub-surface expression of underlying salt diapirs. In some cases, the linear grooves pass over the diapirs and in other instances, they deviate around the features. Up-dip from the grooved zone, the seabed is scoured, with numerous smaller arcuate escarpments 0.5 to 4 km wide and 50 m high. This area passes up-dip to a zone that is much smoother

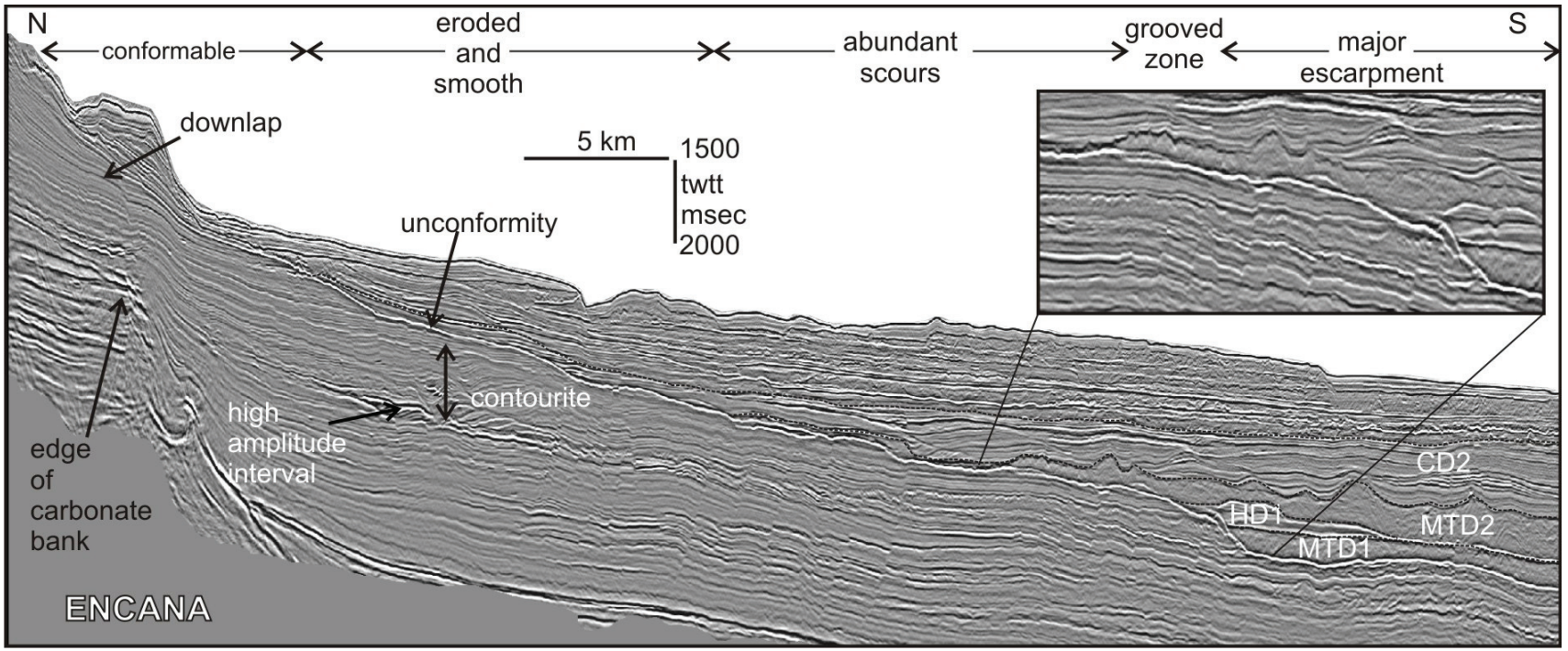

Figure 3.2 Dip-oriented seismic reflection profile from the 3D seismic dataset. An extensive erosional unconformity is imaged below the modern lower slope and rise. Inset shows enlarged portion of line. Line location is shown in Figures 3.1 and 3.4 (Data courtesy of EnCana Corp.).

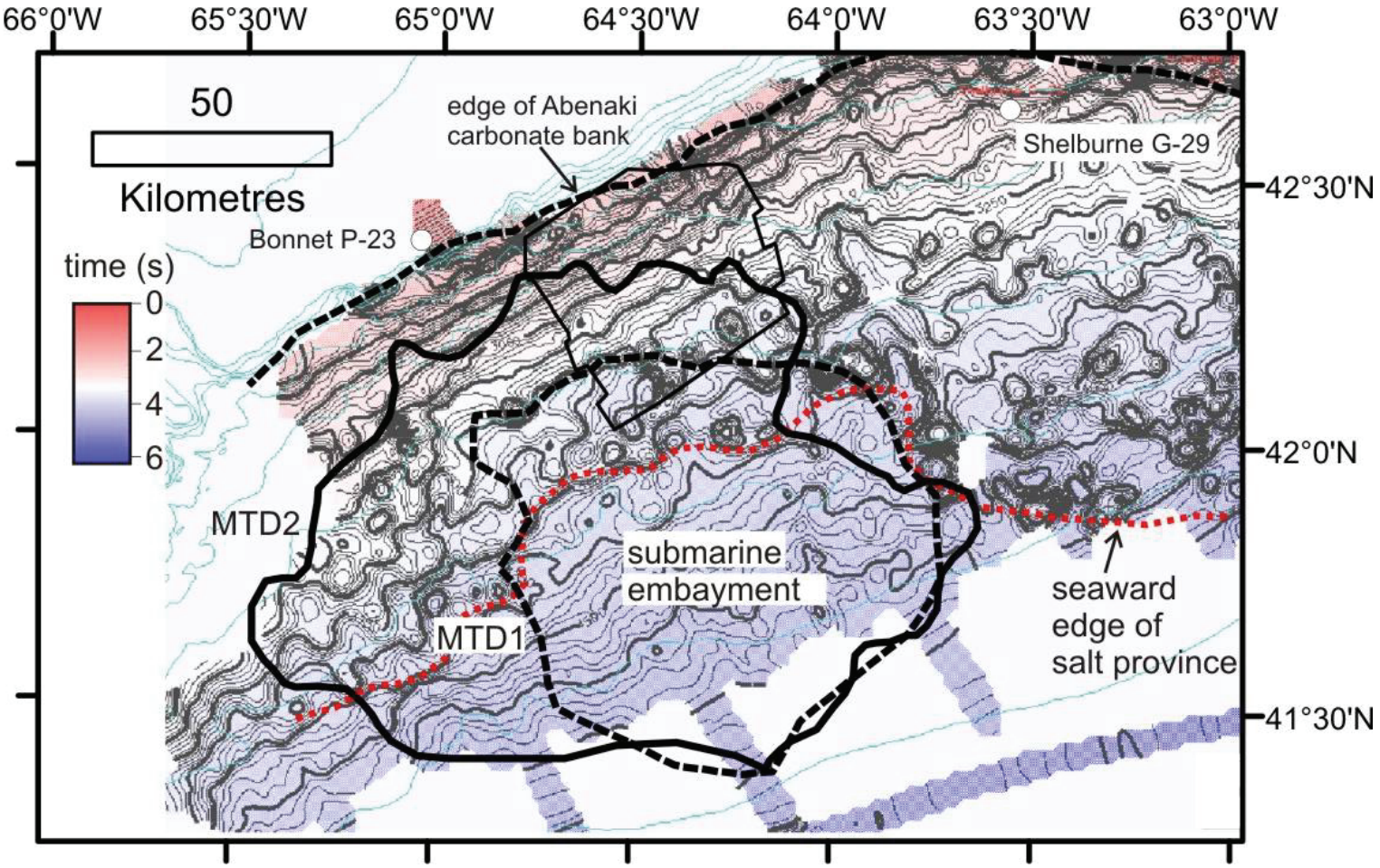

Figure 3.3 Regional time-structure map of the unconformable surface. Note the submarine embayment developed seaward of the salt province. The extents of two major mass-transport deposits (MTD1 and MTD2) are shown in solid and dashed lines.

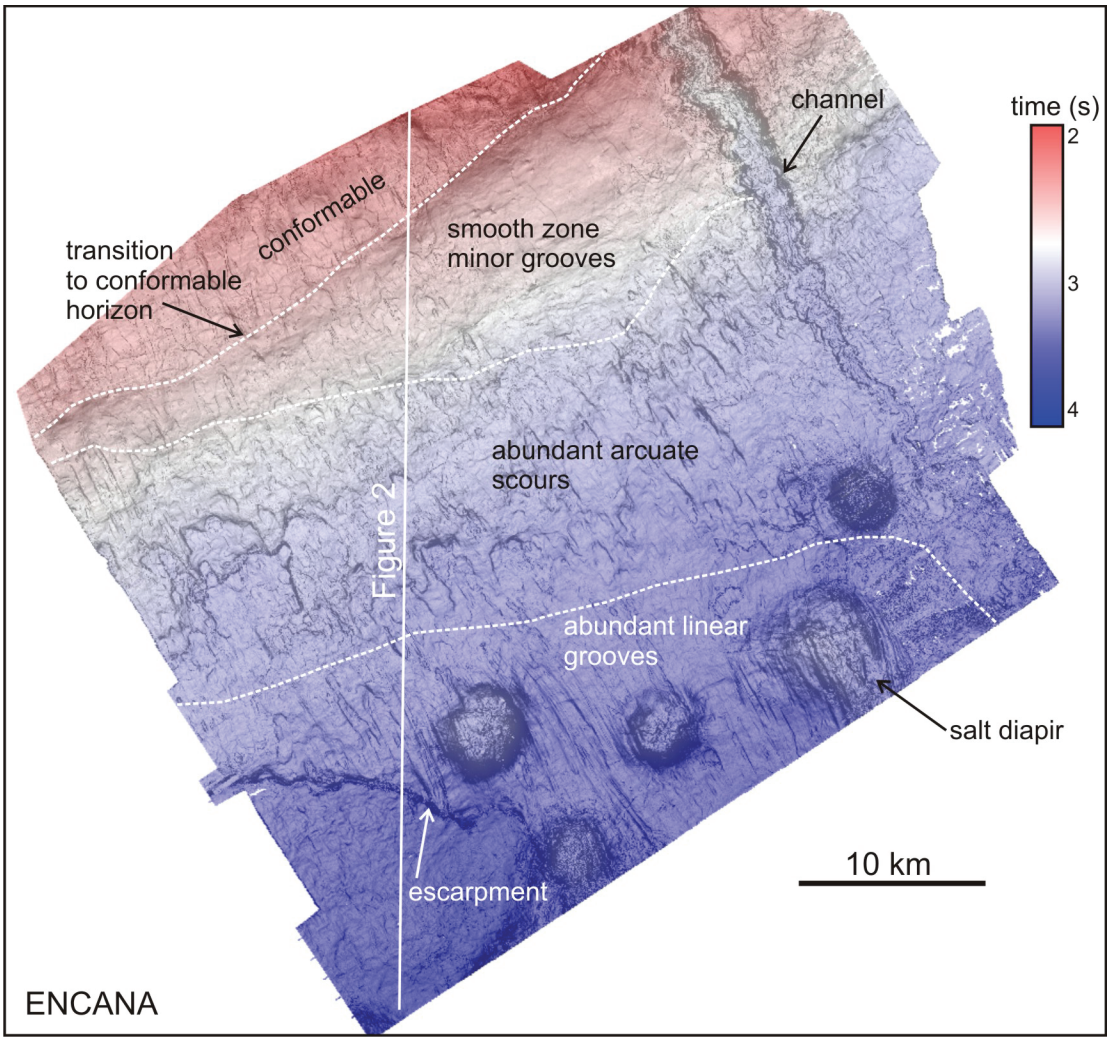

Figure 3.4 Seismic geomorphology (time-structure overlain with dip of maximum similarity) of the unconformity showing evidence of extensive down-slope erosion. Map area located on Figure 3.1 (Data courtesy of EnCana Corp.).

with some subtle scars. The shelfward transition from erosional to conformable character of the surface is marked by a sharp change in gradient. In the eastern part of the 3D seismic dataset, a channel has eroded down to the level of the unconformity. The channel is up to 3 km wide and 370 m deep. The channel walls are scalloped and a sinuous channel thalweg is apparent.

The unconformity marks the top of a reflection package that thins significantly eastward towards the Shelburne G-29 well, with several prominent reflections coalescing at the well location. Biostratigraphic analysis from the well indicates a Late Miocene (Messinian) to Late Eocene (Bartonian) unconformity (Fensome et al. 2008) at the same stratigraphic level as the coalesced reflections. Correlation of the upslope, conformable portion of the erosional surface to the Bonnet P-23 well corresponds to a Middle Miocene age (Table 1), although reflection correlation across the shelf break to this well is tenuous.

Table 3.1 Estimated ages of reflection horizons and units presented in this study.

Horizon/Unit	**Maximum Age**	**Minimum Age**
Contourite deposit 2 (CD2)	Messinian	Late Pliocene
Mass-transport deposit 2 (MTD2)	Messinian	Messinian
Channel (top HD1)	Messinian	Messinian
Hemipelagic interval (HD1)	Messinian	Messinian
Mass-transport deposit 1 (MTD1)	Middle Miocene	Messinian
Contourite deposit 1 (CD1)	Middle Miocene	Messinian
Unconformity	Middle Miocene	Messinian

3.4.2 Seismic reflection character above the unconformity

Five depositional elements were mapped that onlap the unconformity (Figure 3.2, Figure 3.5 – 3.6). The first or oldest deposit has reflection characteristics typical of a separated drift (Faugères et al. 1999), and shows evidence of upslope and eastward migration. This interval is termed CD1. This deposit is recognized in the extreme southwest portion of the study area and possibly correlates with the sediment drift below the unconformity in the 3D dataset (Figure 3.2). A major mass transport deposit (MTD1) overlies CD1 and has typical chaotic to transparent internal reflection character, irregular surface morphology, and mounded and depression-filling geometry. This initial mass transport deposit covers an area of 6200 km^2 and represents a volume of ~300 km^3 of failed material (Figure 3.3). In 3D seismic data, the onlap of MTD1 corresponds with the large escarpment in the southwest portion of the survey and the deeply grooved zone. An

interval of parallel to occasionally wavy, low amplitude reflections (HD1), likely representing hemipelagic and turbidite deposition, overlies MTD1. The deposition of HD1 was concomitant with the development of a large channel imaged in the 3D seismic data (Figure4). West of the large channel, much of HD1 was eroded and redeposited by the fourth element, another mass transport deposit (MTD2) which is much thicker than MTD1, covers an areal extent of 10 500 km^2 and represents a failure volume of ~680 km^3 (Figure 3.3). The failure comprises large rafted blocks up to 5 km long. MTD2 onlaps the unconformity in the intensely scoured zone. A thick contourite interval (CD2) was deposited above MTD2. The onlap of CD2 with the unconformity corresponds to the smooth, up-dip portion of the unconformity in the 3D dataset.

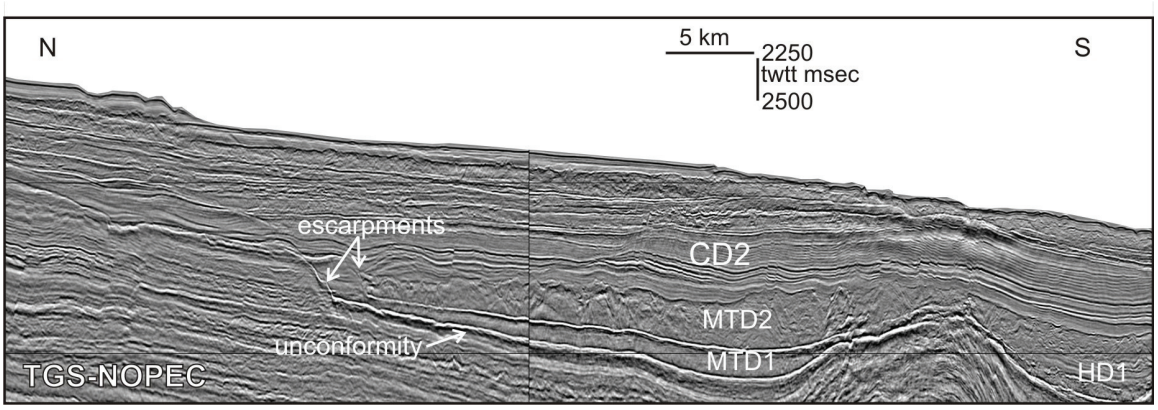

Figure 3.5 Dip-oriented seismic reflection profile from the continental rise showing major escarpments associated with MTD1 and MTD2. Line location is shown in Figure 3.1 (Data courtesy of TGS-Nopec).

Estimated ages of units that onlap the erosional unconformity are based on correlation with the Shelburne G-29 (Figure 3.7) and Bonnet P-23 wells (Table 1). CD1 directly overlies the erosional unconformity in the southwestern part of the study area and possibly underlies the unconformity in the 3D seismic area. Because of this complicated stratigraphic relationship, CD1 is tentatively assigned a Middle to Late Miocene age. In all areas examined, MTD1 immediately overlies CD1 or the unconformity and is therefore younger. HD1, the large channel, and MTD2 are all Late Miocene age and intersect the Shelburne G-29 well at 2200 m- 2320 m, 2190 m, and 2000 m respectively. The second contourite interval, CD2, intersects the well from 2000m – 1660m and is latest Miocene to Late Pliocene age (Figure 3.7).

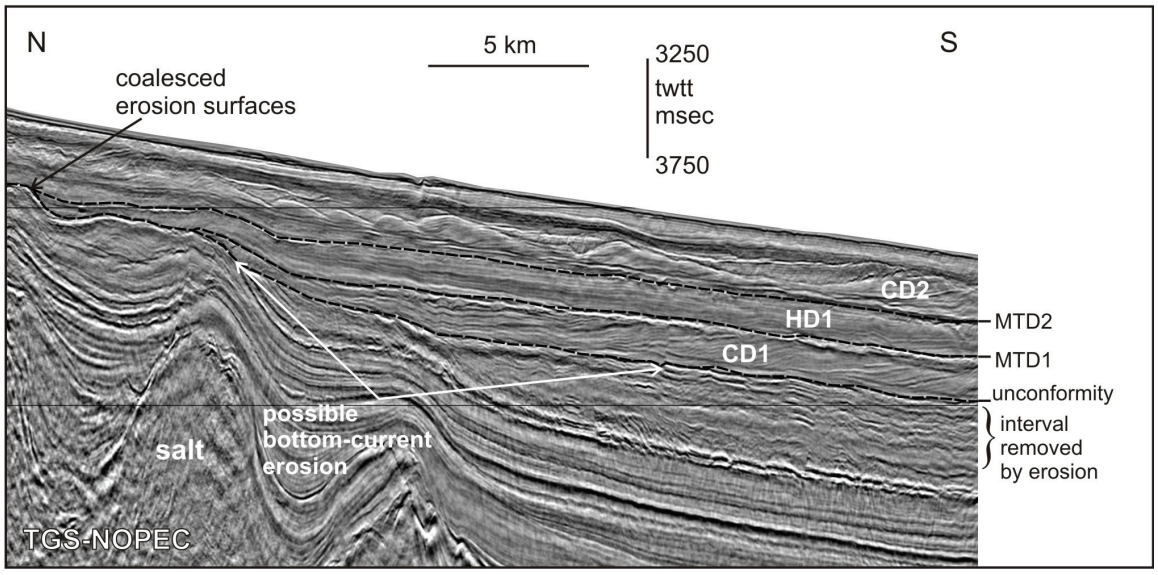

Figure 3.6 Dip-oriented seismic reflection profile from the southwestern part of the study area. The earliest indication of erosion along the unconformity is associated with development of a contourite (CD1) and is enhanced at the edge of a salt diapir. Erosion surfaces merge up-dip to form a single horizon at data resolution. Line location is shown in Figure 3.1 (Data courtesy of TGS-Nopec).

3.5 Discussion

The earliest indication of erosion along the unconformity occurs at the basal surface of contourite interval CD1 (Figures 3.6-3.7). In the western part of the study area, reflections underlying the base of CD1 are truncated and suggest as much as 200 m of sediment was removed from the lower slope, possibly eroded by bottom currents enhanced where the seabed relief changes at the edge of the salt diapirs (Figure 3.6). A second phase of erosion was coeval with the deposition of MTD1 (Figure 3.6). It is likely that failure of contourite deposits in CD1 contributed to the deposits in MTD1 (Figure 3.2). MTD1 is confined to the submarine embayment seaward of the salt province and has a characteristic lower slope escarpment. The deeply grooved surface updip from the escarpment in the 3D dataset suggests some retrogressive failure and translation of intact blocks during formation of MTD1, however it is not possible to determine the extent of

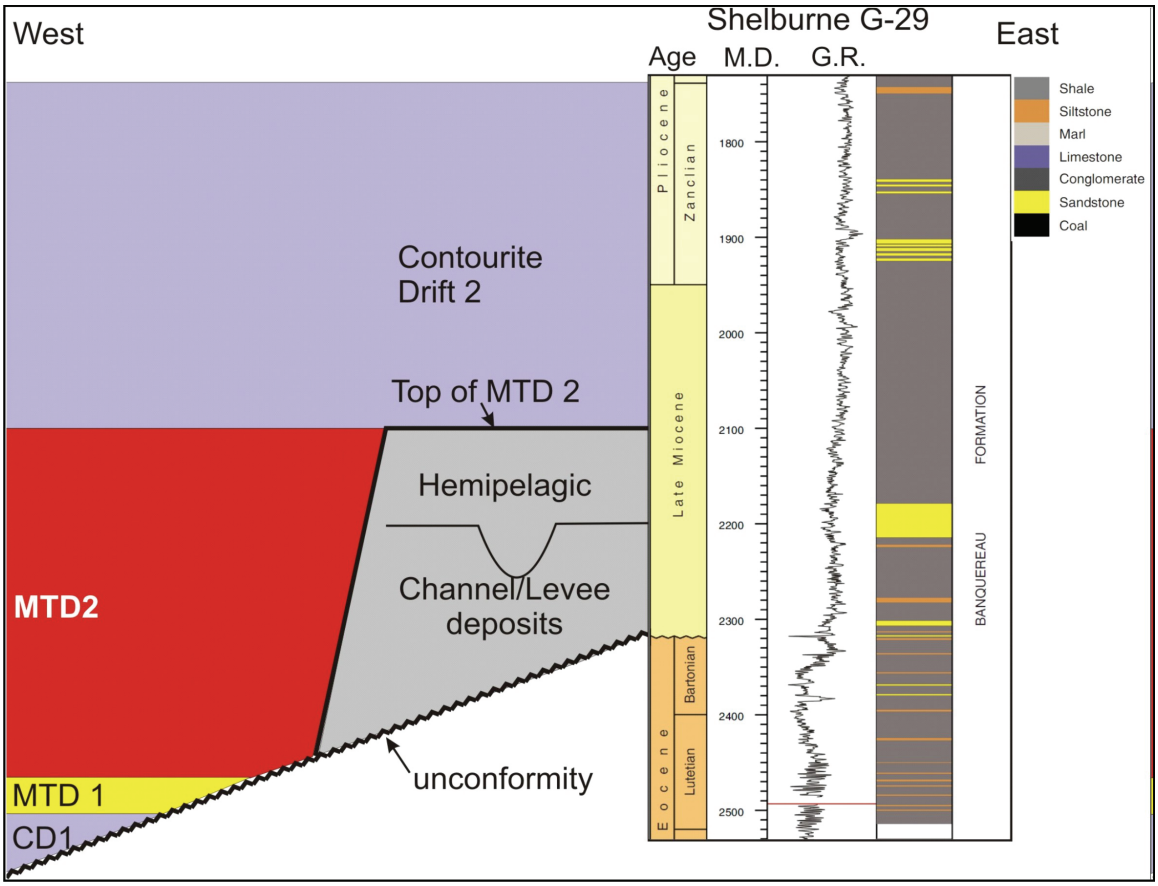

Figure 3.7- A schematic transect from the western part of the study area to the Shelburne G-29 well that illustrates the stratigraphic relationships between the various depositional units discussed in the text and the underlying unconformity. Biostratigraphy is from Fensome et al. (2008).

retrogression because of later erosion by MTD2. The failure of MTD2 was more extensive than MTD1 and transported a large amount of sediment deeper into the basin. The failed material comprised channel and levee sediments of HD1, as well as some contourite material from CD2. MTD2 had a significant retrogressive component and failure deposits are recognized both upslope and down slope of the edge of the salt province.

The 3D seismic reflection data provide the most definitive evidence of the processes responsible for the formation of the erosional surface. The data show that most of the erosion is attributed to mass movement and to a lesser extent, channel formation. MTD1

and MTD2 rank among the largest mass transport deposits reported in the literature (Legros, 2002). Both MTDs were initiated on the continental rise based on the location of the largest failure escarpments. These escarpments are well seaward of the steep Abenaki carbonate bank edge which appears to control the position of the shelf break to this day. More recent failures of Quaternary age were sourced from the steep upper slope area (Mosher and Campbell, 2011). However, in the case of the two MTDs in this study, salt tectonics and perhaps contour current activity played a greater role in slope failure. There is a strong spatial relationship between the distribution of the MTDs and the limit of the salt diapir province (Figure 3.3). Shimeld (2004) reported rejuvenated apparent salt uplift in the study area beginning in the late Paleogene and continuing to the Pliocene. In the study area, contour currents served to build contourite drifts and possibly erode the seabed at topographic highs. It is possible that undercutting by contour currents, supplemented by salt movement, oversteepened the lower slope in this area and contributed to failure.

3.6 Conclusions

This study demonstrates that a widespread, Miocene unconformity preserved below the western Scotian margin is the primarily the product of regional mass-wasting, although erosion via channel incision was important locally and contour currents may have eroded the slope seaward of the 3D survey area. The unconformity appears to be a highly diachronous surface, formed by the coalescing of several erosion surfaces over the course of millions of years. Submarine mass-movements, among the largest reported in the literature, produced large escarpments on the lower slope, eroded long linear grooves at their bases, and created several arcuate scours as they retrogressed. Despite the presence of a steep upper slope in the study area, the unconformity is not due to erosion and bypass of the upper slope, but rather erosion and seabed failure initiated on the continental rise, with salt tectonics and contour current activity providing possible trigger mechanisms.

3.7 Acknowledgements

The authors would like to express their appreciation to EnCana Corp. and TGS-Nopec Geophysical Co. L.P. for data access. Reviews by David Twichell, Serge Berné, David Piper, and John Shimeld improved the manuscript and are appreciated.

3.8 References cited in Chapter 3

Bujak Davies Group 1988. Palynological Analysis of the Interval 440-3950 M, Bonnet P-13, Scotian Shelf. Geological Survey of Canada Open File Report 1858, 19 p

Ebinger C.A. and Tucholke B.E. 1988. Marine Geology of the Sohm Basin, Canadian Atlantic Margin. Bulletin of American Association of Petroleum Geologists, v. 72, p. 1450-1468.

Fensome, R.A., Crux, J.A., Gard, I.G., MacRae, R.A., Williams, G.L., Thomas, F.C., Fiorini, F., and Wach, G., 2008, The last 100 million years on the Scotian Margin, offshore eastern Canada: an event-stratigraphic scheme emphasizing biostratigraphic data: Atlantic Geology, v. 44, p. 93-126.

Frey-Martínez, J., Cartwright, J., and James, D. 2006. Frontally confined versus frontally emergent submarine landslides: a 3D seismic characterization. Marine and Petroleum Geology, v. 23, p. 585-604.

Gee, M.J.R., Gawthorpe, R.L., and Friedmann J.S. 2005. Giant striations at the base of a submarine landslide. Marine Geology, v. 214, p. 287-295.

Hernández-Molina F.J., Llave E., and Stow D.A.V. 2008. Continental slope contourites. In: Rebesco, M. and Camerlenghi, A. (Eds.), Contourites. Elsevier. 379-408.

Jansa L.F. and Wade J.A. 1975. Geology of the continental margin off Nova Scotia and Newfoundland. Geological Survey of Canada Paper 74-30, Offshore geology of eastern Canada, Vol. 2, p. 51-105.

Legros, F. 2002. The mobility of long-runout landslides. Engineering Geology, v. 63, p. 301-331.

Locker S.D. and Laine E.P. 1992. Paleogene-Neogene depositional history of the middle U.S. Atlantic continental rise: mixed turbidite and contourite depositional systems. Marine Geology, v. 103, p. 137–164.

Mosher D.C. and Campbell D.C. 2011. The Barrington submarine landslide, western Scotian Slope. In: Shipp, C., Weimer, P, and Posamentier, H. (Eds.), Mass-Transport Deposits in Deepwater Settings. SEPM Special Publication No. 96, p. 151-159.

Piper, D.J.W. 2005. Late Cenozoic evolution of the continental margin of eastern Canada. Norwegian Journal of Geology, v. 85, p. 231-244.

Shimeld, J., 2004, A comparison of salt tectonic subprovinces beneath the Scotian Slope and Laurentian Fan, *in* Post, P.J., Olson, D.L., Lyons, K.T., Palmes, S.L., Harrison, P.F., and Rosen, N., eds., Salt–sediment Interactions and Hydrocarbon Prospectivity: Concepts, Applications, and Case Studies for the 21st Century. 24th Annual Gulf Coast Section of the Society of Economic Paleontologists and Mineralogists Foundation Bob F. Perkins Research Conference, Houston, Texas, Dec. 5-8, 2004, p. 502-532.

Stow D.A.V. and Mayall M. 2000. Deep-Water Sedimentary Systems: New Models for the 21st Century. Marine and Petroleum Geology, v. 17, p. 125-135.

Swift, S.A., 1987, Late Cretaceous-Cenozoic development of outer continental margin, southwestern Nova Scotia: Bulletin of American Association of Petroleum Geologists, v. 71, p. 678-701.

Wade, J.A. and MacLean, B.C. 1990. The Geology of the Southeastern Margin of Canada, Part 2: Aspects of the Geology of the Scotian Basin from Recent Seismic and Well Data. In Geology of the continental margin off eastern Canada. Edited by M.J. Keen and G.L. Williams. Geological Survey of Canada, Geology of Canada no. 2, p.190-238.

Wade, J.A., MacLean, B.C., and Williams, G.L. 1995. Mesozoic and Cenozoic stratigraphy, eastern Scotian Shelf: New interpretations. Canadian Journal of Earth Sciences, v. 32, p. 1462-1473.

Chapter 4: Geophysical Evidence for Bottom Current Activity Throughout the Cenozoic from the Continental Margin off Nova Scotia, Canada

4.1 Introduction

Contourite depositional systems develop when along-slope geological processes, in part driven by contour-following bottom currents, dominate over down-slope geological processes, driven by gravity (Locker and Laine 1992; Hernandez-Molina et al 2008; Mulder et al. 2008; Hernandez-Molina et al. 2010). In the North Atlantic, contour-following bottom currents flow southward and westward along the continental margin of North America (Worthington 1976; Pickart 1992; Schmitz and McCarthy 1993). Evidence of interaction of these bottom currents with the seabed during the Cenozoic is demonstrated by the widespread presence of contourite drifts that flank the continental margins, from the Gulf of Cadiz to the northern Antilles margin (Figure 4.1a) (Heezen et al. 1966; McCave and Tucholke 1986; Faugères et al. 1993; Wold 1994; Faugères et al. 1999; Faugères et al. 2008). Evidence of bottom current interaction with the seabed is also shown by the development of regional unconformities on the continental slope and rise when bottom current strength was sufficient to hinder deposition or even erode the seabed (Tucholke and Mountain 1979; Mountain and Tucholke 1985; Laberg et al. 2005; Miller et al. 2009).

The paleoceanography of the western North Atlantic is largely based on the analysis of seismic reflection data, supplemented by ocean drilling data, from the United States Atlantic margin (Heezen et al. 1966; Tucholke and Mountain 1979; Mountain and Tucholke 1985; Tucholke and Mountain 1986; McCave and Tucholke 1986). On the U.S. Atlantic margin, bottom current controlled sediment drifts and major erosional periods attributed to strengthened bottom current circulation are recognized from regional 2D seismic data from the continental slope to the lower continental rise. Sediment drift development likely began in the Early Miocene and continued until the Pliocene, occasionally interrupted by pulses of along-slope erosion (Mountain and Tucholke 1985; Locker and Laine 1992). The most extensive Cenozoic erosional pulses resulted in the

formation of regional unconformities A^U (Lower Oligocene), Merlin (Middle Miocene), and Blue (Pliocene) (Tucholke and Mountain 1986; Miller et al. 2009).

Compared to the U.S. Atlantic margin, the Cenozoic paleoceanographic record along the continental margin off Nova Scotia (herein the Scotian margin, Figure 4.1) has not been investigated to the same level of detail, in part due to limited data coverage and in part because of tenuous seismic correlation between the U.S. and Scotian margins. Analysis of the modern bottom current regime along the Scotian margin shows that a southwest flowing western boundary current sweeps the seabed (Smith and Petrie 1982; McCave and Tucholke 1986; Pickart 1992; Pickart et al. 1999). High suspended sediment loads are observed in the nepheloid layer on the Scotian Rise (Amos and Gerard 1979; Biscaye and Eittreim 1977). These currents and high sediment loads suggest that modern conditions are suitable for contourite development. The HEBBLE (High Energy Benthic Boundary Layer Experiment) demonstrated that Holocene contourites are present on the lower Scotian Rise (Nowell and Hollister 1985). Other studies, however, suggest that the Pleistocene geological record is dominated by gravity-driven processes (Hughes-Clarke et al. 1992). Additionally, pre-Quaternary sediment drifts are absent or of limited geographical extent compared to the continental margin to the south and north, although erosional features are recognized on the continental rise (Swift 1987; McCave and Tucholke 1986; Ebinger and Tucholke 1988; McCave et al. 2002). In fact, published maps of the distribution of large contourite drifts in the North Atlantic show that there are no large sediment drifts recognized between the Newfoundland Ridge seaward of the southern Grand Banks, and the Chesapeake Drift seaward of Chesapeake Bay (Figure 4.1a) (McCave and Tucholke 1986; Faugères et al. 1993; Faugères et al. 1999; Faugères et al 2008). This interval is the longest section of North America's Atlantic margin lacking contourite drifts.

This study revisits the issue of the apparent lack of contourite depositional features along the Scotian margin. Analysis of recently acquired two-dimensional (2D) and three-dimensional (3D) seismic reflection data, collected in support of hydrocarbon exploration, reveals that contourite depositional systems *are* extensive along the outer

Scotian Margin (Campbell et al. 2010). The objectives of this paper are to provide new insights into the paleoceanography of the western North Atlantic based on recognition of sedimentary features indicative of contourite depositional systems, as well as new insights into along-slope processes based on interpretations from seismic reflection data. The new geophysical datasets on the Scotian margin allow detailed investigation of contourite depositional systems along the western North Atlantic margin not previously attainable.

4.2 Background and Regional Setting

4.2.1 Geological Setting of Study Area

This study is primarily focused on upper Paleogene and Neogene deposits along the outer Scotian margin in present-day water depths between 200 and 3500 metres below sea level (mbsl) (Figure 4.1). The Scotian margin consists of the continental shelf, slope and rise south of Nova Scotia and forms most of the northern margin of the North American Basin, a large bathymetric depression in the northwest Atlantic Ocean centered on the Bermuda Rise (Figure 4.1) (Jansa et al. 1979). The basin margin formed during the late Triassic and early Jurassic rifting of Pangea and the opening of the Central North Atlantic Ocean (Wade and MacLean 1990). The morphology of the modern Scotian margin includes a >200 km wide continental shelf consisting of transverse troughs and intervening banks, the product of repeated glaciations through the Quaternary (Piper 2005). The shelf break lies at 80-130 mbsl (Mosher et al. 2004) and trends sub-parallel to the coastline for ~1000 km, from Northeast Channel in the west to Laurentian Channel in the east. The present-day slope extends from the shelf break to a decrease in gradient at 2000-2500 mbsl.

Two regional structural features are important for influencing Cenozoic depositional patterns along the outer Scotian margin (McCave et al. 2002). The first is the Jurassic Abenaki carbonate bank that flanks the outer LaHave Platform (Figure 4.1c) (Wade and MacLean 1990). West of 61° 30’ W, the steep buried bank edge follows the approximate

trend of the shelf edge and delimits the interpreted maximum seaward extent of shelf edge progradation throughout the Cenozoic (Campbell and Deptuck In Press). East of 61° 30', the trend of the carbonate bank and LaHave platform changes orientation to the northeast and a major depocenter developed during the Mezozoic below the modern Scotian Shelf. The second feature is a 40-100 km wide belt of shallow salt structures associated with the Triassic Argo Fm (Wade and MacLean 1990; Shimeld 2004) that disrupts the Cenozoic stratigraphy (Figure 4.1c).

Figure 4.1 A) Map of the western North Atlantic showing locations discussed in the text along with the named drifts that flank the continental margin, Eirik Drift (ED), Hamilton Spur (HS), Orphan Spur (OS), Sackville Spur (SP), Newfoundland Ridge (NR), Chesapeake Drift (CD), Hatteras Drift (HD), and Blake Spur (BS). B) Location map of the continental margin off Nova Scotia showing locations discussed in the text. C) Map of data used for this study and major structural elements. Regional 2D seismic reflection data shown as a grid. 3D seismic datasets are shown as white polygons and consist of the Barrington (B), Torbrook (T), and Weymouth (W) survey areas. Exploration wells used for the study are Bonnet P-23 (1), Shelburne G-29 (2), Albatross B-13 (3), Torbrook C-15 (4), Acadia K-62 (5), Shubenacadie H-100 (6), Newburn H-23 (7), and Annapolis G-24 (8). Structural elements were modified from Shimeld (2004).

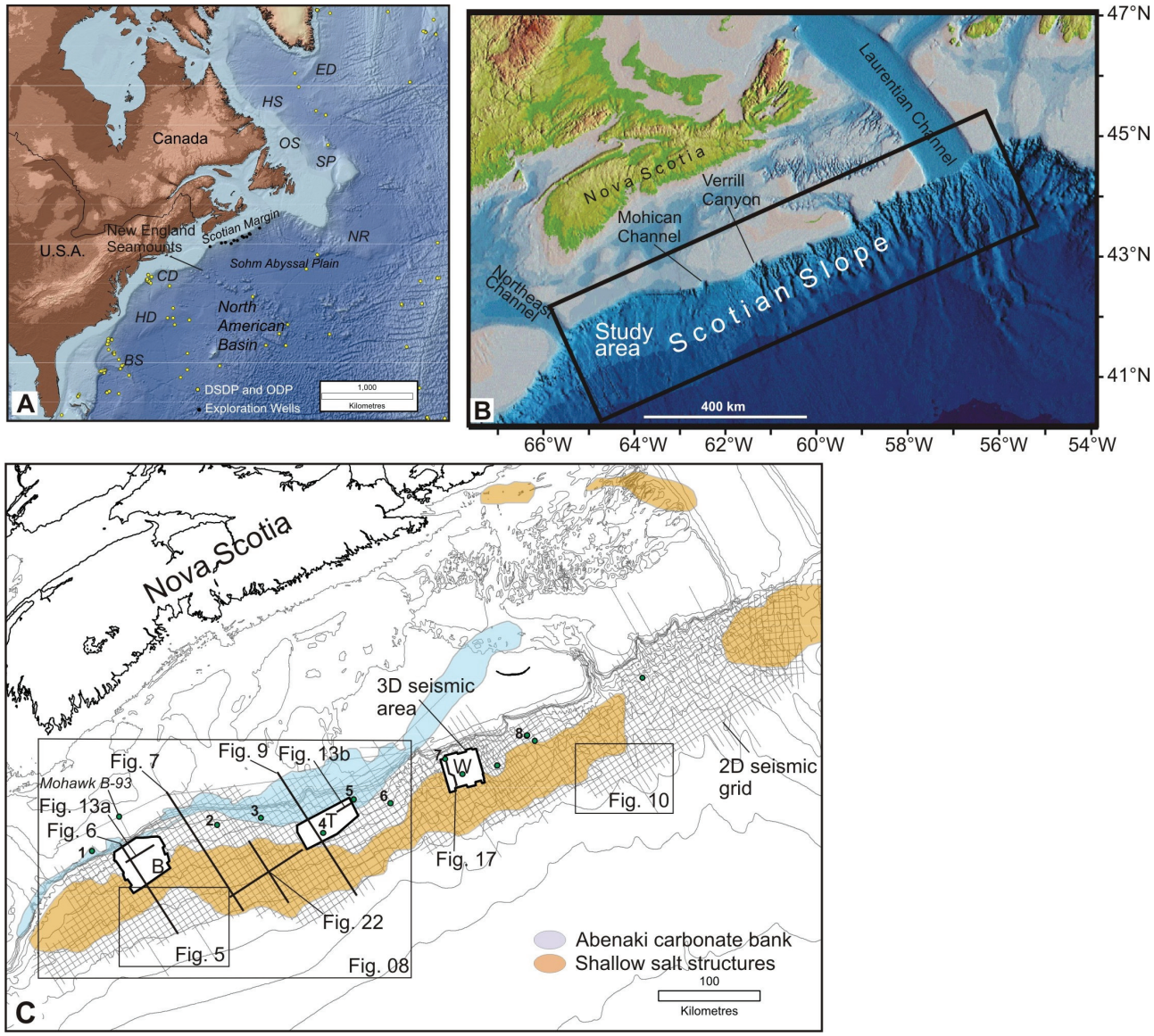
A
Canada
U.S.A.
ED
HS
OS
SP
NR
Scotian Margin
New England Seamounts
Sohm Abyssal Plain
CD
HD
North American Basin
BS
DSDP and ODP
Exploration Wells
1,000
Kilometres
B
Laurentian Channel
Nova Scotia
Verrill Canyon
Mohican Channel
Northeast Channel
Study area
Scotian Slope
400 km
47°N
45°N
43°N
41°N
66°W
64°W
62°W
60°W
58°W
56°W
54°W
C
Nova Scotia
3D seismic area
2D seismic grid
Fig. 7
Fig. 9
Fig. 13b
Mohawk B-93
Fig. 13a
Fig. 6
Fig. 10
Fig. 17
Fig. 22
Fig. 5
Fig. 08
B
W
1
2
3
4
5
6
7
8
Abenaki carbonate bank
Shallow salt structures
100
Kilometres

Upper Paleogene and Neogene deposits on the outer Scotian margin are the distal equivalents of the Upper Cretaceous to Pleistocene Banquereau Formation below the Scotian Shelf (Wade and MacLean 1990; Fensome et al. 2008). Due to a paucity of data, formations along the deep water Scotian margin are not formalized and no detailed lithostratigraphic summary exists. Samples show that the interval is mud-dominated, but like the shelf, has a general coarsening up pattern of deposition. Upper Cretaceous, Paleocene and Lower Eocene chalks, similar age to those on the shelf, are recognized in a number of wells (Fensome et al. 2008). The most detailed published studies of the Cenozoic seismic stratigraphy of the Scotian Slope and Rise off Nova Scotia are by Swift (1987), Ebinger and Tulcholke (1988), and Wade et al. (1995). Because of no direct seismic tie to the well-studied U.S. Atlantic margin, these studies developed Neogene seismic stratigraphies independent from the framework developed along the U.S. margin. Deep water unconformities were interpreted to be produced by bottom current erosion of the continental rise and abyssal plain with inferred ages of Oligocene, Lower Miocene, Middle Miocene, and Pliocene.

4.2.2 The Modern Bottom Current Regime

Several distinct bottom currents flow along the continental margin off Nova Scotia (Figure 4.2). The North Atlantic deep western boundary current (DWBC) moves southward and westward along the continental margin off eastern North America. On the Scotian margin, the DWBC consists of at least three distinct water masses distinguished by their chemical composition, temperature, salinity, and velocity (Pickart 1992; Pickart and Smethie 1998; Smethie et al. 2000). The shallowest, warmest and least dense water mass is Upper Labrador Sea Water (ULSW) which is centred around 700 m water depth and is likely sourced from convection in the southern Labrador Sea. Below this, Classic Labrador Sea Water (CLSW), formed through convection in the Labrador Sea, flows southwestward, centred around 1500 m water depth. The deepest, most dense, and fastest flowing water mass contributing to the DWBC off Nova Scotia, termed overflow water (OW), forms “behind” the Greenland-Iceland-Scotland ridge and overflows into the

North Atlantic, either through the Denmark Strait (Denmark Strait Overflow Water or DSOW) or between Iceland and Scotland (Iceland-Scotland Overflow Water or ISOW).

The Gulf Stream flows northeastward across the Scotian margin. South of the Grand Banks, it contributes to both the North Atlantic Current and a return flow along the Bermuda Rise. Therefore, it is at least a partial deep, mid latitude gyre (Schmitz and McCartney 1992), with an overall clockwise circulation pattern (Laine and Hollister 1982). Although it is primarily a wind-driven current, its deep flow is sufficient to affect the seabed in the northern North American Basin (Laine and Hollister 1982), however its modern mean northern limit is well south of the study area (Figure 4.2). The contribution of the Gulf Stream to the bottom current regime north of the mean Gulf Stream position is less clear. Schmitz and McCartney (1992) propose a second anticlockwise deep gyre north of the Gulf Stream and south of the continental slope that would serve to enhance a DWBC along the Scotian margin. Periodic crossing of the HEBBLE site by warm-cored Gulf Stream rings (clockwise meso-gyres, ~200 km across) caused flow reversals and enhancements, and were implicated as the cause of benthic storms in the area (Weatherly and Kelly 1985; McCave et al. 2002). Pickart et al. (1999) describe the slope water system, a narrow filament of east flowing water resulting from the minor bifurcation of the Gulf Stream south of Nova Scotia, which acts as a coupled system with the westward flowing DWBC adjacent to the continental margin.

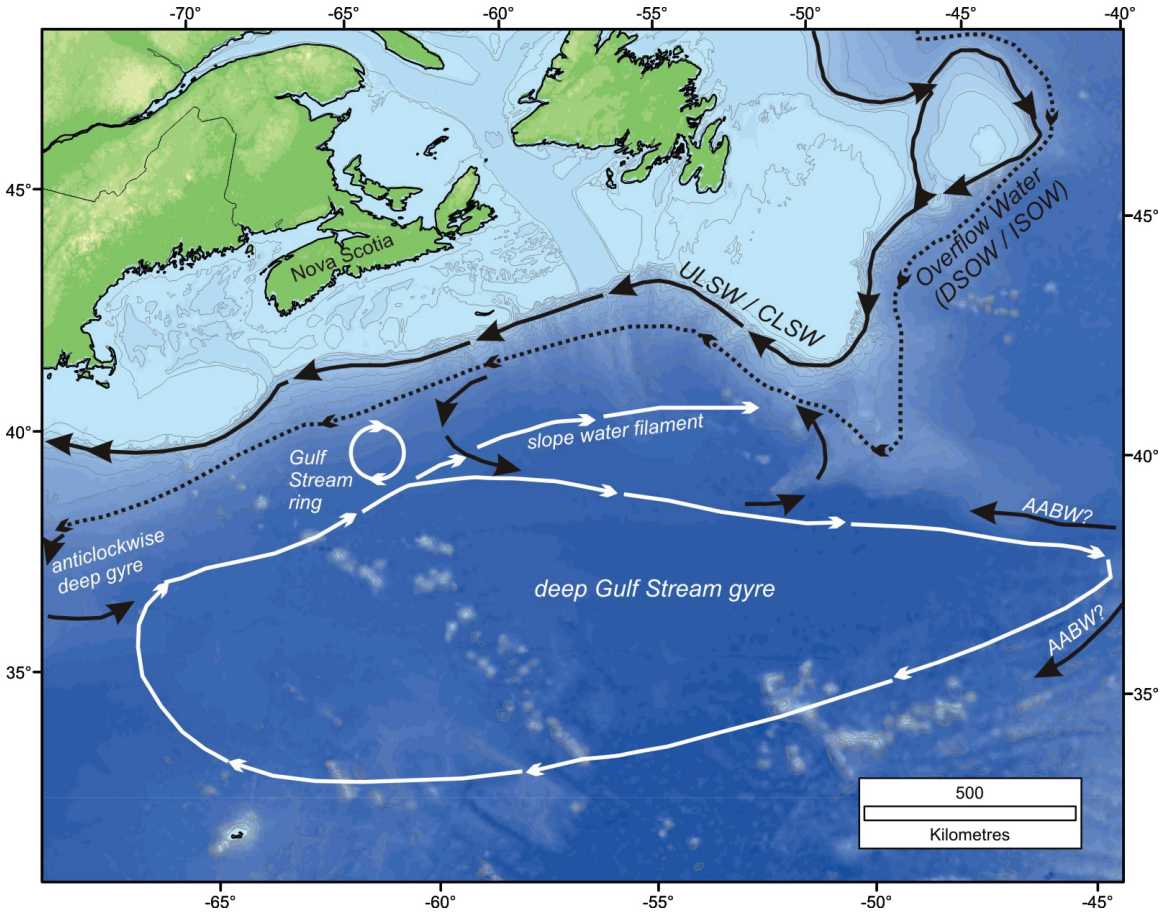

Figure 4.2 Regional map of the modern deep current system off Nova Scotia. The map is compiled from results and observations presented in Laine and Hollister (1982), Schmitz and McCartney (1992), Pickart (1992), Pickart and Smethie (1998), Pickart et al. (1999), and Smethie et al. (2000).

4.3 DATA AND METHODS

4.3.1 Seismic Reflection Data

2D and 3D multichannel seismic reflection data were interpreted for this study. The primary 2D seismic reflection dataset is a regional grid of 80 to 106 fold 2D seismic reflection profiles used to correlate seismic horizons, map the extent of contourite depositional systems, and interpret regional structures (Figure 4.1c). 2D seismic reflection data were acquired by TGS-Nopec Geophysical Company in 1998 and 1999, with a line spacing of 6 km in the strike direction and 3 to 6 km in the dip direction. Hydrophone streamer length was 6 to 8 km and the acoustic source was a 130 L tuned airgun array. Three large 3D seismic surveys were used to examine in detail the seismic geomorphology of contourite depositional systems. The 3D seismic volumes, termed the Barrington, Torbrook, and Weymouth 3D survey areas, were acquired in 2000 and 2001 for EnCana Corporation (then Pan Canadian). Survey parameters are shown in Table 4.1. Processing of both the 2D and 3D datasets was conducted by the data owners prior to this study.

Seismic reflection data were interpreted using SeismicMicro Technologies Kingdom Suite and Schlumberger GeoFrame software packages. For the 3D seismic dataset, reflection horizons were mapped and gridded to produce continuous surfaces with a grid cell size of 25 m. Seismic reflection travel time, amplitude, and geometric attributes were used to interpret the seismic geomorphology. For the 2D seismic dataset, reflection horizons were mapped and gridded to produce continuous surfaces with a grid cell size of 1000 m. Plan view dimensions of morphological features are given in SI units. Two-way travel time (TWTT) was converted to depth and thickness in metres for the seismic structure and isochore maps using the following relationship developed by Campbell et al. (2010) and in Chapter 2.

[Equation 1] $\text{Depth} = 0.5316*(\text{two-way travel time time})^{1.0731}$

The model regression resulted in an R-squared value of 0.97 with a sample size 151 data points.

Table 4.1 3D seismic survey parameters.

3D Survey	Area	Acoustic Source	Frequency Bandwidth	Hydrophone Streamers	Bin Spacing
Barrington	1790 km^2	62 L tuned array	3-180 Hz	6 x 6000 m	12.5 m x 25 m
Torbrook	1560 km^2	62 L tuned array	3-180 Hz	6 x 6000 m	12.5 m x 37.5 m
Weymouth	1270 km^2	62 L tuned array	3-180 Hz	6 x 6000 m	12.5 m x 37.5 m

4.3.2 Geological Sample Control

Geological sample control for the study is provided by samples and well logs from eight hydrocarbon exploration wells (Figure 4.1c). Sample control is limited for the Late Cretaceous and Cenozoic interval, and no conventional cores exist for the Oligocene to Present interval. Instead, most of the geological information is provided by cuttings and sidewall core sample descriptions in well history reports, supplemented by borehole logs and inferences from deep sea drilling results south of the study area. Cutting samples were typically collected over 5 m intervals, while sidewall core sample spacing was less frequent and more variable. Synthetic seismograms were generated from the log data for each well in the study area for correlation of well data to seismic reflection data.

4.3.3 Recognition of Contourite Depositional Systems

Geophysical data play a key role in the study of bottom-current influenced sedimentation in the deep sea (McCave and Tucholke 1986; Faugères et al. 1999; Howe et al. 2008). Classification schemes are proposed that describe the various types of sediment drifts associated with contourite depositional systems primarily based on interpretation of seismic reflection data. In general, nomenclature developed in papers by Faugères et al. (1999), Stow et al. (2002), Faugères and Stow (2008) and Nielsen et al. (2008) are used

in this study. Most sediment drifts have either a sheeted or mounded gross morphology and coherent, divergent to wavy internal reflections. Mounded drifts are further sub-divided into giant plastered, separated, and detached drifts, as well as smaller contourite channel and confined drifts. Criteria for recognition of erosional features include reflection truncation relationships, association with sediment drifts (i.e. forming bounding surfaces in drift systems), or inability to explain erosion by other processes, for example in the deep basin far from the continental margin. Hernandez-Molina et al. (2008) provide a systematic classification scheme for bottom current erosional features on continental margins and recognize six types of features: a) erosional terraces, b) abraded surfaces, c) moats, d) contourite channels, e) marginal valleys or troughs, and f) furrows.

4.4 RESULTS

4.4.1 Seismic Stratigraphy

The details of the regional seismic stratigraphic framework for the Scotian margin are presented by Campbell et al. (2010) and in Chapter 2, and are summarized below and in Figure 4.3 and Table 4.2. Ten regional seismic stratigraphic horizons define four depositional units that span the Upper Cretaceous through Quaternary succession of the outer Scotian margin. Unit 1, spanning the Upper Cretaceous to Upper Eocene, is characterized by mounded and truncated, high amplitude reflections interpreted to represent widespread and repeated periods of gully erosion interspersed with periods of hemipelagic and pelagic sedimentation. Unit 2, spanning the Oligocene to Middle Miocene, is distinctly faulted and dominated by widespread and repeated periods of erosion below the middle slope. Deposition by gravity flow processes and sediment re-working by bottom currents are also apparent throughout Unit 2. Unit 3, spanning the Upper Miocene to Upper Pliocene, is dominated by continuous divergent to wavy reflections interpreted to represent bottom current deposition including stacked sequences of giant sediment waves and large contourite drifts along the lower slope. Unit 4 spans

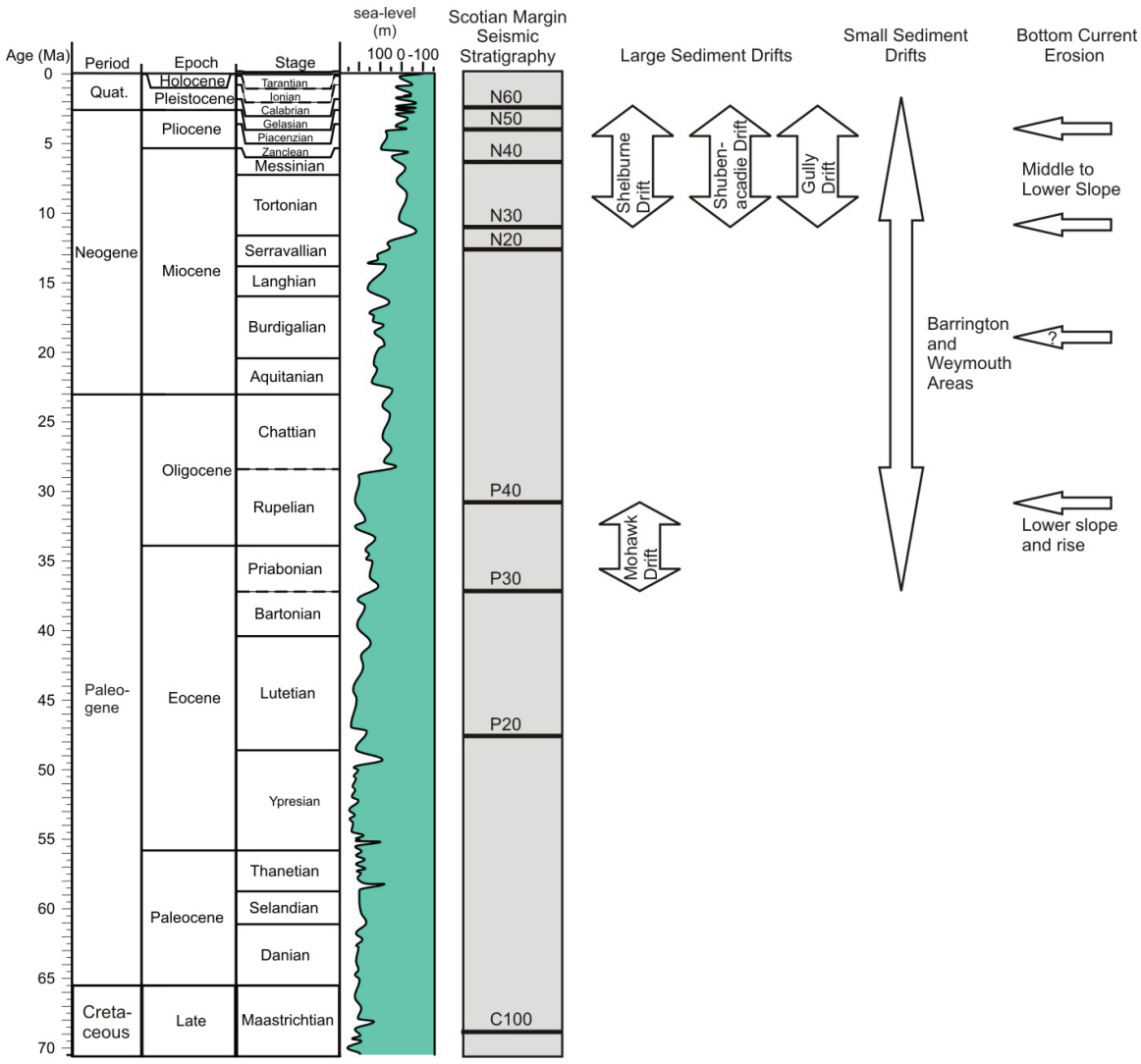

Figure 4.3 Seismic stratigraphy and chronology of sediment drift and erosional features on the Scotian margin. Timescale is modified from TimeScale Creator (www.tscreator.com accessed April 10, 2011).

the Upper Pliocene to present and exhibits a return to gravity flow deposition focused below the upper slope.

4.4.2 Depositional Features

Bottom current depositional features in the study area, interpreted from seismic reflection data, consist of large sediment drifts, small sediment drifts and sediment waves.

Large sediment drifts

Although there is no specific boundary for distinguishing large sediment drifts from small drifts (Faugères and Stow 2008), in this study large drifts are defined as those that cover a significant planview area, on the order of >1000 km^2. The identification of large sediment drifts was based on several criteria. The gross depositional pattern of large drifts is typically elongate along slope. Large sediment drifts are bound above and below by seismic discontinuities or significant changes in acoustic facies. The internal seismic facies is planar to divergent and is occasionally wavy. Large drifts typically thin landward and basinward. Additional identification criteria specific to individual large sediment drifts are included below.

Four large sediment drifts are recognized in the study area (Figure 4.4) and are informally named based on their proximity to physiographic features or hydrocarbon exploration wells. The oldest large sediment drift, termed the *Mohawk Drift*, is in the southwest part of the study area immediately south of the Mohawk B-93 well (Figure 4.1c). Stratigraphically, the drift developed between regional seismic markers P30 and P40

Table 4.2 Summary of the seismic stratigraphic framework characteristics.

Horizon	Reflection Character	Seismic stratigraphic significance	Interval Description	Estimated Age
Seafloor (Top Unit 4)	High positive amplitude reflection.	Top of succession.	N60- Seafloor: Gravity flow predominance and widespread canyons.	Present
N60 (Top Unit 3)	Moderate positive amplitude reflection.	Conformable surface; marks facies change from low amplitude reflections below to high amplitude reflections above.	N40-N60: Regional sediment drift development. Giant sediment wave growth in the SW. Megaslumps appear to be most common in this interval.	Late Pliocene
N50	High positive amplitude reflection.	Erosional surface in east; conformable in the west.		Early Pliocene
N40	High to moderate positive amplitude reflection.	Appears conformable except where associated with channel development. Sands encountered where pene-trated by wells.	N30-N40: Local sediment drift development, mass transport deposits, and channels.	Messinian
N30 (Top Unit 2)	Moderate to high positive amplitude reflection.	Erosional unconformity. Forms marine onlap surface.	N30 often erodes down to N20 or deeper along the middle slope. Local sediment drift development.	Tortonian
N20	Low to moderate positive amplitude reflection.	Marks a faceis change between highly faulted reflections below to less faulted reflection above. Locally associated with channel development.	P40-N20: Interval not represented in most deepwater wells from the margin, but in most cases thickens significantly away from wells. Delta progradation on the shelf and depocenter development on the slope in the central study area. Channel development in many areas. Highly faulted in the west where not associated with down-slope processes.	Serravallian or Tortonian
P40 (Top Unit 1)	Low to moderate positive amplitude reflection.	Conformable except seaward of salt structures where erosional (equiv. to A^U). Marks facies change between undulating, transparent reflections below, to onlaping and higher amplitude/ faulted reflections above.	P30-P40: Distinct, acoustically transparent interval that drapes the top of the Eocene gullied surface. Where sampled, contains less chalk and limestone than underlying strata.	Rupelian
P30	Low positive amplitude reflection.	Erosional unconformity marking top of regional gullied surface. Also appears to separate more calcareous sediment below from less calcareous sediment above.	C100-P30: Complicated interval containing multiple unconformities. In places P30 erodes down to C100 or deeper. Top of interval appears as distinct gullied or canyon surface when mapped. Age equivalent surface recognized on the U.S. margin and described as a "ribbed" surface. Highly faulted in places. Where sampled, the interval consists of chalks and marls with lesser mudstones.	Priabonian
P20	High positive amplitude reflection.	Conformable. Coincides with calcareous chalk and limestone in wells. Drapes erosional surface.		Lutetian

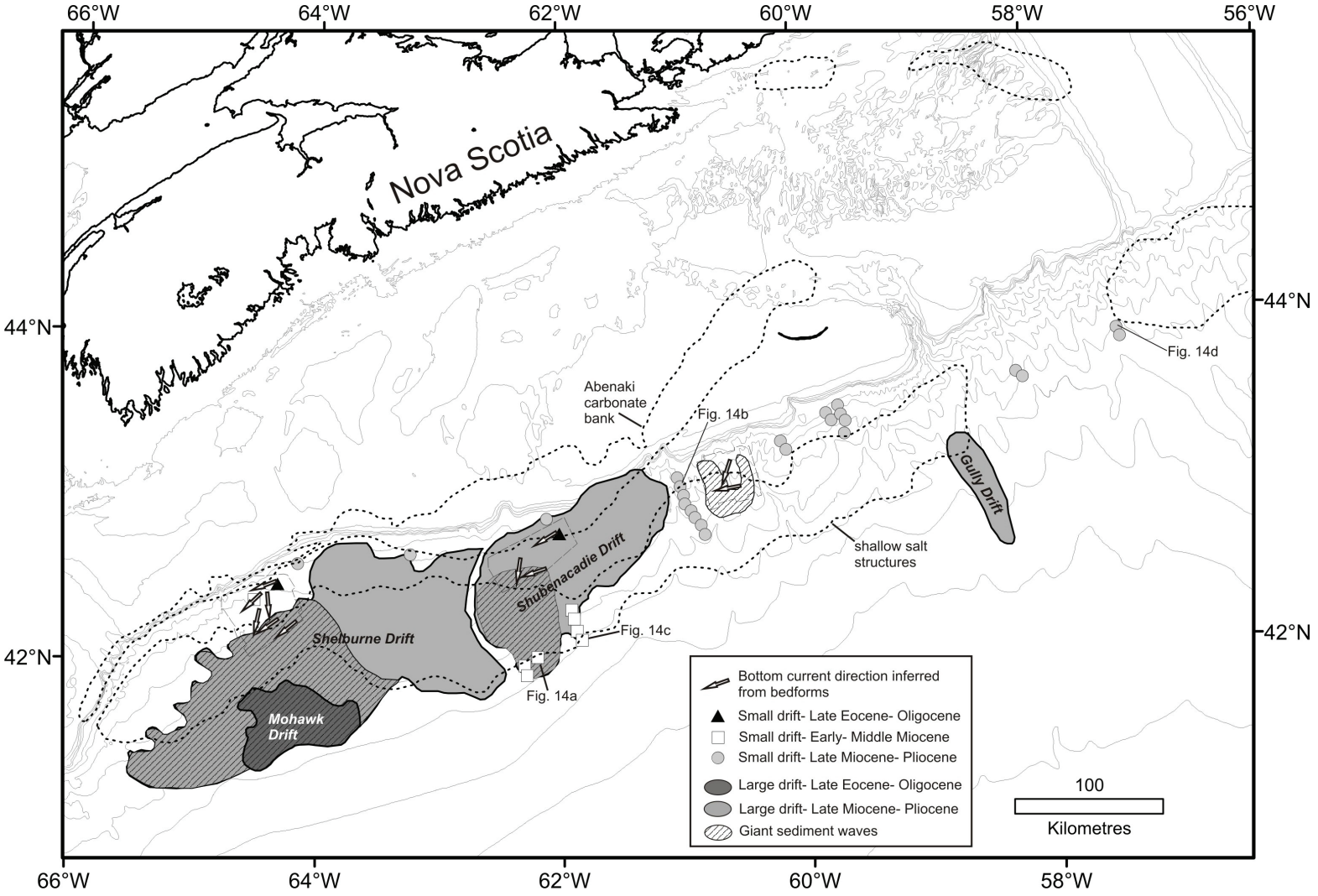

Figure 4.4 Geographical distribution of Cenozoic bottom-current depositional features on the Scotian margin.

(Figure 4.5, 4.6). The drift is within a distinct, acoustically transparent interval estimated to be Priabonian (Table 4.2). The drift covers an area of ~3600 km^2 and has a maximum thickness of 250 m. The lower bounding surface, P30, is an erosional unconformity that marks the end of a period of gully erosion across most of the continental margin. The upper bounding surface, P40, is an erosional unconformity. Within the area of the *Mohawk Drift* below the upper continental rise, P40 appears to be equivalent to horizon A^U, a bottom current eroded unconformity recognized over most of the western North Atlantic and discussed in more detail below (Tucholke and Mountain 1979; Mountain and Tucholke 1985). The internal reflection geometry of the *Mohawk Drift* is faintly stratified with wavy and sigmoidal reflections. Several authors have interpreted this seismic facies as indicative of deepwater sediment waves (eg. Fox et al. 1968; Flood et al. 1993; Wynn and Stow 2002). The waves appear to migrate in an upslope direction (Figure 4.6).

The three other large sediment drifts on the Scotian Slope all occur stratigraphically above a regional Middle to Upper Miocene unconformity termed N30 and below a regional Late Pliocene seismic reflection termed N60. Over much of the study area, N30 is a composite unconformity formed by a variety of processes. For example, in the western part of the study area the formation of N30 is attributed to bottom current erosion in the Middle Miocene followed by gravity driven mass-wasting in the Late Miocene (Figure 4.6) (Campbell and Mosher 2010). The upper bounding surface (N60) separates moderate amplitude, parallel to wavy reflections below from higher amplitude, parallel to chaotic reflections above. N60 is interpreted to mark a transition from along-slope to down-slope predominance over most of the Scotian margin (horizon "E" in Campbell and Deptuck In Press).

Along the western Scotian margin, a large plastered drift, termed the *Shelburne Drift*, named for the Shelburne G-29 well (Figure 4.1c), covers an area of 20 000 km^2 (Figures 4.4, 4.6-4.8). The western part of the *Shelburne Drift* consists of layered sequences of wavy and sigmoidal seismic reflections that converge and onlap the N30 unconformity,

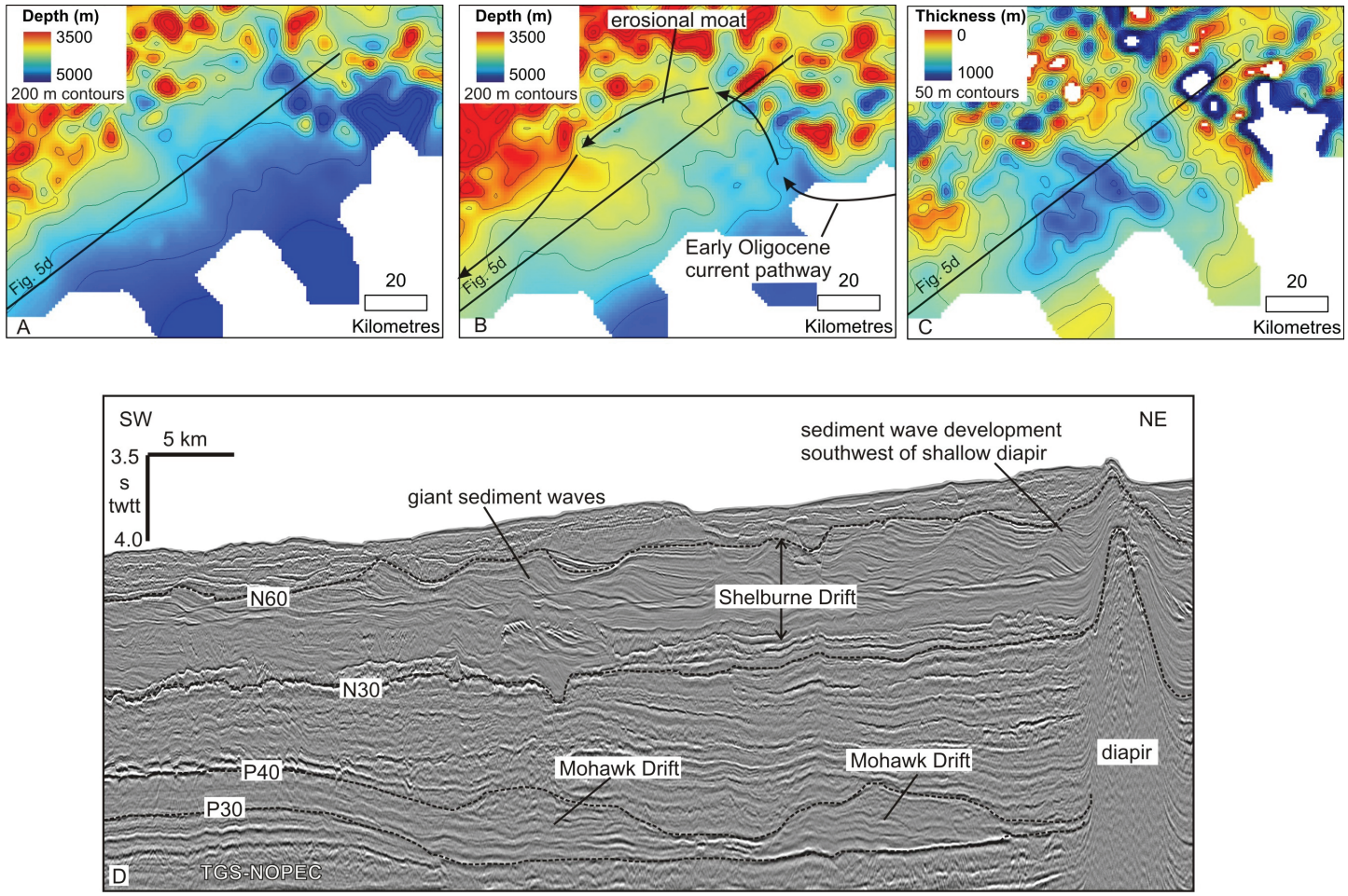

Figure 4.5 A) Stucture map of horizon P30 near the base of the *Mohawk Drift*. B) Structure map of horizon P40 near the top of the *Mohawk Drift*. C) Isochore map of the *Mohawk Drift* (P30 to P40 reflections). D) Seismic reflection profile along the southwest part of the study area showing the *Mohawk* and *Shelburne* drifts.The map location is shown in Figure 4.1. Data are courtesy of TGS-NOPEC Geophysical Company L.P.

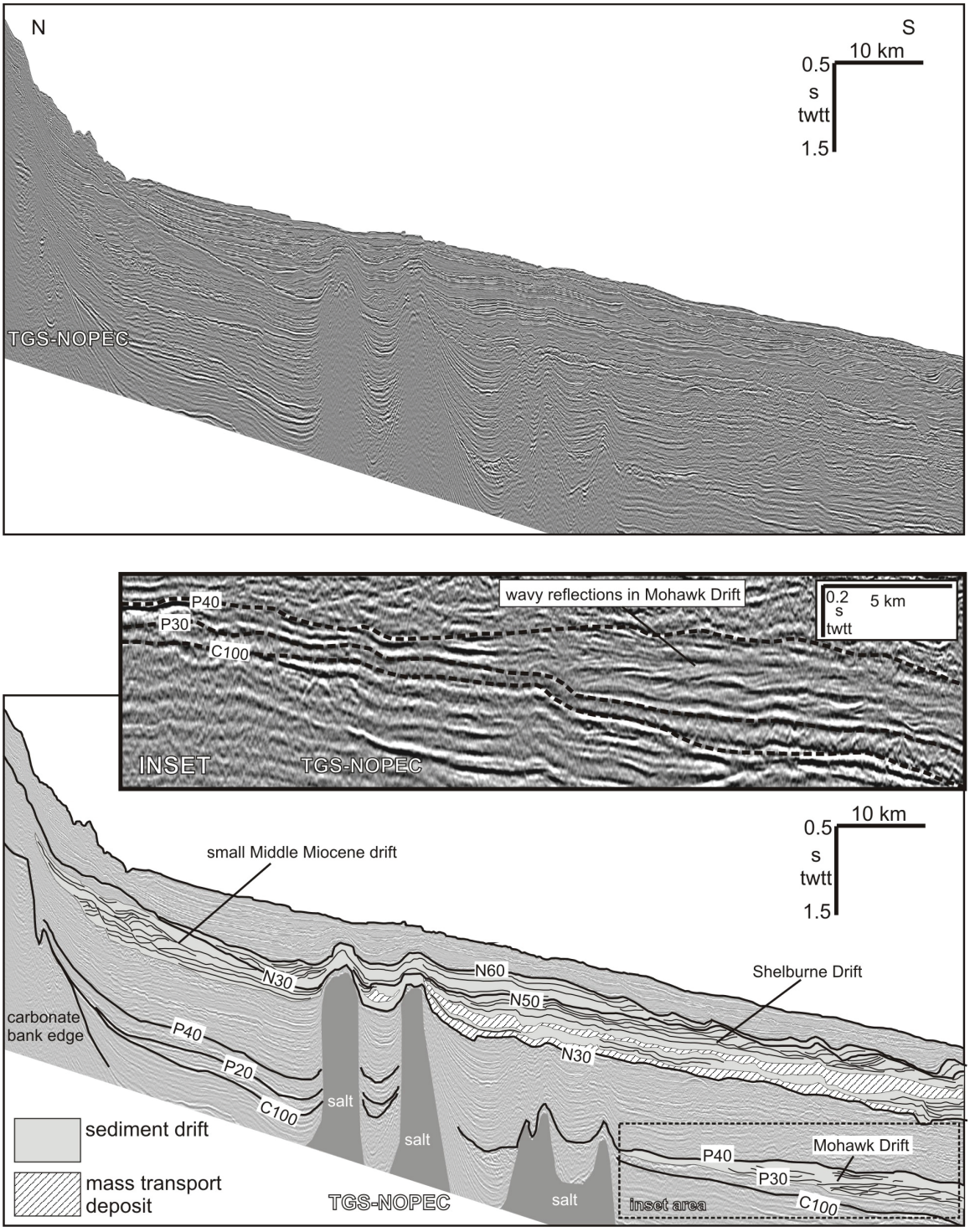

Figure 4.6 Regional seismic reflection profile showing the *Mohawk* and *Shelburne* drifts. Both drifts consist of wavy to sigmoidal reflections interpreted to represent giant sediment waves. Inset shows details of the *Mohawk Drift*. The profile location is shown in Figure 4.1. Data are courtesy of TGS-NOPEC Geophysical Company L.P.

interpreted to represent giant sediment waves (Figures 4.44, 4.5b, 4.6). In strike-oriented seismic profiles, most sediment waves have an apparent migration towards the east, while on dip oriented seismic profiles, most sediment waves appear to migrate upslope. The eastern part of the *Shelburne Drift* consists of stratified, sub-parallel seismic reflections (Figure 4.7). The drift thins landward and basinward, reaching a maximum thickness of ~700 m (Figure 4.8) and has a subtle mounded appearance in dip-oriented seismic profiles.

A large separated or plastered drift is interpreted between Verrill Canyon and Mohican Channel and is termed the *Shubenacadie Drift*, named for the Shubenacadie H-100 well (Figures 4.1c, 4.4, 4.8, 4.9). The *Shubenacadie Drift* is stratigraphically equivalent to the *Shelbune Drift* described above but is much thicker and is partially separated from the *Shelburne Drift* by a channel that subsequently eroded into the drift (Figure 4.8). Near the Torbrook C-15 well, the *Shubenacadie Drift* exceeds 1500 m thickness. In planview, the drift covers an area of 9500 km^2 and the surface morphology has the appearance of a sedimentary ridge (Figure 4.8), similar to the Chesapeake Drift on the U.S. Atlantic margin (Twitchell et al 2009). On dip-oriented seismic profiles, the drift has a distinct lenticular shape (Figure 4.9). Wavy reflections interpreted as sediment waves flank the basinward side of the drift.

The fourth large sediment drift, termed the *Gully Drift* is located on the lower continental slope and upper continental rise, seaward of *The Gully*, one of the largest submarine canyons on the eastern margin of North America (Figure 4.4). The drift deposit covers an area of 1000 km^2 and forms a relatively narrow sedimentary ridge oriented toward the southeast, perpendicular to the trend of the margin. Its orientation suggests that it is a detached drift or a contouritc levee (Faugères et al. 1999) since it is not elongate along slope, but rather normal to the regional slope. Its location coincides with a basinward shift in buried allocthonous salt diapirs (Figures 4.4, 4.10) and with the western flank of large canyon that was the precursor to *The Gully*. The drift developed above the N30 unconformity and reaches a maximum thickness of ~400 m. The internal reflection

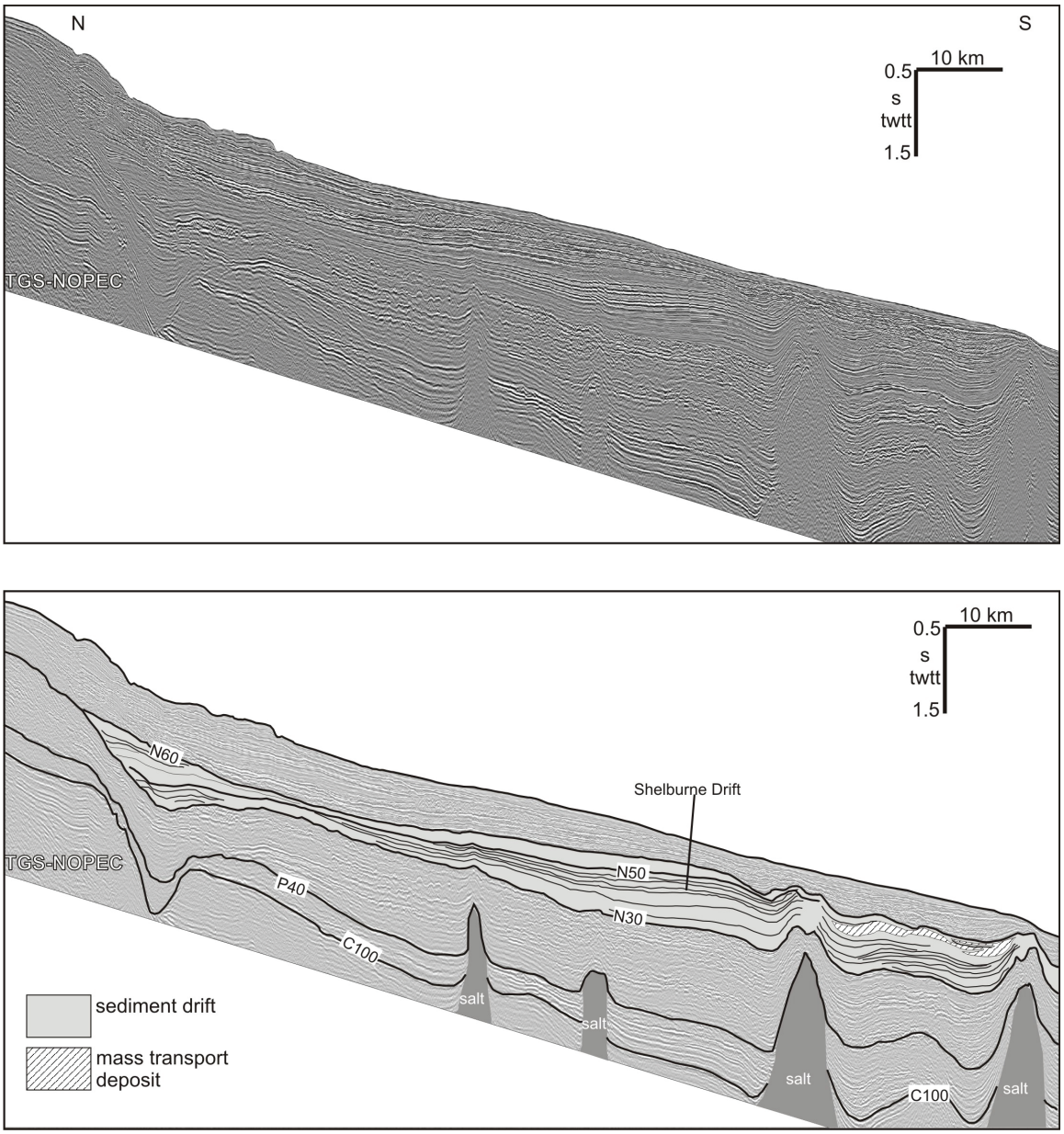

Figure 4.7 Regional seismic reflection profile showing the *Shelburne Drift*. The drift thins landward and basinward, and onlaps the horizon N30. The profile location is shown in Figure 4.1. Data are courtesy of TGS-NOPEC Geophysical Company L.P.

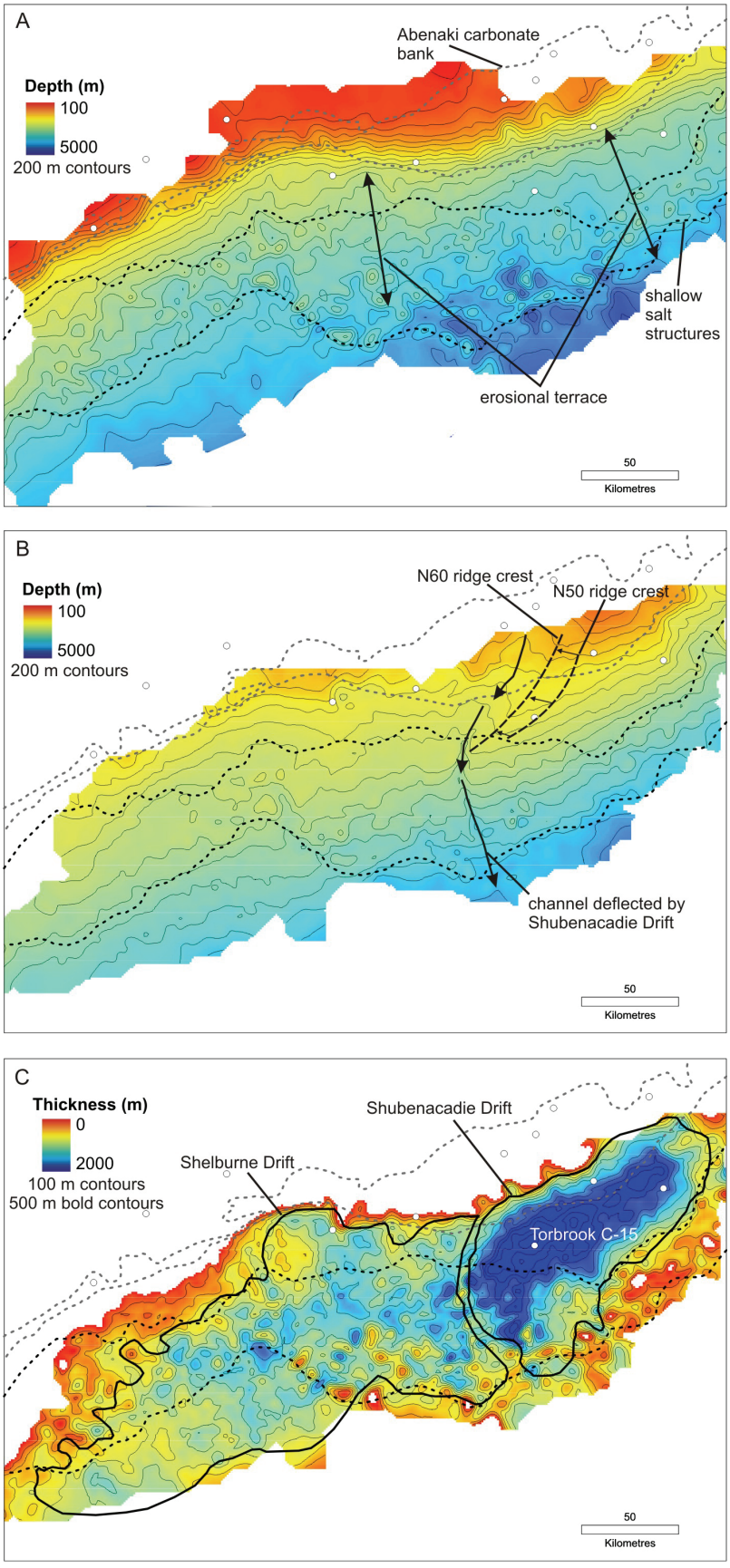

Figure 4.8
A) Stucture map of horizon N30 near the base of the *Shelburne* and *Shubenacadie* drifts. B) Structure map of horizon N60 near the top of the *Shelburne* and *Shubenacadie* drifts. C) Isochore map of the *Shelburne* and *Shubenacadie* drifts. Maps are based on seismic data courtesy of TGS-NOPEC Geophysical Company L.P.

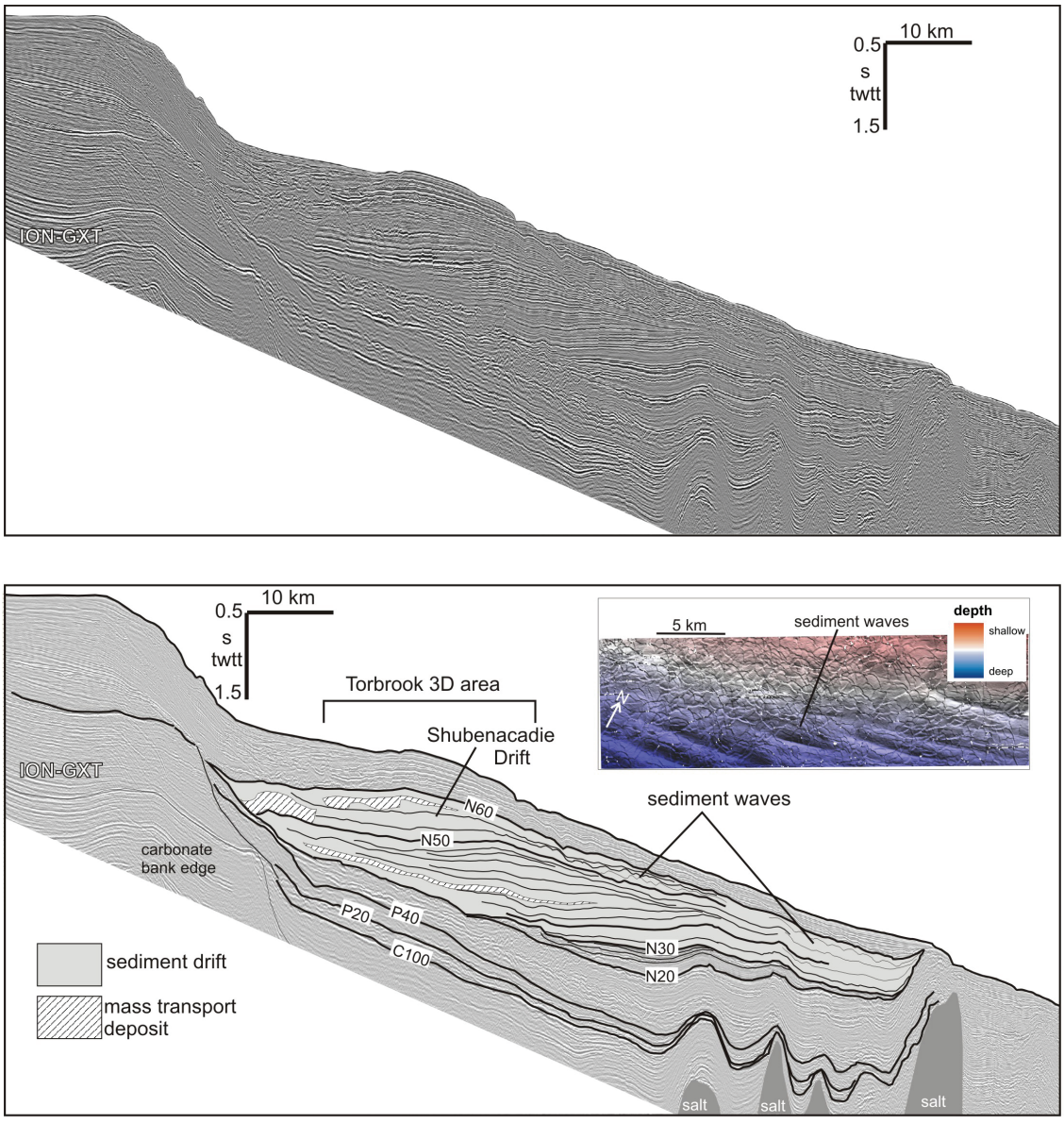

Figure 4.9 Regional seismic reflection profile showing the *Shubenacadie Drift*. The drift has a separated appearance and thins landward and basinward above the N30 horizon. Sediment waves are developed on the basinward limb of the drift. The inset shows a shaded relief image of the sediment waves imaged in the Torbrook 3D dataset. Profile location and Torbrook 3D survey area shown in Figure 4.1. Data are courtesy of TGS-NOPEC Geophysical Company L.P. and EnCana Corporation.

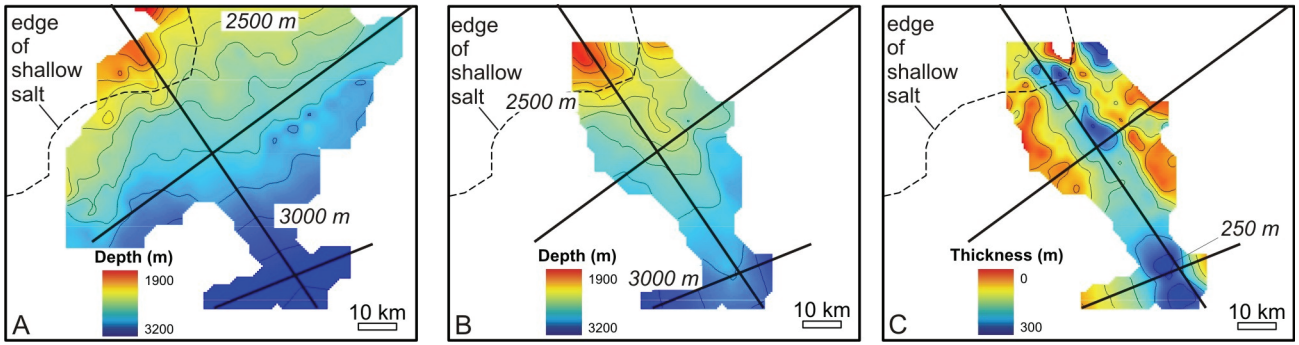

Figure 4.10 A) Stucture map of horizon N30 near the base of the *Gully Drift*. B) Structure map of horizon N60 near the top of the *Gully Drift*. C) Isochore map of the *Gully Drift*. The drift has a detached appearance and forms the western levee of a large channel.

configuration consists of wavy reflections that have an apparent migration upslope and eastward (Figures 4.11, 4.12).

Small sediment drifts

Packages of wavy to sigmoidal reflections, exhibiting an apparent southwest to northeast migration, are observed throughout the study area. These features are interpreted to represent small sediment drifts and are typically elongate in a down-slope direction. Small sediment drifts in the study area extend for 10 km or more down slope, but are of limited along-slope geographical extent- on the order of 10 km or less (Figure 4.13). Most small drifts are located on the western side of seafloor obstacles, such as buried escarpments and buried salt diapirs, or are found within channels. (Figure 4.4, Figures 4.13-4.14). Such small drifts rarely exceed 200 m in total thickness and have the appearance of single sedimentary bedforms. In the Barrington and Torbrook 3D datasets, Priabonian to Rupelian small sediment drifts are recognized between horizons P30 and P40 (Figure 4.13). During the Early to Middle Miocene, small drifts developed in the Barrington 3D data area. The infill of most Middle to Upper Miocene channels exhibit asymmetrical reflection patterns and, in all observed cases, individual channel-fill sequences have a west-to-east fill pattern (Figure 4.14). In some channels, the asymmetrical channel fill continues above the height of channel flanks (e.g. Figure 4.14a).

Sediment waves

Undulating wavy to sigmoidal reflections similar in appearance to multiple adjacent small drifts are interpreted to represent sediment waves (Figures 4.5b, 4.6). Large sediment waves are recognized in a number of locations in the study area (Figure 4.4). In some areas they constitute almost the entire thickness of a sediment drift, for example in the western part of the *Shelburne Drift* (Figures 4.5b, 4.7). In other cases, sediment waves form only part of a larger sediment drift, for example on the *Shubenacadie Drift* (Figure 4.9). Bedform wavelengths are on the order of 3-10 km and wave heights can reach 150 m. Based on the reflection configuration in the 2D seismic reflection data, sediment

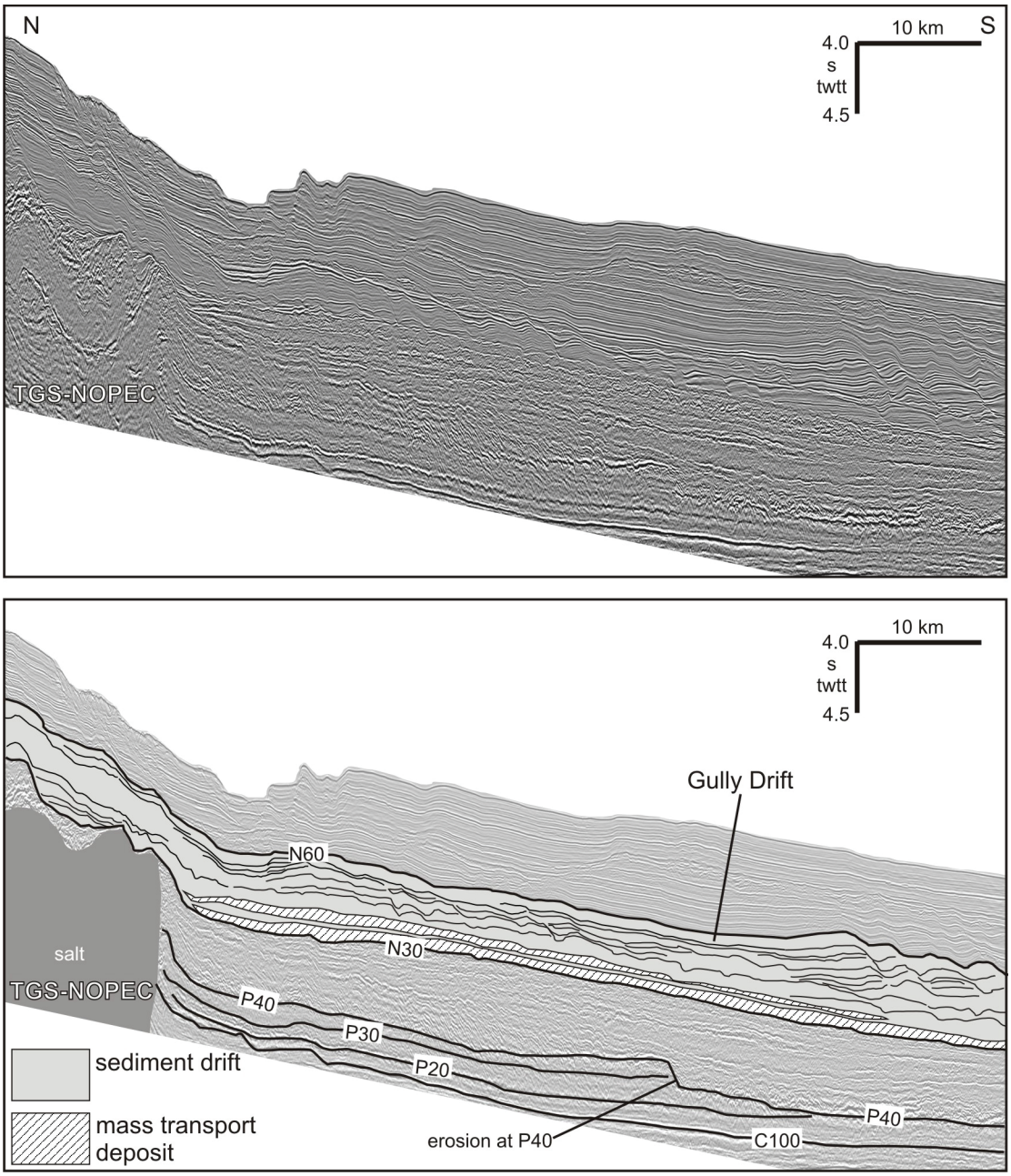

Figure 4.11 Regional seismic reflection profile showing the *Gully Drift*. The drift is constructed from multiple layered sediment waves. Erosion at the P40 horizon is apparent in the deeper part of the profile. The profile location is shown in Figure 4.10. Data are courtesy of TGS-NOPEC Geophysical Company L.P.

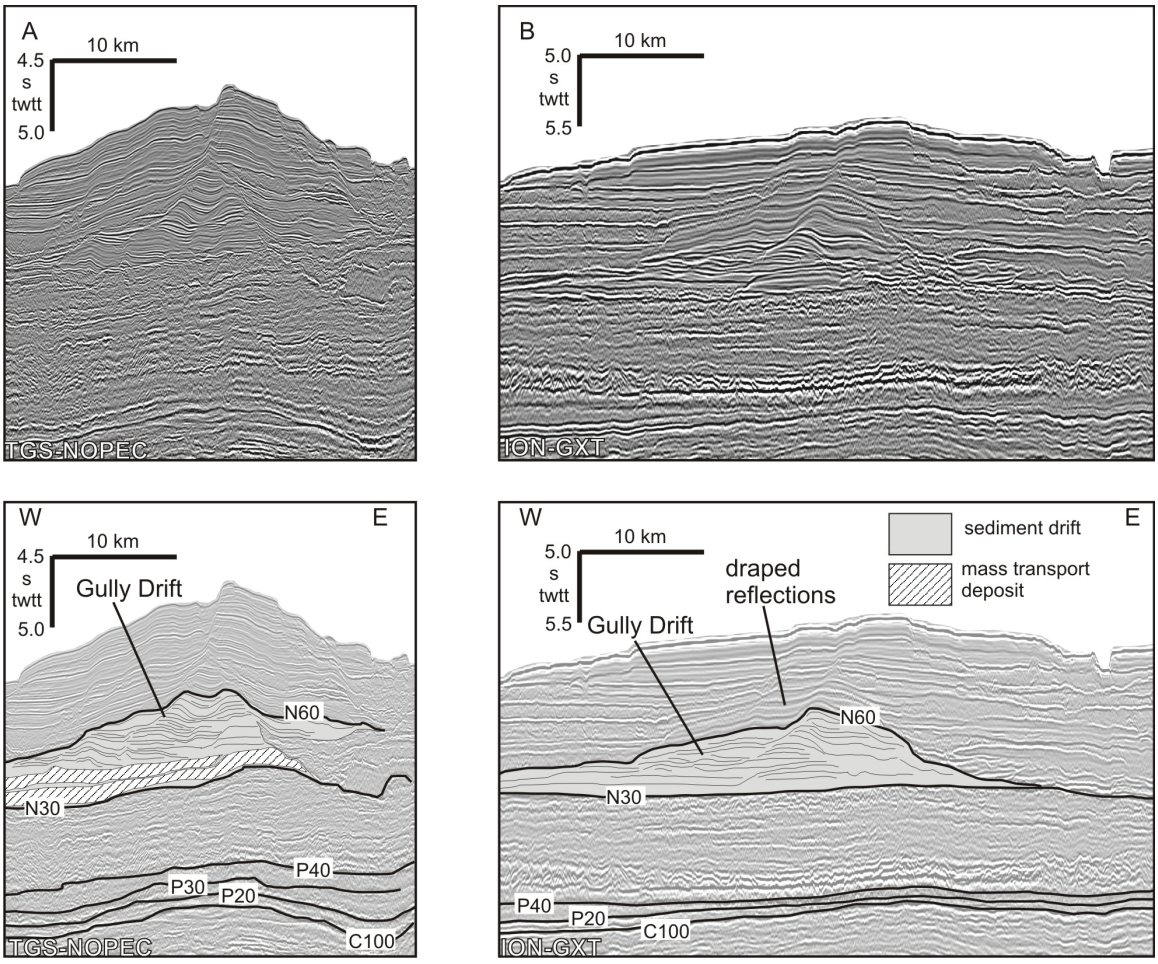

Figure 4.12 Seismic reflection profiles across the *Gully Drift*. A) Northern seismic profile shows west-to-east migration of sediment waves within the drift. The profile location is shown in Figure 4.10. Data are courtesy of TGS-NOPEC Geophysical Company L.P. B) The southern seismic profile also shows west-to-east wave migration and draped reflections above the N60 horizon. The profile location is shown in Figure 4.10. Data are courtesy of ION-GXT.

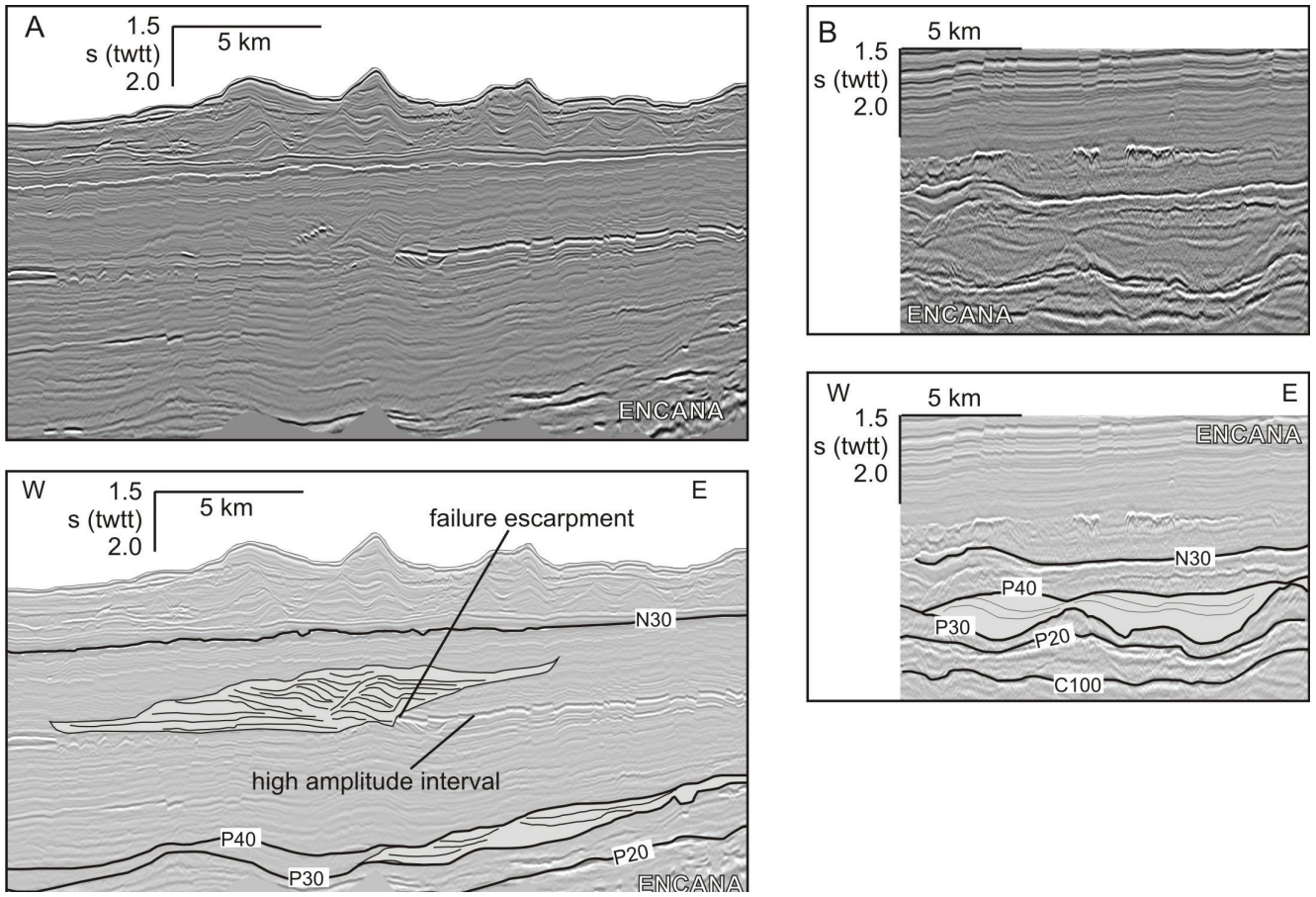

Figure 4.13 Examples of small sediment drifts from the study area (shown in grey). A) Examples from the western Scotian margin showing a drift developed west of a failure escarpment in the Oligocene to Middle Miocene interval. A map of the high amplitude interval is shown in Figure 4.20. Another small drift is developed in probable Upper Eocene sediments between horizons P30 and P40. B) Small Upper Eocene drifts from the central part of the study area between the P30 and P40 horizons. Profile locations are shown in Figure 4.1. Data are courtesy of EnCana Corporation.

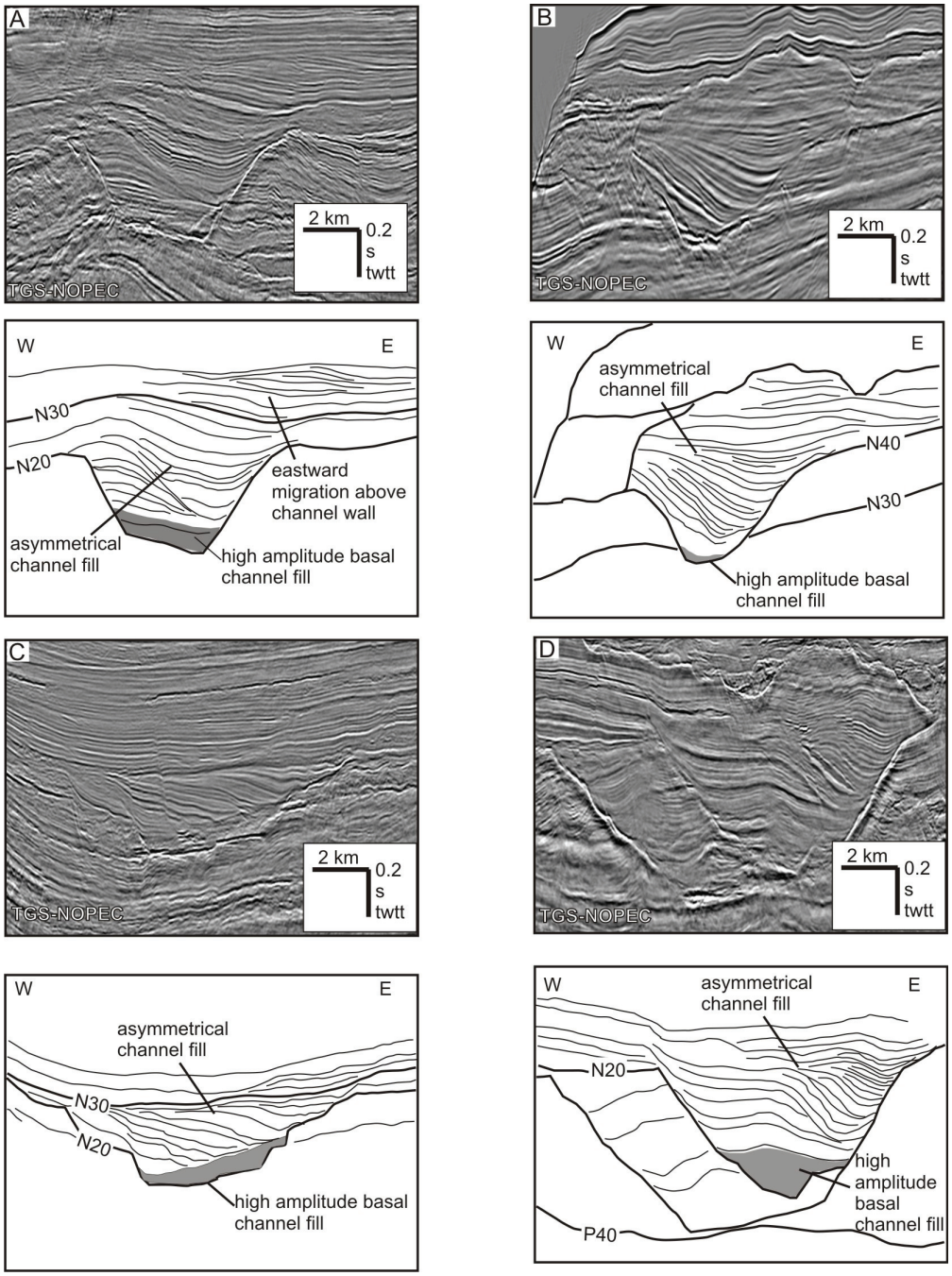

Figure 4.14 Examples of asymmetrical channel fill from the study area. A) Asymmetrical infill of a Middle Miocene channel on the continental rise. Wavy reflections continue above the walls of the canyon. B) Another example of a Middle Miocene channel on the continental rise, however wavy reflections cease to develop above the walls of the canyon. C) Asymmetrical infill of a Late Miocene channel below the continental slope. D) A large Oligocene channel (Brake 2009) partially infilled by wavy reflections above the N20 reflections. Profile locations are shown in Figure 4.4. Data are courtesy of TGS-NOPEC Geophysical Company L.P.

waves migrate from west to east on strike-oriented seismic profiles and from south to north (upslope) on dip-oriented profiles.

Horizontal data density of regional 2D seismic reflection data is not adequate to map in detail the surface morphology and orientation of individual sediment waves, however the detailed geomorphology of these bedforms was examined where they occur in 3D seismic datasets. In the Barrington 3D area, the *Shelburne Drift* thins to near zero thickness as it onlaps the N30 unconformity (Figure 4.6). Here, most sediment waves are 2D linear to curvilinear bedforms and migrate from west to east over the deeper part of the dataset, and upslope in the shallower part of the dataset (Figures 4.5, 4.15-4.16). Locally there are exceptions, for example unique circular bedforms formed west of a shallow buried salt diapir in the dataset (Figure 4.15). For a detailed description of the seismic geomorphology of sediment waves in the Barrington block, see Campbell and Deptuck (In Press, also Chapter 5).

Sediment waves are recognized in both 2D and 3D seismic reflection data on the southern limb of the *Shubenacadie Drift* (Figure 4.9). Some of the sediment waves are imaged in the Torbrook 3D dataset. Mapping results of these sediment waves show they have wavelengths of 5 km and amplitudes of 40 m, have linear wave crests, and show an apparent northward (upslope) migration direction (Figure 4.9). South of the Torbrook 3D dataset, larger sediment waves are imaged on 2D seismic data that also appear to migrate upslope (Figure 4.9).

Sediment waves are imaged in the central part of the study area in the Weymouth 3D dataset (Figures 4.17). Sediment waves in this part of the study area have different internal reflection geometry and different morphology from the sediment waves further west. Layered lenticular packages of parallel to wavy, landward-dipping reflections make up much of the succession between P40 and N30 that correlates to Lower to Middle Miocene deposits at the Newburn H-23 well (Crux and Shaw 2002) (Figure 4.17). Wave crests are oriented northwest to southeast and apparent wave migration direction is towards the north or northeast (predominantly upslope), although it is difficult to interpret

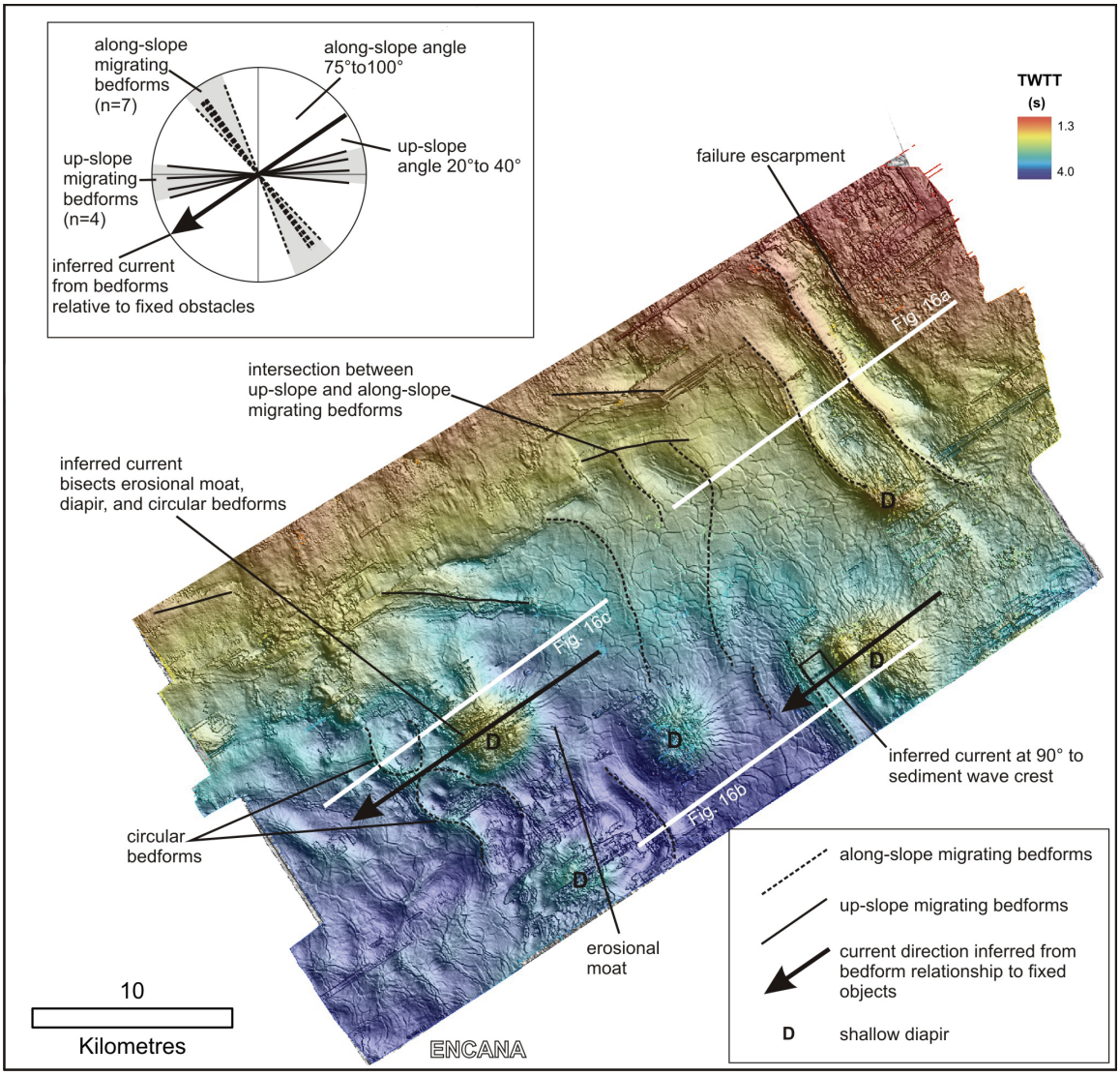

Figure 4.15 Shaded relief image of the N50 horizon from the Barrington 3D dataset. The surface shows widespread development of giant sediment waves in the *Shelburne Drift*. Precise paleo-bottom current direction is determined from the orientation of bedforms relative to fixed objects (e.g. diapirs, escarpments). Sediment waves migrate both along slope on top of the drift and up slope where bedforms onlap the N30 unconformity. Inset shows comparison of along-slope and up-slope wave crest orientations compared to the independently measured bottom current direction. The location of the Barrington 3D dataset is shown in Figure 4.1. Data are courtesy of EnCana Corporation.

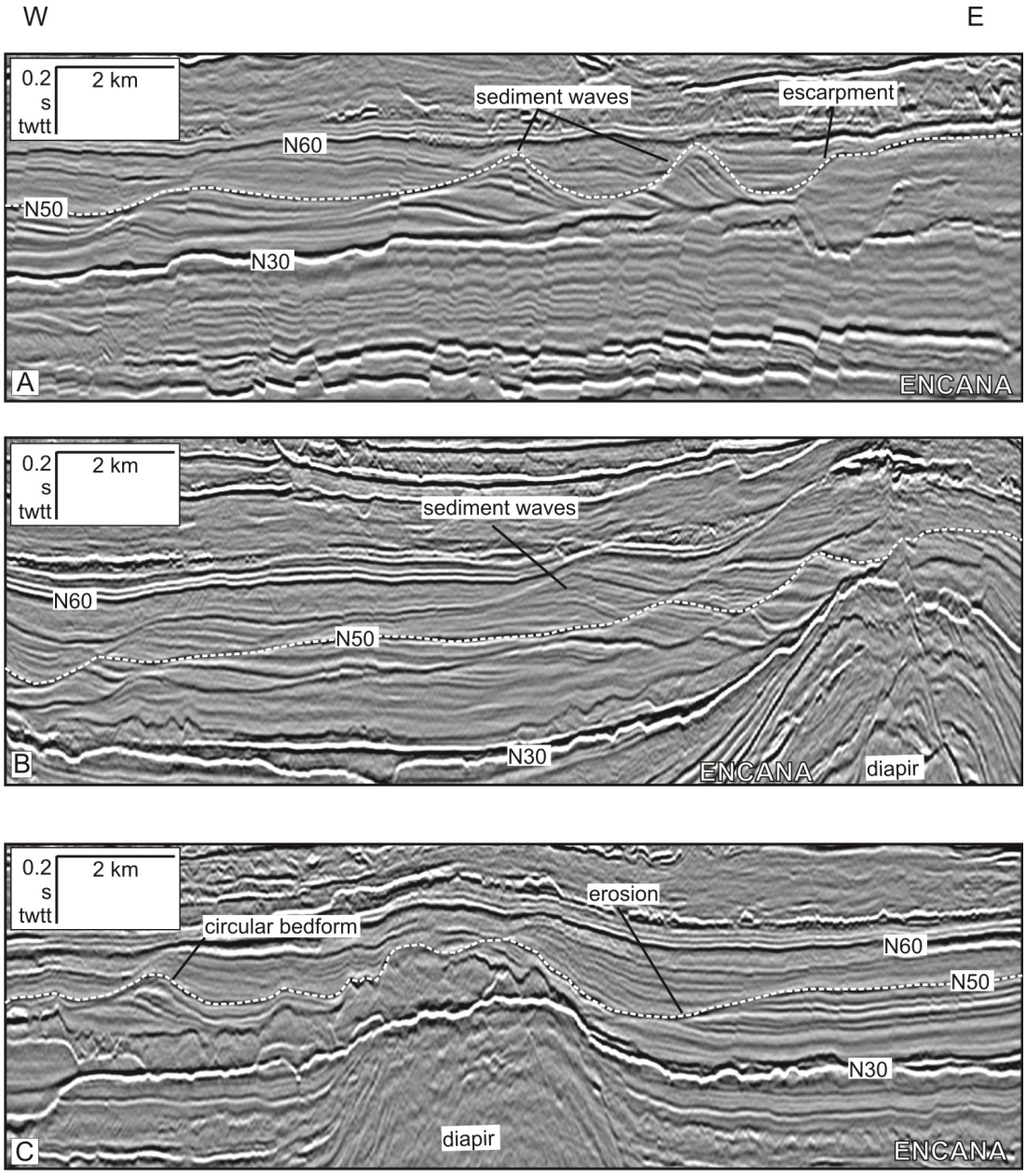

Figure 4.16 Examples of sediment waves and erosional features from the Shelburne drift in the Barrington 3D area. A) Giant sediment waves west of a failure escarpment. B) Giant sediment waves west of a buried diapir. C) Erosion on the east side of a buried diapir and a bedform on the west side that correlate to the circular bedform in Figure 4.15. Profile locations are shown in figure 4.15. Data are courtesy of EnCana Corporation.

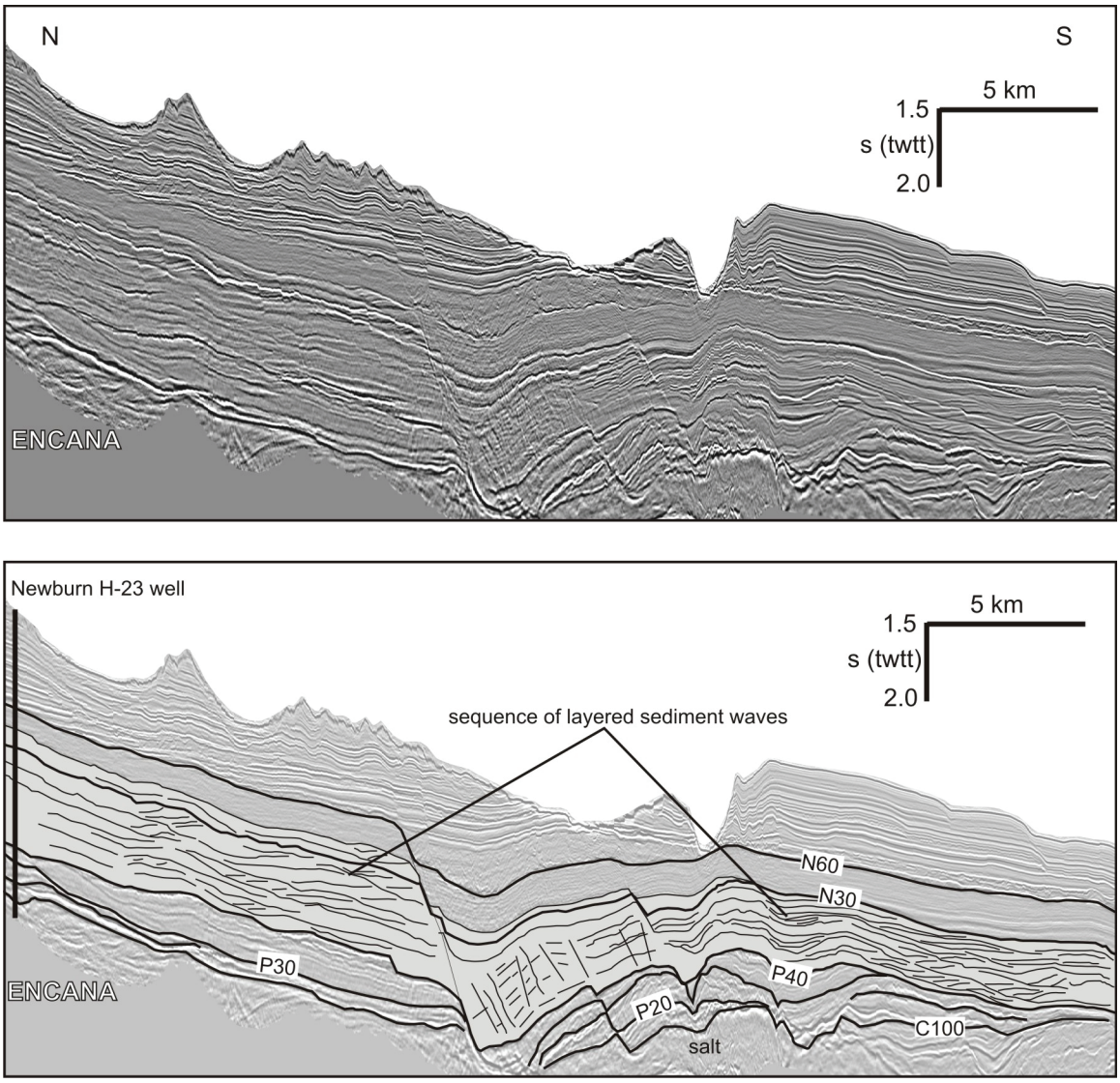

Figure 4.17 Regional seismic profile showing aggrading sediment waves that make up most of the Lower to Middle Miocene succession in the Weymouth 3D area, between horizons P40 and N30. The profile location is shown in Figure 4.1. Data are courtesy of EnCana Corporation.

discrete wave surfaces within the sediment wave interval. Fulthorpe and Carter (1991) interpreted a similar seismic facies to represent accreted sediment drifts in data from the Cantebury Basin of the South Island of New Zealand.

4.4.3 Erosional features

Evidence of bottom current erosion in the study area is divided into large and small features. Large erosional features are associated with the formation of regional unconformities, namely horizons P40, N30, and N50 (Figure 4.3). Small erosional features are of limited geographical extent, for example, features only recognized in a single 3D seismic dataset or on a limited number of regional seismic profiles. In the study area, small erosional features include abraded surfaces, marginal troughs, and possibly helical scour.

Large erosional features

On the eastern and western Scotian margin, at the maximum extent of buried salt diapirs and areas further seaward, 2D seismic reflection data show erosion and the development of abraded surfaces at the P40 unconformity (Figures 4.6, 4.11). The resultant abraded surface is gently undulating and dips slightly seaward (Figure 4.5). In many areas along the upper rise, the erosion at P40 appears to be enhanced at the seaward side of buried salt diapirs. For example, a contourite moat is interpreted in the western part of the study area in such a setting (Figure 4.5). None of the 3D seismic datasets available for use in this study span the area where bottom current erosion at P40 is apparent and therefore it is not possible to determine the detailed seismic geomorphology of the surface. Evidence of erosion by bottom currents at horizon P40 is less obvious within the large area of shallow salt structures and along the slope further landward. At the Annapolis G-24 well, P40 is immediately above a stratigraphic break that separates Priabonian sediments below from Rupelian sediments above (Figure 4.1c) (Robertson Research 2004). A distinct, acoustically transparent interval underlies P40 and is intersected at a number of wells

where it coincides with Priabonian age deposits. Therefore, P40 in the study area is assigned a Rupelian age. A similar age for horizon A^U has been assigned on the U.S. continental margin (Tucholke and Mountain 1979; Mountain and Tucholke 1985).

Horizon N30 marks the approximate base of 3 of the 4 large sediment drifts. Throughout the study area, N30 separates high amplitude and faulted acoustic facies below from stratified, wavy, and locally chaotic reflections above (for example Figures 4.5b, 4.16). Along the western and eastern Scotian margin, prior to drift development, substantial erosion occurred at the level of N30 by large mass wasting processes (Figures 4.6, 4.11) (Campbell and Mosher 2010). Erosion at N30 in the central part of the study area resulted in the formation of a 60 km broad erosional terrace and an abraded surface below the middle slope, landward of salt diapirs (Figure 4.8a). The Torbrook 3D dataset (Figure 4.1c) spans the landward part of the erosional terrace where it merges with a number of other erosional surfaces associated with down-slope processes (Figures 4.9, 4.18). The detailed seismic geomorphology of the surface in the 3D seismic data shows subtle bedforms, interpreted to represent asymmetrical sediment waves on the erosion surface, as well as small arc-shaped bedforms that possibly represent submarine barchan bedforms (Figure 4.18). Although submarine barchans are not widely reported in the literature, bedform dimensions in this study are within the range of those reported for submarine barchan dunes elsewhere (Todd 2005; Kenyon et al. 2002, Daniell and Hughes 2007; Cochonat et al. 1989). In the Weymouth 3D dataset, N30 is a strong seismic reflection that clearly truncates underlying reflections and marks the top of a widespread sediment wave interval (Figure 4.17). In this area, the morphology of the erosional surface is complicated by underlying salt tectonics (see MacDonald 2006). The best age control for the N30 unconformity is Tortonian or Serravallian at the Shubenacadie H-100 well (Fensome et al. 2008). Given its age, its stratigraphic position immediately overlying the Oligocene-Middle Miocene faulted interval, and its erosional character, N30 is approximately equivalent to horizon Merlin on the U.S. Atlantic margin (Mountain and Tucholke 1985)

Extensive erosion at the N50 horizon is recognized over much of the *Shubenacadie Drift* (Figure 4.9). The best age control for the N50 unconformity is at the Shelburne G-29 well

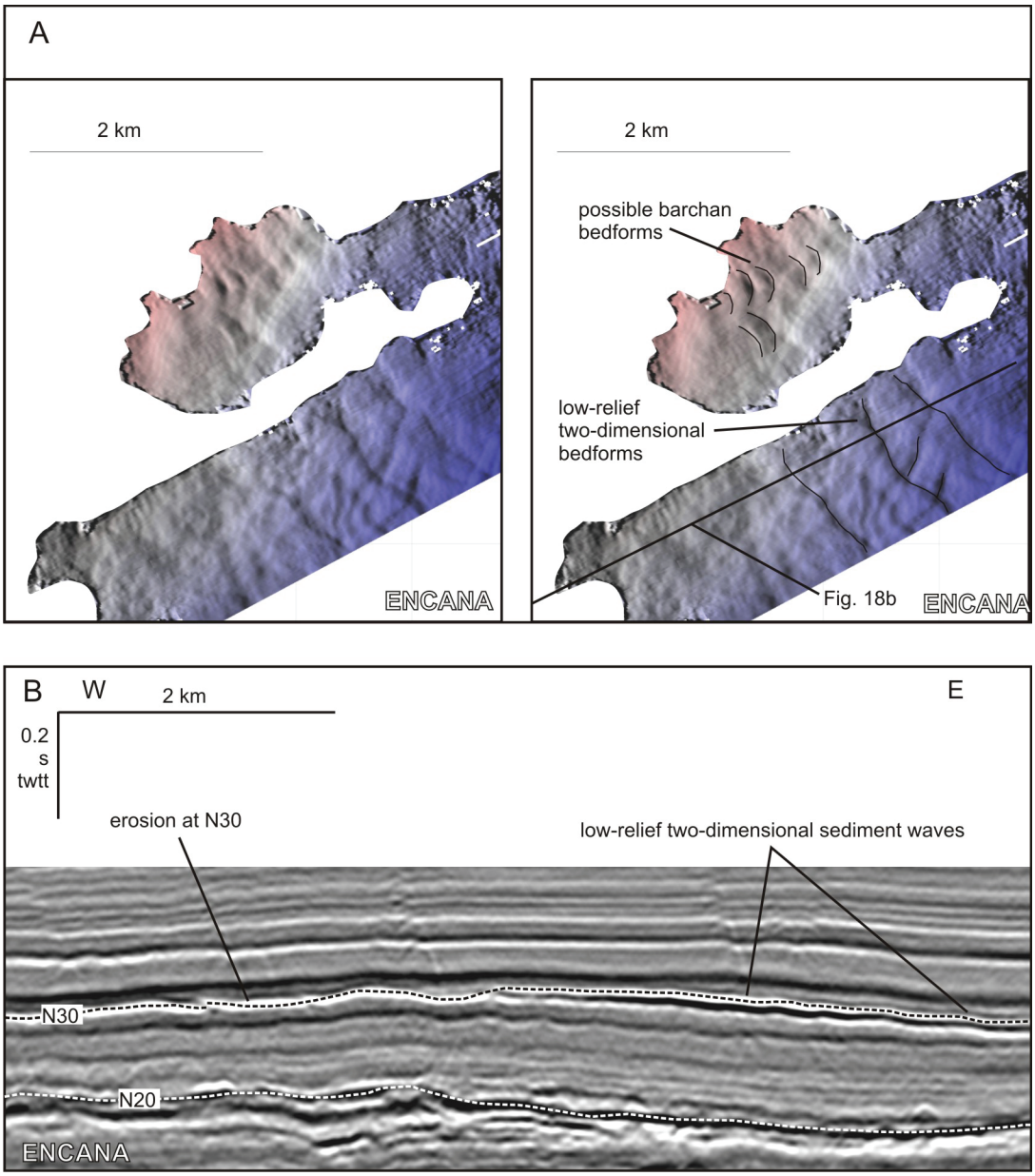

Figure 4.18 A) Shaded relief image of the N30 erosion surface in the Torbrook 3D area. Barchan bedforms and 2D linear bedforms are interpreted to have formed on the surface. Location of the Torbrook 3D dataset is shown in Figure 4.1. B) Seismic reflection profile showing erosion at the N30 unconformity and subtle undulations that possibly represent the 2D bedforms. Profile location is shown in Figure 4.18a. Data are courtesy of EnCana Corporation.

where it coincides to Zanclean deposits (Fensome et al. 2008). Regional mapping of the structure of the N50 horizon shows that it is a gently dipping surface with a subtle southwest-trending ridge that mimics the structure of the top of the *Shubenacadie Drift* (Figures 4.8b, 4.19b). In the Torbrook 3D dataset, the detailed morphology shows a gently undulating surface (Figure 4.19a). The map of the seismic amplitudes of the surface shows patches of high seismic amplitudes that appear to be related to subsurface gas features in the area (Mosher et al. 2005), as well as a slope-parallel, slightly sinuous amplitude anomaly. Such along-slope oriented amplitude anomalies have typically been associated with development of winnowed and abraded surfaces in contourite systems (Hernandez-Molina et al. 2008). On the U.S. Atlantic margin, a pulse in bottom current intensity is proposed for the development of the Blue unconformity in the Pliocene (Mountain and Tucholke 1986). It is possible that N50 records the equivalent increase in bottom current intensity.

Small erosional features

Abraded surfaces of limited geographic extent are recognized in the Barrington and Weymouth 3D datasets. In the Barrington 3D dataset, a prominent erosional surface is recognized in the highly faulted Lower to Middle Miocene succession (Figure 4.20). Correlation of the erosion surface to the Bonnet P-23 well suggests Middle Miocene age (Bujak Davis Group 1988). Although seismic correlation through the interval is difficult, the seismic amplitude map of the surface reveals slope-parallel amplitude anomalies that are interpreted as erosional features of an abraded surface that has been partially deformed by subsequent down-slope mass transport. Similar relationships between along-slope erosion and slope instability are recognized in 3D seismic data from the Santos Basin (Viana et al. 2007).

In the Weymouth 3D dataset, reflections that form the upper and lower bounding surfaces of Lower to Middle Miocene sediment waves have irregular relief and truncate underlying reflections in some locations (Figure 4.21). One surface was mapped in detail and shows a small drift, an erosional moat, along-slope amplitude anomalies, and a cluster of crescent-shaped high amplitudes interpreted to represent submarine barchan

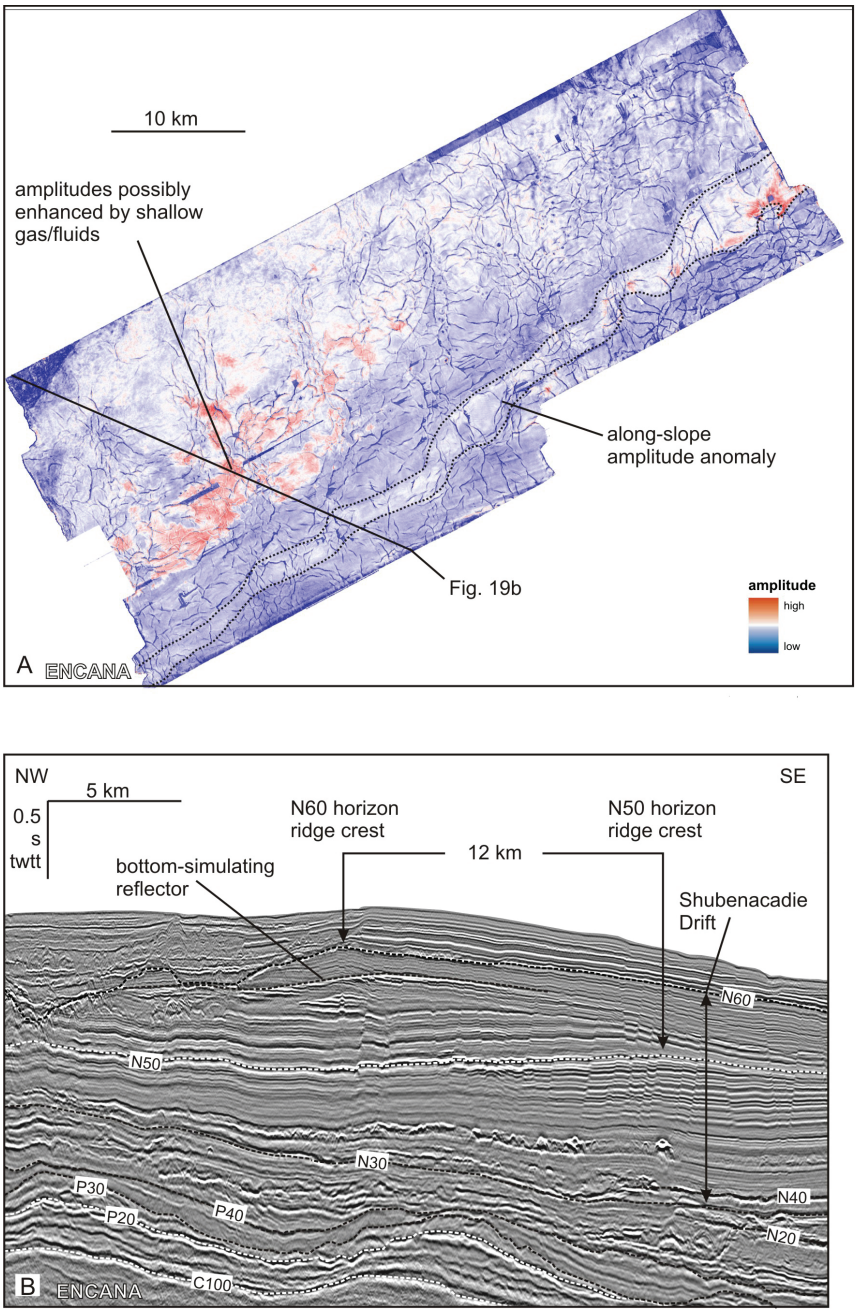

Figure 4.19 A) Map of seismic amplitude and similarity extracted at the N50 horizon in the Torbrook dataset. An along slope, sinuous amplitude anomaly is apparent, as well as amplitude anomalies possibly related to sub-surface fluids. The similarity seismic attribute highlights the polygonal faults that are prominent throughout the drift interval. Location of the Torbrook 3D dataset is shown in Figure 4.1. B) Seismic reflection profile perpendicular to the *Shubenacadie Drift* ridge crest. The drift crest has migrated approximately 12 km between the N50 horizon and the N60 horizon at the top of the drift. A bottom-simulating reflector is apparent near the top of the drift. The profile location is shown in Figure 4.19a. Data are courtesy of EnCana Corporation.

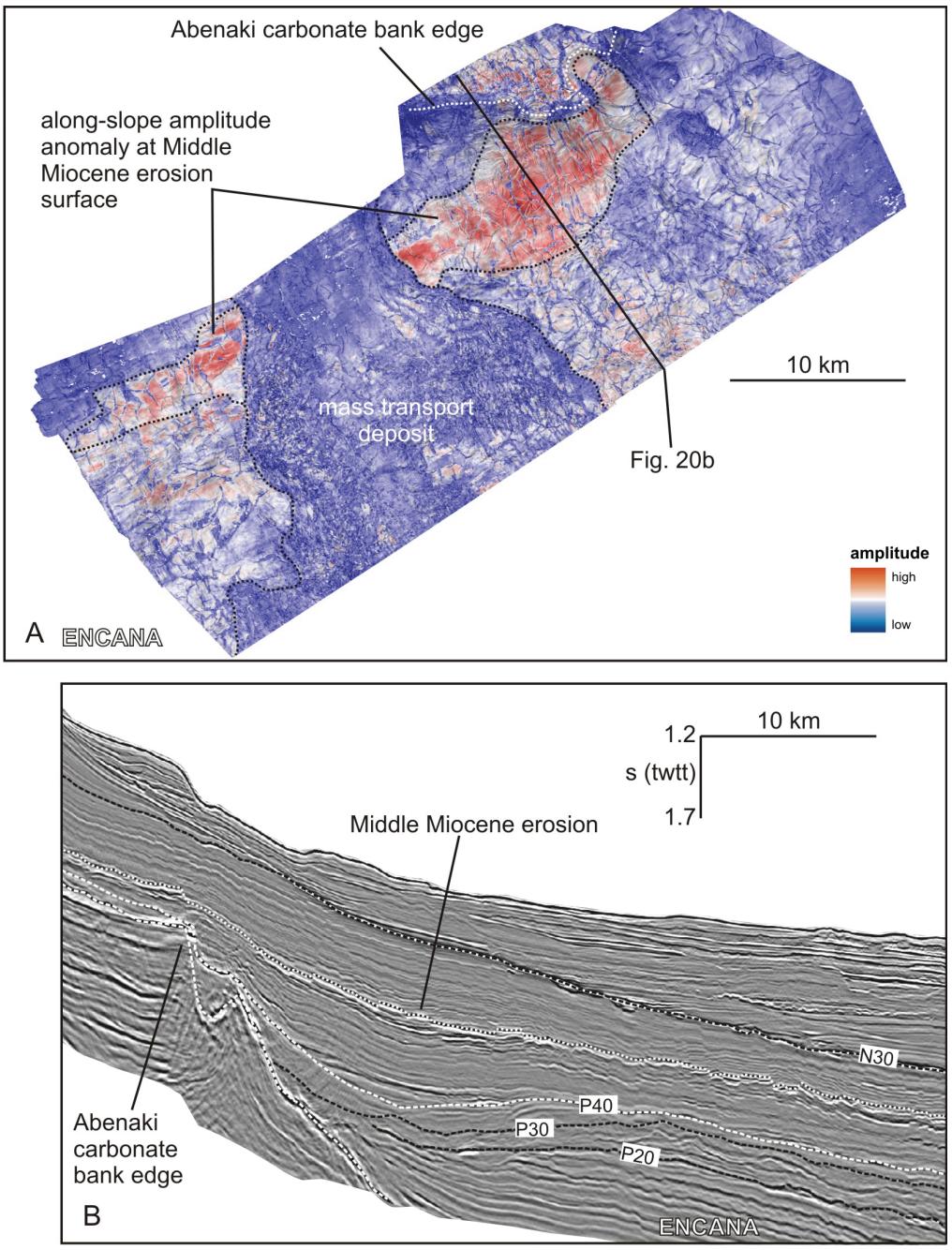

Figure 4.20 A) Map of seismic amplitude and similarity extracted from a prominent high amplitude reflection in the Barrington 3D area. The reflection is between horizons P40 and N30 and is likely Middle Miocene age. The amplitudes reveal an along-slope pattern a few kilometres wide interpreted to represent an abraded surface seaward of the Abenaki carbonate bank. The along-slope pattern is interrupted by a subsequent mass transport deposit. The location of the Barrington 3D area is shown in Figure 4.1. B) Seismic profile showing the high amplitude reflection developed within the highly faulted P40-N30 interval that is also apparent in the similarity data. The profile location is shown in Figure 4.20a. Data are courtesy of EnCana Corporation.

bedforms (Figure 4.21). The barchan bedforms have almost no vertical relief, are ~600 m long, and have a horn width of ~250 m. The bedforms are not sampled by any wells.

Evidence for marginal erosion is common along the flanks of buried salt diapirs, especially within the Middle Miocene to Pliocene succession. For example, in the sequence of giant sediment waves in the Barrington 3D dataset (Figure 4.15), erosional moats formed on the northeastern side of the salt diapir and there is clear merging of reflections and apparent truncation of underlying reflections (Figure 4.16).

Seaward of the Shelburne G-29 and Albatross B-13 wells, a prominent subsurface horizon returns hyperbolic reflections and truncates the underlying N30 reflection in some locations (Figure 4.22). The surface appears erosional. Similar acoustic facies near Blake Ridge and in the Gulf of Mexico were interpreted as representing furrows and helical scour (e.g. McCave and Tucholke 1986; Lee and George 2004). Alternatively the hyperbolic reflections generated at the surface may represent sediment waves. The irregular relief does not appear to be due to faulting as there is no offset above or below the horizon. Also, the facies differs from mass transport deposit facies as there is little thickness variation or association with failure escarpments. Horizontal data density is insufficient where these features occur in the study area to determine the planview geometry of the irregular surface.

Figure 4.21 Middle Miocene erosion in the Weymouth 3D data area between horizons P40 and N30. The location of the Weymouth 3D dataset is shown in Figure 4.1. A) Seismic amplitude draped over shaded relief for an erosional surface within an interval of accreted sediment waves shows an up-slope migrating sediment drift, an erosional moat, and crescentic amplitude anomalies interpreted to be barchan bedforms. B) Detailed seismic amplitude map of the barchan bedforms. C) Comparison of the orientation of the up-slope migrating drift crest and the paleo bottom current direction determined from the barchan bedforms. D) Seismic reflection profile showing the layered and aggrading sediment waves that make up much of the P40-N30 interval in this part of the study area. The erosional surface shown in part A and B is indicated by a dashed white line. Note the subtle amplitude anomalies where the seismic line crosses the “horns” of the barchan bedforms. The location of the profile is shown in Figure 4.21a. Data are courtesy of EnCana Corporation.

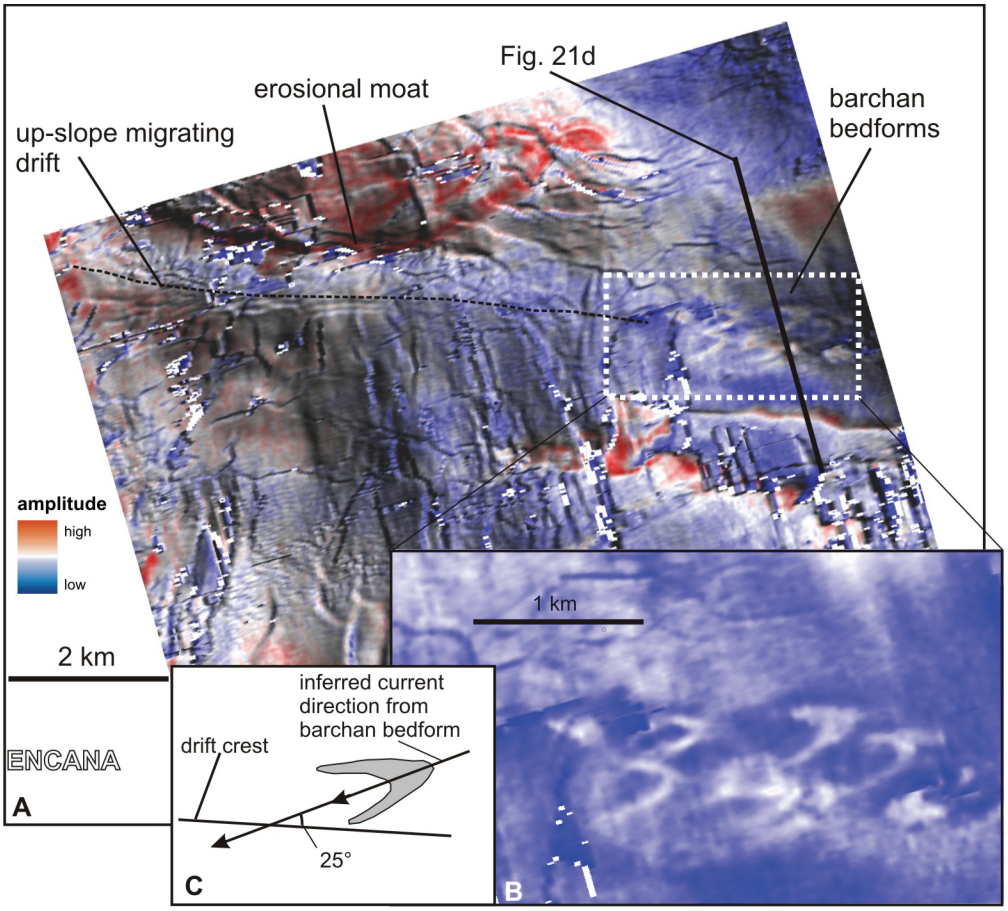
Fig. 21d
erosional moat
up-slope migrating drift
barchan bedforms
amplitude
high
low
2 km
ENCANA
A
1 km
B
inferred current direction from barchan bedform
drift crest
25°
C

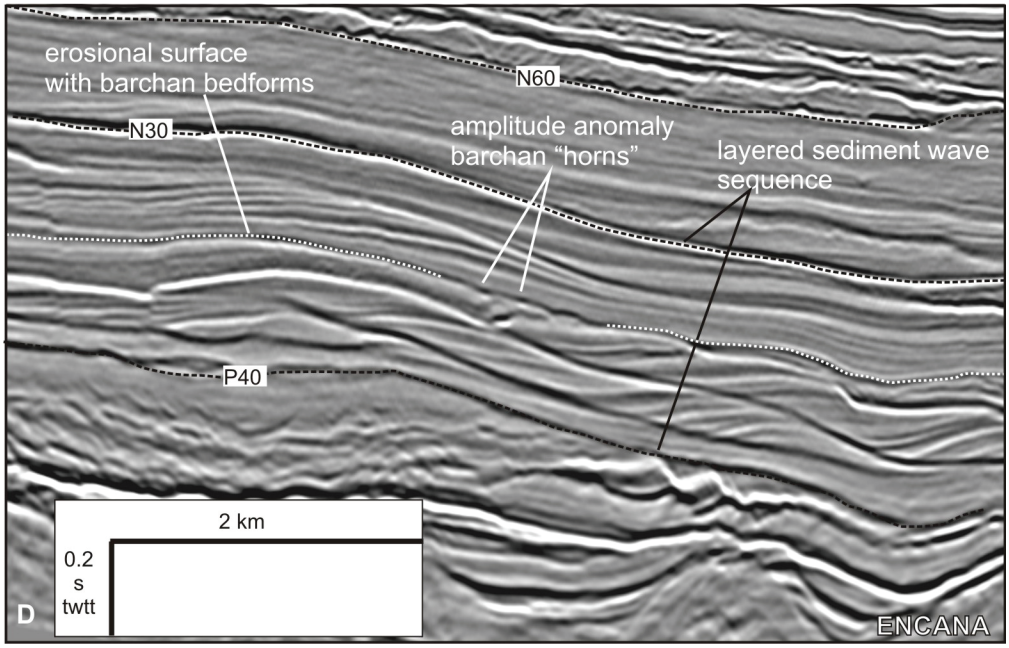
erosional surface with barchan bedforms
N60
N30
amplitude anomaly barchan "horns"
layered sediment wave sequence
P40
2 km
0.2 s twtt
D
ENCANA

Paleocurrent direction indicators

Deep-water sedimentary bedforms preserve important information about long-term mean bottom current characteristics, including flow direction. Bedform migration direction and orientation, erosional feature orientation, and the development of bedforms relative to fixed seafloor obstacles were used to determine paleocurrent direction in the study area (Figure 4.4). In general, giant sediment waves migrate up current when they develop on relatively flat seabed, and up slope and up current at an angle to the mean current when they develop on a slope (Blumsack and Weatherley 1989; Hopfauf and Speiss 2001; Flood and Giosan 2002; Wynn and Masson 2008). Therefore, it is difficult to determine the precise mean current direction for waves that develop on a slope. In Figure 4.4, the approximate current direction was determined by assuming sediment wave migration direction is up-current, 180° from the current direction. As expected, most sediment waves migrate up slope in a north-northeast direction; the exceptions are some of the sediment waves in the Barrington 3D dataset which migrate along slope in a northeast direction (Figure 4.15). Here, wave crest orientation changes abruptly where the *Shelburne Drift* onlaps the more steeply-dipping N30 unconformity. In the case of the 2D, low relief bedforms in the Torbrook 3D dataset, paleo bottom current direction, assumed to be perpendicular to the wave crest, is to the southwest (Figure 4.18).

In this study, more precise methods were developed to determine the paleo-bottom-current direction than simply applying sediment wave migration direction. The position of shallow salt diapirs imaged in the Barrington 3D area likely varied little during the development of the *Shelburne Drift*. In the case of the westernmost diapir in the Barrington 3D area (Figure 4.15), circular bedforms developed on the southwest side of the diapir and erosional moats developed on the northeast side which suggests flow separation and the development of lee vortices (Figure 4.15). A line that bisects the moats, diapir crest, and circular bedforms defines a more accurate estimate of the mean paleo-bottom current direction and suggests a southwest flowing bottom current (Figure 4.15). Comparison of the mean current direction derived from this relationship to

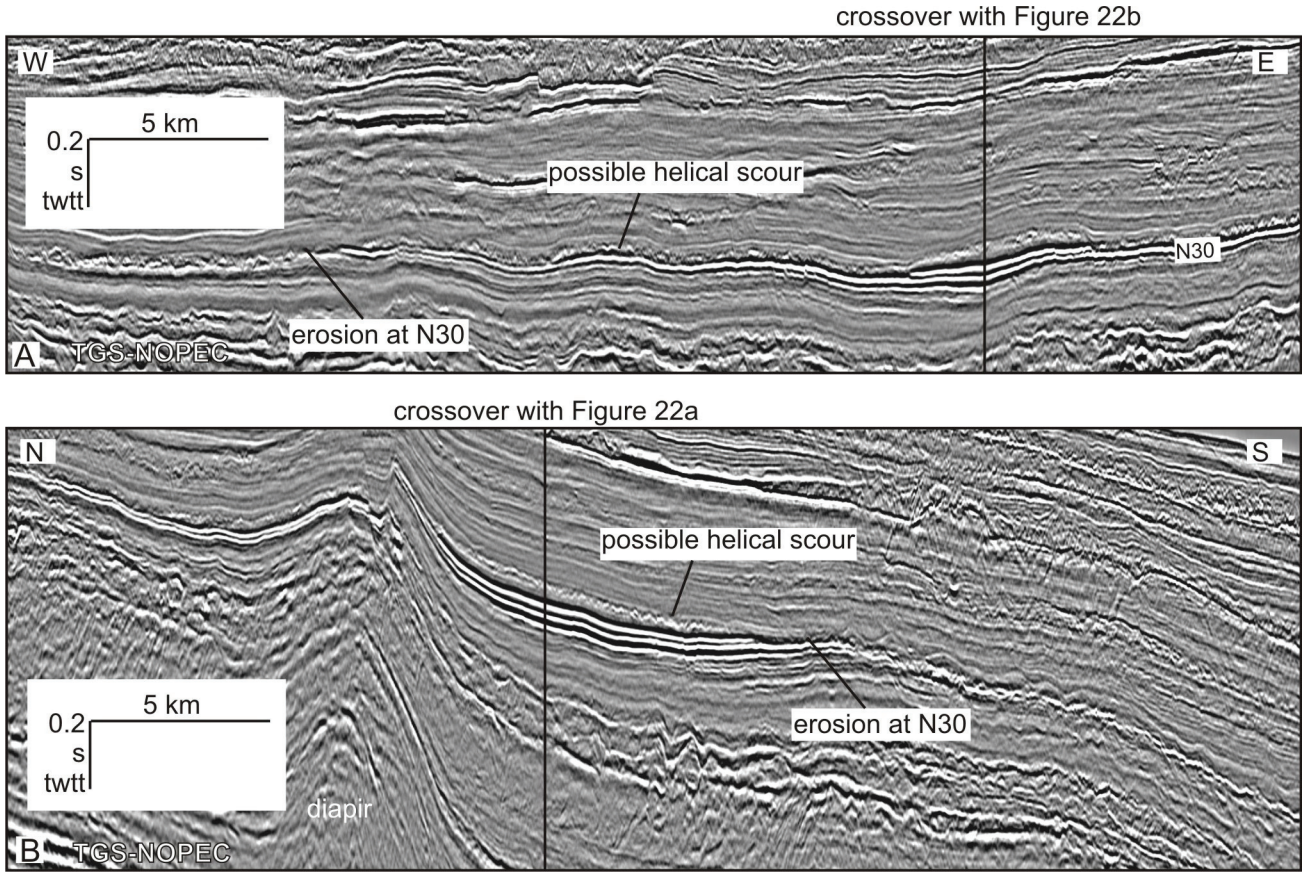

Figure 4.22 Seismic reflection profiles showing an erosional surface above horizon N30 that returns hyperbolic diffractions and possibly represents furrows created by helical scour. Profile locations are shown in Figure 4.1. Data are courtesy of TGS-NOPEC Geophysical Company L.P.

sediment wave orientations elsewhere in the Barrington 3D survey area shows that up-slope migrating bedform crests developed at an angle of 20°-40° to the mean current. In contrast, along-slope migrating bedforms located seaward of the steeply-dipping N30 unconformity migrate at an angle of 75°-100° (approximately perpendicular) to the mean current (Figure 4.15). Another measurement of precise mean paleo-bottom-current direction is derived from the barchan bedforms interpreted in the Torbrook and Weymouth 3D datasets. Barchan bedforms migrate down current and the apexes of the crescents face upcurrent (Todd 2005). Precise paleocurrent directions were determined by bisecting the crescentic bedforms through their apexes (Figures 4.18, 4.21). Analysis of barchan bedforms suggests a southwest flowing bottom current (Figure 4.4). The barchan bedforms in the Weymouth 3D dataset are juxtaposed with up-slope migrating sediment waves (Figure 4.21). Similar to the Barrington 3D area example, the angle between the up-slope migrating wave crest and the paleo-bottom current direction inferred from the barchan bedform orientation is 25° (Figure 4.21).

4.5 Discussion

4.5.1 Comparison with large sediment drifts elsewhere in the North Atlantic

Age

Large Cenozoic sediment drifts are recognized along much of the margin of the North Atlantic (McCave and Tucholke 1986; Faugères et al. 1993; Wold 1994; Faugères et al. 1999; Faugères et al. 2008). The onset of drift construction and enhanced bottom current activity in the North Atlantic occurred during the late Paleogene and early Neogene, and is associated with increased circulation in North Atlantic Deep Water and the opening of northern oceanic gateways such as the Greenland-Scotland Ridge, the Faroe-Shetland gateway, and Fram Strait, and the closing of equatorial gateways at Panama, the Mediterranean, and Indonesia (Wright and Miller 1996; Davies et al. 2001; Jakobsson et al. 2007, Potter and Szatmari 2009). The earliest indication of widespread Cenozoic bottom current activity in the western North Atlantic is the erosion of horizon A^U during

the Early Oligocene over much of the North American Basin (Mountain and Tuchoke 1985), although there is evidence that AABW erosion may have been important as early as the Late Paleocene (Mountain and Miller 1992). In the northern North Atlantic, the onset of development of the Feni and Southeast Faeroes drifts is Early Oligocene and represents the earliest geological evidence of the introduction of northern water masses into North Atlantic circulation (Wold 1993; Davies et al. 2001). In general, sediment drift construction increased substantially in the Middle Miocene and Pliocene throughout the North Atlantic (Mountain and Tucholke 1985; Arthur et al. 1989; Wold 1993; Wright and Miller 1996).

Along the Scotian margin, the earliest evidence of Cenozoic bottom current controlled deposition is the *Mohawk Drift*, which began to develop in the Late Eocene and ceased in the Early Oligocene, prior to the erosion of P40. There are no large drifts preserved between horizons P40 and N30, although regional erosion of N30 by mass wasting (e.g. Campbell and Mosher 2010; Figure 4.6) may have modified the gross structure of a large drift in this interval as to not be recognizable. Other large drifts in the study area all began to develop after formation of the N30 unconformity in the early Late Miocene and continued until the Late Pliocene. Timing of the development of large Neogene sediment drifts in the study area, therefore, is similar to the timing observed for other large sediment drifts in the North Atlantic. Unlike the rest of the North Atlantic, the evidence along the Scotian margin of sediment drift development in the Late Eocene is not widely recognized elsewhere.

Morphology

The coeval *Shubenacadie* and *Shelburne Drifts* are the largest bottom current deposits in the study area, representing more than 20% of the total preserved Upper Cretaceous to Present succession over most of the study area, and over 50% near the Torbrook C-15 well (Campbell et al. 2010 and Chapter 2). The interval was previously interpreted as a turbidite sequence that developed above the N30 unconformity (Swift 1987), or as a sequence of uniform pelagic and hemipelagic sediments deposited during a sealevel highstand (Piper et al. 1987). Sample control from the few wells in the area is insufficient

to determine sedimentologically the nature of the deposit, other than the predominance of mud over coarser lithologies. It is likely that muddy turbidites and hemipelagic sediments provided a sediment source for the drift. It is only through the detailed mapping of the interval on regional seismic profiles that the gross structure and internal architecture becomes apparent, and the importance of along slope bottom currents in moulding the succession becomes evident. The *Shelburne Drift* is interpreted to represent an along-slope continuation of the *Shubenacadie Drift*, separated from each other by the Mohican Channel and having characteristics of a plastered drift rather than a separated drift (Faugères et al. 1999).

The *Shubenacadie Drift* is similar in age and morphology to the Chesapeake Drift on the U.S. Atlantic margin (Mountain and Tucholke 1985; Locker and Laine 1992; Twichell et al. 2009). The drift has the appearance of a separated drift (Faugères et al. 1999). Like the Chesapeake Drift, the *Shubenacadie Drift* developed above the faulted and hummocky Oligocene to Middle Miocene succession, and forms a ridge that is oblique to the regional slope. The morphology of the drift is enhanced by subsequent channel erosion that is deflected towards the west by the pre-existing seafloor relief created by the drift (Figure 4.8). The area between the upper slope and the drift was then back-filled on the on the landward side (Figure 4.9). The drift migrated westward as it developed, for example the crest of the ridge migrated at least 12 km between the N50 and N60 seismic markers over a period of approximately 2 Ma (Figures 4.8, 4.19). The drift shows evidence of a bottom-simulating reflector (Mosher et al. 2005) and is flanked by sediment waves, other elements that are shared with the Chesapeake Drift (Mountain and Tucholke 1985).

The *Gully Drift* is unique in the study area in that it has the morphology of what has typically been described as a detached drift in the literature (McCave and Tucholke 1986; Faugères et al. 1999). The drift appears to be linked to both a basinward shift in underlying salt deposits that changed the trend of the paleoslope, and the development of a channel immediately to the east which likely provided sediment for drift construction (Figure 4.12). The drift forms a large western (right-hand) channel levee and it is likely

that the combined effects of a westward flowing WBUC and Coriolis force led to the construction of the drift.

4.5.2 Sediment wave and small drift formation

Fields of large sediment waves, or giant mud waves, are recognized throughout the study area (Figure 4.4). For example, more than 50% of the area of the *Shelburne Drift* consists of stacked sequences of giant mud waves confined to a submarine embayment where a landward shift in shallow salt diapirs occurs seaward of the Shelburne G-29 well (Figures 4.1c, 4.4). Although the sediment waves are not directly sampled, lateral equivalent sediments are intersected by a few wells suggesting a mud dominated lithology (Campbell and Mosher 2010; Campbell and Deptuck In Press). Similar large sedimentary bedforms are sampled on the U.S. Atlantic margin and are also shown to be mud-dominated (DSDP site 603, Van Hinte, Wise et al. 1983). These sediment waves are associated with the development of the Hatteras Outer Ridge (Fox et al. 1968; Locker and Laine 1992). Such large, mud-dominated bedforms are considered to form under relatively weak bottom currents, on the order of 0.1 to 0.2 m/s (Stow et al. 2009).

Detailed interpretation of 3D seismic data (see also Campbell and Deptuck In Press) shows that development of sediment waves on the Scotian margin is intimately linked to pre-existing seafloor morphology. Sediment wave development, therefore, is related to flow perturbation as the bottom current interacts with seafloor obstacles (Figure 4.15) (Flood 1988; Blumsack and Weatherly 1989; Blumsack 1993; Hopfauf and Speiss 2001). Many of the small drifts observed in the study area develop west or southwest of seafloor obstacles, such as escarpments or diapirs, and likely form under analogous conditions but do not evolve into laterally extensive sediment wave fields. The accreted sediment drifts interpreted in the Weymouth 3D survey area (Figure 4.17) were first interpreted by MacDonald (2006) as two types of sediment waves; bedforms below the upper slope were attributed to formation by turbidity currents, and bedforms below the lower slope were attributed to formation by bottom currents. Further detailed analysis during this

study suggests that there is no obvious reason to propose that two different sediment wave forming processes were responsible for their formation.

The results from this study reveal that the angle between the wave crest orientation of up-slope migrating bedforms and mean paleo-bottom-current direction inferred from independent methods (i.e. from barchan bedfroms or from relationship to fixed seafloor obstacles) is on the order of 20° to 40° (Figures 4.15, 4.21). The apparent upslope migration on slopes may be explained by local changes in helicoidal (secondary) flow dynamics because the bottom current becomes more confined as it approaches the more steeply-dipping slope, resulting in differential velocities between the sloping and flat seabed (e.g. Hernandez-Molina et al. 2008). Additionally, it is possible that bottom current flow parallel to the wave crest versus perpendicular to wave crest plays a greater role in bedform formation on slopes than on relatively flat areas. In the Argentine Basin, Blumsack and Weatherly (1989) recognized that sediment waves were not aligned perpendicular to mean current direction and that a crest-parallel bottom current velocity component was important for sediment wave growth.

The two-dimensional, low relief sediment waves, barchan bedforms, and possible helical scour in the study area are associated with erosional surfaces (Figures 4.18, 4.21-4.22). In the Weymouth 3D dataset, MacDonald (2006) identified a zone of closely-spaced along-slope amplitude anomalies within the Pliocene interval and also suggested a bottom current scour origin. None of these features are sampled in the study area, but elsewhere similar features are generally considered to be coarser grained and attributed to higher bottom current velocities, on the order of 0.5 to 1.2 m/s (Stow et al. 2009; Viana 2007). Barchan bedforms form in sediment-starved conditions, where there is limited mobile sediment available. Most examples of submarine barchans in the literature are from areas where glaciomarine sediments are reworked and barchans typically consist of mud and sand overlying a sandy to gravelly lag (Cochonat et al. 1989; Wynn et al. 2002; Todd 2005). Miocene sediments on the outer Scotian margin are mud-dominated and non-glaciomarine (Fensome et al. 2008), so it is difficult to suggest that a similar lithological relationship would exist for the barchan bedforms shown in Figure 4.21. Kenyon et al.

(2002) describe deepwater barchans in the Gulf of Mexico, where glaciomarine sediments are absent, and postulate that the bedforms are composed of foraminiferal sands overlying a cohesive foram ooze, although sample control is not available. A similar process may be responsible for the features observed in Miocene sediments on the Scotian margin.

The unique case of asymmetrical channel infill

Most Miocene channels in the study area are relatively straight and show a similar pattern of a west-to-east channel infill and preferential deposition on the western channel wall (Figure 4.14). Such asymmetrical development of channel infill has been attributed elsewhere to the influence and interaction of bottom currents with channel forming processes (Faugères et al. 1999; Mulder et al. 2008; Zhu et al. 2010). The observation that asymmetrical channel fill continues above the height of the channel flanks (Figure 4.14a) suggests that the processes that lead to the channel infill are different than the processes that eroded the channel. If the dynamics proposed in the lee-wave and flow perturbation models proposed by Flood (1988), Blumsack and Weatherly (1989) and Hopfauf and Speiss (2001) are applied to a bottom current flowing perpendicular to a channel, as the bottom current flows from east to west and encounters a channel, the flow first accelerates down the eastern wall of the channel, then decelerates as it meets the western wall, resulting in decreased deposition or erosion in the east and deposition in the west (Figure 4.23). Therefore, it would seem that the channel infill pattern observed in the study area supports this model. Additionally, the Scotian margin is in a mid-latitude position and it is likely that Coriolis forces influence turbidity currents, deflecting the flow towards the west (Cossu et al. 2010), possibly resulting in the observed asymmetry (Figure 4.23). At this time it is difficult to determine the relative importance of either processes, however the asymmetry observed in the nearby western levee of Laurentian Channel was attributed to the combined effects of WBUC and Coriolis forces (Skene and Piper 2006; Faugères et al. 1999), and it is likely that Coriolis forces enhance the WBUC in the study area.

4.5.3 New insights into Cenozoic circulation in the Western North Atlantic

Major erosional surfaces generated by along-slope processes mark significant changes in ocean circulation and often coincide with tectonic events, such as the opening of oceanic gateways (Wright and Miller 1996, Faugères et al. 2008). Along the U.S. Atlantic margin, regional seismic horizons A^U (early Oligocene), Merlin (late Middle Miocene) and Blue (Pliocene) (Mountain and Tucholke 1985) are interpreted to represent pulses in WBUC intensity that resulted in local erosion. Over much of the Scotian margin, within the constraints of biostratigraphic age control, equivalent age horizons are recognized as P40 (A^U), N30 (Merlin) and N50 (Blue). P40 and N30 are readily identifiable, not only because they appear erosional in many areas, but because they mark distinct changes in

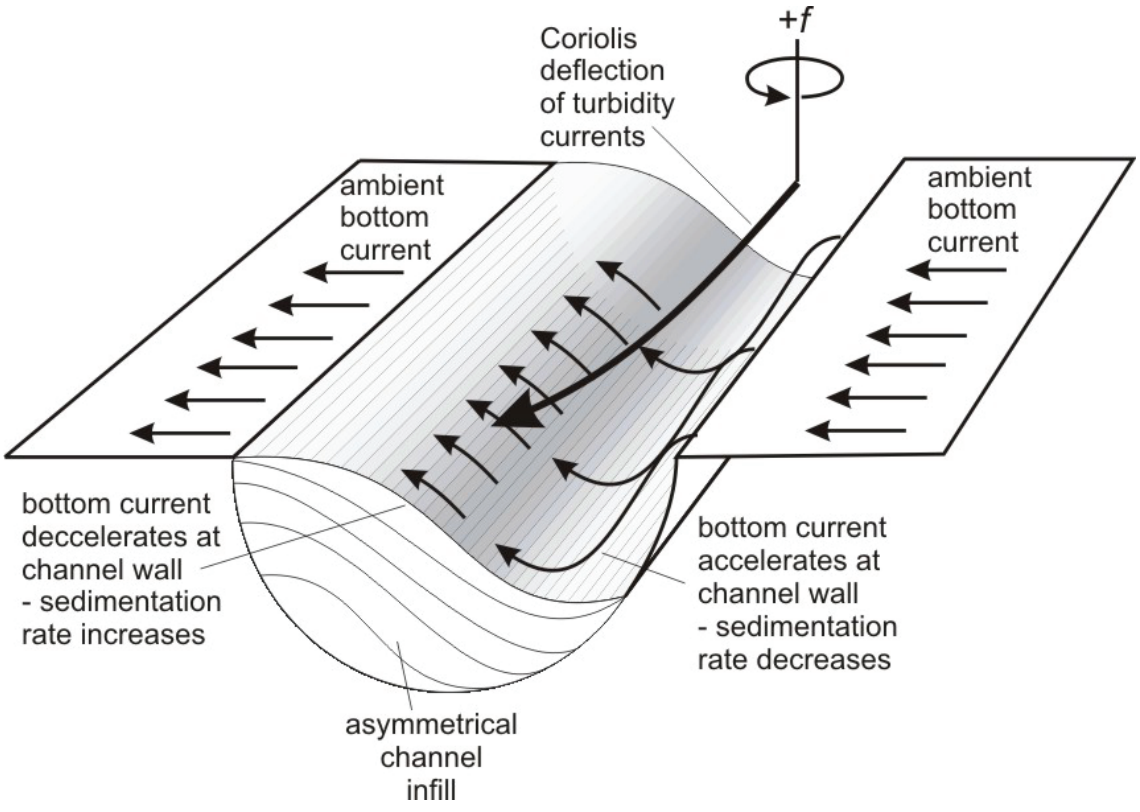

Figure 4.23 Cartoon illustrating processes that lead to asymmetrical infill of channels in the study area. *+f* is the Coriolis parameter in the northern hemisphere.

acoustic facies above and below. Horizons P40 and N30 often form the lower and upper boundary of the distinct hummocky and faulted Oligocene to Middle Miocene succession (e.g. Figures 4.7, 4.8, 4.10). In contrast, horizon N50 forms an erosional unconformity over parts of the *Shubenacadie Drift*, but because it is not associated with a marked acoustic facies change above and below, it is less easily identified away from areas of erosion.

The effects of along-slope erosion and deposition during the Late Eocene and Oligocene, for example the construction of the *Mohawk Drift* and the erosion of P40, are more apparent along the upper continental rise seaward of shallow salt structures on the Scotian margin. The pattern suggests that the effects of bottom currents are better preserved in the deep basin either because the evidence further up slope was removed by subsequent erosion, or bottom currents were more intense along the deep basin margin and basin floor at this time (Figure 4.24). If the latter, this deep basin erosion possibly represents incursion of AABW onto the Scotian Rise (Figure 4.2). Subsequent or concurrent gravity flow processes due to sea-level lowering later in the Oligocene possibly mask the geological evidence for along slope erosion further landward as suggested for the U.S. continental margin (Mountain and Tucholke 1985; Miller et al.1985). If widespread downslope erosion occurred on the Scotian margin during the Early Oligocene, it would be expected that downslope flows would be focussed in the ubiquitous gullies that formed during the Paleocene and Eocene (Figure 4.19b). This pattern occurred in at least one location along the margin (e.g. Brake 2009), however over much of the Scotian margin, a distinct Priabonian mud-dominated unit is preserved in gullies and is eroded on interfluves. In fact, small drifts are recognized in the Upper Eocene and Lower Oligocene succession below the middle slope in some locations (Figures 4.4, 4.13). Although these drifts are not widespread, they indicate that bottom currents were active but probably not as significant landward of the diapir province during the Early Oligocene (Figure 4.4). In contrast, erosion during the Neogene, for example during the formation of the N30 and N50 unconformities, was focussed further landward in what were probably shallower water depths, below the modern middle slope (Figure 4.24). Additionally, Neogene sediment drifts are recognized over the extent of the

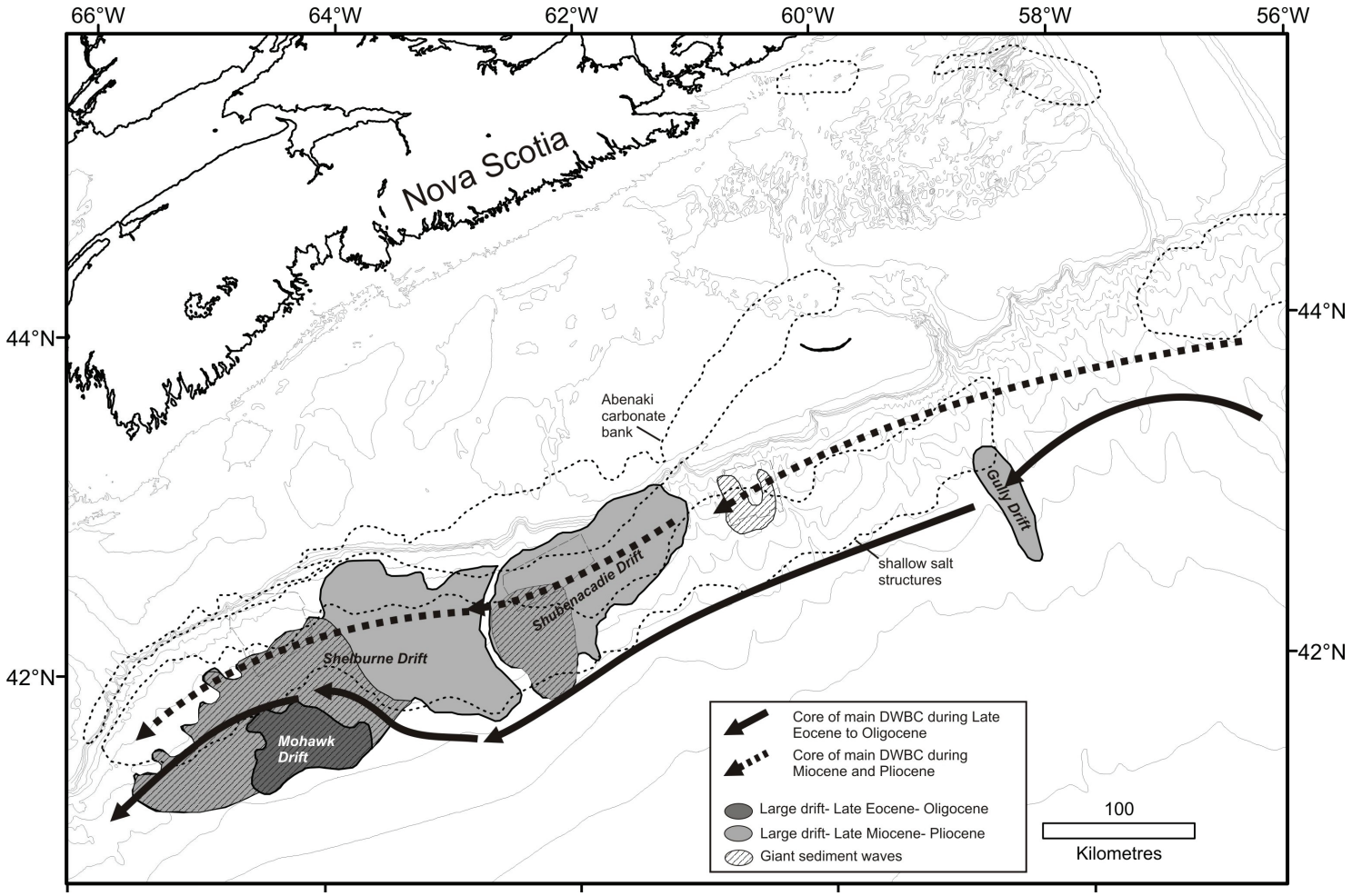

Figure 4.24 Map showing the core positions of the DWBC during the Late Eocene and Oligocene, and during the Miocene and Pliocene. The positions are based on the locations of maximum erosion, although data suggests that an east-to-west flowing bottom current swept most of the margin during much of the late Paleogene and Neogene.

Scotian margin, from the upper slope to the upper rise. This distribution suggests a general change in the location of the DWBC, from confinement to the continental rise and deep basin in the Oligocene, to shallower water depths through the Neogene. Increased contribution from northern water masses originating in the Labrador Sea are a likely cause for the observed shift.

The results from this study overwhelmingly indicate that where Cenozoic contourite depositional systems are observed on the Scotian margin, a northeast to southwest flowing, slope parallel bottom current was responsible for their formation. Whether this evidence is indicative of the anticlockwise gyre north of the Gulf Stream suggested by Schmitz and McCartney (1992) (Figure 4.2), or simply a continuation of the DWBC around the southern Grand Banks suggested by several others (McCave and Tucholke 1986; Pickart 1992; Pickart and Smethie 1998) is not clear. There is no geological evidence, however, of northward encroachment of the Gulf Stream onto the Scotian margin which would result in a west to east bottom current as hypothesized in the absence of a Labrador Current (e.g. Barron and Peterson 1991). There is also no preserved evidence of Gulf Stream ring interaction with the seabed as recognized in the present day at the HEBBLE site (Weatherley and Kelley 1985).

4.6 Conclusions

1. This study represents the first detailed investigation of contourite depositional systems along the Western North Atlantic margin using modern 2D and 3D seismic reflection data. These data provide a unique opportunity to investigate the preserved geomorphology of large sedimentary features in three dimensions and determine the long-term mean bottom current flow characteristics throughout the Cenozoic.

2. The results show that sediment drifts, previously considered absent or of limited geographical extent, are widespread and make up much of the Cenozoic section preserved below the outer Scotian margin. Large sediment drifts developed in the Late

Eocene to Early Oligocene, and during the Late Miocene to Pliocene. Small sediment drifts developed locally throughout the late Paleogene and Neogene, either southwest and down current of seafloor obstacles or fill channels.

3. Significant and sustained erosional pulses in bottom current circulation contribute to the formation of regional seismic markers, first along the continental rise in the Early Oligocene, then along the continental slope during the Late Miocene and Pliocene. The timing of these erosional pulses appears to be similar to the timing on the U.S. Atlantic margin. 3D seismic data show that locally, erosion surfaces preserve along slope amplitude anomalies and bedforms indicative of relatively strong currents, and possible evidence of helical scour.

4. 3D seismic data allow determination of paleo bottom-current direction using multiple criteria. All bottom current evidence suggests a northeast-to-southwest, along-slope flowing Deep Western Boundary Current during the Cenozoic.

5. The results show an active Western Boundary Under Current at least as early as the Late Eocene. An increase in intensity of the WBUC in shallower water depths occurred during the Miocene and possibly represents increased contribution from Labrador Sea water masses. There is no preserved evidence of northward encroachment of the Gulf Stream or Gulf Stream Rings.

4.7 Acknowledgements

The authors would like to express appreciation to EnCana Corp., TGS-Nopec Geophysical Co. L.P., and ION-GXT for data access.

4.8 References cited in Chapter 4

Amos, A.F., and Gerard, R.D. 1979. Anomalous bottom water south of the grand-banks suggests turbidity current activity. Science, v. 203, p. 894-897.

Arthur, M., Srivastava, S.P., Kamiski, M., Jarrad, R., Osler, J., 1989. Seismic stratigraphy and history of deep circulation and sediment drift development in the Baffin Bay and the Labrador Sea, in: Srivastava, S.P., Arthur, M., Clement, B. (Eds.), Proc. ODP Sci. Res. College Station, TX (Ocean Drilling Program), Vol. 105, pp. 957–988.

Biscaye, P.E., and Eittreim, S.L. 1977. Suspended particulate loads and transports in the nepheloid layer of the abyssal Atlantic Ocean. Marine Geology, v. 23, p. 155-172.

Blumsack, S.L., 1993. A model for the growth of mudwaves in the presence of time varying currents. Deep-sea Research II 40 (4/5), 963–974.

Blumsack, S.L. and Weatherly, G.L. 1989. Observations of the nearby flow and a model for the growth of mudwaves. Deep Sea Reseach Part A. v. 36, p. 1327-1339.

Brake, V.I. 2009. Evolution of an Oligocene Canyon System on the Eastern Scotian Margin. Unpublished M.Sc. Thesis, Dalhousie University, Halifaxm Nova Scotia, Canada.

Bujak Davies Group 1988. Palynological Analysis of the Interval 440-3950 M, Bonnet P-13, Scotian Shelf. Geological Survey of Canada Open File 1858, 19 p.

Campbell, D.C. and Deptuck, M.E. In Press. Alternating bottom current dominated and gravity flow dominated deposition in a lower slope and rise setting- Insights from the seismic geomorphology of the western Scotian margin, Eastern Canada. SEPM special publication.

Campbell, D.C. and Mosher, D.C. 2010. Middle to Late Miocene slope failure and the generation of a regional unconformity beneath the western Scotian Slope, eastern Canada. Submarine Mass Movements and Their Consequences, Advances in Natural and Technological Hazards Research, v. 28, p. 645-655.

Campbell, D.C., Mosher, D.C., and Shimeld, J.W. 2010. Erosional Unconformities, Megaslumps and Giant Mud Waves: Insights into passive margin evolution from the continental slope off Nova Scotia. Conjugate Margins II, Lisbon 2010, Metodo Directo, v. IV, p. 37-41, ISBN: 978-989-96923-1-2, http://metododirecto.pt/CM2010

Cochonat, P., Ollier, G., and Michel, J.L. 1989. Evidence for slope instability and current-induced sediment transport, the RMSTitanic wreck search area, Newfoundland rise. Geo-Marine Letters, v. 9, p. 145-152.

Cossu, R., M. G. Wells, and A. K. Wåhlin (2010), Influence of the Coriolis force on the velocity structure of gravity currents in straight submarine channel systems, Journal of Geophysical Research, v. 115, C11016, doi:10.1029/2010JC006208.

Crux, J.A. and Shaw, D. 2002. Biostratigraphy of the Chevron et al. Newburn H-23 well, offshore Nova Scotia. 37 p.

Daniell, J.J., and Hughes, M. 2007. The morphology of barchan-shaped sand banks from western Torres Strait, northern Australia. Sedimentary Geology, v. 202, p. 638-652.

Davies, R., Cartwright, J., Pike, J., and Line, C. 2001. Early Oligocene initiation of North Atlantic Deep Water formation. Nature, v. 410, p. 917–920.

Ebinger C.A., and Tucholke, B.E., 1988, Marine Geology of the Sohm Basin, Canadian Atlantic Margin: Bulletin of American Association of Petroleum Geologists, v. 72, p. 1450-1468.

Faugères, J.-C., Mezerais, M.L., and Stow, D.A.V. 1993. Contourite drift types and their distribution in the North and South Atlantic Ocean basins. Sedimentary Geology, v. 82, p.189–203.

Faugères, J-C, Stow, D.A.V., Imbert, P., and Viana, A., 1999, Seismic features diagnostic of contourite drifts: Marine Geology, v. 162, p. 1-38.

Faugères, J.C., and Stow, A.V., 2008. Contourite drifts: nature, evolution and controls. In: Rebesco, M., Camerlenghi, A. (Eds.), Contourites. Developments in Sedimentology, vol. 60. Elsevier, p. 259-288.

Fensome, R.A., Crux, J.A., Gard, I.G., MacRae, R.A., Williams, G.L., Thomas, F.C., Fiorini, F., and Wach, G., 2008, The last 100 million years on the Scotian Margin, offshore eastern Canada: an event-stratigraphic scheme emphasizing biostratigraphic data: Atlantic Geology, v. 44, p. 93-126.

Flood, R.D., 1988, A lee wave model for deep-sea mudwave activity: Deep-Sea Research, v 35, p. 973-983.

Flood, R.D., Giosan, L., 2002. Migration history of a fine-grained abyssal sediment wave on the Bahama Outer Ridge. Marine Geology, v. 192, 259–274.

Flood, R.D., Shor, A.N., Manley, P.L., 1993. Morphology of abyssal mud waves at Project MUDWAVES sites in the Argentine Basin. Deep-Sea Res. II 40, 859-888.

Fox, P.J., Heezen, B.C., and Harian, A.M. 1968. Abyssal anti-dunes. Nature, v. 220, p.470-472.

Heezen, B.C., Hollister, C.D., and Ruddiman, W.F. 1966. Shaping of the continental rise by deep geostrophic contour currents. Science, v. 152, p. 502–508.

Hernández-Molina, F.J., Llave, E., and Stow, D.A.V. 2008. Continental slope contourites. In: M. Rebesco and A. Camerlenghi (eds.). Contourites. Developments in Sedimentology, v. 60, Elsevier, p. 379- 408.

Hernández-Molina, F.J., Paterlini, M., Somoza, L., Violante, R., Arecco, M.A., de Isasi, M., Rebesco, M., Uenzelmann-Neben, G., Neben, S., and Marshall, P. 2010. Giant mounded drifts in the Argentine Continental Margin: Origins, and global implications for the history of thermohaline circulation. Marine and Petroleum Geology, v. 27, p. 1508-1530, ISSN 0264-8172, DOI: 10.1016/j.marpetgeo.2010.04.003.

Hopfauf, V., and Spiess, V., 2001, A three-dimensional theory for the development and migration of deep sea sediment waves: Deep-Sea Research I, v. 48, p. 2497–2519.

Howe, J.A. 2008. Methods for Contourite Research, In: Rebesco, M., Camerlenghi, A. (Eds.), Contourites. Developments in Sedimentology, vol. 60. Elsevier, p. 19-33.

Hughes Clarke, J.E., O'leary, D.W., and Piper, D.J.W. 1992. Western Nova Scotia continental rise: relative importance of mass wasting and deep boundary-current activity. In: Poag, C.W., De Graciansky, P.C. (Eds.) Geologic Evolution of Atlantic Continental Rises. Van Nostrand Reinhold, New York, p. 266-281.

Jakobsson, M., Backman, J., Rudels, B., Nycander, J., Frank, M., Mayer, L., Jokat, W., Sangiorgi, F., O'Regan, M., Brinkhuis, H., King, J., Moran, K., 2007. The early Miocene onset of a ventilated circulation regime in the Arctic Ocean. Nature, v. 447, p. 986–990.

Jansa, L.F., Enos, P., Tucholke, B.E., Gradstein, F.M. and Sheridan, R.E. 1979. Mesozoic-Cenozoic sedimentary formations of the North American Basin: Western North Atlantic. In Deep Drilling Results in the Atlantic Ocean: continental margins and paleoenvironment, Edited by M. Talwani, W. Hay and W.B.F. Ryan, American Geophysical Union Maurice Ewing Series, v. 3 , p. 1–57.

Kenyon, N.H., Akhmetzhanov, A.M., Twichell, D.C. 2002. Sand wave fields beneath the Loop Current, Gulf of Mexico: reworking of fan sands. Marine Geology, v.192, p. 297–307.

Laberg, J.S., Stoker, M.S., Dahlgren, K.I.T., de Haas, H., Haflidason, H., Hjelstuen, B.O., Nielsen, T., Shannon, P.M., Vorren, T.O., Van Weering, T.C.E., Ceramicola, S. 2005. Cenozoic alongslope processes and sedimentation on the NW European Atlantic margin. Marine and Petroleum Geology, v. 22, p.1,069-1,088.

Lee, Y.-D.E., and George, R.A. 2004. High-resolution geological AUV survey results across a portion of the eastern Sigsbee Escarpment. AAPG Bulletin, v. 88, p. 747-764.

Locker, S.D., and Laine, E.P., 1992, Paleogene-Neogene depositional history of the middle U.S. Atlantic continental rise: mixed turbidite and contourite depositional systems: Marine Geology, v. 103, p. 137-164.

MacDonald, A.W.A. 2006. Cenozoic structural and stratigraphic evolution, faulting and geohazard issues influenced by shallow salt tectonics in the Weymouth prospect of the Scotian Slope, offshore Nova Scotia. Unpublished M.Sc. thesis, St. Mary's University, Halifax, Nova Scotia.

McCave I.N. and Tucholke B.E. 1986. Deep current controlled sedimentation in the western North Atlantic. in: The geology of North America vol. M: The western North Atlantic region. Vogt P.R. & Tuchkolke B.E. (eds.). Geological Society of America. p. 451–468.

McCave, I.N., Chandler, R.C., Swift, S.A., and Tucholke, B.E. 2002. Contourites of the Nova Scotian continental rise and the HEBBLE area. Geological Society, London, Memoirs, v. 22, p. 21-38.

Miller, K.G., Mountain, G.S., and Tucholke, B.E. 1985. Oligocene glacio–eustasy and erosion on the margins of the North Atlantic. Geology, v. 13, p. 10-13.

Miller, K.G., Wright, J.D., Katz, M.E., Wade, B.S., Browning, J.V., Cramer, B.S., and Rosenthal, Y. 2009. Climate threshold at the Eocene-Oligocene transition: Antarctic ice sheet influence on ocean circulation, in Koeberl, C., Montanari, A., (Eds.) The Late Eocene Earth—Hothouse, Icehouse, and Impacts: Geological Society of America Special Paper 452, p. 169–178, doi: 10.1130/2009.2452(11).

Mosher, D.C., Piper, D.J.W., Campbell, D.C., and Jenner, K.A., 2004, Near-surface geology and sediment-failure geohazards of the central Scotian Slope: American Association of Petroleum Geologists Bulletin, v. 88, p. 703-723.

Mosher, D.C., Louden, K., LeBlanc, C., Shimeld, J.W., and Osadetz, K.G. 2005. Gas Hydrates Offshore Eastern Canada: Fuel for the Future? Offshore Technology Conference paper 17588. In: Offshore Technology Conference. Houston, Tx. 2-5 May 2005.

Mountain, G.S. and Tucholke, B.E. 1985. Mesozoic and Cenozoic Geology of the U.S. Atlantic Continental Slope and Rise. in: Geologic Evolution of the U.S. Atlantic Margin. C.W. Poag (ed.). Van Nostrand Reinhold. p. 293-341.

Mountain, G.S., and Miller, K.G. 1992. Seismic and geologic evidence for early Paleogene deepwater circulation in the western North Atlantic. Paleoceanography, v. 7, p. 23-43.

Mulder, T., Faugères, J-C, Gonthier, E. 2008. Mixed turbidite-contourite systems. In: M. Rebesco and A. Camerlenghi (eds.). Contourites. Developments in Sedimentology, v. 60, Elsevier, p. 435-456.

Nielsen, T., Knutz, P.C., and Kuijpers, A. 2008. Seismic Expression of Contourite Depositional Systems. In: M. Rebesco and A. Camerlenghi (eds.). Contourites. Developments in Sedimentology, v. 60, Elsevier, p. 301-321.

Nowell, A.R.M., and Hollister, C.D. (Eds.). 1985. Deep Ocean Sediment Transport – Preliminary Results of the High Energy Benthic Boundary Layer Experiment, Marine Geology, v. 66, 420 pp.

Pickart, R.S. 1992. Water mass components of the North Atlantic Deep Western Boundary Current. Deep-Sea Research, v. 39, p. 1553-1572.

Pickart, R.S., McKee, T.K., Torres, D.J., and Harrington, S.A. 1999. On the mean structure and interannual variability of the slopewater system south of Newfoundland. Journal of Physical Oceanography, v. 29, p. 2541–2558.

Pickart, R. S., and Smethie, W.M. 1998. Temporal evolution of the deep western boundary current where it enters the sub-tropical domain. Deep-Sea Research, v. 45, p. 1053–1083.

Piper, D.J.W. 2005. Late Cenozoic evolution of the continental margin of eastern Canada. Norwegian Journal of Geology, v. 85, p. 231-244.

Piper, D.J.W., Normark, W.R., and Sparkes, R. 1987. Late Cenozoic Stratigraphy of the central Scotian Slope, Eastern Canada. Canadian Bulletin of Petroleum Geology, v. 35, p. 1-11.

Potter, P.E., and Szatmari, P. 2009. Global Miocene tectonics and the modern world. Earth-Science Reviews, v. 96, p. 279-295

Robertson Research. 2004. Nova Scotia Shelf: Biostratigraphic and Sequence Stratigraphic Correlation of the Early Cretaceous Strata in Seven Wells - Report No.6620/Ib. Canada-Nova Scotia Offshore Petroleum Board File SR(E) 2004-1, 47 p.

Schmitz , W.J., and McCartney, M.S. 1993. On the North Atlantic Circulation. Reviews of Geophysics, v. 31, p. 21-39.

Shimeld, J., 2004, A comparison of salt tectonic subprovinces beneath the Scotian Slope and Laurentian Fan, *in* Post, P.J., Olson, D.L., Lyons, K.T., Palmes, S.L., Harrison, P.F., and Rosen, N., eds., Salt–sediment Interactions and Hydrocarbon Prospectivity: Concepts, Applications, and Case Studies for the 21st Century. 24th Annual Gulf Coast Section of the Society of Economic Paleontologists and Mineralogists Foundation Bob F. Perkins Research Conference, Houston, Texas, Dec. 5-8, 2004, p. 502-532.

Skene, K.I., and Piper, D.J.W. 2006. Late Cenozoic evolution of Laurentian Fan: Development of a glacially-fed submarine fan. Marine Geology, v. 227, p. 67-92.
Smethie, W.M., Fine, R.A., Putzuka, A., and Jones, P. 2000. Tracing the flow of North Atlantic Deep Water using chlorofluorocarbons. Journal of Geophysical Research, v. 105, p. 14297-14323.

Smith, P.C., and Petrie, B.D. 1982. Low-frequency circulation at the edge of the Scotian Shelf. Journal of Physical Oceanography, v. 12, p. 28-46.

Stow, D.A.V., Faugères, J.C., Howe, J.A., Pudsey, C.J., Viana, A., 2002a. Contourites, bottom currents and deep-sea sediment drifts: current state-of-the-art. In: Stow, D.A.V., Pudsey, C.J., Howe, J.A., Faugères, J.C., Viana, A.R. (Eds.), Deep-Water Contourite Systems: Modern Drifts and Ancient Series, Seismic and Sedimentary Characteristics. Geological Society of London, Memoirs 22, 7-20.

Swift, S.A., 1987, Late Cretaceous-Cenozoic development of outer continental margin, southwestern Nova Scotia: Bulletin of American Association of Petroleum Geologists, v. 71, p. 678-701.

Todd, B.J. 2005. Morphology and composition of submarine barchan dunes on the Scotian Shelf, Canadian Atlantic margin. Geomorphology, v. 67, p. 487-500.

Tucholke, B. E., and Mountain, G.S. 1979. Seismic stratigraphy, lithostratigraphy and paleosedimentation patterns in the North American Basin, Edited by M. Talwani, W. Hay, and W. B. F. Ryan, Deep Drilling Results in the Atlantic Ocean: continental margins and paleoenvironment, American Geophysical Union Maurice Ewing Series, 3: 58-86.

Tucholke, B. E., and Mountain, G.S. 1986. Tertiary paleoceanography of the western North Atlantic Ocean. In The Geology of North America, Vol. M, The Western North Atlantic Region (ch. 38), Edited by Vogt, P.R. and Tucholke, B.E., Geological Society of America, Boulder, CO, p. 631–650.

Twichell, D.C., Chaytor, J.D., ten Brink, U.S., and Buczkowski, B. 2009. Morphology of late Quaternary submarine landslides along the U.S. Atlantic continental margin. Marine Geology, v. 264, p. 4-15.

Viana, A.R., Almeida Jr., W., Nunes, C.V., and Bulhões, E.M. 2007. The Economic importance of contourites. In Viana, A.R., Rebesco, M., eds.. Economic and Palaeoceanographic Significance of Contourite Deposits: Geological Society of London Special Publication v. 276, p. 1–23.

Wade, J.A. and MacLean, B.C. 1990. The Geology of the Southeastern Margin of Canada, Part 2: Aspects of the Geology of the Scotian Basin from Recent Seismic and

Well Data. In Geology of the continental margin off eastern Canada. Edited by M.J. Keen and G.L. Williams. Geological Survey of Canada, Geology of Canada no. 2, p.190-238.

Weatherly, G.L., and Kelley, E.A. 1985. Storms and flow reversals at the HEBBLE site. Marine Geology, v. 66, p. 205-218.

Wise, S.W. and van Hinte, J.E. 1987. Mesozoic-Cenozoic depositional environments revealed by Deep Sea Drilling Project Leg 93 Drilling on the continental rise off the eastern United States: cruise summary, In: Initial Reports of the Deep Sea Drilling Project, v. 93, p. 1367-1423.

Wold, C.N. 1994. Cenozoic sediment accumulation on drifts in the northern North Atlantic. Paleoceanography, v. 9, p. 917–941.

Worthington, L. V., 1976: On the North Atlantic Circulation. The Johns Hopkins Oceanographic Studies, No. 6, 110 pp.

Wright, J.D., Miller, K.G. 1996. Control of North Atlantic Deep Water circulation by the Greenland- Scotland Ridge. Paleoceanography, v. 11, p. 157–170.

Wynn, R.B. and Masson, D.G. 2008. Sediment waves and bedforms. In: M. Rebesco and A. Camerlenghi (eds.). Contourites. Developments in Sedimentology, v. 60, Elsevier, p 289-300.

Wynn, R.B., Masson, D.G., and Bett, B.J. 2002. Hydrodynamic significance of variable ripple morphology across deep-water barchan dunes in the Faroe–Shetland Channel. Marine Geology, v. 192, p. 309– 319.

Wynn, R.B., and Stow, D.A.V. 2002. Classification and characterization of deep-water sediment waves. Marine Geology, v. 192: 7-22.

Zhu, M., Graham, S., Pang, X., and McHargue, T. 2010. Characteristics of migrating submarine canyons from the middle Miocene to present: Implications for paleoceanographic circulation, northern South China Sea. Marine and Petroleum Geology, v. 27, p. 307-319

Chapter 5: Alternating Bottom Current Dominated and Gravity Flow Dominated Deposition in a Lower Slope and Rise Setting- Insights from the Seismic Geomorphology of the Western Scotian Margin, Eastern Canada*

5.1 Introduction

Mixed turbidite and contourite depositional systems exist on many continental margins (e.g. Locker and Laine 1992; Carter and McCave 1994; Rebesco and Stow 2001; Knutz and Cartwright 2003; Hernández-Molina et al. 2006; Uenzelmann-Neben 2006). Deposition in such systems is focussed along the lower continental slope and rise and occurs under the influence of relatively short-lived, sporadic, gravity-driven currents, as well as long-lived steady along-slope currents (Heezen et al. 1966; Locker and Laine 1992; Mulder et al. 2008). The interaction of gravity and bottom currents is most apparent where low frequency alternations of contourite and turbidite predominance are preserved (Mulder et al. 2008), and depositional elements are resolved in seismic reflection data. In such cases, it is likely that pre-existing morphology influenced the character of deposits originating from both down-slope gravity currents and along-slope bottom currents (Locker and Laine 1992; Uenzelmann-Neben 2006; Mulder et al. 2008). For instance, in the case of gravity flows, it is recognized that receiving basin configuration is one of the primary factors controlling lithofacies distribution as gravity flows transit from shelf areas into deeper water (Prather 2003; Steffens et al. 2003). Similarly for sediment drifts, pre-existing seafloor irregularities appear to be loci for the initiation of deepwater bottom current deposits (Faugères et al. 1999; Viana et al. 2007; Hopfauf and Spiess 2001; Wynn and Masson 2008).

Although conceptual models of the interaction of sedimentary processes in mixed turbidite and contourite systems have been proposed (Heezen et al. 1966; Locker and Laine 1992; Hernández-Molina et al. 2008; Viana 2008), relatively few published studies

have used 3D seismic data to clearly demonstrate the effects of morphological heritage in alternating gravity current and bottom current deposition. Viana et al. (2007) indicate that most studies of deepwater seismic geomorphology focus on describing and understanding depositional elements associated with downslope sediment transport primarily because of exploration interest in turbidite reservoirs (e.g. Posamentier and Kolla 2003; Deptuck et al., 2003; Davies et al. 2004). Recently, a number of authors have demonstrated the effectiveness of applying 3D seismic data to sediment drift studies (Knutz and Cartwright 2003; Hohbein and Cartwright 2006; Viana et al 2007) and have emphasized the need for more detailed examination of these deposits. In many areas, sediment drifts contribute significantly to the depositional record along the lower continental slope and rise (Wynn and Stow 2002; Hernàndez-Molina et al. 2008).

Across much of the western Scotian margin off eastern Canada (Figure 5.1), seismic reflection data reveal evidence of alternating down-slope and along-slope deposition throughout the Neogene (Campbell and Mosher 2010). A 3D seismic dataset located at the transition from the modern slope to continental rise provides an excellent opportunity to study in detail the seismic geomorphology and geological evolution of a mixed turbidite and sediment drift system. The objectives of this study are to describe the seismic geomorphology of the paleo-seabed immediately preceding the onset of drift construction and illustrate the close association between inherited seabed relief and drift morphology. Additionally, this study examines the seismic geomorphology of the sediment drift and its effect on receiving basin configuration as the system switched back to downslope-dominated sediment transport.

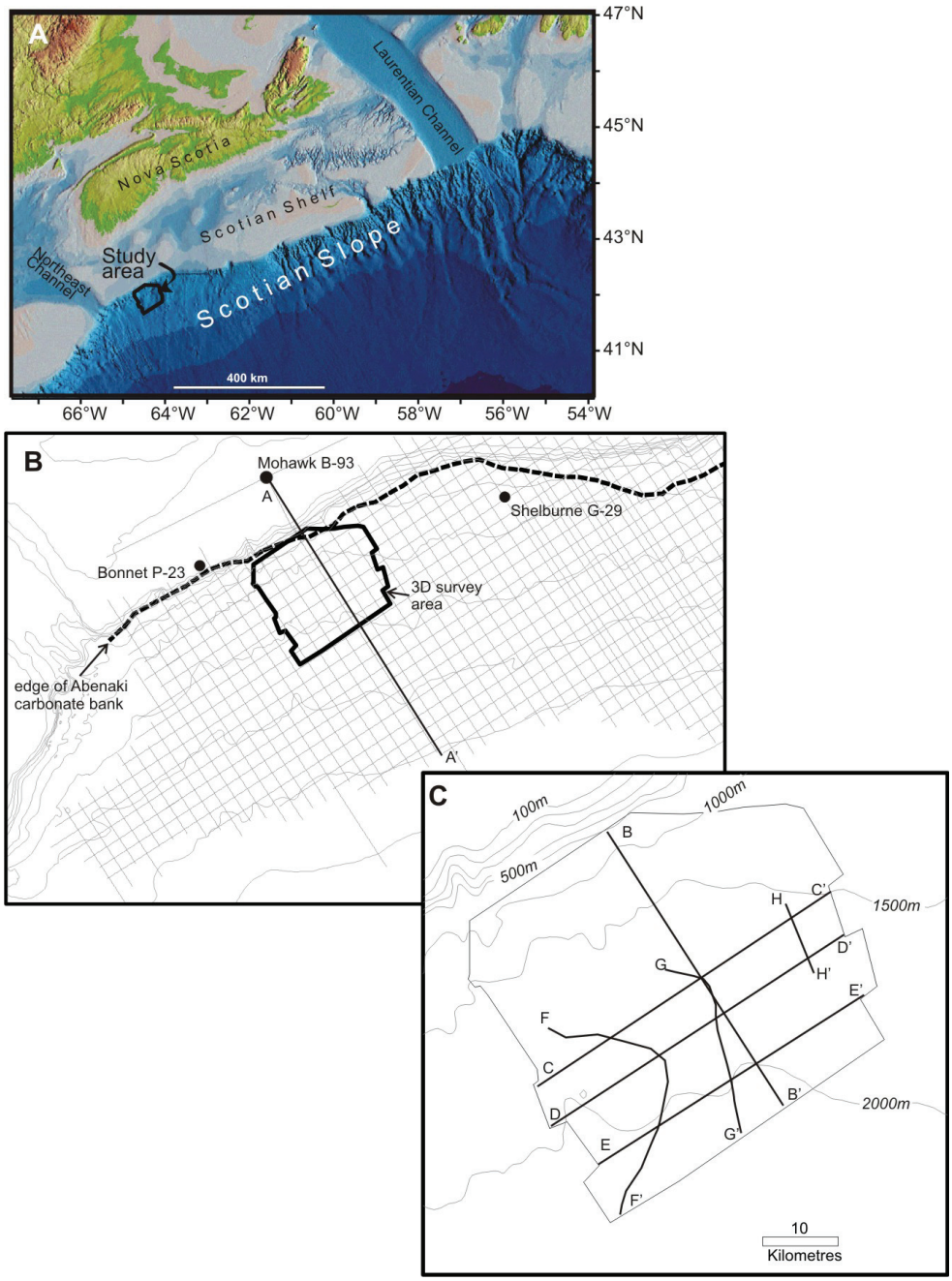

Figure 5.1 Location maps of study area. A) Regional map of the geomorphology of the continental margin off Nova Scotia (Modified from Shaw and Courtney 2004) B) Location map of the continental margin off western Nova Scotia, Canada showing coverage of 2D and 3D seismic reflection data, the buried edge of the Abenaki carbonate bank, and the location of cross-section A-A'. C) Location map of study area showing position of various seismic profiles discussed in the text.

5.2 GEOLOGICAL SETTING AND PREVIOUS WORK

The study area spans the middle continental slope to upper continental rise off southwestern Nova Scotia, Canada, in present-day water depths between 500 and 2900 metres below sea level (mbsl) (Figure 5.1). The morphology of the modern Scotian margin includes a >200 km wide continental shelf consisting of transverse troughs and intervening banks, the product of repeated glaciations through the Quaternary (Piper 1988). The shelf break lies at 80-130 mbsl (Mosher et al. 2004) and trends sub-parallel to the coastline for ~1000 km, from Northeast Channel in the west to Laurentian Channel in the east. The present-day slope extends from the shelf break to a decrease in gradient at 2000-2500 mbsl. The modern western Scotian margin has the characteristics of a bypass margin (Ross et al. 1994) with a steep (>4°) upper slope that extends to ~1000 mbsl and a gentler (<2°) lower slope and rise (Figure 5.2).

Published studies of the Cenozoic geological history of the Scotian margin focus on the area near Sable Island, east of the study area, where data density is greatest (e.g. Swift 1985; Swift et al. 1986; Swift 1987; Ebinger and Tucholke, 1988; Wade et al. 1995; Long 2002; Thomas 2005; MacDonald 2006; Fensome et al. 2008; Brake, 2009). In general, sediment accumulation appears to have been broadly controlled by changes in relative sealevel; however, local sediment distribution patterns were strongly influenced by local variations in sediment supply, slope morphology, erosion by bottom currents, and salt tectonics. Below the modern continental shelf and upper slope, episodes of localized outer shelf progradation occurred in the Paleocene, Eocene, and Miocene (Wade et al. 1995; MacDonald 2006), and major periods of channel formation and canyon incision occurred in the Paleocene, Eocene, Oligocene, Miocene and Pleistocene (Thomas 2005; MacDonald 2006; Fensome et al. 2008; Brake 2009). On the lower continental slope and rise, Swift (1987) and Ebinger and Tulcholke (1988) reported a number of erosional unconformities in seismic reflection data and suggested a bottom current origin with inferred ages of Oligocene, Early Miocene, Middle Miocene, and Pliocene.

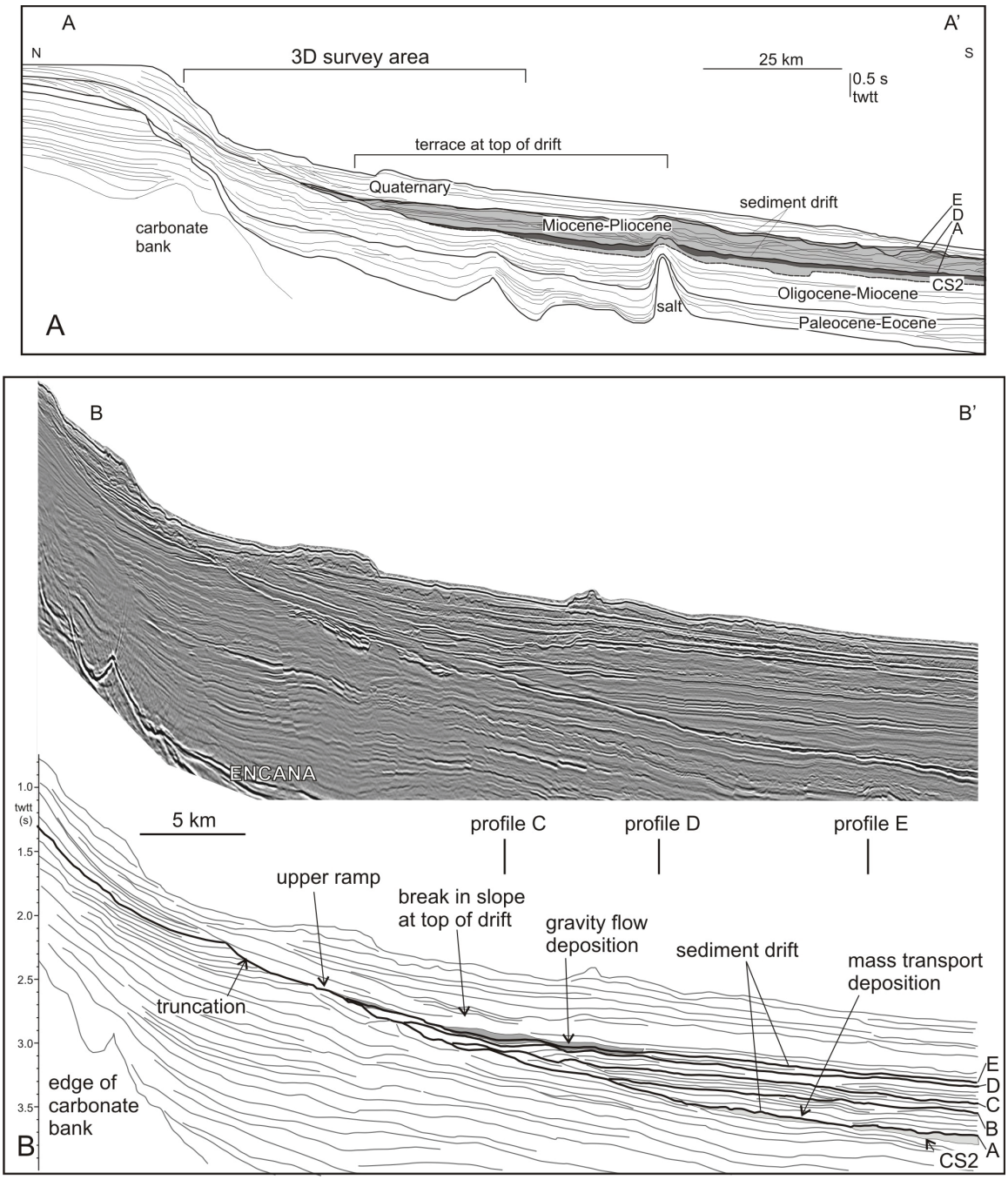

Figure 5.2 A) Schematic dip-oriented cross-section of Cenozoic deposits and older structural elements in the study area. The studied interval is highlighted in grey. Location of profile is given on Figure 5.1b. B) Dip-oriented seismic reflection profile and line interpretation through the central part of the study area. Note the major erosive unconformity and onlapping deposits which are the focus of this study (Horizons A-E). Location of profile is given in Figure 5.1c. Data are courtesy of EnCana Corp. and TGS-Nopec.

The Miocene to Pliocene seismic stratigraphy of the study area is described by Campbell and Mosher (2010). In the study area, the edge of the Jurassic Abenaki carbonate bank appears to have controlled the maximum seaward position of the shelf break throughout the Cenozoic and contributed to the development of a steep upper slope (Figure 5.2) (Campbell and Mosher 2010). In contrast, further east the carbonate bank edge controlled the steepness of the paleoslope until the Late Miocene, after which the relief of the bank was healed over (Swift 1987). Seaward of the carbonate bank, a widespread erosional unconformity was formed in the Miocene and is tentatively correlated to horizon CS2 of Swift (1987) (Figure 5.2). The unconformity is complex and developed through repeated erosion episodes, with the oldest recognized erosion forming the basal surface of a sediment drift (Campbell and Mosher 2010). Swift (1987) suggested CS2 was of lower to lower-middle Miocene age and equivalent to horizon Merlin from the U.S. continental margin dated at ~12 Ma (Tucholke and Mountain 1986), although no direct seismic reflection tie of Merlin to the Scotian margin exists. Both CS2 and Merlin are attributed to erosion by bottom currents (Swift 1987; Tucholke and Mountain 1986) and the position of the horizon at the base of a sediment drift in the study area supports this interpretation. Two subsequent and extensive periods of mass wasting, as well as channel incision, further eroded the surface in the study area. The net result of these erosion events was the creation of a submarine embayment near the seaward edge of buried autochthonous salt deposits (Figure 5.3a). In the study area, CS2 is onlapped by mass transport and sediment drift deposits.

5.3 Data and methods

Both 2D and 3D multichannel seismic reflection data were interpreted for this study and integrated with biostratigraphic (Fensome et al. 2008) and geological (Petro-Canada Inc. 1985) information from the Shelburne G-29 exploration well (Figure 5.1). A regional grid of 80 to 106 fold 2D seismic reflection profiles was used to map the extent of depositional elements, interpret regional structures, and to correlate seismic horizons into Shelburne G-29. These profiles were acquired by TGS-Nopec Geophysical Company in

1998 and 1999, with a line spacing of 8 km in the strike direction and 4 to 8 km in the dip direction. Hydrophone streamer length was 6 to 8 km and the acoustic source was a 130 L tuned airgun array.

A large 3D seismic survey was used to map five key surfaces and to subdivide the drift deposits into sub units. The surfaces were also used to study the geomorphological evolution of the drift deposits. The 3D seismic volume, termed the Barrington 3D survey, was acquired in 2001 by EnCana Corporation. The survey covers an area of approximately 1790 km^2. Data were recorded by eight 6000 m long hydrophone streamers, each with 240 channels. Channel separation was 25 m and bin spacing was 12.5 m. The acoustic source was a 62 L tuned airgun array generating a peak frequency of 70 Hz and a bandwidth of 5-100 Hz, implying about 5.5 m vertical resolution at water velocity. Processing of both datasets was conducted by the data owners prior to this study.

Seismic reflection data were interpreted using SeismicMicro Technologies Kingdom Suite and Schlumberger GeoFrame software packages. For the 3D seismic dataset, reflection horizons were mapped and gridded to produce continuous surfaces with a grid cell size of 25 m. Seismic reflection travel time, amplitude, and dip of maximum similarity attributes were used to interpret the seismic geomorphology. The dip of maximum similarity is a geometric attribute computed by first determining similarity (e.g. semblance) of adjacent traces over a sliding time window and range of dips, and then extracting the dip of maximum semblance within the time window. It is useful for identifying structural discontinuities. Plan view dimensions of morphological features are given in SI units, and vertical dimensions, such as thickness and height, are given in milliseconds (ms) of two-way travel time (TWTT) or, in some cases, in metres using an interval velocity of 1800 m/s for conversion based on measured velocities for the interval from the Shelburne G-29 well.

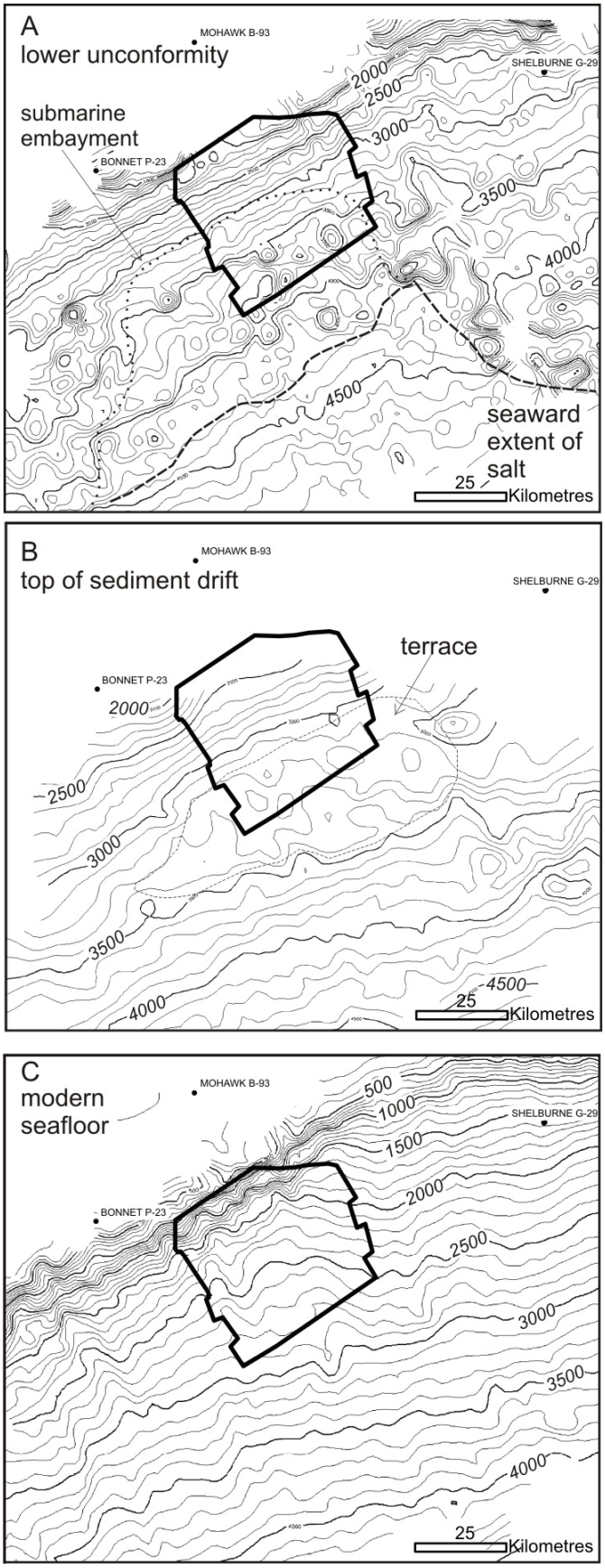

Figure 5.3 Time structure maps of the regional Late Miocene to recent evolution of the western Scotian margin. A) Time structure of the lower unconformity and the location of the seaward extent of autochthonous salt (from Shimeld 2004) and a submarine embayment (Modified from Campbell and Mosher 2010). B), Time structure of the top of the sediment drift. Note the broad terrace. C) Morphology of present seafloor (Modified from Shaw and Courtney 2004). Contour interval for all maps is 100 ms (twtt). Data are courtesy of TGS-Nopec.

5.4 RESULTS

The study interval is located between seismic reflection horizons A and E (discussed below) and comprises a buried succession of wavy to concordant reflections on the lower slope and rise interpreted to represent alternating deposits from bottom currents and sediment gravity flows (Figures 5.2, 5.4-5.7). In the 3D survey area, the interval is up to 450 ms thick and thins to zero thickness upslope. The basal bounding surface of the succession is the top of a regional mass transport deposit (MTD) and associated erosional unconformity (CS2) which together form a widespread marine onlap surface (Figure 5.2; see also Campbell and Mosher 2010). The upper bounding surface of the succession is defined by an abrupt transition to chaotic and transparent reflections interpreted as an interval of stacked mass transport deposits. Five seismic horizons were correlated over the 3D seismic dataset and include the upper and lower bounding surfaces (Table 1). At Shelburne G-29, this interval correlates to upper Miocene to lower Pliocene strata (Fensome et al. 2008).

Table 5.1 Seismic stratigraphy. Age estimates are from correlation to the Sheburne G-29 well and biostratigraphy from Fensome et al. (2008).

Horizon	**Age**	**Geological Significance**
A	Late Miocene	Basal surface. Regional unconformity and top of associated MTD.
B	Late Miocene-Zanclean	Onset of sediment drift development.
C	Zanclean	Middle of sediment drift sequence.
D	Zanclean	Top of sediment drift sequence.
E “complex”	Late Pliocene	Return to gravity flow predominance.

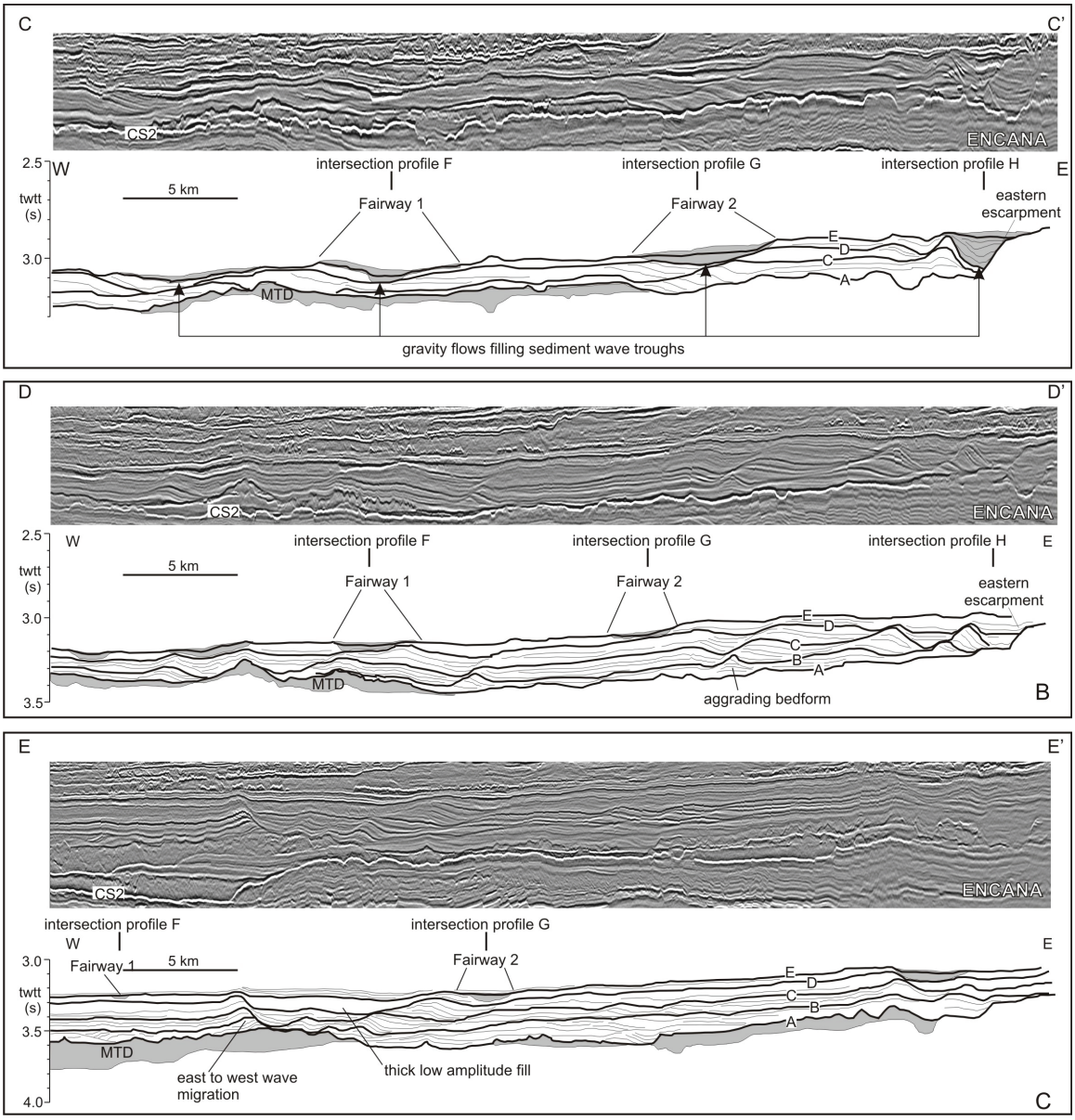

Figure 5.4- Series of three strike-oriented seismic profiles and line interpretations from the study area. Profile C-C' is located just seaward of the break in slope associated with the top of the sediment drift and shows that gravity flows (grey stipple) at Horizon E are concentrated in sediment wave troughs. Profile D-D' is 7 km seaward of C-C' and shows that gravity flow focusing in wave troughs is less apparent. Profile E-E' is 10 km seaward of D-D' and shows little evidence of the thick, high seismic amplitude facies of the Horizon E complex. Note that in most cases, sediment wave migration direction is from west to east. Locations for profiles are given in Figure 5.1c and Figures 5.8-5.14. Data are courtesy of EnCana Corp.

5.4.1 Horizon CS2/Merlin

The seismic geomorphology of horizon CS2 is presented in Campbell and Mosher (2010). CS2 is interpreted to be an erosional unconformity and appears as a strong, negative reflection that overlies a highly faulted interval (Figure 5.2, Figure 5.4). The unconformity is complex, formed by multiple, coalesced erosion surfaces within the area of the 3D seismic data. The seismic geomorphology of CS2 in the 3D seismic dataset shows evidence of pronounced down-slope erosion (Figure 5.8). In the southwestern corner of the 3D dataset, a long arcuate escarpment more than 220 m high corresponds to the headscarp of a large MTD. Immediately north and east of the escarpment, long, linear grooves up to 14 km long and 400 m wide, are oriented down-dip and characterize much of the unconformity. Five domal structures are present on the CS2 surface and are the sub-surface expression of underlying salt diapirs. Up-dip from the grooved zone, the seabed is scoured, with numerous smaller arcuate escarpments 0.5 to 4 km wide and 50 m high. This area passes up-dip to a zone that is much smoother with some subtle scars. The shelfward transition from erosional to conformable character of the surface is marked by a sharp change in gradient (Figure 5.2). In the eastern part of the 3D seismic dataset, a channel eroded down to the level of CS2. The channel is up to 3 km wide and 370 m deep. The channel walls are scalloped and a sinuous channel thalweg is apparent.

5.4.2 Horizon A

Horizon A forms the lower boundary of the succession examined in this study (Figure 5.9). The horizon can be broadly divided into two zones: an upslope portion corresponding to the first peak reflection above the prominent trough of the underlying CS2 unconformity (described above), and a downslope portion that corresponds to the top boundary of the final mass transport deposit associated with CS2. The morphology of the upslope portion of Horizon A is very similar to the underlying erosive surface where it directly drapes CS2 (Figures 5.5, 5.8-5.9), consisting of curvilinear and arcuate escarpments and elongated scours that developed during earlier mass wasting. The downslope portion of Horizon A is separated from the underlying CS2 by an up to 300

ms thick interval dominated by chaotic mass transport deposits. The downslope morphology is rugose, due to the surface relief of massive blocks associated with the underlying MTD. This MTD is up to 280 ms thick and individual blocks have lengths up to 4 km and relief up to 100 ms (Figure 5.9). A large sidewall escarpment is preserved at the eastern margin of the MTD (herein referred to as the eastern escarpment) (Figures 5.4a and 5.4b) and is over 20 km long with a maximum height of 150 ms.

In addition to relief due to gravity flow processes, five buried salt diapirs create domal structures on this surface (Figure 5.9c). Some of the salt doming is inferred to have been present at the time of formation of the pre-drift surface based on the subtle diversion of gravity flow striations around diapirs (Campbell and Mosher 2010). It is also possible that younger folding of strata above the salt diapirs could have produced this pattern.

5.4.3 Horizon B

Horizon B is a prominent reflection that onlaps Horizon A along the middle slope and also onlaps mass transport deposits and salt diapirs where they have high positive relief (Figure 5.2, Figure 5.4). The isochron map of the Horizon A-B interval (Figure 5.10c) illustrates that deposition was focused in the depression between the eastern escarpment and an area of blocky mass transport deposition, leading to the development of a terrace. There was little or no deposition on the salt diapir crests and in areas east of the eastern escarpment.

The Horizon A-B interval shows early development of several sediment waves and the smoothing of relief associated with the basal Horizon A surface (Figure 5.10). Much of the blocky and irregular relief apparent on the Horizon A surface is subdued or even absent at the Horizon B level. Sediment waves developed near the eastern escarpment (Figure 5.4, Figure 5.10) are continuous over distances up to 10 km, with up to 1 km of northeastward wave crest migration between Horizons A and B. Wave amplitudes are up to 90 m, with an average wavelength between the two crests of 4 km. Wave flank gradients are on the order of 5°. Sediment waves southwest of the salt diapirs are curvilinear, with wave crests that can be followed for up to 10 km, and average

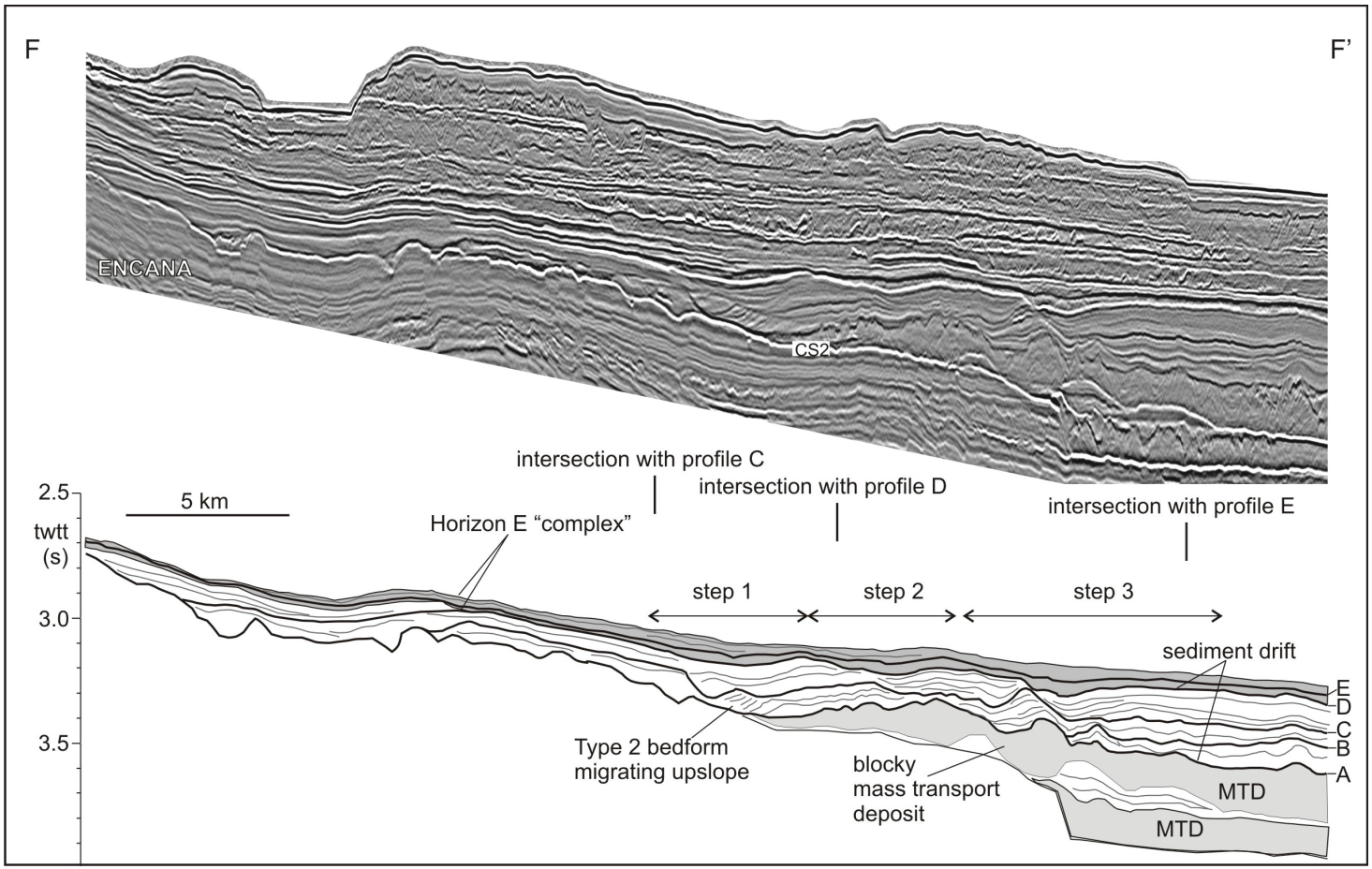

Figure 5.5 Seismic reflection profile and line interpretation F-F'. Profile is a dip-oriented line down the axis of sediment Fairway 1. The Horizon E "complex" is thickest above three steps formed by the inherited morphology of the underlying sediment drift and MTD. Note the apparent up slope sediment wave migration of type 2 bedforms. Location of profile is given in Figure 5.1c and Figures 5.8-5.14. Data are courtesy of EnCana Corp.

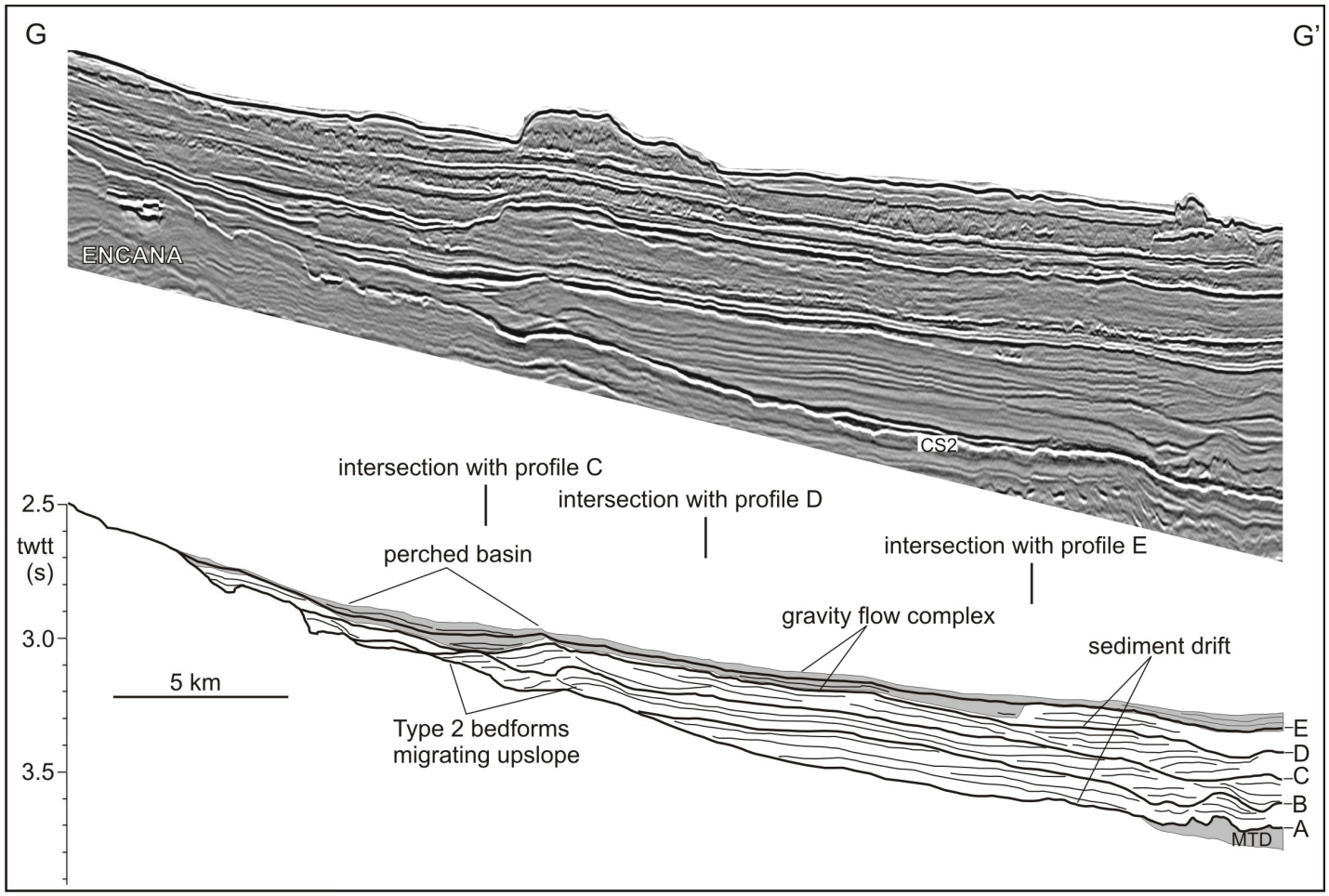

Figure 5.6- Seismic reflection profile and line interpretation G-G'. Profile is a dip-oriented line down the axis of sediment Fairway 2. A perched basin was created by a large type 2 bedform that migrated upslope and was filled by a thick succession of gravity flow deposits (grey stipple). Location of profile is given in Figure 5.1c and Figures 5.8-5.14. Data are courtesy of EnCana Corp.

wavelengths of 3 km. These sediment waves have crests that bend northward around the northern curved flank of underlying diapirs (Figure 5.10). Near the updip limit, where Horizon B onlaps Horizon A, additional smaller bedforms have an east-west crest orientation and an apparent south to north migration direction (Figure 5.5, Figure 5.10). The wave field in the SW corner of the study area overlying the buried mass transport deposit is complex with highly discontinuous wave crests with variable orientations.

5.4.4 Horizon C

Horizon C is a high seismic amplitude wavy reflection in the middle of the sediment drift sequence (Figure 5.2, Figure 5.4). Horizon C appears to corresponds to a time of maximum bedform relief across most of the study area. An isochron map between Horizon B and C shows that maximum deposition is located at the two large sediment waves west of the eastern escarpment and immediately west of the salt diapirs (Figure 5.11c).

Both the direction and magnitude of wave crest migration vary between Horizons B and C. Near the eastern escarpment, the dominant migration direction is to the northeast with up to 2 km of wave crest migration near the eastern escarpment (Figure 5.4). Interestingly, at least one wave crest migrated in the opposite direction towards the southwest (Figure 5.11e) and is likely caused by changing current parameters as the bottom current interacted with the eastern escarpment and the buried salt diapir to the south. Variations in the amount of wave crest migration on most sediment waves also result in a subtle change of orientation of the wave crests at Horizon C compared to Horizon B. Wave amplitudes, particularly near the eastern escarpment, increased significantly from <90 m at Horizon B to > 150 m at Horizon C, with the steeper flanks of the bedforms showing a sharp increase in gradient to 9°.

Sediment waves southwest of the salt diapirs continue to develop in a curvilinear pattern around the diapirs. At Horizon C, these sediment waves are linked to low amplitude two-dimensional waves north of the diapirs that trace up dip to where they intersect or

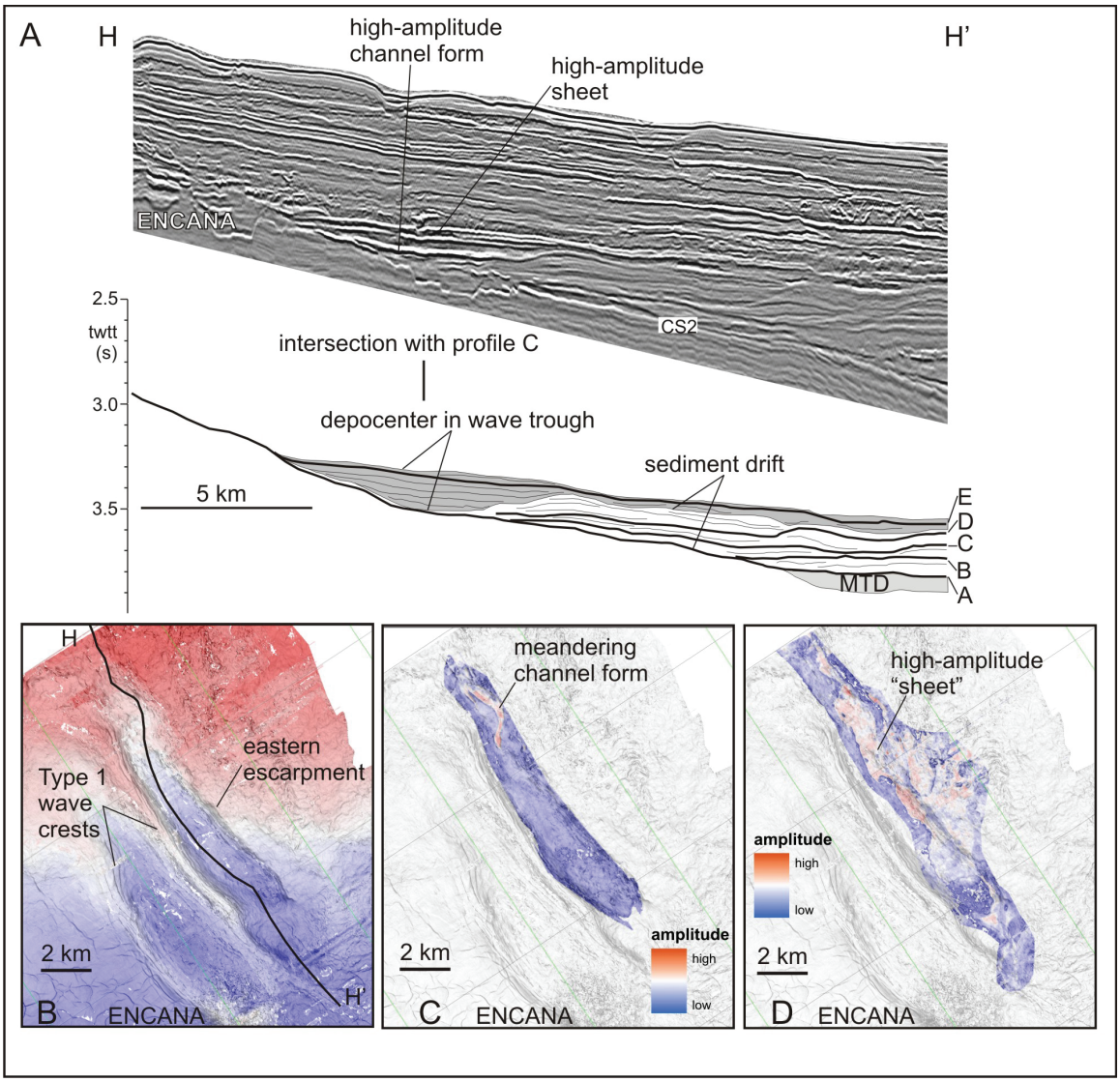

Figure 5.7- A) Seismic reflection profile and line interpretation H-H'. Profile is a dip-oriented line down the axis of a large sediment wave trough in the eastern part of the study area. Location of profile is given in Figure 5.1c and Figures 5.8-5.14. B) Detailed morphology of the wave trough at Horizon C and the location of profile H-H'. C) and D) Seismic amplitude and similarity of the depression-filling deposits. The large depression formed by the wave trough effectively trapped a thick succession of gravity flow deposits. Seismic amplitudes suggest confined flow (channel form geometry) in the lower part of the trough and less confined flow (high-amplitude sheets) in the upper part of the trough. Data are courtesy of EnCana Corp.

transition to east-west oriented waves (Figure 5.11). East-west oriented waves are more common at the Horizon C level than Horizon B and have continuous crests for up to 5 km. In the area overlying the buried MTD in the southwest, many of the discontinuous bedforms observed at Horizon B have become linked, forming larger and more organized bedforms with curvilinear to circular planform shapes (Figure 5.11).

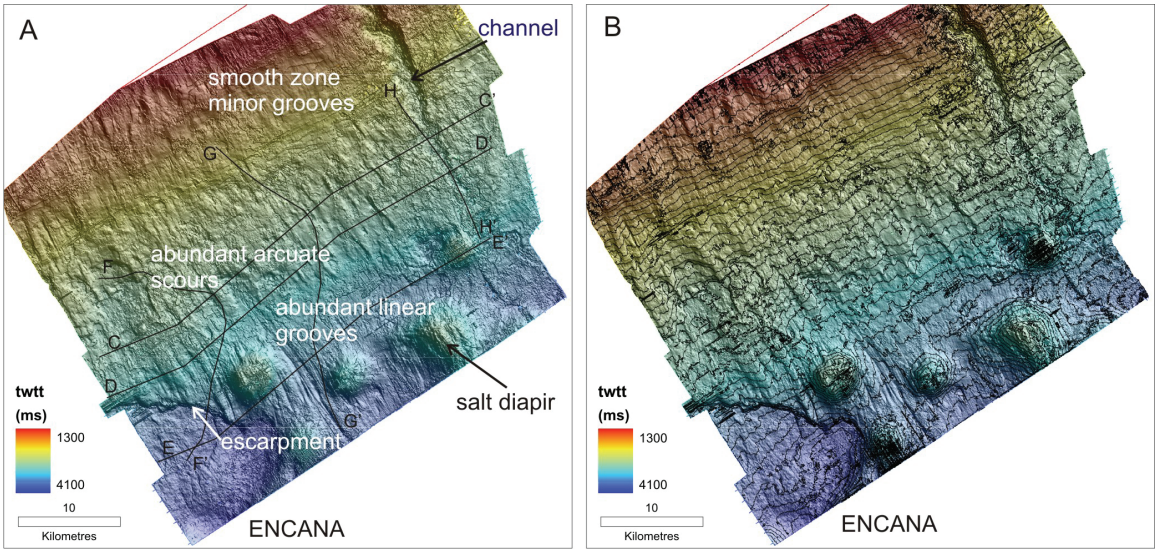

Figure 5.8 Seismic geomorphology of Horizon CS2, a widespread Miocene erosional unconformity within the study area and described in detail in Campbell and Mosher (2010). A) Shaded relief of the surface showing major morphological elements. B) Time structure contours (50 ms (twtt) contour interval). Data are courtesy of EnCana Corp.

5.4.5 Horizon D

Horizon D (Figure 5.12) coincides with a decrease in sediment wave growth and migration (Figures 5.4-5.6). The horizon C-D interval shows evidence of sediment wave migration and growth, as well as some draping and ponding in bathymetric lows (Figure 5.4). The isochron map of the interval between horizons C and D (Figure 5.12c) illustrates that sedimentation was greatest along the crests of large sediment waves in the eastern part of the study area, in contrast to the western part of the study area where sediment draping dominated in the wave troughs and little deposition occurred at wave crests.

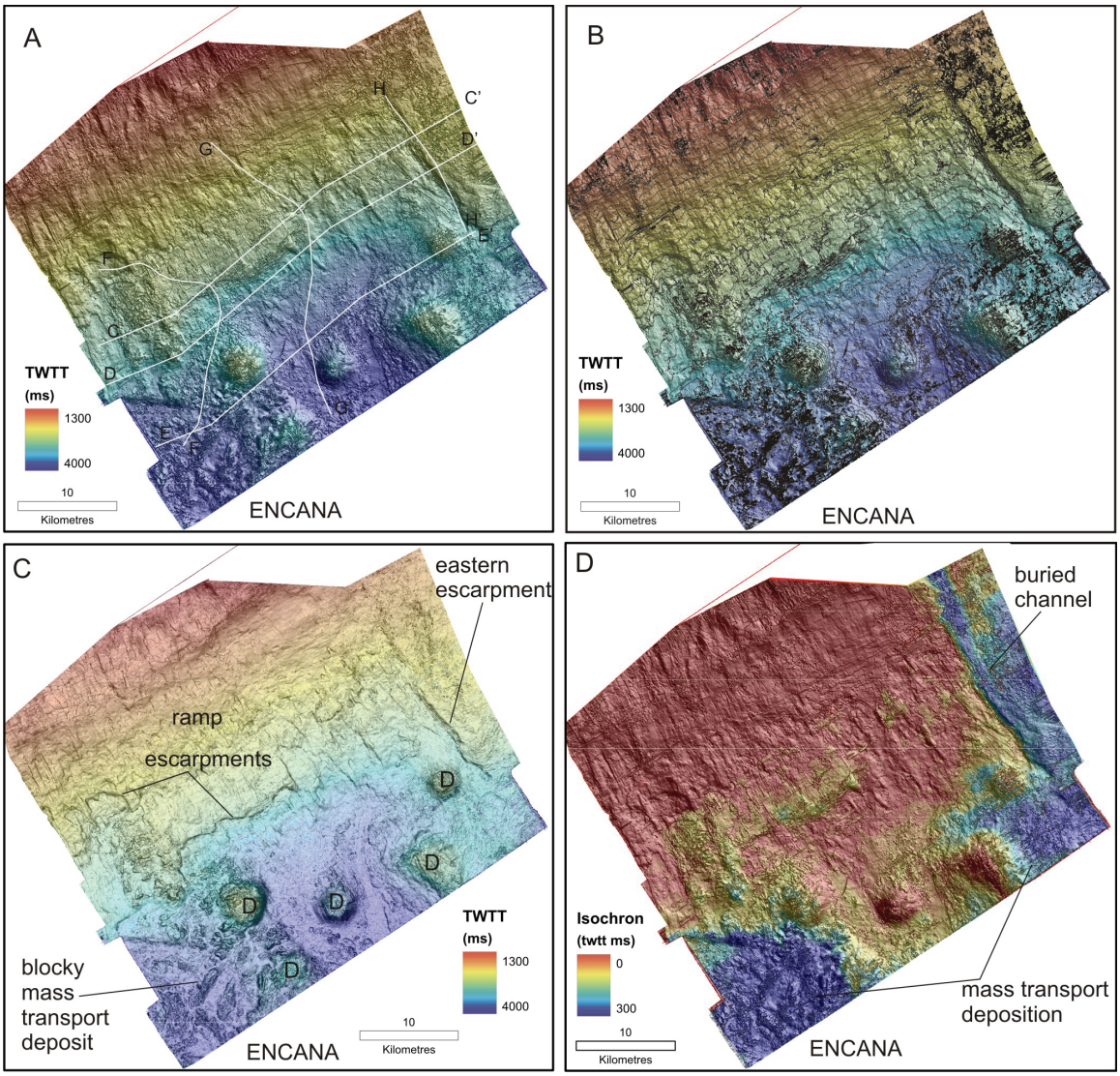

Figure 5.9 Seismic geomorphology of Horizon A. A) Shaded-relief map. B) Time structure contours (50 ms (twtt) contour interval). C) Dip of maximum similarity overlain on structure in order to highlight the morphology of the large MTD. The tops of salt diapirs are indicated with a "D". D) Isochron map of the Horizon CS2-A interval. Data are courtesy of EnCana Corp.

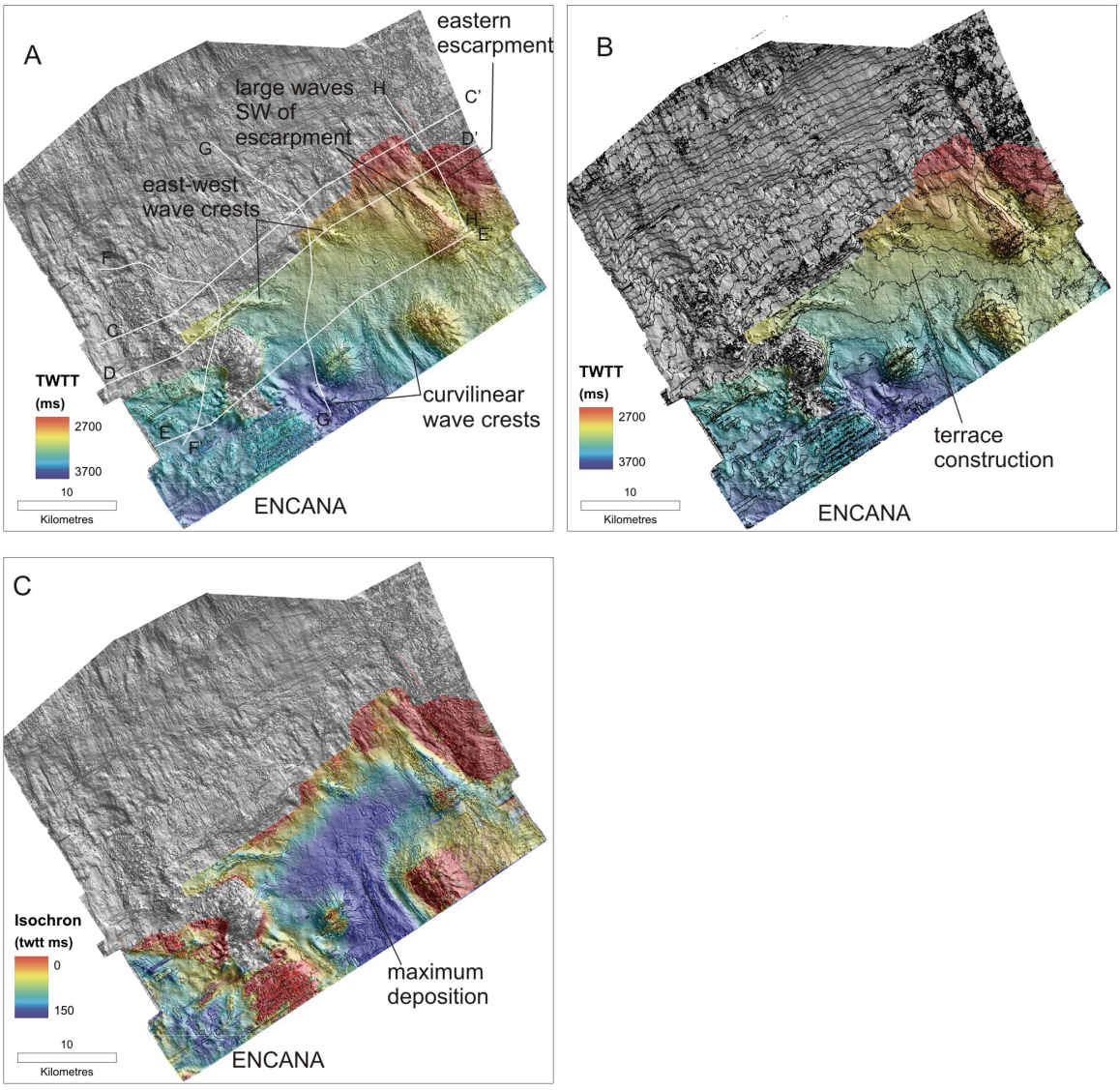

Figure 5.10 Seismic geomorphology of Horizon B. A) Shaded-relief map. B) Time structure contours (50 ms (twtt) contour interval). C) Isochron map of the Horizon A-B interval. Data are courtesy of EnCana Corp.

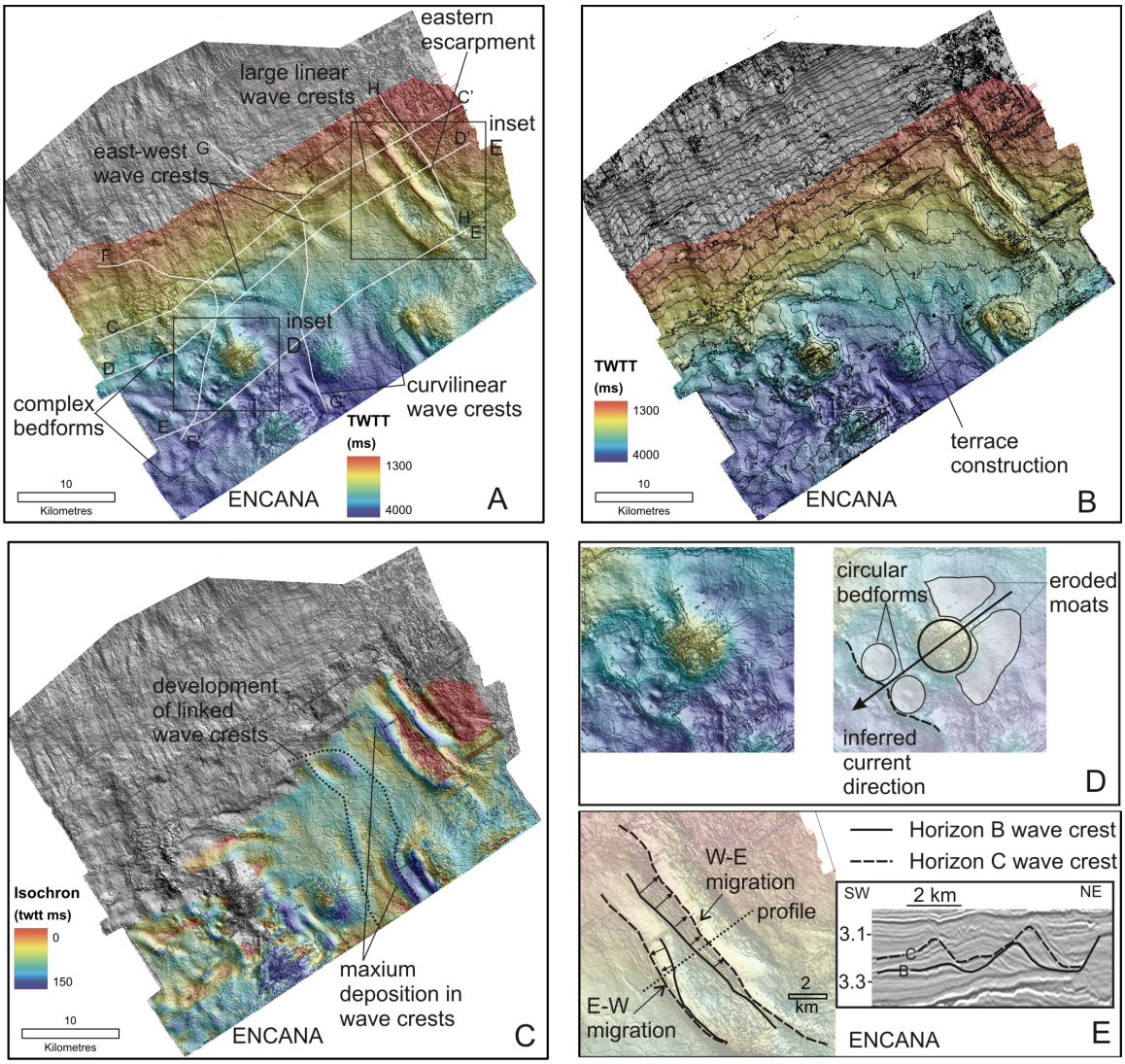

Figure 5.11 Seismic geomorphology of Horizon C. A) Shaded-relief map. B) Time structure contours (50 ms (twtt) contour interval). C) Isochron map of the Horizon B-C interval. D) Detailed map of type 3 circular bedforms west of a salt diapir, suggesting flow separation in the bottom current with erosion on the eastern (up current) side of the diaper. E) Examples of sediment wave migration patterns between Horizon B and C. Note that in one case the waves migrate from east to west and in another from west to east. The amount of migration varies along each crest. Data are courtesy of EnCana Corp.

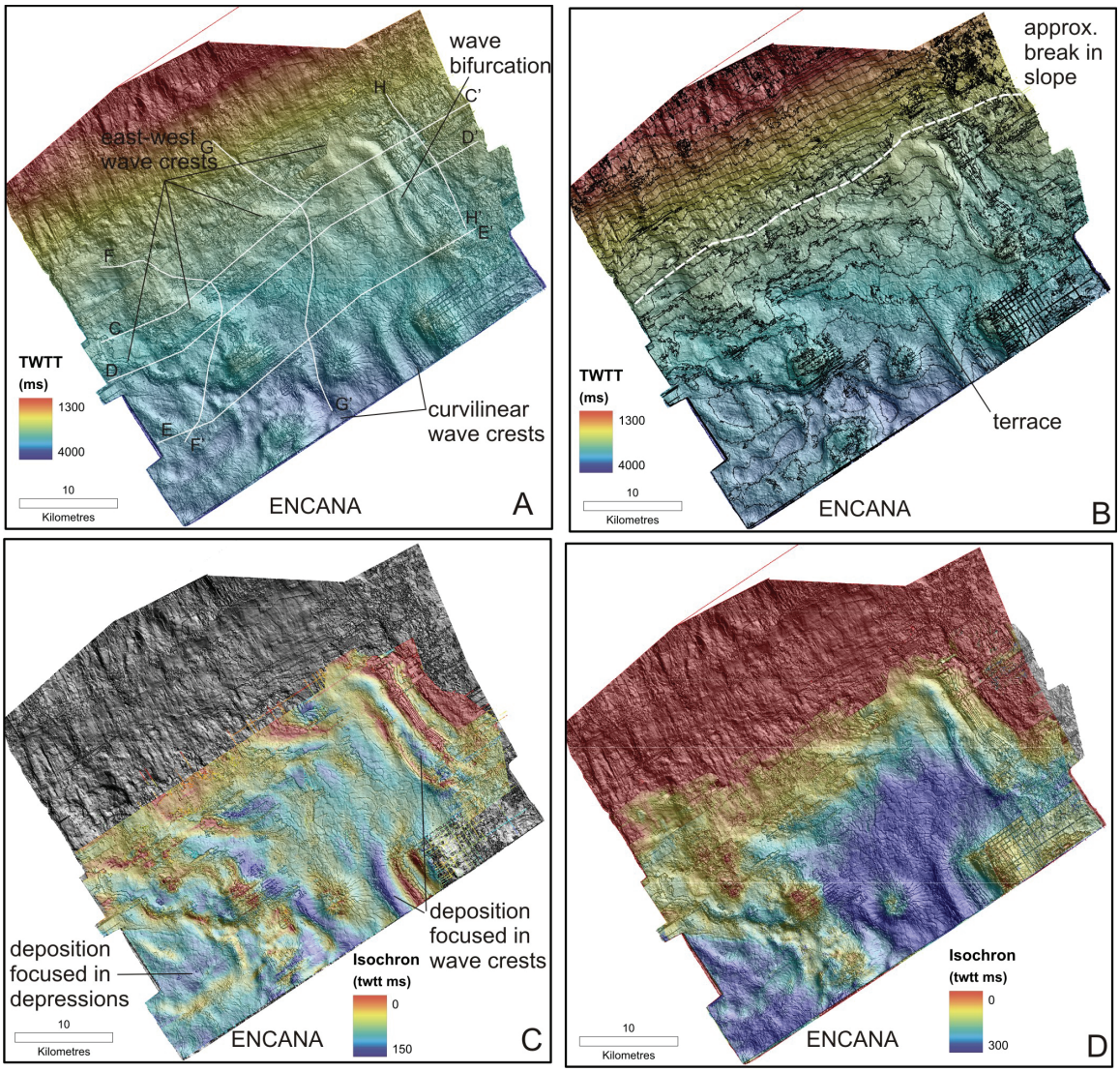

Figure 5.12 Seismic geomorphology of Horizon D. A) Shaded-relief map. B) Time structure contours (50 ms (twtt) contour interval). C) Isochron map of the Horizon C-D interval. D) Isochron map of the entire sediment drift (Horizon A-D interval). Data are courtesy of EnCana Corp.

Along the eastern escarpment, compared to Horizon C, the waves are lower amplitude and there is bifurcation of one of the wave crests (Figure 5.12). Large sediment waves continue to develop southwest of the salt diapirs and the crests of the east-west oriented waves are more continuous, reaching lengths up to 10 km. Above the buried MTD in the southwest, two large curvilinear sediment waves are apparent.

Time structure maps show that cumulative deposition of the sediment drift resulted in the construction of a bathymetric step in the southern half of the 3D survey area (Figure 5.12b). The step extends up to 50 km seaward, forming a prominent regional terrace (Figure 5.3b).

5.4.6 Horizon E Complex

Over much of the study area, Horizon E consists of a single high positive amplitude reflection; however, in some paleo-bathymetric lows, the horizon splits into 2 or more high positive amplitude reflections (Figures 5.4-5.7). Horizon E marks an abrupt change in the seismic facies character and geomorphology within the study interval. Much of the wavy and undulating nature of the underlying sediment drift was healed over at the Horizon E level, with only sediment waves adjacent to salt diapirs still present (Figure 5.13a). A seismic reflection line along strike to the regional slope near the foot of the ramp shows that deposition of the Horizon E complex is focused in sediment wave troughs (Figure 5.4a).

The Horizon D-E interval generally lacks the internal sediment wave geometry of underlying deposits. The interval is divided into two parts; a lower low-amplitude and reflection-free section that immediately overlies Horizon D, and a high amplitude section assigned to the Horizon E complex (Figures 5.4-5.7). An RMS amplitude map of the Horizon D-E interval (Figure 5.13d) and the amplitude map of Horizon E show several amplitude anomalies that have ribbon to sub-ellipsoid shape (Figure 5.13d, Figure 5.14). They generally have a downslope orientation, with trajectories that avoid the crests of salt diapirs. Highest seismic amplitudes are located at the foot of the steep ramp at the up dip

limit of the sediment drift. Deposits associated with the Horizon E complex are thickest and have the greatest amplitude in the troughs of bedforms in the underlying sediment drift (Figure 5.4, Figure 5.14).

Two depositional fairways are recognized from the seismic amplitude maps (Figure 5.14) and seismic reflection data (Figures 5.4-5.6). These are interpreted to mark the transition back to gravity driven deposition with sediment transport dominantly oriented in the downslope direction. Fairway 1 is the westernmost depositional fairway. It changes orientation downslope, from a southeast to a southwest direction (Figure 5.14). An axial dip profile down the fairway reveals deposits of variable thickness between horizons D and E (Figure 5.5). In plan view on the RMS amplitude map (Figure 5.14), the fairway becomes a narrow, < 500 m wide ribbon downslope where it intersects profile E-E' (Figure 5.4c). Fairway 2 is located in the central part of the study area and its plan view geometry appears similar to Fairway 1 (Figure 5.14). Like Fairway 1, Fairway 2 changes orientation downslope, from southeast to southwest. An axial dip profile down Fairway 2 shows that the Horizon E complex bifurcates into a number of reflections immediately updip of a large sediment wave crest (Figure 5.6).

In addition to the two depositional fairways, two other depocenters are recognized (Figure 5.4, Figure 5.14). In the extreme western part of the study area, a moderate to high amplitude lobe is present within a depression formed by the erosion and deposition of the large MTD associated with Horizon A (Figure 5.14). The downslope limit of the high amplitude reflection is controlled by a ridge formed by a sediment wave crest. Downslope from the ridge, the Horizon D-E interval consists of lower amplitude reflections. In the eastern part of the study area, a large depression located within the trough of a sediment wave is a second depocenter (Figure 5.7). The depression fill (Horizon E complex) thins upslope and downslope and onlaps the flanks of the sediment wave. Reflection amplitudes within the fill show evidence of channel development, with meandering channel forms and high amplitude sheets (Figure 5.7).

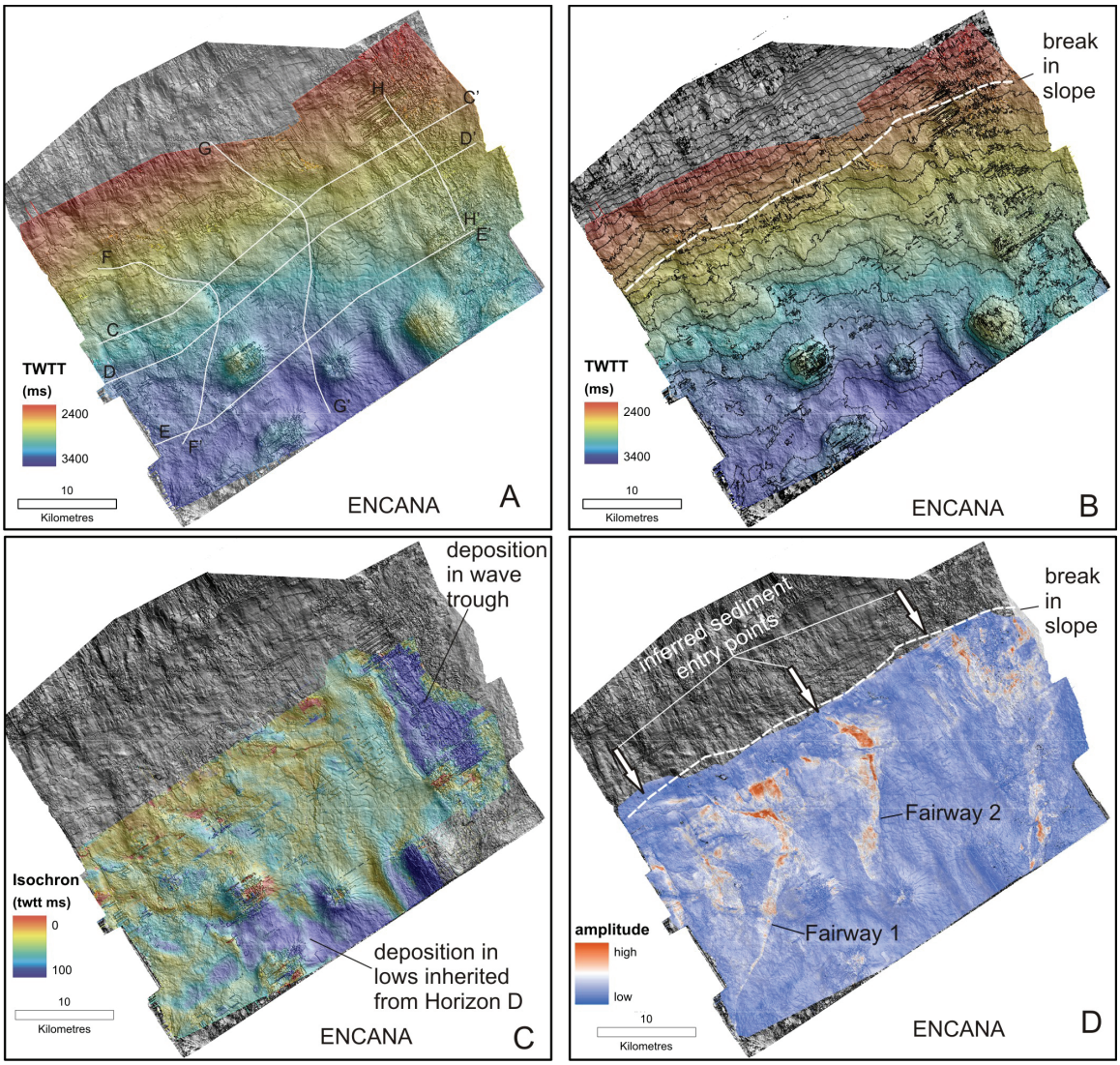

Figure 5.13 Seismic geomorphology of Horizon E. A) Shaded-relief map. B) Time structure contours (50 ms (twtt) contour interval). C) Isochron map of the Horizon D-E interval. D) RMS seismic amplitude of extracted from the Horizon D-E interval. Note the interpretation of depositional fairways and inferred sediment entry points. Data are courtesy of EnCana Corp.

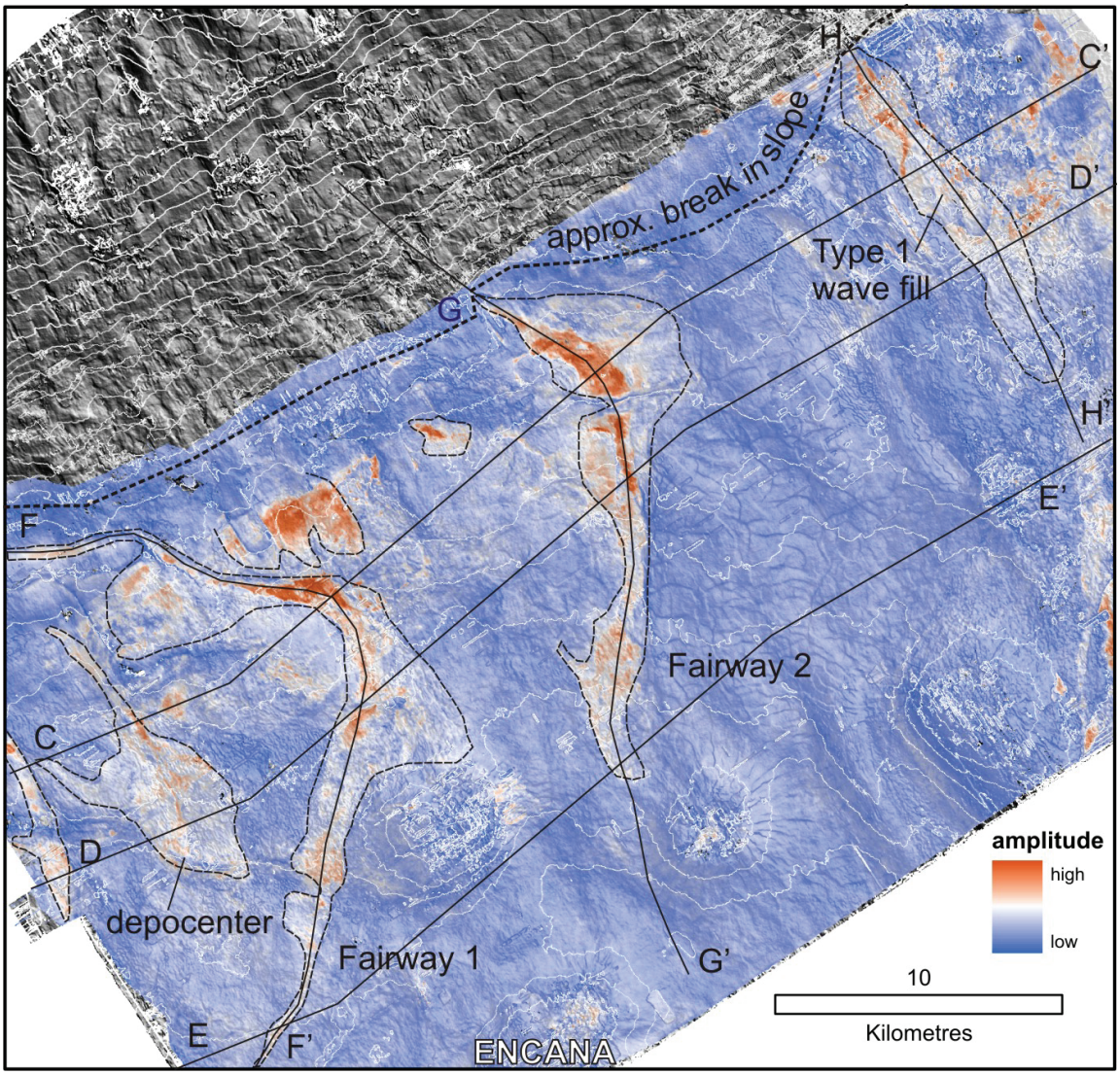

Figure 5.14 Detailed RMS seismic amplitude map of the D-E interval and interpretation. Zones of high seismic amplitude are highlighted by dashed lines. The highest amplitudes are just seaward of the break in slope and are confined to depressions inherited from the underlying sediment drift. Data are courtesy of EnCana Corp.

5.5 Discussion

5.5.1 Bedform Classification

The geomorphology of Horizons A through D is dominated by sedimentary bedforms that are broadly divided into three types (Figures 5.11a-b). Type 1 bedforms are most common and comprise two-dimensional sediment waves with crests oriented northwest-southeast (Figure 5.11a). Their crests extend up to 20 km in length, their wavelengths are 2-4 km, and their amplitudes are up to 150 m. Wave amplitude is greatest immediately west of abrupt negative changes in seafloor relief, such as west-dipping escarpments and west-dipping diapir flanks. Type 2 bedforms are two-dimensional sediment waves with crests oriented east-west. They are confined to areas of steeper slopes and gullies up-dip of Type 1 bedforms. Type 2 bedforms have wave crests that typically extend for 5 km, wavelengths of 3 km, and wave amplitudes up to 75 m (Figure 5.11a). Type 3 bedforms are circular to curvilinear bedforms located on the west side of three closely-spaced salt diapirs in the 3D seismic survey area (Figures 5.11a-c). This bedform type is less organized than Types 1 and 2.

Wave migration through the Horizon B-C interval is interpreted from comparison of changes in wave crest position at the Horizon B and C level, as well as the intervening asymmetrical and sinusoidal seismic reflection geometries. Most Type 1 bedforms migrate from west to east (Figure 5.4). An exception includes the second wave crest west of the eastern escarpment which appears to migrate from east to west along part of the bedform (Figure 5.11e). Additionally, wave crest migration can vary along an individual wave, for example, along the large wave immediately west of the eastern escarpment. On this bedform, the wave appears to have remained stationary at the southern end of the wave and migrated over 1 km at the northern end of the wave crest (Figure 5.11e). Type 2 bedforms migrate up slope as revealed by arbitrary seismic profiles perpendicular to the wave crest (Figure 5.2, Figures. 5.5-5.6). Type 3 bedform migration direction is highly variable, from laterally climbing bedforms to vertically aggrading bedforms (Figure 5.4).

5.5.2 Alternation of Depositional Modes and the Effects of Inherited Morphology

Widespread Slope Failure and Mass Transport Deposition-

Horizon CS2, a regional deepwater unconformity, formed in the Middle to Late Miocene in the study area through periods of major slope failure and, to a lesser extent, bottom current erosion and channel incision (Campbell and Mosher 2010). Gravity-driven mass wasting had a marked effect on subsequent depositional patterns. The erosional surface modified the pre-existing slope morphology and created a broad ramp on the middle to lower slope. The steep, upper portion of the ramp created a by-pass zone that persisted for millions of years and likely restricted the accumulation of gravity flow deposits to areas further seaward. The last phase of slope failure resulted in the formation of the eastern escarpment which controlled the development of large sediment waves to the west.

The Development of a Sediment Drift-

On a regional scale, sediment drift construction contributed to the infilling of the submarine embayment related to the erosion of CS2 (Figure 5.3a) and created a broad terrace up to 50 km wide (Figure 5.3b), forming an abrupt break in slope where the drift onlaps Horizon A (Figure 5.2). The drift was constructed through the stacking of sediment wave packages and, within the area of 3D seismic data, reached a maximum thickness of ~380 ms (Figure 5.12d). The drift appears to have grown from the deeper part of the basin and back-stepped up the slope rather than developing a plastered component over the steep ramp. This architecture suggests that some of the sediment comprising the sediment wave field was likely pirated from turbidity currents that would have bypassed the ramp, only to perhaps get entrained in a bottom current on the rise, forming sediment waves. Such a process has been suggested by He et al. (2008) and the formation of muddy sediment waves would only require a bottom current with a velocity of 0.05- 0.25 m/s (Stow et al. 2009). Alternatively, the back-stepping and onlapping architecture may have resulted from bottom current acceleration across the ramp, preventing deposition, although there is no evidence of along-slope erosion on the ramp.

The initiation process for fine-grained sediment waves generated by bottom currents is not well understood (Flood 1988; Blumsack 1993, Hopfauf and Spiess 2001; Wynn and Stow 2002), but in general is attributed to the presence of seafloor irregularities which cause the bottom-current velocity perturbations required for wave development (Hopfauf and Spiess 2001, Blumsack 1993). Detailed analysis of the Horizon A-D interval in this study provides some insight into deep-water sediment-wave forming processes. Seafloor irregularities at Horizon A result from the surface expression of five salt diapirs, and rugose erosional and depositional features (escarpments, blocky MTDs) associated with seabed failure (Figure 5.9). Sediment wave development is greatest immediately southwest of these features (Figures 5.10-5.12). On basin floors, wave crest are usually oriented perpendicular to current direction (Wynn and Stow 2002). For the study area, this fact implies a northeast to southwest bottom current flow direction, approximately perpendicular to the regional slope. On steeper slopes at the northern limit of the sediment wave field, Type 2 bedforms migrate in a northerly to a northwesterly direction. This observation implies that sediment waves on slopes migrate up slope and up current which is consistent with observations from Wynn and Stow (2002). The geomorphology of Horizon C shows an abrupt transition from Type 1 to Type 2 bedforms, apparently related to an increase in the gradient of the underlying seabed (Figure 5.6, Figure 5.11). Type 3 bedforms exhibit complicated geometries that likely result from bottom currents flowing over complex topography. For example, bedform geometry around the salt diapir shown in Figure 5.11d suggests flow separation and formation of lee vortices on the down current side. This phenomenon was modeled for fluid flow around 3-dimensional objects (Smolarkiewicz and Rotunno 1989), and is known to occur in alluvial channels (Best and Brayshaw 1985). Flow separation has been suggested as a process for complex contourite depositional systems where multiple current pathways exist (Hernández-Molina et al. 2008).

The sediment drift is not sampled in the study area. Fifty kilometres east of the study area at the Shelburne G-29 well, sidewall cores of age-equivalent strata are predominantly composed of dark-grey brown to dark grey-green claystone (Petro-Canada Inc., 1985);

however, sediment waves are not present at the well site. Biostratigraphic data at the Shelburne G-29 well (Fensome et al. 2008) shows that the drift formed during the Late Miocene to Middle Pliocene and is therefore of similar age to a large sediment wave field on the New Jersey continental rise (Poag and Mountain, 1987). Off New Jersey (e.g. Deep Sea Drilling Program site 603), the sediment wave interval consists of dark grayish green hemipelagic claystone. Locker and Laine (1992) suggested that the New Jersey margin sediment waves formed through entrainment of fine grained turbidity currents and hemipelagic sediments in a southwest flowing bottom current.

Miocene and Pliocene age sediment drifts along the Scotian margin are underreported in the literature. Apart from identification of a small zones of sediment waves (e.g. Swift 1987, MacDonald 2006), the role of bottom currents in shaping the margin has focused on recognition of seismic reflection horizons attributed to bottom current erosion (Swift 1987, Ebinger and Tucholke 1988). During construction of the sediment drift in this study, paleo-current direction indicators suggest mean bottom-current flow was from the northeast to the southwest. It therefore appears likely that the sediment drift was deposited under the influence of a western boundary undercurrent. Using the sediment drift categories defined by Rebesco (2005), the sediment drift in this study could be defined as a sheeted or infill drift based on its low relief, large area, and the observation that it fills the submarine embayment formed by the erosion of CS2.

Return to Gravity Flow Deposition

The Horizon E “complex” is interpreted to represent a transition back to gravity flow dominated deposition based on a change in reflection character and geometry at this level. The complex is correlated on 2D seismic data to the Shelburne G-29 well where it corresponds to an ~50 m thick interval of interbedded, well–sorted, fine grained sandstone and claystone (Petro-Canada Inc. 1985). The greatest seismic amplitudes of Horizon E, both in terms of magnitude and area, are located just seaward of the break in slope (Figure 5.14). Seismic reflection onlap relationships and thickness variations suggest that gravity flow deposits preferentially filled sediment wave troughs. This observation is most apparent near the break in slope (Figure 5.4). In Fairway 1, gravity

flow deposits form a series of three elongated, stepped basins (Figure 5.5). Sills were formed by inherited relief from sediment wave crests and the buried irregular MTD surface. The fairway was laterally confined either by position within wave troughs, or structural highs related to salt diapirs. In Fairway 2, a perched basin was formed by a large Type 2 sediment wave at the break in slope (Figure 5.6, Figure 5.14). In this example, a Type 2 wave crest created a sill, and gravity flow deposits accumulated behind the sill until it was breached. In the large sediment wave trough in the eastern part of the study area (Figure 5.7), repeated gravity flows filled the depression, creating a high amplitude wedge. A similar model for formation of ponded basins by sediment wave morphology was suggested by Viana (2008).

There are several places in the study area where large depressions at the Horizon D surface were filled with low seismic amplitude deposits instead of the high amplitude Horizon E complex (Figure 5.4). The precise position along slope where gravity flows bypassed the ramp and reached the terrace was controlled by factors further up slope outside the study area (e.g. the position of failures or turbidity currents generated at the shelf edge or upper slope). Once flows reached the break in slope, they presumably accumulated in the closest depression, which once filled overflowed into the next depression downslope in a cascading manner. Large depressions on the Horizon D surface that were not connected to gravity flow inputs were filled with lower seismic amplitude deposits of the Horizon D-E interval. Therefore, it appears that proximity to the input point of gravity flows, proximity to the base of slope, and connectivity between adjacent depressions were more important factors than depression size for accumulating the high seismic amplitude deposits associated with the Horizon E complex.

5.6 Summary and Conclusions

In the study area, the seismic stratigraphy reveals abrupt changes in depositional styles and sedimentary processes. Initially, seabed failure and deposition of the large MTD associated with the pre-drift surface represented rapid erosion of the middle to lower

slope and sediment transfer into the deeper basin. This period was followed by sediment drift development and construction of a large terrace at the foot of slope. Finally, an apparently sudden transition to gravity flow (turbidity current) input occurred that was contemporaneous with a termination of sediment wave development, suggesting that either bottom current intensity decreased or gravity flow input overwhelmed the bottom current signal.

Within the study area, inherited morphology affected subsequent deposition patterns for both along-slope and down-slope deposits. Regionally, the sediment wave field developed within a submarine embayment created by mass-wasting and channel incision. Locally, seafloor irregularities due to mass-wasting and protruding salt diapirs controlled the precise locations of maximum sediment wave growth. With the return to gravity-flow dominated deposition, the highest seismic amplitudes occur at the break in slope formed by the drift terrace. At the break in slope proximal to gravity flow input points, local topographic features at the scale of individual sediment waves controlled the distribution of gravity flows.

The studied interval on the western Scotian margin represents alternations from gravity flow dominated to bottom current dominated to gravity flow dominated deposition. The results demonstrate the importance of morphological heritage in controlling subsequent deposition patterns. The morphologies of the bedforms observed in the study area provide insights into the hydrodynamics of bottom currents and sediment wave forming processes. With the onset of gravity flow deposition, the regional terrace formed by the sediment drift effectively trapped gravity flows that may have otherwise been transported to deeper parts of the basin. Locally, sediment wave morphology strongly influenced the locations of gravity flow conduits and depocenters.

5.7 Acknowledgements

The authors would like to express appreciation to EnCana Corp. and TGS-Nopec Geophysical Co. L.P. for data access. Reviews of the manuscript by Dr. David Mosher, Mr. John Shimeld, Dr. David Van Rooij, and Dr. Douglas Masson substantially improved the manuscript.

5.8 References cited in Chapter 5

Best, J.L. and Brayshaw, A.C. 1985. Flow separation—a physical process for the concentration of heavy minerals within alluvial channels. Journal of the Geological Society, v. 142, p. 747-755.

Blumsack, S.L. 1993. A model for the growth of mudwaves in the presence of time varying currents. Deep-sea Research II, v. 40, p. 963–974.

Brake, V.I. 2009. Evolution of an Oligocene Canyon System on the Eastern Scotian Margin: Unpublished M.Sc. Dissertation [M.Sc. Thesis], Dalhousie University, Halifax, Nova Scotia, Canada, 113 p.

Campbell, D.C., and Mosher, D.C. 2010. Middle to Late Miocene slope failure and the generation of a regional unconformity beneath the western Scotian Slope, eastern Canada. In: Mosher, D.C., Shipp, C., Moscardelli, L., Chaytor, J., Baxter, C., Lee, H. and Urgeles, R., eds., Submarine Mass Movements and Their Consequences IV: Advances in Natural and Technological Hazards Research v. 28, Springer, The Netherlands, p. 645-755.

Carter, L. and McCave, I.N. 1994. Development of sediment drifts approaching an active plate margin under the SW Pacific deep western boundary current. Paleoceanography, v. 9, p. 1061-1085.

Davies, R.J., Stewart, S.A., Cartwright, J.A., Lappin, M., Johnston, R., Fraser, S.I., and Brown, A.R. 2004. 3D Seismic Technology: Are We Realising Its Full Potential? In: Davies, R.J., Stewart, S.A., Cartwright, J.A., Lappin, M. (eds.) 3D Seismic Technology; Application to the Exploration of Sedimentary Basins: Geological Society of London Memoirs v. 29, p. 1-10.

Deptuck, M.E., Steffens, G.S., Barton, M., Pirmez, C. 2003. Architecture and evolution of upper fan channel-belts on the Niger Delta slope and in the Arabian Sea. Marine and Petroleum Geology, v. 20, p. 649–676.

Faugères, J-C, Stow, D.A.V., Imbert, P., and Viana, A. 1999. Seismic features diagnostic of contourite drifts. Marine Geology, v. 162, p. 1-38.

Ebinger C.A., and Tucholke, B.E. 1988. Marine Geology of the Sohm Basin, Canadian Atlantic Margin. Bulletin of American Association of Petroleum Geologists, v. 72, p. 1450-1468.

Fensome, R.A., Crux, J.A., Gard, I.G., MacRae, R.A., Williams, G.L., Thomas, F.C., Fiorini, F., and Wach, G. 2008. The last 100 million years on the Scotian Margin, offshore eastern Canada: an event-stratigraphic scheme emphasizing biostratigraphic data. Atlantic Geology, v. 44, p. 93-126.

Flood, R.D. 1988. A lee wave model for deep-sea mudwave activity. Deep-Sea Research, v 35, p. 973-983.

He, Y., Duan, T., and Gao, Z. 2008. Sediment entrainment. In: Rebesco, M. and Camerlenghi, A. eds., Contourites: Developments in Sedimentology v. 60, Elsevier, p. 101-119.

Heezen, B.C., Hollister, C.D., Ruddiman, W.F. 1966. Shaping of the continental rise by deep geostrophic contour currents. Science, v. 152, p. 502–508.

Hernández-Molina, F.J., Llave, E., and Stow, D.A.V. 2008. Continental slope contourites. In: Rebesco, M. and Camerlenghi, A. (eds.), Contourites: Developments in Sedimentology v. 60, Elsevier, p. 379- 408.

Hernández-Molina, F.J., Llave, E., Stow, D.A.V., García, M., Somoza, L., Vázquez, J.T., Lobo, F., Maestro, A., Díaz del Río, V., León, R., Medialdea, T., and Gardner, J. 2006. The Contourite Depositional System of the Gulf of Cadiz: A sedimentary model related to the bottom current activity of the Mediterranean Outflow Water and the continental margin characteristics. Deep-Sea Research I, v. 53, p. 1420–1463.

Hohbein, M., Cartwright, J. 2006. 3D seismic analysis of the West Shetland Drift system: Implications for Late Neogene palaeoceanography of the NE Atlantic. Marine Geology, v. 230, p. 1-20.

Hopfauf, V., and Spiess, V., 2001. A three-dimensional theory for the development and migration of deep sea sediment waves. Deep-Sea Research I, v. 48, p. 2497–2519.

Knutz, P.C., and Cartwright, J. 2003. Seismic stratigraphy of the West Shetland Drift: Implications for Late Neogene paleocirculation in the Faeroe-Shetland Gateway. Paleoceanography, v. 18, p. 1093, doi: 10.1029/2002PA000786.

Locker, S.D., and Laine, E.P. 1992. Paleogene-Neogene depositional history of the middle U.S. Atlantic continental rise: mixed turbidite and contourite depositional systems: Marine Geology, v. 103, p. 137-164.

Long, M.T. 2002. A sequence stratigraphic analysis of Campian to Middle Miocene sediments of the Sable Island area, Offshore Nova Scotia, Eastern Canada. Unpublished M.Sc. Dissertation [M.Sc. Thesis], Rice University, Houston, Texas, 143 p.

MacDonald, A.W.A. 2006. Cenozoic seismic stratigraphy of the central Nova Scotian continental margin: the interplay of erosion, deposition and salt tectonics, offshore Nova Scotia. Unpublished M.Sc. Dissertation [M.Sc. Thesis], St. Mary's University, Halifax, Nova Scotia, 152 p.

Mosher, D.C., Piper, D.J.W., Campbell, D.C., and Jenner, K.A. 2004. Near-surface geology and sediment-failure geohazards of the central Scotian Slope. American Association of Petroleum Geologists Bulletin, v. 88, p. 703-723.

Mulder, T., Faugères, J-C, and Gonthier, E. 2008. Mixed turbidite-contourite systems. In: Rebesco, M. and Camerlenghi, A. (eds.) Contourites: Developments in Sedimentology v. 60, Elsevier, p. 435-456.

Petro-Canada Inc. 1985. Well History Report Petro-Canada et al. Shelburne G-29: 116 p.

Piper D.J.W. 1988. Glaciomarine sediments on the continental slope off eastern Canada. Geoscience Canada, v. 15, p. 23-28.

Poag, C.W. and Mountain, G.S. 1987. Late Cretaceous and Cenozoic evolution of the New Jersey continental slope and upper rise: An integration of borehole data with seismic reflection profiles. Initial Reports, Deep-Sea Drilling Project Leg 95, p. 673-724.

Posamentier, H.W., and Kolla, V. 2003. Seismic geomorphology and stratigraphy of depositional elements in deep-water settings. Journal of Sedimentary Research, v. 73, p. 367-388.

Prather, B.E. 2003. Controls on reservoir distribution, architecture and stratigraphic trapping in slope settings. Marine and Petroleum Geology, v. 20, p. 527–543.

Rebesco, M. 2005. Contourites. In: Selley, R.C., Cocks, L.R.M., and Plimer, I.R. (eds.) Encyclopedia of Geology: Elsevier, Oxford, v. 4., p. 513-527.

Rebesco, M., and Stow, D.A.V. 2001. Seismic Expression of Contourites and Related Deposits: A Preface. Marine Geophysical Researches, v. 22, p. 303-308.

Ross, W.C., Halliwell, B.A., May, J.A., Watts, D.E., and Syvitski, J.P.M. 1994. Slope readjustment: a new model for the development of submarine fans and aprons. Geology, v. 22, p. 511–514.

Shaw, J., and Courtney, R.C. 2004. Digital elevation model of Atlantic Canada: Geological Survey of Canada Open File 4634.

Shimeld, J. 2004. A comparison of salt tectonic subprovinces beneath the Scotian Slope and Laurentian Fan. In: Post, P.J., Olson, D.L., Lyons, K.T., Palmes, S.L., Harrison, P.F., and Rosen, N. (eds.) Salt–sediment Interactions and Hydrocarbon Prospectivity: Concepts, Applications, and Case Studies for the 21st Century. 24th Annual Gulf Coast Section of the Society of Economic Paleontologists and Mineralogists Foundation Bob F. Perkins Research Conference, Houston, Texas, Dec. 5-8, 2004, p. 502-532.

Smolarkiewicz, P.K., and Rotunno, R. 1989. Low Froude Number Flow Past Three-Dimensional Obstacles. Part I: Baroclinically Generated Lee Vortices. Journal of Atmospheric Sciences, v. 46, p. 1154-1164.

Steffens, G.S., Biegert, E.K., Sumner, S., and Bird, D. 2003. Quantitative bathymetric analyses of selected deepwater siliciclastic margins: receiving basin configurations for deepwater fan systems. Marine and Petroleum Geology, v. 20, p. 547-561.

Stow, D.A.V., Hernández-Molina, F.J., Llave, E., Sayago-Gil, M., Díaz del Río, V., and Branson, A. 2009. Bedform-velocity matrix: The estimation of bottom current velocity from bedform observations. Geology, v. 37, p. 327-330.

Swift, S.A. 1985. Cenozoic geology of the continental slope and rise off western Nova Scotia. Unpublished PhD dissertation [PhD thesis], Massachusetts Institute of Technology, Cambridge, Massachusetts, 188 p.

Swift, S.A. 1987. Late Cretaceous-Cenozoic development of outer continental margin, southwestern Nova Scotia. Bulletin of American Association of Petroleum Geologists, v. 71, p. 678-701.

Swift, S.A., Ebinger, C.J., and Tucholke, B.E. 1986, Seismic stratigraphic correlations across the New England Seamounts, western North Atlantic Ocean. Geology, v. 14, p. 346-349.

Thomas, F.C. 2005. Oligocene benthic foraminifera from the Paleogene Wenonah Canyon, Scotian Shelf- normal versus canyon assemblages. Atlantic Geology, v. 41, p 1-16.

Tucholke, B.E., and Mountain, G.S. 1986. Tertiary paleoceanography of the western North Atlantic Ocean. In: Vogt, P.R., and Tucholke, B.E. (eds.) The Geology of North America, Vol. M, The Western North Atlantic Region (ch. 38): Geological Society of America, Boulder, CO, p. 631–650.

Uenzelmann-Neben, G. 2006. Depositional patterns at Drift 7, Antarctic Peninsula: Along-slope versus down-slope sediment transport as indicators for oceanic currents and climatic conditions. Marine Geology, v. 233, p. 49-62.

Viana, A.R. 2008. Economic relevance of contourites. In: Rebesco, M. and Camerlenghi, A. (eds.) Contourites: Developments in Sedimentology v. 60, Elsevier, p. 493-510.

Viana, A.R., Almeida, Jr., W., Nunes, M.C.V., Bulhöes, E.M. 2007. The economic importance of contourites. In: Viana, A.R., Rebesco, M., eds.. Economic and Palaeoceanographic Significance of Contourite Deposits: Geological Society of London Special Publication v. 276, p. 1–23.

Wade, J.A., MacLean, B.C., and Williams, G.L. 1995. Mesozoic and Cenozoic stratigraphy, eastern Scotian Shelf: New interpretations. Canadian Journal of Earth Sciences, v. 32, p. 1462-1473.

Wynn, R.B., and Masson, D.G. 2008. Sediment waves and bedforms. In: Rebesco, M. and Camerlenghi, A. (eds.) Contourites: Developments in Sedimentology v. 60, Elsevier, p 289-300.

Wynn, R.B., and Stow, D.A.V. 2002. Classification and characterization of deep-water sediment waves. Marine Geology, v. 192, p. 7-22.

Chapter 6: Conclusions

6.1 Introduction

The four objectives described in detail in Chapter 1 lead to (1) an improved understanding of the Late Cretaceous and Cenozoic geological history of the outer Scotian margin and how it relates to the geological history determined elsewhere along the North American Basin margin, (2) new insights into the Cenozoic paleoceanography of the North Atlantic, and (3) new insights into the general slope processes of mass transport, unconformity formation, and bottom current erosion and deposition. This chapter summarizes the significance of key results and conclusions of the research, and identifies directions for future research.

6.2 Significance of Key Results

6.2.1 Late Cretaceous and Cenozoic geological history of the outer Scotian margin

Prior to this study, relatively little was known about the Cenozoic geological history of the outer Scotian margin. The Scotian margin lies northeast of the U.S. Atlantic margin, one of the most thoroughly studied passive margins in the world (specifically the New Jersey margin). The Scotian margin's close proximity to the New Jersey margin makes it an ideal location to test concepts of global and local controls on continental margin evolution; if the geological evolution of the Scotian margin differs significantly from the New Jeresy margin, then clearly local processes dominate. Regional mapping of the Upper Cretaceous and Cenozoic succession of the Scotian margin reveals two large depocenters; one that coincides with the Laurentian Fan on the eastern Scotian margin and one that lies between Verrill Canyon and Northeast Channel along the western margin (Figure 6.1). Chapter 2 presents the detailed depositional history of the large

depocenter in the west. Marked changes in seismic facies and depositional style occurred in the depocenter during the Late Cretaceous, at the Eocene-Oligocene transition, in the Middle Miocene, and Pleistocene. The bulk of the preserved succession within the depocenter can either be attributed to mass transport deposits and sediment drift (bottom current modified) deposits in the Oligocene -Middle Miocene interval, or sediment drift deposits in the Late Miocene and Pliocene. Compared to the depocenter associated with Laurentian Fan in the east, there are no obvious large submarine fans and channel-levee systems are rare.

Previous to this study, the most detailed published study of the Upper Cretaceous and Cenozoic geological history of the outer Scotian margin was by S.A. Swift in his PhD thesis and subsequent publications (Swift 1985; Swift et al 1986; Swift 1987). Although there are many shared results between the work by Swift and this study, important differences also exist. Firstly, Swift (1985, 1987) interpreted the mounded seismic facies that make up much of the Upper Cretaceous to Eocene succession as "chalky fans". The current study clearly demonstrates strong evidence that the mounded features are erosional remnants that form interfluves between broad gullies. Secondly, Swift (1985, 1987) proposed that the Abenaki carbonate bank remained exposed until the Late Cretaceous. The current study proposes that a widespread period of erosion of the upper slope during the Paleogene, possibly related to the Montagnais meteorite impact, exhumed to Lower Cretaceous or earlier deposits. The abrupt truncation of reflections above the Abenaki bank near the bank edge suggests that in many parts of the study area the bank edge was buried prior to this intense erosional phase in the Paleogene and was not exposed. Finally, Swift (1985, 1987) stated that the only bottom current deposits in the area are a <300 m thick interval of Pliocene sediment waves restricted to the lowermost continental rise. The current study demonstrates that bottom current deposits are much more widespread than indicated by previous researchers (e.g. Swift (1985, 1987), McCave et al. (2002)).

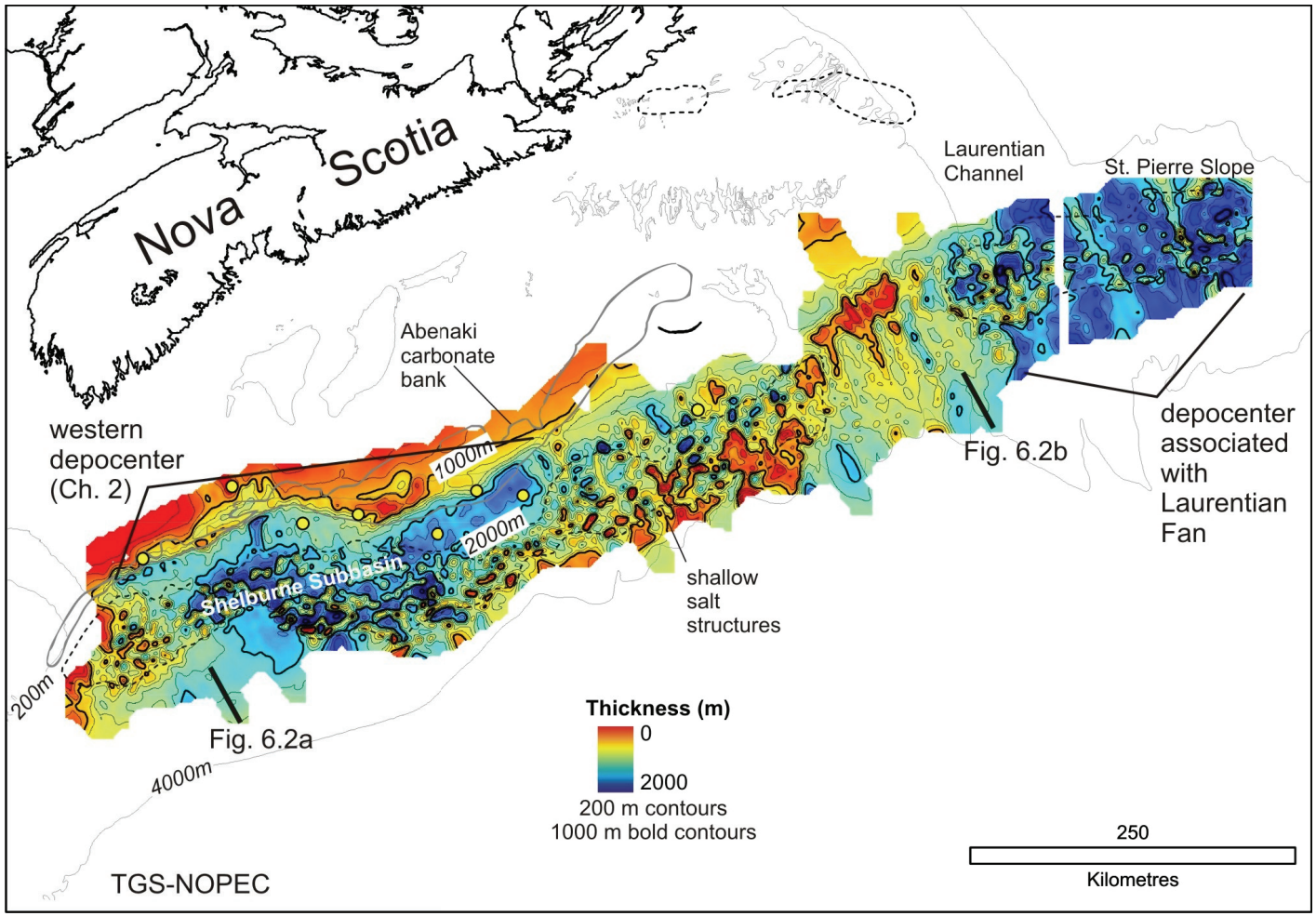

Figure 6.1 Isochore map of Upper Cretaceous to Present succession on the Scotian margin. The depocenter apparent in the western part of the margin was the focus of Chapter 2. Map is derived from data that are courtesy of TGS-Nopec.

Although the seismic stratigraphic framework presented in Chapter 2 was developed along a particular segment of the margin, additional work conducted during the course of the research, but not included in Chapters 2-5, shows that the seismic stratigraphy appears consistent across the entire Scotian margin, particularly seaward of salt structures. For example, Figure 6.2 shows two seismic reflection profiles that are suprisingly similar, even though they are separated by over 650 km. Despite the availability of a dense seismic grid for this study, uncertainty in seismic reflection correlation from below the slope and rise onto the shelf remains high because intervals become condensed and are poorly imaged below the outer shelf and upper slope. For these reasons, lateral correlation of the deepwater seismic stratigraphy developed in this study provides better stratigraphic control for the deepwater Scotian margin than attempting to correlate from the shelf to slope. The seismic framework developed in this study will be useful for providing stratigraphic constraints for future studies of the Scotian margin, and will be tested and refined if further scientific or exploration drilling is conducted. The interpreted relationship between the Scotian margin seismic stratigraphic framework and the seismic stratigraphic framework developed along the U.S. Atlantic margin is given in Chapter 2. The Upper Cretaceous and Cenozoic seismic architecture between the two areas appears remarkably similar. This study marks a significant northeastward expansion of the North American Basin framework; therefore, it allows regional extension of the interpretation of the paleoceanography and geological history of the Northwest Atlantic.

6.2.2 Cenozoic paleoceanography of the North Atlantic

Chapter 4 represents the first detailed investigation of contourite depositional systems along the Western North Atlantic margin using modern 2D and 3D seismic reflection data. These data provide the unique opportunity to investigate the preserved geomorphology of large sedimentary features in three dimensions and determine the long-term mean bottom current flow characteristics throughout the Cenozoic. Regional mapping of the Upper Cretaceous and Cenozoic seismic stratigraphy of the outer Scotian margin in Chapter 2 revealed that contourite depositional systems were a major contributor to the preserved succession. Prior to this study, the Scotian margin was

anomalous among the margins of the Northwest Atlantic insofar as contourite depositional features and sediment drifts were considered absent apart from minor Holocene and Pliocene features on the lower continental rise (Swift 1987; McCave and Tucholke 1986; Ebinger and Tucholke 1988; McCave et al. 2002). New results from this study show that evidence of bottom current activity throughout the Cenozoic along the Scotian margin is widespread.

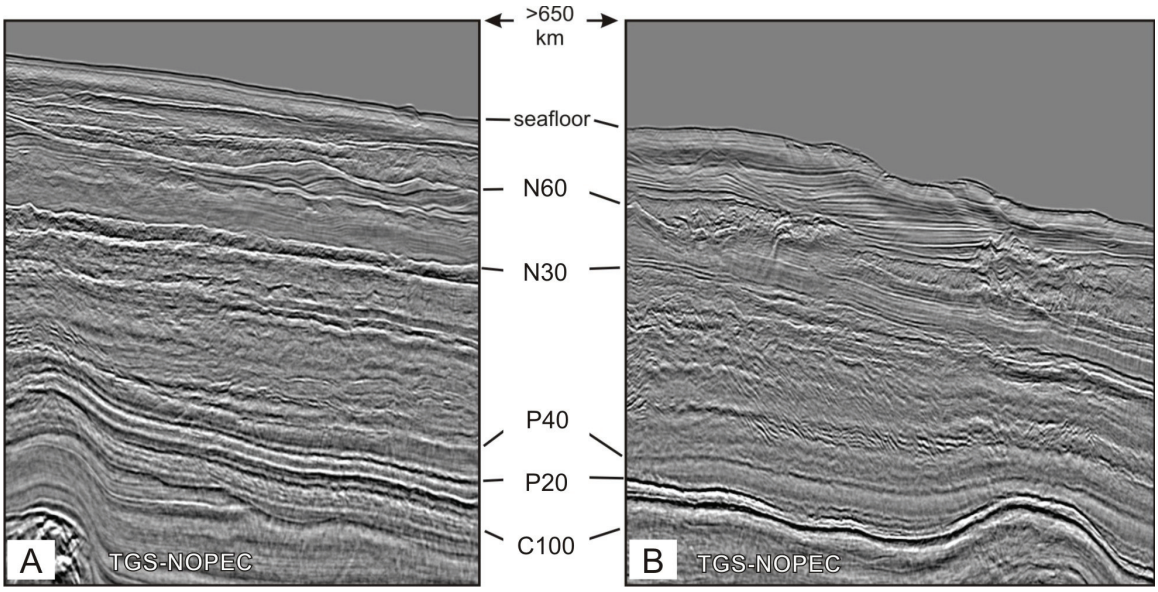

Figure 6.2 Example of two seismic reflection profiles from the outer Scotian margin, beyond the seaward extent of shallow salt structures. The two profiles are separated by over 650 km yet the seismic reflection character and stratigraphy is remarkably similar. Line locations are shown on Figure 6.1. Data are courtesy of TGS-Nopec.

In general, the results from this study agree with the Cenozoic bottom current histories derived elsewhere in the North Atlantic. On the Scotian margin, stacked sequences of giant sediment waves and elongate sediment drifts make up much of the Upper Miocene and Pliocene succession along the western Scotian margin. Evidence for bottom current activity is also recognized in the Upper Eocene and Oligocene- Middle Miocene succession. Major erosional pulses contribute to the formation of regional seismic markers, first along the continental rise in the Early Oligocene, then along the continental slope during the Late Miocene and Pliocene. The current study augments the existing scientific understanding of the paleoceanography of the Northwest Atlantic. Most studies report that the onset of an active deep western boundary current in the North Atlantic

occurred in the Early Oligocene driven by the development of large Antarctic ice sheets (Miller et al. 2008). In the study area, the recognition of Late Eocene bottom current activity suggests that an active western boundary current was present earlier in the Paleogene. Throughout the Cenozoic, local bottom current erosion is recognized at several stratigraphic levels and appears related to nearby seafloor perturbations (discussed further below). Novel methods were applied to determine direct measurements of paleo-bottom current direction and estimations of current strength through bedforms imaged in 3D seismic data. All bottom current evidence overwhelmingly suggests a northeast-to-southwest flowing Deep Western Boundary Current during the Cenozoic.

6.2.3 Slope processes

Most studies of deepwater seismic geomorphology focus on describing and understanding depositional elements associated with down slope sediment transport primarily because of hydrocarbon exploration interest in turbidite reservoirs (e.g. Posamentier et al. 2007; Posamentier and Kolla 2003; Deptuck et al., 2003; Davies et al. 2004). Because this study examined the entire range of processes that resulted in the seismic reflection architecture of the outer Scotian margin rather than focusing on a single process or depositional element (e.g. submarine fans or channels), the seismic geomorphology of features not traditionally examined in detail using 3D seismic data were investigated. In particular, Chapters 2 and 3 discuss processes that led to the development of deepwater unconformities, Chapter 3 examines mass wasting processes, Chapters 4 and 5 investigate contourite depositional systems, and Chapter 5 addresses the interaction of along-slope and down-slope processes. These results contribute significantly to the general understanding of how such features form, have applications globally where similar features exist, and provide important insights into understanding how continental margins evolve.

Deep water unconformities

Below the continental shelf, it is relatively easy to imagine that raising and lowering sea-level, changing rates of sediment supply, and creating and removing accommodation

space would, through time, lead to the formation of widespread unconformities. These unconformities form useful seismic stratigraphic markers and underpin sequence stratigraphy (Catuneanu et al. 2009). Below the continental slope and rise, regional unconformities are also recognized, and similarly form useful seismic stratigraphic horizons. Beyond the shelf edge, these deep water unconformities cannot be directly attributed to sea-level change and their formation is less clear. Deep water unconformities are the focus of Chapter 3, but are also discussed elsewhere throughout the thesis.

The results from this study show that processes that led to the formation of regional deep water seismic stratigraphic unconformities are complex and in most cases are attributed to both along slope and down slope processes. For example, the sequence of events that formed the N30 unconformity during the Middle to Late Miocene in the western part of the Scotian margin was examined in detail in Chapter 3. The N30 horizons appears equivalent to the Merlin unconformity recognized along much of the North American Basin margin to the south (Mountain and Tucholke 1985; Swift 1987). As discussed in Chapters 2 and 3, its origin is uncertain; in places attributed to down-slope erosional process and elsewhere attributed to along-slope erosional processes. On the Scotian margin, N30 is often a composite unconformity, formed by the merging of a number of erosional surfaces. Chapter 3 demonstrates that given sufficient data coverage, it is possible to dissect the various events that led to the formation of this unconformity. For the first time, the 3D seismic geomorphology of this important regional seismic stratigraphic horizon was determined and seismic stratigraphic analysis shows that it formed through multiple periods of bottom current erosion, large mass wasting events, and channel incision.

Mass transport deposition

Submarine mass transport deposits are an important component in the evolution of continental margins (Piper et al 1997; Canals et al. 2004; Bull et al. 2009; Mosher et al. 2010) and are included in some proposed deep water sequence stratigraphic models (Posamentier and and Kolla 2003; Catuneanu et al. 2009) . Because of their episodic nature and location in the marine realm, direct observation of submarine mass transport events is lacking. Most of what is known about submarine mass movements is from

geophysical studies that reveal their seafloor and seismic expression and, to a much lesser extent, outcrop and borehole investigations that reveal detailed structure, sedimentology, and physical properties. Increased collection of 3D seismic datasets in deep water by the petroleum industry, and access to these datasets by researchers over the last ten years, have been major contributors to an improved understanding of mass transport processes.

In Chapter 3, two large mass transport deposits were investigated in detail. The purpose was to determine their contribution to erosion of the N30 unconformity along the western Scotian Slope. The areal extent and volume of the deposits presented in Chapter 3 are among the largest reported in the literature (Lipman et al. 1988; Hampton et al. 1996; Legros 2002). The results in Chapter 3 show that these mass wasting events appear to have initiated on the lower slope in the vicinity of shallow salt diapirs far away from the shelf edge. Individual intact blocks within the failures exceed 5 km in length and up to 200 m in thickness and would likely be difficult to identify in outcrop given their size. Striae at the base of mass transport deposits provide information about the failure kinematics. There was no obvious direct sea level driver for the deposits discussed in Chapter 3; they do not appear to have formed by the collapse of shelf margin deltas, although loading of the outer shelf and upper slope may have driven salt tectonism contributing to failure in the vicinity of diapirs. Additionally, in the particular case of the failures examined in Chapter 3, deep bottom currents may have been sufficient to undercut the seabed on the seaward side of salt structures and precondition the seabed for failure. Finally, rare large earthquakes, as occurred in the 1929 Grand Banks earthquake (Piper et al. 1999), are the likely ultimate triggers for these large submarine mass movements.

Deep water sedimentary bedforms

Along much of the Earth's continental margins, sediment drift deposits contribute significantly to the depositional record along the lower continental slope and rise (Wynn and Stow 2002; Hernàndez-Molina et al. 2008). Results presented in Chapters 2 and 4 in this thesis show that they are a major contributor to the preserved Cenozoic succession along the Scotian margin. Relatively few published studies have used 3D seismic data to

investigate sediment drifts and contourite depositional systems. A number of recent studies have demonstrated the effectiveness of applying 3D seismic data to understanding these systems (Knutz and Cartwright 2003; Hohbein and Cartwright 2006; Viana et al 2007) but emphasize the need for more detailed examination of these deposits. Chapters 4 and 5 in this thesis provide new results about deep water sedimentary bedforms and contourite drifts primarily through the analysis of 2D and 3D seismic data.

Conceptual and numerical models of deepwater giant sediment wave formation attempt to explain the observed natural characteristics of these features (Flood 1988; Blumsack and Weatherly 1988; Blumsack 1993; Hopfauf and Speiss 2001). There is still considerable uncertainty as to the criteria required to initiate sediment wave development and the relationship of bedform migration direction to long-term mean bottom currents (Wynn and Stow 2002; Flood and Giosan 2002; Wynn and Masson 2008). During the Late Miocene and Pliocene, giant sediment waves covered approximately 40% of the slope and upper rise along the western Scotian margin (Figure 4.4) and approximately 30% of the continental rise of the eastern U.S. (see Figure 8-34 in Mountain and Tucholke 1985). Chapter 5 applied a novel approach to analysis of 3D seismic data from the southwest Scotian margin to investigate a sequence of giant sediment waves. The detailed mapping of multiple reflection horizons within the sediment wave interval reveals details about bedform initiation and migration not previously known. For example, sediment waves are shown to migrate both up-current and down-current, bottom current interaction with the seabed is interpreted to result in the creation of lee vortices, and flow separation appears to occur across shallow salt structures. In Chapters 4 and 5, numerous examples demonstrate the close association between seafloor perturbations and sediment wave initiation. The clearest case is presented in Chapter 5 where the development of several individual sedimentary bedforms is directly tied to pre-existing seafloor obstacles such as escarpments or shallow salt diapirs.

In Chapter 4, novel methods were used to estimate the paleo-bottom current direction. Previous authors assumed that giant sediment waves are antidunal bedforms that migrated up current and used this assumption combined with sediment wave crest

orientation to estimate paleo-bottom current direction (Flood 1988; Flood and Giosan 2002; Wynn and Stow 2002). In Chapter 4, methods that avoid such assumptions were used. The orientation of bedforms relative to fixed obstacles, for example diapir crests or escarpments, was one such method. Convincing examples of buried submarine barchan bedforms are shown in Chaper 4 and their orientation provides another measure of paleo-bottom current direction. The results show that on relatively flat areas, bedform crest orientation is approximately perpendicular (at 90°) to mean current direction, while on slopes, bedform crest orientation is oblique to bottom current direction with the acute angle of 20° - 40°.

The role of pre-existing seafloor topography

The importance of pre-existing seafloor morphology in influencing the character of deposits originating from both down-slope gravity currents and along-slope bottom currents is becoming more apparent (Locker and Laine 1992; Uenzelmann-Neben 2006; Mulder et al. 2008). In the case of gravity flows, it is recognized that receiving basin configuration is one of the primary factors controlling lithofacies distribution as gravity flows transit from shelf areas into deeper water (Prather 2003; Steffens et al. 2003). Similarly for sediment drifts, pre-existing seafloor irregularities appear to be loci for the initiation of deepwater bottom current deposits (Faugères et al. 1999; Viana et al. 2007; Hopfauf and Spiess 2001; Wynn and Masson 2008).

Within the study area, inherited morphology affected subsequent deposition patterns for both along-slope and down-slope deposits. The bulk of the Upper Cretaceous and Cenozoic depocenter discussed in Chapter 2 is confined to the area between the steep carbonate bank edge on the landward side, and the zone of shallow salt structures on the basinward side. On a more local scale, erosional or constructional terraces or depressions (e.g. the gullies that characterize seismic unit 1, the erosional terrace formed by N30 in the east, or the constructional terrace created by the *Shelburne Drift* in the west) created deep water accommodation space in the sense of Prather (2003) and Steffens et al. (2003). Chapters 2 and 5 show that regionally, the Upper Miocene and Pliocene sediment wave field along the southwest Scotian margin developed within a submarine embayment

created by mass-wasting and channel incision. Locally, seafloor irregularities due to mass-wasting and protruding salt diapirs controlled the precise locations of maximum sediment wave growth as shown in Chapter 5. The transition from seismic stratigraphic unit 3 to 4 saw a return to gravity-flow dominated deposition across the entire Scotian margin. In many parts of the study area, the highest seismic amplitudes in Unit 4 occur at the break in slope formed where the *Shelburne* and *Shubenacadie Drifts* onlap the N30 unconformity. Detailed investigation has shown that where gravity flows entered the system, local topographic features at the scale of individual sediment waves controlled their distribution.

6.3 Conclusions

1. The Upper Cretaceous and Cenozoic seismic stratigraphy of the outer Scotia margin is broadly divisible into four units: 1) Unit 1 (Upper Cretaceous to Upper Eocene) consists of high-amplitude, discontinuous and mounded reflections. The formation of this unit is attributed to repeated, widespread erosion events interspersed with periods of hemipelagic and pelagic, carbonate rich sedimentation. There is extensive evidence of slope instability in Unit 1 below the modern upper slope. 2) Unit 2 (Lower Oligocene to Middle Miocene) consists of a variety of seismic facies (e.g. channels, mass transport deposition, sediment drift and hemipelagic facies) overprinted by dense, small-offset faults that are diagnostic of this unit, 3) Unit 3 (Middle Miocene to Upper Pliocene) is dominated by low to moderate amplitude, parallel to wavy reflections interpreted to represent sediment drift, or bottom current-modified deposition, 4) Unit 4 (Upper Pliocene to Present) consists of high amplitude, sub-parallel to chaotic reflections and shows evidence of channel development and gravity flow deposition. The majority of the Upper Cretaceous and Cenozic deposits preserved below the modern western Scotian Slope and upper rise belong to seismic units 2 and 3 (Lower Oligocene to Upper Pliocene). These deposits are mainly confined to the area seaward of the Abenaki carbonate bank and landward of salt structures below the slope.

2. The processes that led to the regionally identifiable seismic stratigraphic horizons that were used to divide and sub-divide the the seismic stratigraphic units were complex. In some instances, these stratigraphic horizons do not appear to be erosional and, instead, appear due to changes in lithology or seismic facies. In other cases, the bounding surfaces are clearly erosional and the formation processes are attributed to down-slope erosion by large mass-wasting events, down-slope erosion by channels, and along-slope erosion by bottom currents. The specific processes that lead to margin erosion become less obvious moving from the lower continental rise to the slope as unconformities merge, preserving only evidence of the most recent erosion event.

3. Cenozoic depositional patterns along the outer Scotian margin were strongly influenced by northeast-to-southwest flowing bottom currents. The earliest indication of bottom current activity was in the Eocene when small sediment drifts filled numerous gullies below the slope and larger sediment drifts developed on the upper rise. Localized small sediment drifts also developed in the Middle Miocene, but it is only in the Upper Miocene and Pliocene succession that sediment drifts are the dominant depositional feature. Upper Miocene and Pliocene sediment drifts contribute substantially to the preserved succession in the Shelburne sub-basin, representing >50% of the stratigraphic section in the thickest part of the depocenter. Erosion of the outer margin by bottom currents occurred in the Early Oligocene, Middle Miocene, and Pliocene. In the Early Oligocene, erosion appears to have been confined to the area below the upper continental rise, while later in the Neogene, the effects of bottom current erosion appear more pronounced below the slope.

4. In the case of the Upper Cretaceous and Cenozoic succession along the outer western Scotian margin, gross receiving basin configuration appears to be controlled on the landward side by the Abenaki carbonate bank and on the seaward side by shallow salt structures. Locally, however, modification of the slope profile through processes related to mass-wasting and bottom current erosion and deposition greatly influenced subsequent depositional patterns.

6.4 SUGGESTIONS FOR FUTURE RESEARCH

1) Improved geological sample control for deposits along the outer Scotian margin would greatly improve understanding of the lithostratigraphy of the margin. Chapter 2 demonstrates that a significant portion of the Cenozoic succession is undersampled. In particular, the existing exploration wells do not sample the Pleistocene section and are positioned such that most of the Upper Eocene to Middle Miocene interval is not sampled. Sampling of the Upper Eocene to Middle Miocene succession on the U.S. margin has also been problematic (Poag and Mountain 1987). Compared to the U.S. margin where Eocene sediments outcrop along much of the slope, the western Scotian margin has not suffered erosion of Oligocene to present sediments to the same extent. The mapping results in Chapter 2 provide an excellent first step towards developing a scientific drilling plan to effectively sample the seismic stratigraphic units where they are thickest and best preserved.

2) Results from Chapter 2 should be integrated with the geological history and sequence stratigraphy of the continental shelf off Nova Scotia where there is superior sample control. Where data allows, it should be possible to determine if there are relationships between the acoustic facies on the slope and shelf, e.g. do periods of shelf margin progradation coincide with channel formation on the slope, is there a relationship between sediment drift development and sea-level position. Some of the shelf work exists already in the form of publications and M.Sc. theses (e.g. Wade et al. 1995; Long 2002; MacDonald 2006; Fensome et al. 2008).

3) Scientific drilling of several of the contourite depositional and erosional features identified in this study would improve understanding of the rate in which deepwater sediment waves migrate and the lithology of erosional lag surfaces, for example along the N30 unconformity or in areas of barchan bedforms.

4) The seismic stratigraphy developed in this study should be extended eastward and northward along the Scotian margin to the Grand Banks margin, ideally to tie into the

framework developed by Deptuck (2003) for the Jean D'Arc Basin and Flemish Pass, and to the stratigraphy of the Newfoundland Basin. The margin decreases in age moving eastward and northward and differences in the Upper Cretaceous and Paleogene stratigraphy should be apparent. For example, it is important to determine how far the mounded and erosional seismic Unit 1 continues towards the north and to determine whether there are differences in the bottom current history moving away from the influence of the Gulf Stream.

5) More detailed investigation of the multiple erosional surfaces within the Upper Cretaceous to Middle Eocene succession may unravel the importance of meteorite impacts in margin erosion.

6) Preliminary interpretation of seismic data seaward of the Abenaki carbonate bank edge along the western Scotian margin shows the presence of extensive deepwater sediment waves in Cretaceous deposits that underlie the C100 (Upper Cretaceous) reflection. These bedforms are significant because they suggest an active deep current system in the Mesozoic which is not widely recognized and should be examined in more detail.

7) More research should be done on the polygonal fault system that characterizes the Oligocene to Middle Miocene succession, but are also found in the Late Miocene and Pliocene succession. The Oligocene to Middle Miocene faulted interval is recognized across the entire U.S. and Nova Scotian Atlantic margin (Mountain and Tucholke 1985; Chapter 2). Cryptic high amplitude reflections within the interval may be indicative of diagentic boundaries. Detailed analysis of the 3D seismic data in the Barrington area may reveal details about fault kinematics. The Bonnet P-23 well possibly provides some lithological control for the interval. Preliminary analyis of data from the Torbrook 3D dataset (e.g. 4.19a) suggests that the fault pattern is at least in part inherited from the underlying mounded Upper Cretaceous to Eocene succession and may be related to differential compaction. The faults appear to be conduits for fluid flow (Mosher 2011).

6.5 REFERENCES CITED IN CHAPTER 6

Blumsack, S.L., 1993. A model for the growth of mudwaves in the presence of time varying currents. Deep-sea Research II 40 (4/5), 963–974.

Blumsack, S.L. and Weatherly, G.L. 1989. Observations of the nearby flow and a model for the growth of mudwaves. Deep Sea Reseach Part A. v. 36, p. 1327-1339.

Bull, S., Cartwright, J.A., and Huuse, M. 2009. A review of kinematic indicators from mass-transport complexes using 3D seismic data. Marine and Petroleum Geology *26*, 1132-1151

Canals, M., Lastras, G., Urgeles, R., Casamor, J.L., Mienert, J., Cattaneo, A., De Batist, M., Halfidason, H., Y. Imbo, Y., Laberg, J.S., Locat, J., Long, D., Longva, O., Masson, D.G., Sultan, N., Trinardi, F. and Bryn, P. 2004. Slope failure dynamics and impacts from seafloor and shallow sub-seafloor geophysical data: case studies from the COSTA project. Marine Geology, v. 213, p. 9-72.

Catuneanu, O., Abreu, V., Bhattacharya, J.P., Blum, M.D., Dalrymple, R.W., Eriksson, P.G., Fielding, C.R., Fisher, W.L., Galloway, W.E., Gibling, M.R., Giles, K.A., Holbrook, J.M., Jordan, R., Kendall, C.G.St.C., Macurda, B., Martinsen, O.J., Miall, A.D., Neal, J.E., Nummedal, D., Pomar, L., Posamentier, H.W., Pratt, B.R., Sarg, J.F., Shanley, K.W., Steel, R.J., Strasser, A., Tucker, M.E. and Winker, C. 2009. Towards the standardization of sequence stratigraphy. Earth-Science Reviews, Vol. 92, p. 1-33.

Davies, R.J., Stewart, S.A., Cartwright, J.A., Lappin, M., Johnston, R., Fraser, S.I., and Brown, A.R. 2004. 3D Seismic Technology: Are We Realising Its Full Potential?, *in* Davies, R.J., Stewart, S.A., Cartwright, J.A., Lappin, M., eds., 3D Seismic Technology; Application to the Exploration of Sedimentary Basins: Geological Society of London Memoirs v. 29, p. 1-10.

Deptuck, M.E., Steffens, G.S., Barton, M., Pirmez, C. 2003. Architecture and evolution of upper fan channel-belts on the Niger Delta slope and in the Arabian Sea. Marine and Petroleum Geology, v. 20, p. 649–676.

Ebinger C.A., and Tucholke, B.E., 1988, Marine Geology of the Sohm Basin, Canadian Atlantic Margin: Bulletin of American Association of Petroleum Geologists, v. 72, p. 1450-1468.

Fensome, R.A., Crux, J.A., Gard, I.G., MacRae, R.A., Williams, G.L., Thomas, F.C., Fiorini, F., and Wach, G. 2008. The last 100 million years on the Scotian Margin, offshore eastern Canada: an event-stratigraphic scheme emphasizing biostratigraphic data. Atlantic Geology, v. 44, p. 93-126.

Faugères, J-C, Stow, D.A.V., Imbert, P., and Viana, A. 1999. Seismic features diagnostic of contourite drifts. Marine Geology, v. 162, p. 1-38.

Flood, R.D., 1988, A lee wave model for deep-sea mudwave activity: Deep-Sea Research, v 35, p. 973-983.

Flood, R.D., Giosan, L., 2002. Migration history of a fine-grained abyssal sediment wave on the Bahama Outer Ridge. Marine Geology, v. 192, 259–274.

Hampton, M.A., Lee, H.J., Locat, J. 1996. Submarine landslides. Reviews of Geophysics, v. 34, p. 33– 59.

Hernández-Molina, F.J., Llave, E., and Stow, D.A.V. 2008. Continental slope contourites. In: M. Rebesco and A. Camerlenghi (eds.). Contourites. Developments in Sedimentology, v. 60, Elsevier, p. 379- 408.

Hohbein, M., Cartwright, J.A. 2006. 3D seismic analysis of the West Shetland Drift system: Implications for Late Neogene palaeoceanography of the NE Atlantic. Marine Geology, v. 230, p. 1-20.

Hopfauf, V., and Spiess, V., 2001, A three-dimensional theory for the development and migration of deep sea sediment waves: Deep-Sea Research I, v. 48, p. 2497–2519.

Knutz, P.C., and Cartwright, J.A. 2003. Seismic stratigraphy of the West Shetland Drift: Implications for Late Neogene paleocirculation in the Faeroe-Shetland Gateway. Paleoceanography, v. 18, p. 1093, doi: 10.1029/2002PA000786.

Legros, F. 2002. The mobility of long-runout landslides. Engineering Geology, v. 63, p. 301-331.

Lipman, P.W., Normark, W.R., Moore, J.G., Wilson, J.B., Gutmacher, C.E. 1988. The giant submarine Alika debris slide, Mauna Loa, Hawaii. Journal of Geophysical Research, v. 93, p. 4279– 4299.

Locker, S.D., and Laine, E.P., 1992, Paleogene-Neogene depositional history of the middle U.S. Atlantic continental rise: mixed turbidite and contourite depositional systems: Marine Geology, v. 103, p. 137-164.

Long, M.T. 2002. A sequence stratigraphic analysis of Campian to Middle Miocene sediments of the Sable Island area, Offshore Nova Scotia, Eastern Canada. Unpublished M.Sc. Dissertation [M.Sc. Thesis], Rice University, Houston, Texas, 143 p.

MacDonald, A.W.A. 2006. Cenozoic seismic stratigraphy of the central Nova Scotian continental margin: the interplay of erosion, deposition and salt tectonics, offshore Nova Scotia. Unpublished M.Sc. Dissertation [M.Sc. Thesis], St. Mary's University, Halifax, Nova Scotia, 152 p.

McCave I.N. and Tucholke B.E. 1986. Deep current controlled sedimentation in the western North Atlantic. in: The geology of North America vol. M: The western North Atlantic region. Vogt P.R. & Tuchkolke B.E. (eds.). Geological Society of America. p. 451–468.

McCave, I.N., Chandler, R.C., Swift, S.A., and Tucholke, B.E. 2002. Contourites of the Nova Scotian continental rise and the HEBBLE area. Geological Society, London, Memoirs, v. 22, p. 21-38.

Mosher, D.C. 2011. A margin-wide BSR gas hydrate assessment: Canada's Atlantic margin. Marine and Petroleum Geology, v. 28, p. 1540-1553.

Mosher, D.C., Shipp, C., Moscardelli, L., Chaytor, J., Baxter, C., Lee, H., Urgeles, R. (eds.) 2010. Submarine Mass Movements and Their Consequences. Springer, Advances in Natural and Technological Hazards Research, v. 28, 786 p.

Mountain, G.S. and Tucholke, B.E. 1985. Mesozoic and Cenozoic Geology of the U.S. Atlantic Continental Slope and Rise. in: Geologic Evolution of the U.S. Atlantic Margin. C.W. Poag (ed.). Van Nostrand Reinhold. p. 293-341.

Mulder, T., Faugères, J-C, Gonthier, E. 2008. Mixed turbidite-contourite systems. In: M. Rebesco and A. Camerlenghi (eds.). Contourites. Developments in Sedimentology, v. 60, Elsevier, p. 435-456.

Piper D.J.W, Cochonat P., and Morrison M.L. 1999. The sequence of events around the epicentre of the 1929 Grand Banks earthquake: initiation of debris flows and turbidity currents inferred from sidescan sonar. Sedimentology. V. 46, p. 79–97.

Piper, D.J.W., Pirmez, C., Manley, P.L., Long, D., Flood, R.D., Normark, W.R. and Showers, W. 1997. Mass Transport Deposits of the Amazon Fan. In: Proc. ODP Sci. Results, 155. R.D. Flood, D.J.W. Piper, A. Klaus and L.C. Peterson (eds.). Ocean Drilling Program, College Station, TX. p. 109-146.

Posamentier, H.W., and Kolla, V. 2003. Seismic geomorphology and stratigraphy of depositional elements in deep-water settings. Journal of Sedimentary Research, v. 73, p. 367-388.

Posamentier, H.W., Davies, R.J., Cartwright, J.A., and Wood, L.J. 2007. Seismic geomorphology; an overview. Seismic geomorphology; applications to hydrocarbon exploration and production, Geological Society Special Publications 277, p. 1-14.

Prather, B. E. 2003. Controls on reservoir distribution, architecture and stratigraphic trapping in slope settings. Marine and Petroleum Geology, v. 20, p. 527–543.

Steffens, G.S., Biegert, E.K., Sumner, S., and Bird, D. 2003. Quantitative bathymetric analyses of selected deepwater siliciclastic margins: receiving basin configurations for deepwater fan systems. Marine and Petroleum Geology, v. 20, p. 547-561.

Swift, S.A. 1985. Cenozoic geology of the continental slope and rise off western Nova Scotia. PhD Thesis, Massachusetts Institute of Technology, Cambridge, Massachusetts, 188 p.

Swift, S.A., Ebinger, C.J., and Tucholke, B.E., 1986, Seismic stratigraphic correlations across the New England Seamounts, western North Atlantic Ocean: Geology, v. 14, p. 346-349.

Swift, S.A., 1987, Late Cretaceous-Cenozoic development of outer continental margin, southwestern Nova Scotia: Bulletin of American Association of Petroleum Geologists, v. 71, p. 678-701.

Uenzelmann-Neben, G. 2006. Depositional patterns at Drift 7, Antarctic Peninsula: Along-slope versus down-slope sediment transport as indicators for oceanic currents and climatic conditions. Marine Geology, v. 233, p. 49-62.

Viana, A.R., Almeida, Jr., W., Nunes, M.C.V., Bulhões, E.M. 2007. The economic importance of contourites. In: Viana, A.R., Rebesco, M., (eds.) Economic and Palaeoceanographic Significance of Contourite Deposits: Geological Society of London Special Publication v. 276, p. 1–23.

Wade, J. A., MacLean, B. C., and Williams, G. L. 1995. Mesozoic and Cenozoic stratigraphy, eastern Scotian Shelf: New interpretations. Canadian Journal of Earth Sciences, v. 32, p. 1462-1473.

Wynn, R.B. and Masson, D.G. 2008. Sediment waves and bedforms. In: M. Rebesco and A. Camerlenghi (eds.). Contourites. Developments in Sedimentology, v. 60, Elsevier, p 289-300.

Wynn, R.B., and Stow, D.A.V. 2002. Classification and characterization of deep-water sediment waves. Marine Geology, v. 192: 7-22.

References

Amos, A.F., and Gerard, R.D. 1979. Anomalous bottom water south of the grand-banks suggests turbidity current activity. Science, v. 203, p. 894-897.

Archibald, M. 2003. Geological report for Marathon Canada Ltd. Annapolis G-24 exploration well. 95 p.

Arthur, M., Srivastava, S.P., Kamiski, M., Jarrad, R., Osler, J., 1989. Seismic stratigraphy and history of deep circulation and sediment drift development in the Baffin Bay and the Labrador Sea, in: Srivastava, S.P., Arthur, M., Clement, B. (Eds.), Proc. ODP Sci. Res. College Station, TX (Ocean Drilling Program), Vol. 105, pp. 957–988.

Ascoli, P. 1988. Mesozoic-Cenozoic foraminiferal, ostracod and calpionellid zonation of the north Atlantic margin of North America: Georges Bank-Scotian basins and northeastern Grand Banks. Geological Survey of Canada Open File 1791. 41 p.

Aurnhammer, M., and Mayoral, R. 2004. Improving seismic horizon matching by ordinal measures. In Proceedings of the 17th International Conference on Pattern Recognition, Vol. 3, pp. 642-645.

Best, J.L. and Brayshaw, A.C. 1985. Flow separation—a physical process for the concentration of heavy minerals within alluvial channels. Journal of the Geological Society, v. 142, p. 747-755.

Biscaye, P.E. and Eittreim, S.L. 1977. Suspended particulate loads and transports in the nepheloid layer of the abyssal Atlantic Ocean. Marine Geology, v. 23, p. 155-172.

Blumsack, S.L. 1993. A model for the growth of mudwaves in the presence of time varying currents. Deep-sea Research II, v. 40, p. 963–974.

Blumsack, S.L. and Weatherly, G.L. 1989. Observations of the nearby flow and a model for the growth of mudwaves. Deep Sea Reseach Part A. v. 36, p. 1327-1339.

Boggs, S. 1995. Principles of Sedimentology and Stratigraphy. Prentice-Hall, Inc., Englewood Cliffs, New Jersey.

Bond, C.E., Gibbs, A.D., Shipton, Z.K., and Jones, S. 2007. What do you think this is? "Conceptual uncertainty" in geoscience interpretation. GSA Today, v. 17. p. 4-10.

Bottomley, R. and York D. 1988. Age measurement of the submarine Montagnais impact crater. Geophysical Research Letters, v. 15, p. 1409-1412.

Brake, V.I. 2009. Evolution of an Oligocene Canyon System on the Eastern Scotian Margin. Unpublished M.Sc. Thesis, Dalhousie University, Halifax, Nova Scotia, Canada.

Bujak Davies Group 1988. Palynological Analysis of the Interval 440-3950 M, Bonnet P-13, Scotian Shelf. Geological Survey of Canada Open File 1858, 19 p.

Bujak Davies Group 1988a. Palynological Analysis of the Interval 1875-4045 M, Albatross B-13, Scotian Shelf. GSC Open File 1857, 13 p

Bull, S., Cartwright, J.A., and Huuse, M. 2009. A review of kinematic indicators from mass-transport complexes using 3D seismic data. Marine and Petroleum Geology 26, 1132-1151

Campbell, D.C. and Deptuck, M.E. In Press. Alternating bottom current dominated and gravity flow dominated deposition in a lower slope and rise setting- Insights from the seismic geomorphology of the western Scotian margin, Eastern Canada. SEPM special publication.

Campbell, D.C. and Mosher, D.C. 2010. Middle to Late Miocene slope failure and the generation of a regional unconformity beneath the western Scotian Slope, eastern Canada. Submarine Mass Movements and Their Consequences, Advances in Natural and Technological Hazards Research, v. 28, p. 645-655.

Campbell, D.C., Mosher, D.C., and Shimeld, J.W. 2010. Erosional Unconformities, Megaslumps and Giant Mud Waves: Insights into passive margin evolution from the continental slope off Nova Scotia. Conjugate Margins II, Lisbon 2010, Metodo Directo, v. IV, p. 37-41, ISBN: 978-989-96923-1-2, http://metododirecto.pt/CM2010

Canals, M., Lastras, G., Urgeles, R., Casamor, J.L., Mienert, J., Cattaneo, A., De Batist, M., Halfidason, H., Y. Imbo, Y., Laberg, J.S., Locat, J., Long, D., Longva, O., Masson, D.G., Sultan, N., Trinardi, F. and Bryn, P. 2004. Slope failure dynamics and impacts from seafloor and shallow sub-seafloor geophysical data: case studies from the COSTA project. Marine Geology, v. 213, p. 9-72.

Carter, L. and McCave, I.N. 1994. Development of sediment drifts approaching an active plate margin under the SW Pacific deep western boundary current. Paleoceanography, v. 9, p. 1061-1085.

Cartwright, J.A. and Dewhurst, D.N. 1998. Layer-bound compaction faults in fine-grained sediments. Geological Society of America Bulletin, v. 110, p 1242-1257.

Carvajal, C., Steel, R., and Petter, A. 2009. Sediment supply: The main driver of shelf-margin growth. Earth-Science Reviews, v. 96, p. 221–248.

Catuneanu, O., Abreu, V., Bhattacharya, J.P., Blum, M.D., Dalrymple, R.W., Eriksson, P.G., Fielding, C.R., Fisher, W.L., Galloway, W.E., Gibling, M.R., Giles, K.A., Holbrook, J.M., Jordan, R., Kendall, C.G.St.C., Macurda, B., Martinsen, O.J., Miall, A.D., Neal, J.E., Nummedal, D., Pomar, L., Posamentier, H.W., Pratt, B.R., Sarg, J.F.,

Shanley, K.W., Steel, R.J., Strasser, A., Tucker, M.E. and Winker, C. 2009. Towards the standardization of sequence stratigraphy. Earth-Science Reviews, Vol. 92, p. 1-33.

Chaplot, V., Darboux, F., Bourennane, H., Leguédois, S., Silvera, N., and Phachomphon, K. 2006. Accuracy of interpolation techniques for the derivation of digital elevation models in relation to landform types and data density. Geomorphology, v. 77, p. 126-141.

Chen, J. and Schuster, G.T. 1999. Resolution limits of migrated images. Geophysics, v. 64, p. 1046-1053.

Chevron et al. 2002. Well history report for Chevron et al. Newburn H-23. 486 p.

Cochonat, P., Ollier, G., and Michel, J.L. 1989. Evidence for slope instability and current-induced sediment transport, the RMS Titanic wreck search area, Newfoundland rise. Geo-Marine Letters, v. 9, p. 145-152.

Cossu, R., M. G. Wells, and A. K. Wåhlin 2010., Influence of the Coriolis force on the velocity structure of gravity currents in straight submarine channel systems, Journal of Geophysical Research, v. 115, C11016, doi:10.1029/2010JC006208.

Crux, J.A. and Shaw, D. 2002. Biostratigraphy of the Chevron et al. Newburn H-23 well, offshore Nova Scotia. 37 p.

Daniell, J.J., and Hughes, M. 2007. The morphology of barchan-shaped sand banks from western Torres Strait, northern Australia. Sedimentary Geology, v. 202, p. 638-652.

Davies, R., Cartwright, J., Pike, J., and Line, C. 2001. Early Oligocene initiation of North Atlantic Deep Water formation. Nature, v. 410, p. 917–920.

Davies, R.J., Ireland, M.T., amd Cartwright, J.A. 2009. Differential compaction due to the irregular topology of a diagenetic reaction boundary: a new mechanism for the formation of polygonal faults. Basin Research, v. 21, p 354-359.

Davies, R.J., Posamentier, H.W., Wood, L.J., and Cartwright, J.A. (eds.) 2007. Seismic geomorphology: applications to hydrocarbon exploration and production. Geological Society of London, Special Publications, v. 277, 274 p.

Davies, R.J., Stewart, S.A., Cartwright, J.A., Lappin, M., Johnston, R., Fraser, S.I., and Brown, A.R. 2004. 3D Seismic Technology: Are We Realising Its Full Potential? In: Davies, R.J., Stewart, S.A., Cartwright, J.A., Lappin, M. (eds.) 3D Seismic Technology; Application to the Exploration of Sedimentary Basins: Geological Society of London Memoirs v. 29, p. 1-10.

Deptuck, M.E. 2003. Post-rift geology of the Jeanne d'Arc basin, with a focus on the architecture and evolution of early Paleogene submarine fans, and insights from modern deepwater systems. PhD. Thesis, Dalhousie University. 326pp, plus appendices.

Deptuck, M.E., Steffens, G.S., Barton, M., Pirmez, C. 2003. Architecture and evolution of upper fan channel-belts on the Niger Delta slope and in the Arabian Sea. Marine and Petroleum Geology, v. 20, p. 649–676.

Dypvik, H. and Jansa, L.F. 2003. Sedimentary signatures and processes during marine bolide impacts: a review. Sedimentary Geology, v. 161, p. 309-337.

Ebinger C.A., and Tucholke, B.E. 1988. Marine Geology of the Sohm Basin, Canadian Atlantic Margin. Bulletin of American Association of Petroleum Geologists, v. 72, p. 1450-1468.

Emery, K.O., Uchupi, E., Phillips, J.D., Brown, C.O., Bunce, E.T., and Knott, S.T. 1970. Continental rise off eastern North America. AAPG Bulletin, v. 54, 44-108.

EnCana 2003a. Well history report, EnCana Torbrook C-15 volume 2. 129 p.

EnCana 2003b. Well history report, EnCana Weymouth A-45 volume 2. 189 p.

Faugères, J.C., and Stow, A.V., 2008. Contourite drifts: nature, evolution and controls. In: Rebesco, M., Camerlenghi, A. (Eds.), Contourites. Developments in Sedimentology, vol. 60. Elsevier, p. 259-288.

Faugères, J.-C., Mezerais, M.L., and Stow, D.A.V. 1993. Contourite drift types and their distribution in the North and South Atlantic Ocean basins. Sedimentary Geology, v. 82, p.189–203.

Faugères, J-C, Stow, D.A.V., Imbert, P., and Viana, A. 1999. Seismic features diagnostic of contourite drifts. Marine Geology, v. 162, p. 1-38.

Fensome, R.A., Crux, J.A., Gard, I.G., MacRae, R.A., Williams, G.L., Thomas, F.C., Fiorini, F., and Wach, G. 2008. The last 100 million years on the Scotian Margin, offshore eastern Canada: an event-stratigraphic scheme emphasizing biostratigraphic data. Atlantic Geology, v. 44, p. 93-126.

Fisher, P.F., and Tate, N.J. 2006. Causes and consequences of error in digital elevation models. Progress in Physical Geography, v. 30, p. 467-489.

Flood, R.D. 1988. A lee wave model for deep-sea mudwave activity. Deep-Sea Research, v 35, p. 973-983.

Flood, R.D. and Giosan, L. 2002. Migration history of a fine-grained abyssal sediment wave on the Bahama Outer Ridge. Marine Geology, v. 192, 259–274.

Flood, R.D., Shor, A.N., Manley, P.L. 1993. Morphology of abyssal mud waves at Project MUDWAVES sites in the Argentine Basin. Deep-Sea Res. II 40, 859-888.
Fox, P.J., Heezen, B.C., and Harian, A.M. 1968. Abyssal anti-dunes. Nature, v. 220, p.470-472.

Frey-Martínez, J., Cartwright, J., and James, D. 2006. Frontally confined versus frontally emergent submarine landslides: a 3D seismic characterization. Marine and Petroleum Geology, v. 23, p. 585-604.

Gee, M.J.R., Gawthorpe, R.L., and Friedmann J.S. 2005. Giant striations at the base of a submarine landslide. Marine Geology, v. 214, p. 287-295.

Gradstein F.M., Jansa L.F., Srivastava S.P., Williamson M.A., Bonham Carter G., and Stam B. 1990. Aspects of North Atlantic paleoceanography. In Geology of the continental margin off eastern Canada. Edited by M.J. Keen and G.L. Williams. Geological Survey of Canada, Geology of Canada no. 2, p. 351-389.

Haggerty, J., Sarti, M., von Rad, U., Ogg, J.G., and Dunnet, D.A. 1987. Late Aptian to Recent sedimentological history of the lower continental rise off New Jersey, Deep Sea Drilling Project Site 603. Initial Reports Deep Sea Drilling Project, v. 93, p. l285-l304.

Hampton, M.A., Lee, H.J., and Locat, J. 1996. Submarine landslides. Reviews of Geophysics, v. 34, p. 33– 59.

Hansen, D.M., Shimeld, J.W., Williamson, M.A., and Lykke-Andersen, H. 2004. Development of a major polygonal fault system in Upper Cretaceous chalk and Cenozoic mudrocks of the Sable Subbasin, Canadian Atlantic margin. Marine and Petroleum Geology, v. 21, p. 1205-1219.

Hansen, R.O. 1993. Interpretive gridding by anisotropic kriging. Geophysics, v. 58, p. 1491-1497.

Hardy, I.A. 1975. Lithostratigraphy of the Banquereau Formation of the Scotian Shelf. In Offshore geology of eastern Canada. Edited by W.J.M. van der Linden and J.A. Wade, Geological Survey of Canada Paper 74-30, pp. 163–174.

He, Y., Duan, T., and Gao, Z. 2008. Sediment entrainment. In: Rebesco, M. and Camerlenghi, A. eds., Contourites: Developments in Sedimentology v. 60, Elsevier, p. 101-119.

Heezen, B.C., Hollister, C.D., and Ruddiman, W.F. 1966. Shaping of the continental rise by deep geostrophic contour currents. Science, v. 152, p. 502–508.

Hernández-Molina, F.J., Llave, E., and Stow, D.A.V. 2008. Continental slope contourites. In: Rebesco, M. and Camerlenghi, A. (Eds.), Contourites. Developments in Sedimentology, v. 60, Elsevier, p. 379- 408.

Hernández-Molina, F.J., Llave, E., Stow, D.A.V., García, M., Somoza, L., Vázquez, J.T., Lobo, F., Maestro, A., Díaz del Río, V., León, R., Medialdea, T., and Gardner, J. 2006. The Contourite Depositional System of the Gulf of Cadiz: A sedimentary model related to the bottom current activity of the Mediterranean Outflow Water and the continental margin characteristics. Deep-Sea Research I, v. 53, p. 1420–1463.

Hernández-Molina, F.J., Paterlini, M., Somoza, L., Violante, R., Arecco, M.A., de Isasi, M., Rebesco, M., Uenzelmann-Neben, G., Neben, S., and Marshall, P. 2010. Giant mounded drifts in the Argentine Continental Margin: Origins, and global implications for the history of thermohaline circulation. Marine and Petroleum Geology, v. 27, p. 1508-1530, ISSN 0264-8172, DOI: 10.1016/j.marpetgeo.2010.04.003.

Hohbein, M., Cartwright, J. 2006. 3D seismic analysis of the West Shetland Drift system: Implications for Late Neogene palaeoceanography of the NE Atlantic. Marine Geology, v. 230, p. 1-20.

Hopfauf, V., and Spiess, V. 2001. A three-dimensional theory for the development and migration of deep sea sediment waves. Deep-Sea Research I, v. 48, p. 2497–2519.

Howe, J.A. 2008. Methods for Contourite Research, In: Rebesco, M., Camerlenghi, A. (Eds.), Contourites. Developments in Sedimentology, vol. 60. Elsevier, p. 19-33.

Hughes Clarke, J.E., O'leary, D.W., and Piper, D.J.W. 1992. Western Nova Scotia continental rise: relative importance of mass wasting and deep boundary-current activity. In: Poag, C.W. and De Graciansky, P.C. (Eds.), Geologic Evolution of Atlantic Continental Rises. Van Nostrand Reinhold, New York, p. 266-281.

Hurd, D.C., Pankratz, H.S., Asper, V., Fugate, J., and Morrow, H. 1981. Changes in the physical and chemical properties of biogenic silica from the central equatorial Pacific: Part III, Specific pore volume, mean pore size, and skeletal ultrastructure of acid cleaned samples. American Journal of Science, v. 281, p. 833-895.

Imperial Oil Resources Ventures Ltd. 2003. Vol. 2 well history report, IORVL et al. Balvenie B-79 offshore nova Scotia. 229 p.

Ireland, M.T., Goulty, N.R., and Davies, R.J. 2010. Influence of stratigraphic setting and simple shear on layer-bound compaction faults offshore Mauritania. Journal of Structural Geology, v. 33, p. 487-499.

Jakobsson, M., Backman, J., Rudels, B., Nycander, J., Frank, M., Mayer, L., Jokat, W., Sangiorgi, F., O'Regan, M., Brinkhuis, H., King, J., Moran, K., 2007. The early Miocene onset of a ventilated circulation regime in the Arctic Ocean. Nature, v. 447, p. 986–990.

Jansa, L. F., and Wade, J. A. 1975. Geology of the continental margin off Nova Scotia and Newfoundland: Geological Survey of Canada Paper 74-30, Offshore geology of eastern Canada, v. 2: p. 51-105.

Jansa, L.F. and Pe-Piper, G. 1987. Identification of an underwater extraterrestrial impact crater. Nature, v. 327, p. 612- 614.

Jansa, L.F., Pe-Piper, G., Robertson, P.B., and Friedenreich, O. 1989. Montagnais: A submarine impact structure on the Scotian Shelf, eastern Canada. Geological Society of America Bulletin, v. 101, p. 450-463.

Jansa, L.F., Enos, P., Tucholke, B.E., Gradstein, F.M. and Sheridan, R.E. 1979. Mesozoic-Cenozoic sedimentary formations of the North American Basin: Western North Atlantic. In Deep Drilling Results in the Atlantic Ocean: continental margins and paleoenvironment, Edited by M. Talwani, W. Hay and W.B.F. Ryan, American Geophysical Union Maurice Ewing Series, v. 3 , p. 1–57.

Keen, M.J. and Piper, D.J.W. 1990. Geophysical and historical perspective. In: Keen, M.J. and Williams, G.L. (Eds.), Geology of the Continental Margin of Eastern Canada. Geological Survey of Canada, Geology of Canada v. 2, p. 5–30.

Kenyon, N.H., Akhmetzhanov, A.M., and Twichell, D.C. 2002. Sand wave fields beneath the Loop Current, Gulf of Mexico: reworking of fan sands. Marine Geology, v.192, p. 297–307.

Knutz, P.C., and Cartwright, J.A. 2003. Seismic stratigraphy of the West Shetland Drift: Implications for Late Neogene paleocirculation in the Faeroe-Shetland Gateway. Paleoceanography, v. 18, p. 1093, doi: 10.1029/2002PA000786.

Laberg, J.S., Stoker, M.S., Dahlgren, K.I.T., de Haas, H., Haflidason, H., Hjelstuen, B.O., Nielsen, T., Shannon, P.M., Vorren, T.O., Van Weering, T.C.E., and Ceramicola, S. 2005. Cenozoic along slope processes and sedimentation on the NW European Atlantic margin. Marine and Petroleum Geology, v. 22, p.1069-1088.

Lee, Y.-D.E., and George, R.A. 2004. High-resolution geological AUV survey results across a portion of the eastern Sigsbee Escarpment. AAPG Bulletin, v. 88, p. 747-764.

Legros, F. 2002. The mobility of long-runout landslides. Engineering Geology, v. 63, p. 301-331.

Lewis, D.G. and Pandachuck, P.N. 1978. Well history report, Chevron PEX Shell Acadia A K-62 well. 87 p.

Lipman, P.W., Normark, W.R., Moore, J.G., Wilson, J.B., Gutmacher, C.E. 1988. The giant submarine Alika debris slide, Mauna Loa, Hawaii. Journal of Geophysical Research, v. 93, p. 4279– 4299.

Locker, S.D., and Laine, E.P. 1992. Paleogene-Neogene depositional history of the middle U.S. Atlantic continental rise: mixed turbidite and contourite depositional systems. Marine Geology, v. 103, p. 137-164.

Long, M.T. 2002. A sequence stratigraphic analysis of Campian to Middle Miocene sediments of the Sable Island area, Offshore Nova Scotia, Eastern Canada. Unpublished M.Sc. Dissertation [M.Sc. Thesis], Rice University, Houston, Texas, 143 p.

MacDonald, A.W.A. 2006. Cenozoic seismic stratigraphy of the central Nova Scotian continental margin: the interplay of erosion, deposition and salt tectonics, offshore Nova Scotia. Unpublished M.Sc. Dissertation [M.Sc. Thesis], St. Mary's University, Halifax, Nova Scotia, 152 p.

MacLean, B.C. and Wade, J.A. 1993. Seismic markers and stratigraphic picks in Scotian Basin wells. Atlantic Geoscience Center, Geological Survey of Canada, 276 p.

McCave I.N. and Tucholke B.E. 1986. Deep current controlled sedimentation in the western North Atlantic. In: Vogt P.R. and Tuchkolke B.E. (Eds.), The Geology of North America vol. M: The Western North Atlantic region. Geological Society of America. p. 451–468.

McCave, I.N., Chandler, R.C., Swift, S.A., and Tucholke, B.E. 2002. Contourites of the Nova Scotian continental rise and the HEBBLE area. Geological Society, London, Memoirs, v. 22, p. 21-38.

McIver, N. L. 1972. Cenozoic and Mesozoic stratigraphy of the Nova Scotia Shelf. Canadian Journal of Earth Sciences, v. 9, p. 54-70.

Miall, A.D., Balkwill, H.R. and McCracken, J. 2008. Chapter 14- The Atlantic Margin Basins of North America. In: Miall, A.D. (Ed.), Sedimentary Basins of the World. Elsevier, Volume 5- The Sedimentary Basins of the United States and Canada, p. 473-504.

Miller, K.G., Mountain, G.S., and Tucholke, B.E. 1985. Oligocene glacio–eustasy and erosion on the margins of the North Atlantic. Geology, v. 13, p. 10-13.

Miller, K.G., Wright, J.D., Katz, M.E., Wade, B.S., Browning, J.V., Cramer, B.S., and Rosenthal, Y. 2009. Climate threshold at the Eocene-Oligocene transition: Antarctic ice sheet influence on ocean circulation, in Koeberl, C., Montanari, A., (eds.) The Late Eocene Earth—Hothouse, Icehouse, and Impacts: Geological Society of America Special Paper 452, p. 169–178, doi: 10.1130/2009.2452(11).

Mosher, D.C. 2011. A margin-wide BSR gas hydrate assessment: Canada's Atlantic margin. Marine and Petroleum Geology, v. 28, p. 1540-1553.

Mosher D.C. and Campbell D.C. 2011. The Barrington submarine landslide, western Scotian Slope. In: Shipp, C., Weimer, P, and Posamentier, H. (Eds.), Mass-Transport Deposits in Deepwater Settings. SEPM Special Publication No. 96, p. 151-159.

Mosher, D.C., Bigg, S. and LaPierre, A. 2006. 3D seismic versus multibeam sonar seafloor surface renderings for geohazard assessment: Case examples from the central Scotian Slope. The Leading Edge, v. 25, p. 1484-1494.

Mosher, D.C., Louden, K., LeBlanc, C., Shimeld, J.W., and Osadetz, K.G. 2005. Gas Hydrates Offshore Eastern Canada: Fuel for the Future? Offshore Technology Conference paper 17588. In: Offshore Technology Conference. Houston, Tx. 2-5 May 2005.

Mosher, D.C., Piper, D.J.W., Campbell, D.C., and Jenner, K.A. 2004. Near-surface geology and sediment-failure geohazards of the central Scotian Slope. American Association of Petroleum Geologists Bulletin, v. 88, p. 703-723.

Mosher, D.C., Shipp, C., Moscardelli, L., Chaytor, J., Baxter, C., Lee, H., Urgeles, R. (eds.) 2010. Submarine Mass Movements and Their Consequences. Springer, Advances in Natural and Technological Hazards Research, v. 28, 786 p.

Mountain, G.S. 1987. Cenozoic Margin Construction and Destruction Offshore New Jersey. in: C.Ross and D. Haman (eds.), Cushman Foundation for Foraminiferal Research, Special Publication. 24, p. 57-83.

Mountain, G.S. and Tucholke, B.E. 1985. Mesozoic and Cenozoic Geology of the U.S. Atlantic Continental Slope and Rise. in: Geologic Evolution of the U.S. Atlantic Margin. C.W. Poag (ed.). Van Nostrand Reinhold. p. 293-341.

Mountain, G.S., and Miller, K.G. 1992. Seismic and geologic evidence for early Paleogene deepwater circulation in the western North Atlantic. Paleoceanography, v. 7, p. 23-43.

Mountain, G.S., Burger, R.L., Delius, H., Fulthorpe, C.S., Austin, J.A., Goldberg, D.S., Steckler, M.S., et al. 2007. The long-term stratigraphic record on continental margins. In: Nittrouer, C.A., Austin, J.A., Field, M.E., Kravitz, J.H., Syvitski, J.P.M., and Wiberg, P.L. (Eds.), Continental margin sedimentation: from sediment transport to sequence stratigraphy. International Association of Sedimentologists Special Publication. v. 37, p. 381–458.

Mulder, T., Faugères, J-C, and Gonthier, E. 2008. Mixed turbidite-contourite systems. In: Rebesco, M. and Camerlenghi, A. (eds.) Contourites: Developments in Sedimentology v. 60, Elsevier, p. 435-456.

Neagu, R.C., Cartwright, J., Davies, R., and Jensen, L. 2010. Fossilisation of a silica diagenesis reaction front on the mid-Norwegian margin, Marine and Petroleum Geology, v. 27, p. 2141-2155.

Nielsen, T., Knutz, P.C., and Kuijpers, A. 2008. Seismic Expression of Contourite Depositional Systems. In: M. Rebesco and A. Camerlenghi (eds.). Contourites. Developments in Sedimentology, v. 60, Elsevier, p. 301-321.

Nittrouer, C.A., Austin, J.A., Field, M.E., Kravitz, J.H., Syvitski, J.P.M., and Wiberg, P.L. 2007. Writing a Rosetta stone: insights into continental-margin sedimentary processes and strata., In: Nittrouer, C.A., Austin, J.A., Field, M.E., Kravitz, J.H., Syvitski, J.P.M., and Wiberg, P.L. (Eds.), Continental margin sedimentation: from sediment transport to sequence stratigraphy. International Association of Sedimentologists Special Publication. v. 37, p. 1-48.

Nowell, A.R.M., and Hollister, C.D. (Eds.). 1985. Deep Ocean Sediment Transport – Preliminary Results of the High Energy Benthic Boundary Layer Experiment, Marine Geology, v. 66, 420 pp.

Parsons, M. G., 1975, The geology of the Laurentian Fan and the Scotia Rise, in C. J. Yorath, E. R. Parker, and D. J. Glass, eds., Canada's continental margins and offshore petroleum exploration: Canadian Society of Petroleum Geologists Memoir 4, p. 155-167.

Payton, C.E. (Ed.). 1977. Seismic stratigraphy- Applications to hydrocarbon exploration. AAPG Memoir 26, American Association of Petroleum Geologists, 502 p.

Petro-Canada Inc. 1985. Well History Report Petro-Canada et al. Shelburne G-29: 116 p.

Pickart, R. S., and Smethie, W.M. 1998. Temporal evolution of the deep western boundary current where it enters the sub-tropical domain. Deep-Sea Research, v. 45, p. 1053–1083.

Pickart, R.S. 1992. Water mass components of the North Atlantic Deep Western Boundary Current. Deep-Sea Research, v. 39, p. 1553-1572.

Pickart, R.S., McKee, T.K., Torres, D.J., and Harrington, S.A. 1999. On the mean structure and interannual variability of the slopewater system south of Newfoundland. Journal of Physical Oceanography, v. 29, p. 2541–2558.

Piper D.J.W. 1988. Glaciomarine sediments on the continental slope off eastern Canada. Geoscience Canada, v. 15, p. 23-28.

Piper D.J.W., Normark W.R., and Sparkes 1987. Late Cenozoic stratigraphy of the central Scotian Slope, Eastern Canada. Canadian Bulletin of Petroleum Geology, v. 35, p. 1-11.

Piper, D.J.W. 2005. Late Cenozoic evolution of the continental margin of eastern Canada. Norwegian Journal of Geology, v. 85, p. 231-244.

Piper, D.J.W. and Normark, W.R. 2009. Processes that initiate turbidity currents and their influence on turbidites: A marine geology perspective: Journal of Sedimentary Research, v. 79, p. 347-362.

Piper D.J.W, Cochonat P., and Morrison M.L. 1999. The sequence of events around the epicentre of the 1929 Grand Banks earthquake: initiation of debris flows and turbidity currents inferred from sidescan sonar. Sedimentology. V. 46, p. 79–97.

Piper, D.J.W., Normark, W.R., and Sparkes, R. 1987. Late Cenozoic Stratigraphy of the central Scotian Slope, Eastern Canada. Canadian Bulletin of Petroleum Geology, v. 35, p. 1-11.

Piper, D.J.W., Pirmez, C., Manley, P.L., Long, D., Flood, R.D., Normark, W.R. and Showers, W. 1997. Mass Transport Deposits of the Amazon Fan. In: Proc. ODP Sci. Results, 155. R.D. Flood, D.J.W. Piper, A. Klaus and L.C. Peterson (eds.). Ocean Drilling Program, College Station, TX. p. 109-146.

Poag, C.W. and Mountain, G.S. 1987. Late Cretaceous and Cenozoic evolution of the New Jersey continental slope and upper rise: An integration of borehole data with seismic reflection profiles. Initial Reports, Deep-Sea Drilling Project Leg 95, p. 673-724.

Poag, C.W. and Ward, L.W. 1993. Allostratigraphy of the U.S. Middle Atlantic continental margin- Characteristics, distribution, and depositional history of principal unconformity bounded Upper Cretaceous and Cenozoic sedimentary units. U.S. Geological Survey Professional Paper 1542, 81 p.

Posamentier, H.W., and Kolla, V. 2003. Seismic geomorphology and stratigraphy of depositional elements in deep-water settings. Journal of Sedimentary Research, v. 73, p. 367-388.

Posamentier, H.W., Davies, R.J., Cartwright, J.A., and Wood, L.J. 2007. Seismic geomorphology; an overview. Seismic geomorphology; applications to hydrocarbon exploration and production, Geological Society Special Publications 277, p. 1-14.

Potter, P.E., and Szatmari, P. 2009. Global Miocene tectonics and the modern world. Earth-Science Reviews, v. 96, p. 279-295

Prather, B.E. 2003. Controls on reservoir distribution, architecture and stratigraphic trapping in slope settings. Marine and Petroleum Geology, v. 20, p. 527–543.

Ramsayer, G.R. 1979. Seismic stratigraphy, a fundamental exploration tool. Offshore Technology Conference Paper OTC 3568, p. 1859-1862.

Rebesco, M. 2005. Contourites. In: Selley, R.C., Cocks, L.R.M., and Plimer, I.R. (eds.) Encyclopedia of Geology: Elsevier, Oxford, v. 4., p. 513-527.

Rebesco, M., and Stow, D.A.V. 2001. Seismic Expression of Contourites and Related Deposits: A Preface. Marine Geophysical Researches, v. 22, p. 303-308.

Robertson Research. 2004. Nova Scotia Shelf: Biostratigraphic and Sequence Stratigraphic Correlation of the Early Cretaceous Strata in Seven Wells - Report No.6620/Ib. Canada-Nova Scotia Offshore Petroleum Board File SR(E) 2004-1, 47 p.

Rona, P.A. 1969. Linear "lower continental rise hills" off Cape Hatteras. Journal of Sedimentary Petrology, v. 39, p. 1132-1141.

Ross, W.C., Halliwell, B.A., May, J.A., Watts, D.E., and Syvitski, J.P.M. 1994. Slope readjustment: a new model for the development of submarine fans and aprons. Geology, v. 22, p. 511–514.

Sangree, J.B. and Widmier, J.M. 1979. Interpretation of depositional facies from seismic data. Geophysics, v. 44, p. 131-160.

Schlee, J.S., Poag, C.W. and Hinz, K. 1985. Seismic stratigraphy of the continental slope and rise seaward of Georges Bank. in C.W. Poag, ed., Geologic evolution of the United States Atlantic margin: New York, Van Nostrand, p. 265-292.

Schmitz , W.J. and McCartney, M.S. 1993. On the North Atlantic Circulation. Reviews of Geophysics, v. 31, p. 21-39.

Shannon, P. M, Stoker, M. S., Praeg, D., van Weeringc, T.C.E., de Haasc, H., Nielsend, T., Dahlgrene, K.I.T., and Hjelstuenf, B.O. 2005. Sequence stratigraphic analysis in deep-water, underfilled NW European passive margin basins. Marine and Petroleum Geology, v. 22, p. 1185–1200.

Shaw, J., and Courtney, R.C. 2004. Digital elevation model of Atlantic Canada: Geological Survey of Canada Open File 4634.

Shell Canada Reources Limited. 1983. Well history report Shell et al. Shubenacadie H-100. 115 p.

Sheriff, R.F., 1985, Aspects of Seismic Resolution. In: Berg, O.R. and Woolverton, D.G. (Eds.), Seismic Stratigraphy II - An Integrated Approach. AAPG Memoir 39, American Association of Petroleum Geologists, p. 1-10.

Shimeld, J. 2004. A comparison of salt tectonic subprovinces beneath the Scotian Slope and Laurentian Fan. In: Post, P.J., Olson, D.L., Lyons, K.T., Palmes, S.L., Harrison, P.F., and Rosen, N. (eds.) Salt–sediment Interactions and Hydrocarbon Prospectivity:

Concepts, Applications, and Case Studies for the 21st Century. 24th Annual Gulf Coast Section of the Society of Economic Paleontologists and Mineralogists Foundation Bob F. Perkins Research Conference, Houston, Texas, Dec. 5-8, 2004, p. 502-532.

Shimeld, J.W., Warren, S.N., Mosher, D.C., and MacRae, R.A. 2003. Tertiary-aged megaslumps under the Scotian Slope, south of the Lahave Platform, offshore Nova Scotia (abs.). Geological Society of America, Northeastern Section Conference, Halifax, April, 2003, Program with Abstracts v. 35, no. 3.

Skene, K.I., and Piper, D.J.W. 2006. Late Cenozoic evolution of Laurentian Fan: Development of a glacially-fed submarine fan. Marine Geology, v. 227, p. 67-92.

Smethie, W.M., Fine, R.A., Putzuka, A., and Jones, P. 2000. Tracing the flow of North Atlantic Deep Water using chlorofluorocarbons. Journal of Geophysical Research, v. 105, p. 14297-14323.

Smith, P.C., and Petrie, B.D. 1982. Low-frequency circulation at the edge of the Scotian Shelf. Journal of Physical Oceanography, v. 12, p. 28-46.

Smith, R.S. and O'Connell, M.D. 2005. Interpolation and gridding of aliased geophysical data using constrained anisotropic diffusion to enhance trends. Geophysics, v. 70, V121-V127.

Smolarkiewicz, P.K., and Rotunno, R. 1989. Low Froude Number Flow Past Three-Dimensional Obstacles. Part I: Baroclinically Generated Lee Vortices. Journal of Atmospheric Sciences, v. 46, p. 1154-1164.

Steeves, G.B. 1984. Well history report Petro-Canada et al. Bonnet P-23. 198 p.

Steeves, G.B. 1985a. Well history report Petro-Canada et al. Albatross B-13. 143 p.

Steeves, G.B. 1985b. Well history report Petro-Canada et al. Shelburne G-29. 116 p.

Steffens, G.S., Biegert, E.K., Sumner, S., and Bird, D. 2003. Quantitative bathymetric analyses of selected deepwater siliciclastic margins: receiving basin configurations for deepwater fan systems. Marine and Petroleum Geology, v. 20, p. 547-561.

Stoker, M.S., Praeg, D., Hjelstuen, B.O., Laberg, J.S., Nielsen, T., and Shannon, P.M. 2005. Neogene stratigraphy and the sedimentary and oceanographic development of the NW European Atlantic margin. Marine and Petroleum Geology, v. 22. p. 977-1005.

Stow D.A.V. and Mayall M. 2000. Deep-Water Sedimentary Systems: New Models for the 21st Century. Marine and Petroleum Geology, v. 17, p. 125-135.

Stow, D.A.V., Faugères, J.C., Howe, J.A., Pudsey, C.J., Viana, A., 2002. Contourites, bottom currents and deep-sea sediment drifts: current state-of-the-art. In: Stow, D.A.V.,

Pudsey, C.J., Howe, J.A., Faugères, J.C., Viana, A.R. (Eds.), Deep-Water Contourite Systems: Modern Drifts and Ancient Series, Seismic and Sedimentary Characteristics. Geological Society of London, Memoirs 22, 7-20.

Stow, D.A.V., Hernández-Molina, F.J., Llave, E., Sayago-Gil, M., Díaz del Río, V., and Branson, A. 2009. Bedform-velocity matrix: The estimation of bottom current velocity from bedform observations. Geology, v. 37, p. 327-330.

Swift, S.A. 1985. Cenozoic geology of the continental slope and rise off western Nova Scotia. PhD Thesis, Massachusetts Institute of Technology, Cambridge, Massachusetts, 188 p.

Swift, S.A., 1987, Late Cretaceous-Cenozoic development of outer continental margin, southwestern Nova Scotia: Bulletin of American Association of Petroleum Geologists, v. 71, p. 678-701.

Swift, S.A., Ebinger, C.J., and Tucholke, B.E. 1986, Seismic stratigraphic correlations across the New England Seamounts, western North Atlantic Ocean. Geology, v. 14, p. 346-349.

Thomas, F.C. 2001. Cenozoic micropaleontology of three wells, Scotian Shelf and Slope. Geological Survey of Canada Open File 4014, 42 p.

Thomas, F.C. 2005. Oligocene benthic foraminifera from the Paleogene Wenonah Canyon, Scotian Shelf- normal versus canyon assemblages. Atlantic Geology, v. 41, p 1-16.

Todd, B.J. 2005. Morphology and composition of submarine barchan dunes on the Scotian Shelf, Canadian Atlantic margin. Geomorphology, v. 67, p. 487-500.

Tucholke, B.E., 1979, Relationships between acoustic stratigraphy and lithostratigraphy in the western North Atlantic basin, in Tucholke, B.E., Vogt, P.R., and others, Initial reports of the Deep Sea Drilling Project, v. 43, p. 827-846.

Tucholke, B. E. and Mountain, G.S. 1979. Seismic stratigraphy, lithostratigraphy and paleosedimentation patterns in the North American Basin. In: Talwani M., Hay, W., and Ryan, W.B.F. (Eds.), Deep Drilling Results in the Atlantic Ocean: continental margins and paleoenvironment. American Geophysical Union Maurice Ewing Series, v. 3 ,p. 58-86.

Tucholke, B. E. and Mountain, G.S. 1986. Tertiary paleoceanography of the western North Atlantic Ocean. In: Vogt, P.R. and Tucholke, B.E (Eds.), The Geology of North America, Vol. M, The Western North Atlantic Region, Geological Society of America, Boulder, CO, p. 631–650.

Twichell, D.C., Chaytor, J.D., ten Brink, U.S., and Buczkowski, B. 2009. Morphology of late Quaternary submarine landslides along the U.S. Atlantic continental margin. Marine Geology, v. 264, p. 4-15.

Uchupi, E., and Austin, J.A. 1979. The geological history of the passive margin off New England and the Canadian Maritime provinces. Tectonophysics, v. 59, p. 53-69.

Uchupi, E. and Swift, S. A. 1991. Plio-Pleistocene slope construction off western Nova Scotia, Canada. Cuadernos de Geologia Iberica, Special Issue no. 15, p.15-35.

Uenzelmann-Neben, G. 2006. Depositional patterns at Drift 7, Antarctic Peninsula: Along-slope versus down-slope sediment transport as indicators for oceanic currents and climatic conditions. Marine Geology, v. 233, p. 49-62.

Vail, P. R., R. G. Todd, and J. B. Sangree 1977. Seismic Stratigraphy and Global Changes of Sea Level: Part 5. Chronostratigraphic Significance of Seismic Reflections. In: Payton, C.E. (Ed.), Seismic stratigraphy- Applications to hydrocarbon exploration. AAPG Memoir 26, American Association of Petroleum Geologists, p. 99 – 116.

Vecsie. A. and Hoppie, B.W. 1996. Sequence stratigraphy and diagenesis of the Miocene-Oligocene below the New Jersey continental slope: Implications of physical properties and mineralogical variations. Proceedings of the Ocean Drilling Program, Scientific Results, v. 150, p. 361- 376.

Viana, A.R. 2008. Economic relevance of contourites. In: Rebesco, M. and Camerlenghi, A. (eds.) Contourites: Developments in Sedimentology v. 60, Elsevier, p. 493-510.

Viana, A.R., Almeida, Jr., W., Nunes, M.C.V., Bulhöes, E.M. 2007. The economic importance of contourites. In: Viana, A.R., Rebesco, M., (eds.) Economic and Palaeoceanographic Significance of Contourite Deposits: Geological Society of London Special Publication v. 276, p. 1–23.

Vorren, T.O. and Laberg, J.S. 1997. Trough mouth fans- Palaeoclimate and ice-sheet monitors. Quaternary Science Reviews, v. 16, p. 865-881.

Wade, J. A., MacLean, B. C., and Williams, G. L. 1995. Mesozoic and Cenozoic stratigraphy, eastern Scotian Shelf: New interpretations. Canadian Journal of Earth Sciences, v. 32, p. 1462-1473.

Wade, J.A. and MacLean, B.C. 1990. The Geology of the Southeastern Margin of Canada, Part 2: Aspects of the Geology of the Scotian Basin from Recent Seismic and Well Data. In Geology of the continental margin off eastern Canada. Edited by M.J. Keen and G.L. Williams. Geological Survey of Canada, Geology of Canada no. 2, p.190-238.

Wade, J.A., MacLean, B.C., and Williams, G.L. 1995. Mesozoic and Cenozoic stratigraphy, eastern Scotian Shelf: New interpretations. Canadian Journal of Earth Sciences, v. 32, p. 1462-1473.

Weatherly, G.L., and Kelley, E.A. 1985. Storms and flow reversals at the HEBBLE site. Marine Geology, v. 66, p. 205-218.

White, R. and Simm, R. 2003. Tutorial: Good practice in well ties. First Break, v.21, p. 75-83.

Wise, S.W. and van Hinte, J.E. 1987. Mesozoic-Cenozoic depositional environments revealed by Deep Sea Drilling Project Leg 93 Drilling on the continental rise off the eastern United States: cruise summary, In: Initial Reports of the Deep Sea Drilling Project, v. 93, p. 1367-1423.

Wold, C.N. 1994. Cenozoic sediment accumulation on drifts in the northern North Atlantic. Paleoceanography, v. 9, p. 917–941.

Worthington, L. V., 1976. On the North Atlantic Circulation. The Johns Hopkins Oceanographic Studies, No. 6, 110 pp.

Wright, J.D., Miller, K.G. 1996. Control of North Atlantic Deep Water circulation by the Greenland- Scotland Ridge. Paleoceanography, v. 11, p. 157–170.

Wynn, R.B. and Masson, D.G. 2008. Sediment waves and bedforms. In: M. Rebesco and A. Camerlenghi (eds.). Contourites. Developments in Sedimentology, v. 60, Elsevier, p 289-300.

Wynn, R.B., and Stow, D.A.V. 2002. Classification and characterization of deep-water sediment waves. Marine Geology, v. 192, p. 7-22.

Wynn, R.B., Masson, D.G., and Bett, B.J. 2002. Hydrodynamic significance of variable ripple morphology across deep-water barchan dunes in the Faroe–Shetland Channel. Marine Geology, v. 192, p. 309– 319.

Yilmaz, O. 1987. Seismic Data Processing, v. 2. Society of Exploration Geophysicists, Tulsa Oklahoma.

Zhu, M., Graham, S., Pang, X., and McHargue, T. 2010. Characteristics of migrating submarine canyons from the middle Miocene to present: Implications for paleoceanographic circulation, northern South China Sea. Marine and Petroleum Geology, v. 27, p. 307-319

Appendices

APPENDIX I- DATA USED FOR CONVERTING TWO-WAY TRAVEL TIME TO DEPTH

Two-way travel time and depth data for the velocity model used in Chapters 2 and 4 (Figure 2.3)

Well	Depth Below Seabed (m)	Two-way Travel Time Below Seabed (ms)	Well	Depth Below Seabed (m)	Two-way Travel Time Below Seabed (ms)
Shubenacadie H-100	30	36	Albatross B-13	255	315.99
Shubenacadie H-100	121	160	Albatross B-13	355	423.99
Shubenacadie H-100	221	276	Albatross B-13	455	528.09
Shubenacadie H-100	321	388	Albatross B-13	480.2	553.58
Shubenacadie H-100	421	498	Albatross B-13	605	679.79
Shubenacadie H-100	521	608	Albatross B-13	755	834.29
Shubenacadie H-100	621	714			
Shubenacadie H-100	716	814	Bonnett P-23	249.9	296.52
Shubenacadie H-100	825	928	Bonnett P-23	259.2	306.62
Shubenacadie H-100	919	1026	Bonnett P-23	301.9	353
Shubenacadie H-100	1038	1146	Bonnett P-23	584.7	640.72
Shubenacadie H-100	1121	1232	Bonnett P-23	859.7	894.68
Shubenacadie H-100	1196	1294	Bonnett P-23	1114.6	1108.48
Shubenacadie H-100	1246	1344	Bonnett P-23	1314.5	1282.58
Shubenacadie H-100	1271	1374	Bonnett P-23	1516.5	1452.12
Shubenacadie H-100	1321	1428			
Shubenacadie H-100	1396	1496	Torbrook C-15	808.302	1055.87
Shubenacadie H-100	1446	1542	Torbrook C-15	839.9	1095.95
Shubenacadie H-100	1496	1584	Torbrook C-15	855.1	1111.36
Shubenacadie H-100	1546	1646	Torbrook C-15	870.2	1125.78
Shubenacadie H-100	1596	1688	Torbrook C-15	885.3	1140.6
Shubenacadie H-100	1646	1736	Torbrook C-15	900.4	1156.22
Shubenacadie H-100	1696	1782	Torbrook C-15	915.5	1170.83
Shubenacadie H-100	1746	1832	Torbrook C-15	930.6	1186.05
Shubenacadie H-100	1796	1874	Torbrook C-15	945.8	1201.07
Shubenacadie H-100	1846	1922	Torbrook C-15	960.9	1215.08
Shubenacadie H-100	1896	1958	Torbrook C-15	976	1230.3
Shubenacadie H-100	1946	2012	Torbrook C-15	991.1	1244.71
Shubenacadie H-100	2021	2078	Torbrook C-15	1006.2	1259.33
Shubenacadie H-100	2096	2146	Torbrook C-15	1021.3	1274.75
Shubenacadie H-100	2146	2188	Torbrook C-15	1036.5	1288.96
Shubenacadie H-100	2196	2230	Torbrook C-15	1051.6	1303.58
Shubenacadie H-100	2246	2268	Torbrook C-15	1066.7	1320
Shubenacadie H-100	2321	2322	Torbrook C-15	1071	1324.3
Shubenacadie H-100	2371	2362	Torbrook C-15	1081.9	1335.03
Shubenacadie H-100	2421	2406	Torbrook C-15	1097	1348.4
Shubenacadie H-100	2471	2444	Torbrook C-15	1112.1	1362.37
Shubenacadie H-100	2521	2482	Torbrook C-15	1127.2	1376.33
Shubenacadie H-100	2621	2560	Torbrook C-15	1142.3	1388.33
Shubenacadie H-100	2718	2636	Torbrook C-15	1157.4	1402.1
			Torbrook C-15	1172.5	1416.07
Shelburne G-29	287.5	340.62	Torbrook C-15	1187.6	1429.84
Shelburne G-29	412.2	468.16	Torbrook C-15	1202.7	1442.43
Shelburne G-29	487.5	545.18	Torbrook C-15	1217.8	1456.2
Shelburne G-29	702.5	773.92	Torbrook C-15	1232.9	1469.77
Shelburne G-29	887.5	963.22	Torbrook C-15	1248.1	1483.15

Well	Depth Below Seabed (m)	Two-way Travel Time Below Seabed (ms)	Well	Depth Below Seabed (m)	Two-way Travel Time Below Seabed (ms)
Shelburne G-29	1087.5	1156.82	Torbrook C-15	1263.3	1498.49
Shelburne G-29	1302.5	1358.76	Torbrook C-15	1278.4	1511.67
Shelburne G-29	1397.5	1444.46	Torbrook C-15	1293.5	1524.85
Shelburne G-29	1482.5	1516.98	Torbrook C-15	1308.6	1537.64
Shelburne G-29	1532.5	1562.2	Torbrook C-15	1323.8	1551.21
Shelburne G-29	1662.5	1677.28	Torbrook C-15	1338.9	1563.6
Shelburne G-29	1722.5	1725.36	Torbrook C-15	1354	1575.6
Shelburne G-29	1822.5	1810.1	Torbrook C-15	1369.1	1587
Shelburne G-29	1887.5	1858.24	Torbrook C-15	1384.3	1599.8
Shelburne G-29	2037.5	1984.18	Torbrook C-15	1399.4	1612.6
Shelburne G-29	2187.5	2097.54	Torbrook C-15	1414.5	1625.2
Shelburne G-29	2287.5	2175.14	Torbrook C-15	1429.6	1637.6
Shelburne G-29	2382.5	2236.98	Torbrook C-15	1444.8	1649.6
Shelburne G-29	2491.5	2315.06	Torbrook C-15	1459.9	1662.6
Shelburne G-29	2627.5	2398.02	Torbrook C-15	1475	1675.2
Shelburne G-29	2631	2400.15	Torbrook C-15	1490.1	1687.6
			Torbrook C-15	1505.3	1699.8
Acadia K-62	239	309.6	Torbrook C-15	1520.4	1711.6
Acadia K-62	275	348	Torbrook C-15	1535.5	1723.4
Acadia K-62	428	501.6	Torbrook C-15	1550.6	1735.6
Acadia K-62	580	691.6	Torbrook C-15	1565.6	1747.2
Acadia K-62	732	845.8	Torbrook C-15	1580.7	1758.6
Acadia K-62	842	957.8	Torbrook C-15	1595.8	1770.6
Acadia K-62	1037	1151.8	Torbrook C-15	1610.9	1782.8
Acadia K-62	1190	1299.8	Torbrook C-15	1626.3	1795.8
Acadia K-62	1342	1437.8	Torbrook C-15	1641.4	1808.2
Acadia K-62	1464	1568	Torbrook C-15	1656.5	1820
Acadia K-62	1649	1703.8	Torbrook C-15	1671.7	1831.2
Acadia K-62	1839	1840	Torbrook C-15	1686.7	1847.2
			Torbrook C-15	1701.8	1858.2
			Torbrook C-15	1716.9	1871.4
			Torbrook C-15	1732	1881.6
			Torbrook C-15	1762.627	1902.29

APPENDIX II- WELL LOG PLOTS AND SYNTHETIC SEISMOGRAMS FOR EXPLORATION WELLS EXAMINED IN THIS STUDY

Appendix II shows detailed plots of well logs (sonic, density, and gamma ray), sythentic seismograms generated for each well for correlation to seismic reflection profiles, and intersection depths for named seismic stratigraphic horizons in chapters 2 and 4. On the following page, an annotated version of the synthetic seismogram plot for Shubenacaide H-100 is shown, with items within the plot described. Following this example, each well in the thesis is presented in alphabetical order. The vertical scale on the left of each plot shows depth (measured depth) in metres, as well as two-way travel time in seconds. The plots are scaled for equal depth with 100 m graduations. The synthetic seismograms were generated by convolving the reflection coefficient series calculated from the well logs with a source wavelet derived from the seismic reflection data closest to the well over the depth range that was of interest (as described by White and Simm (2003)). The synthetic seismograms show positive and negative polarity plots that are compared to a plot of the average seismic trace closest to the well. The average seismic trace was calculated from the closest seismic profile to each well within a set radius and typically represents an average of 10 to 15 traces. See chapter 2 (particularly Table 2.1) for detailed lithological and age information for the seismic stratigraphy.

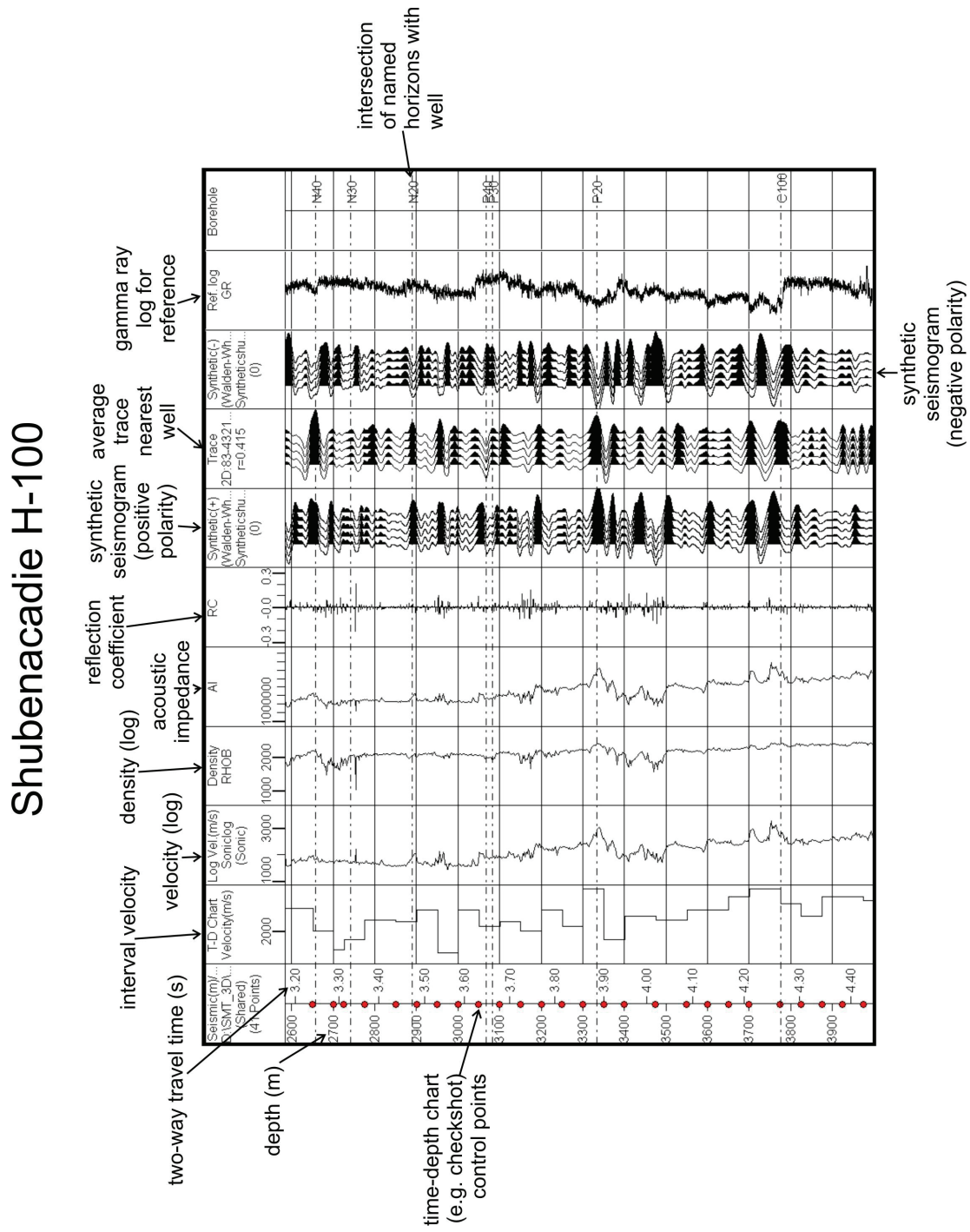
Shubenacadie H-100
interval velocity
velocity (log)
density (log)
acoustic impedance
reflection coefficient
synthetic seismogram (positive polarity)
average trace nearest well
gamma ray log for reference
intersection of named horizons with well
synthetic seismogram (negative polarity)
two-way travel time (s)
depth (m)
time-depth chart (e.g. checkshot) control points
Seismic(m)/...
T-D Chart Velocity(m/s)
Log Vel.(m/s) Sonicilog (Sonic)
Density RHOB
AI
RC
Synthetic(+) (Walden-Wh... Syntheticshu... (0)
Trace 2D:83-4321... r=0.415
Synthetic(-) (Walden-Wh... Syntheticshu... (0)
Ref_log GR
Borehole
N40
N30
N20
P40
P30
P20
E100

Acadia K-62

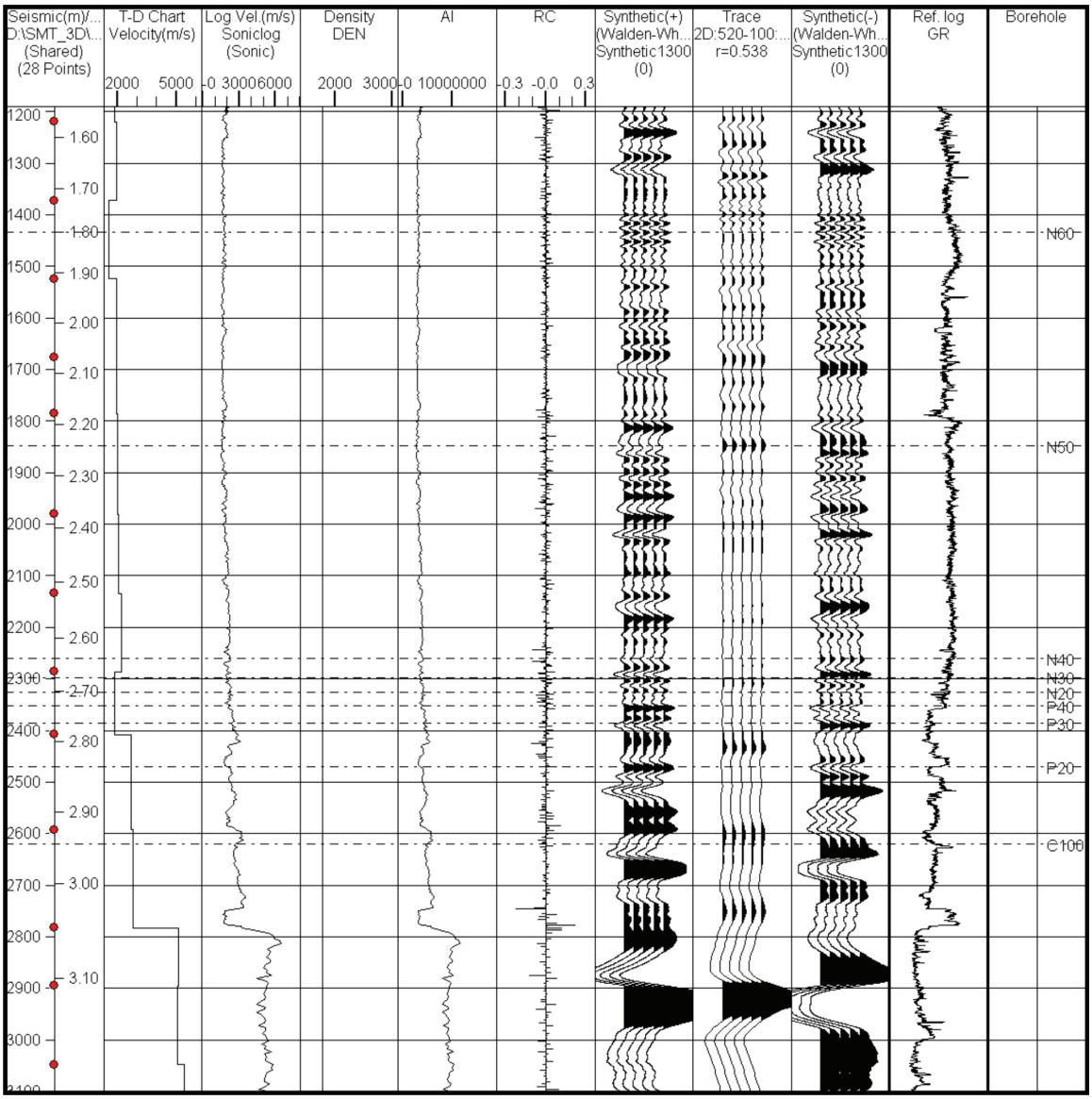

Location	42.862294 -61.916636
Drilling reference	Rotary table
Reference elevation (for measured depths)	12.8 m
Water depth	866.3 m
Total depth	5287.4 m

Albatross B-13

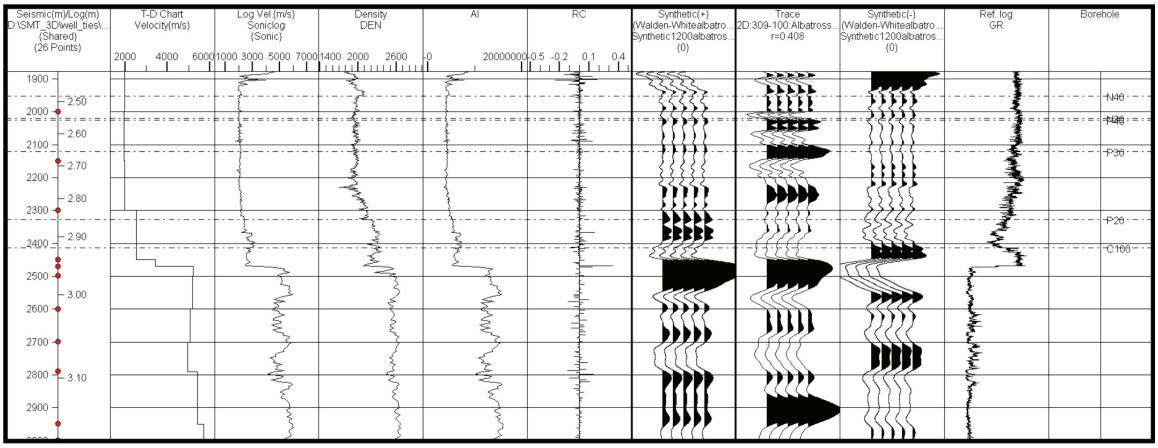

Location	42.703036 -63.035917
Drilling reference	Rotary table
Reference elevation (for measured depths)	24 m
Water depth	1341 m
Total depth	4047.5 m

Annapolis G-24

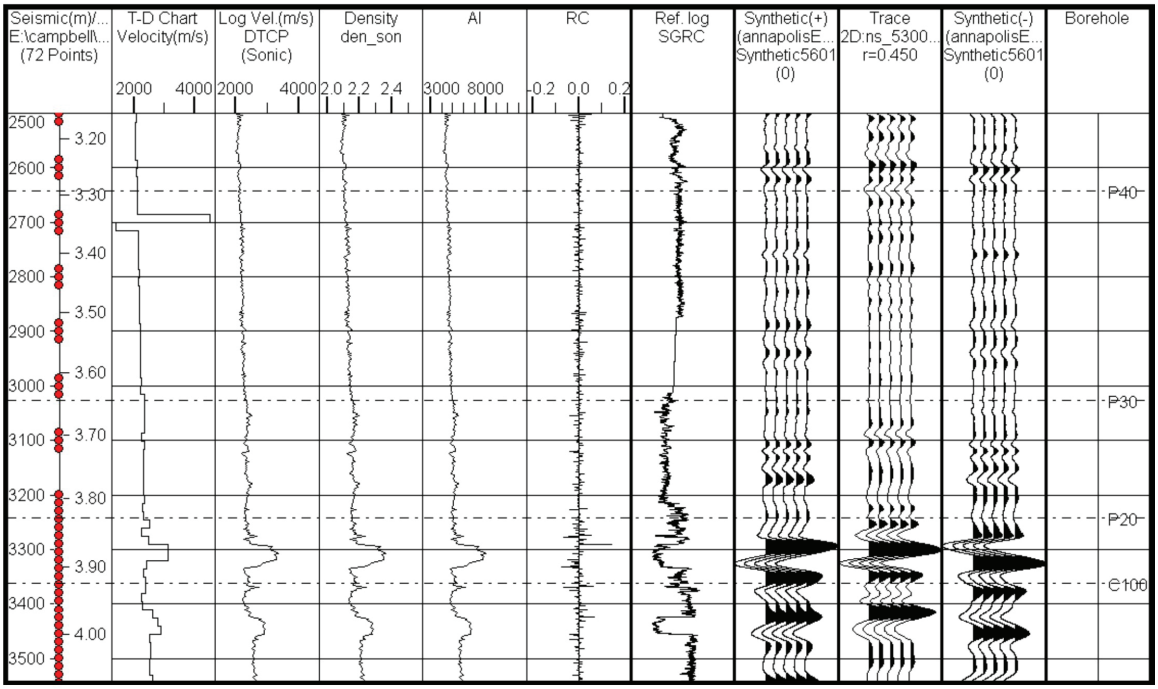

Location	43.389781 -59.807345
Drilling reference	Rotary table
Reference elevation (for measured depths)	36 m
Water depth	1678 m
Total depth	6182 m

Balvenie B-79

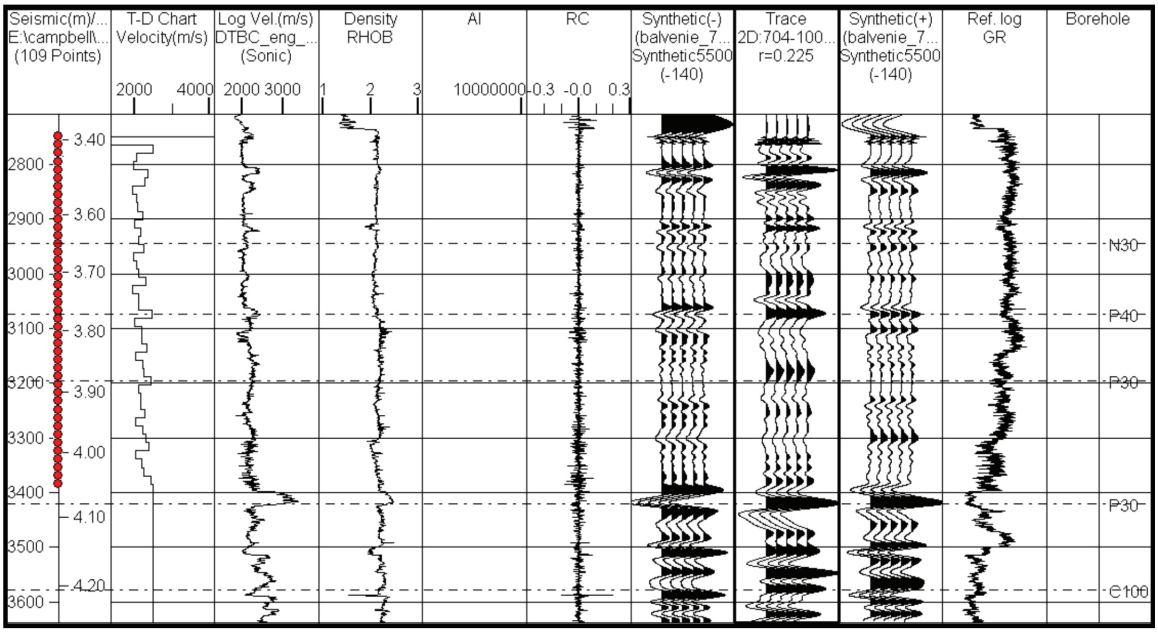

Location	43.133769 -60.181682
Drilling reference	Rotary table
Reference elevation (for measured depths)	25 m
Water depth	1803 m
Total depth	4750 m

Bonnet P-23

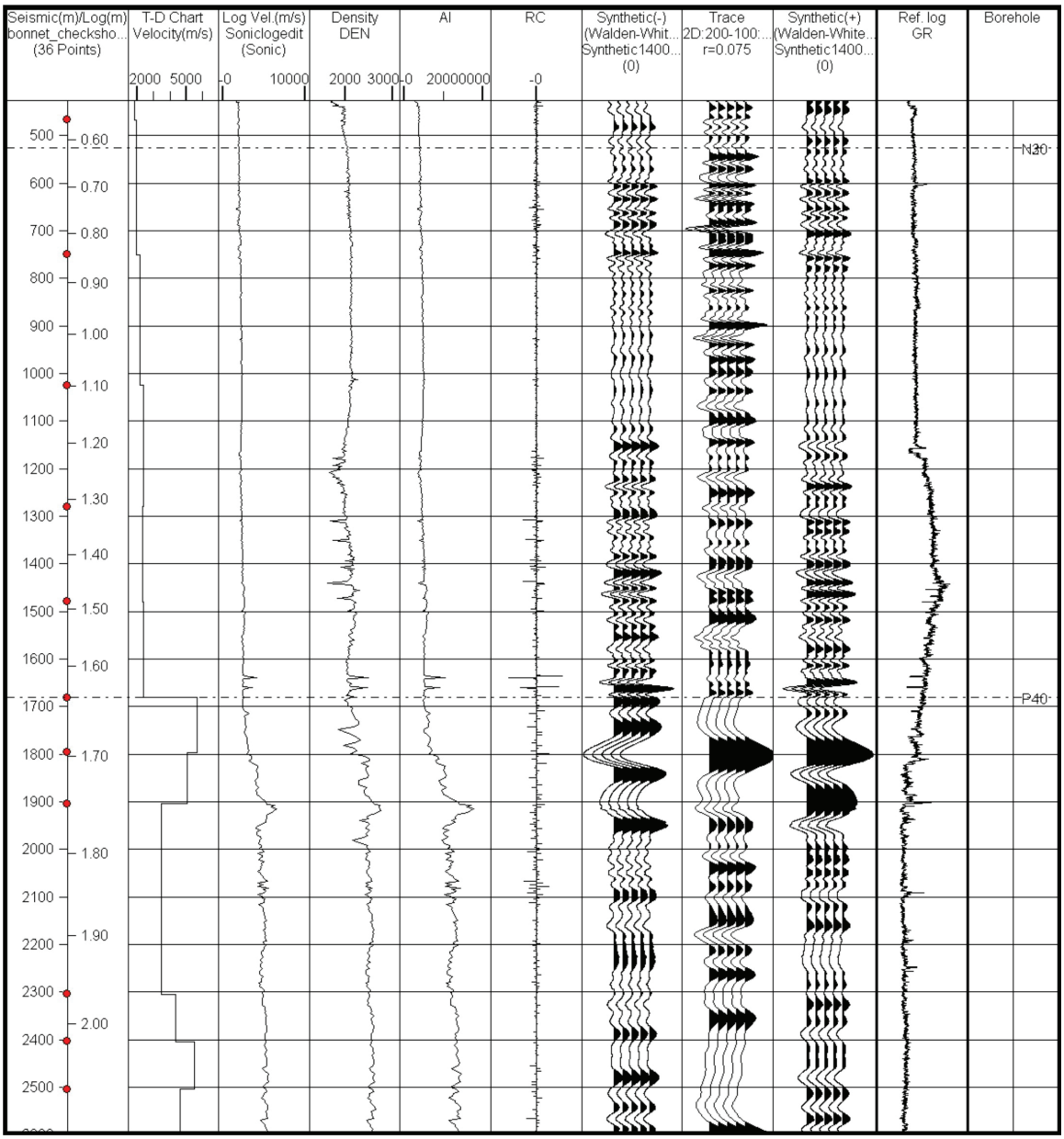

Location	42.380267 -65.049881
Drilling reference	Rotary table
Reference elevation (for measured depths)	25 m
Water depth	133.5 m
Total depth	4336 m

Newburn H-23

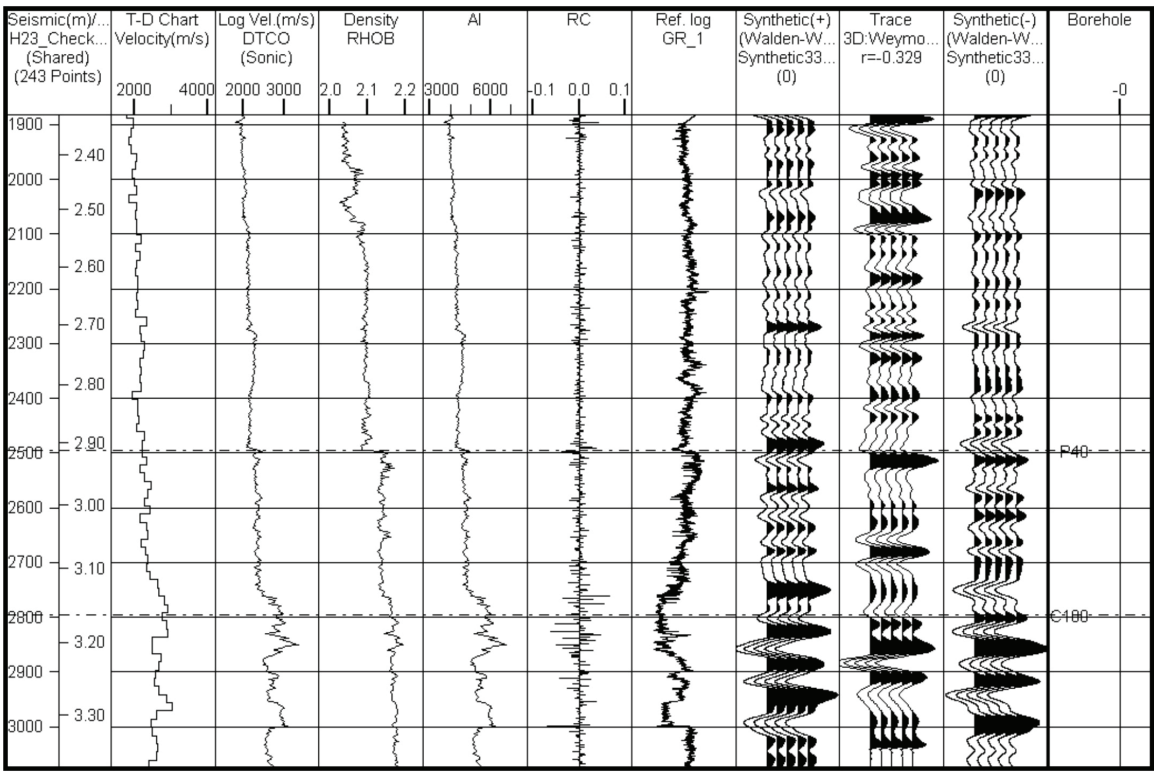

Location	43.204646 -60.805123
Drilling reference	Rotary table
Reference elevation (for measured depths)	24 m
Water depth	977 m
Total depth	6070 m

Shelburne G-29

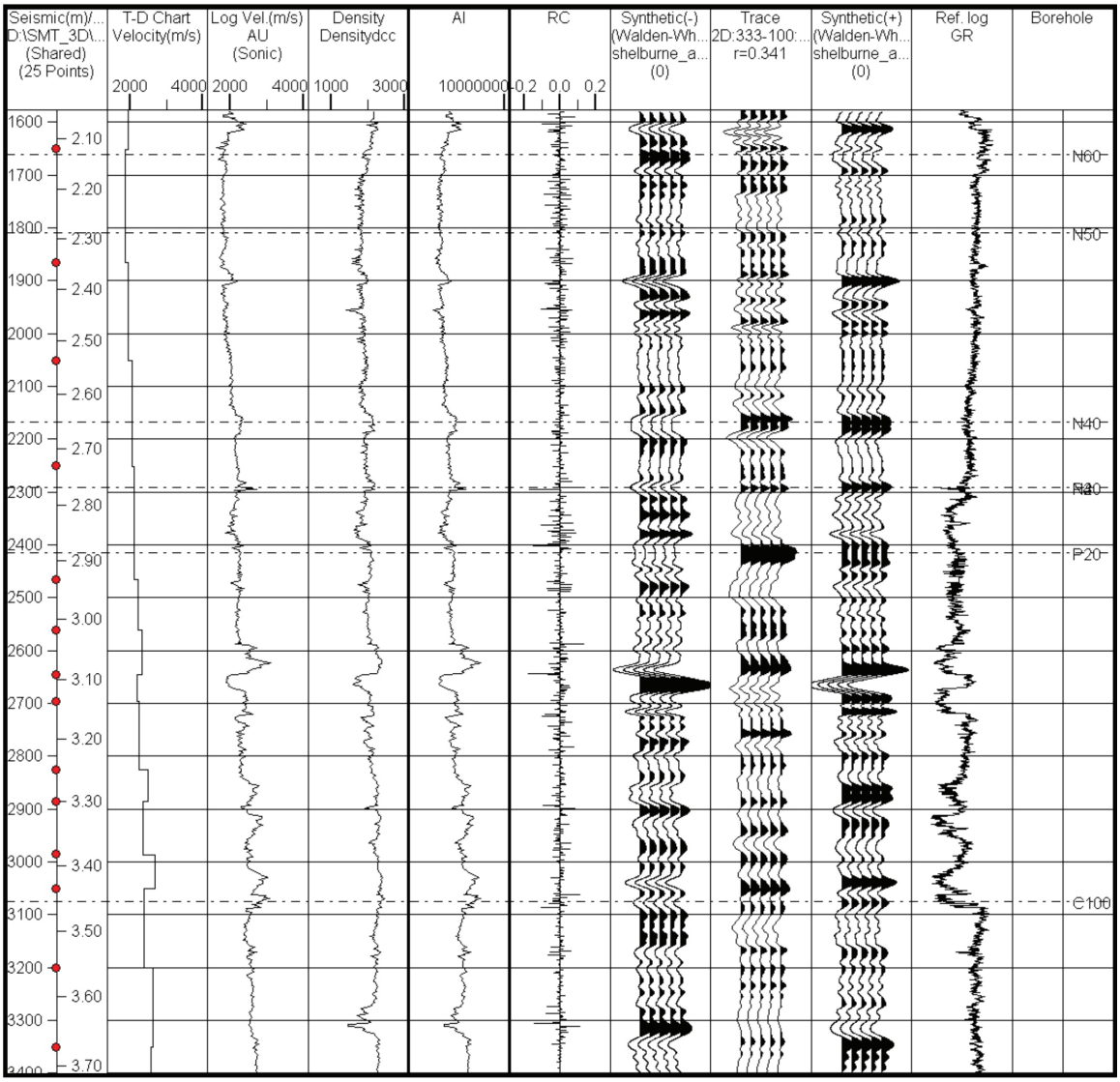

Location	42.640869 -63.558608
Drilling reference	Rotary table
Reference elevation (for measured depths)	24 m
Water depth	1153.5 m
Total depth	4005 m

Shubenacadie H-100

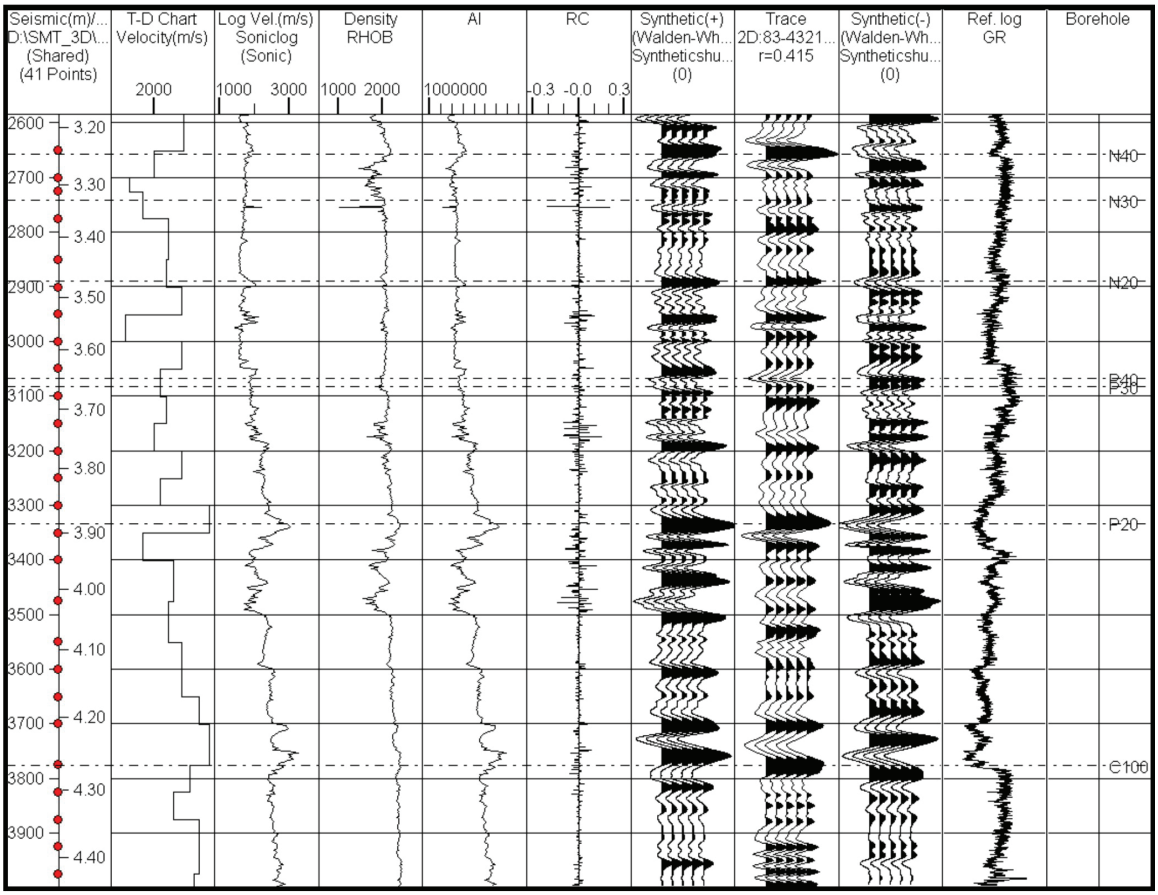

Location	42.824644 -61.477811
Drilling reference	Rotary table
Reference elevation (for measured depths)	24 m
Water depth	1476.5 m
Total depth	4200 m

Torbrook C-15

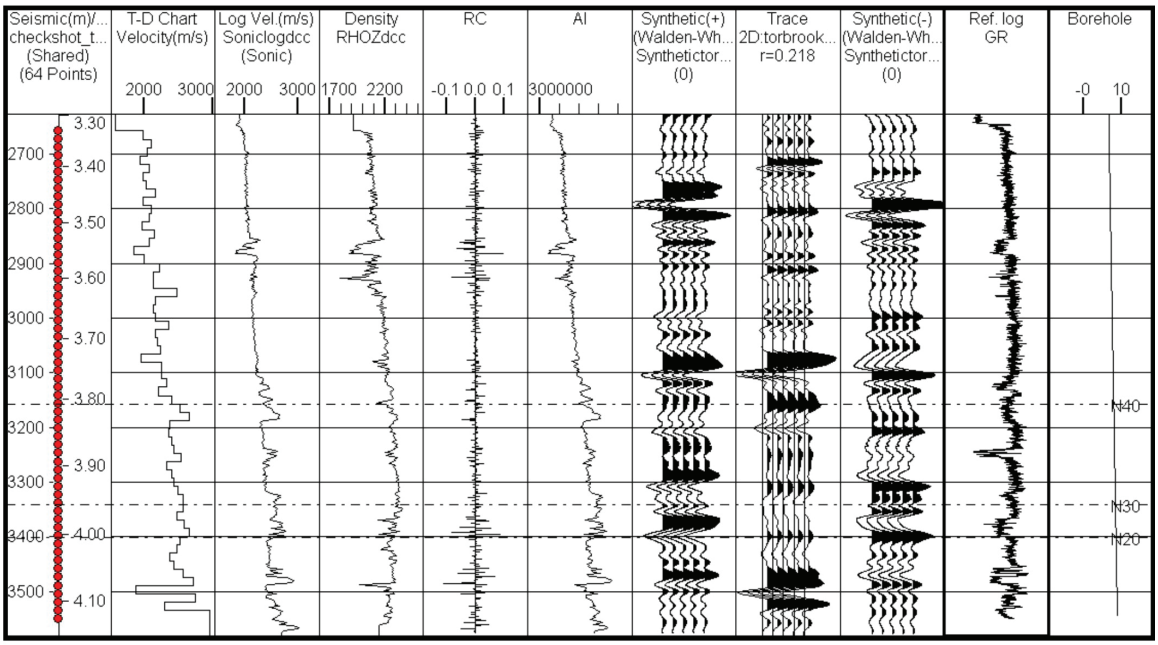

Location	42.567511 -62.292587
Drilling reference	Rotary table
Reference elevation (for measured depths)	25 m
Water depth	1674 m
Total depth	3600 m

Weymouth A-45

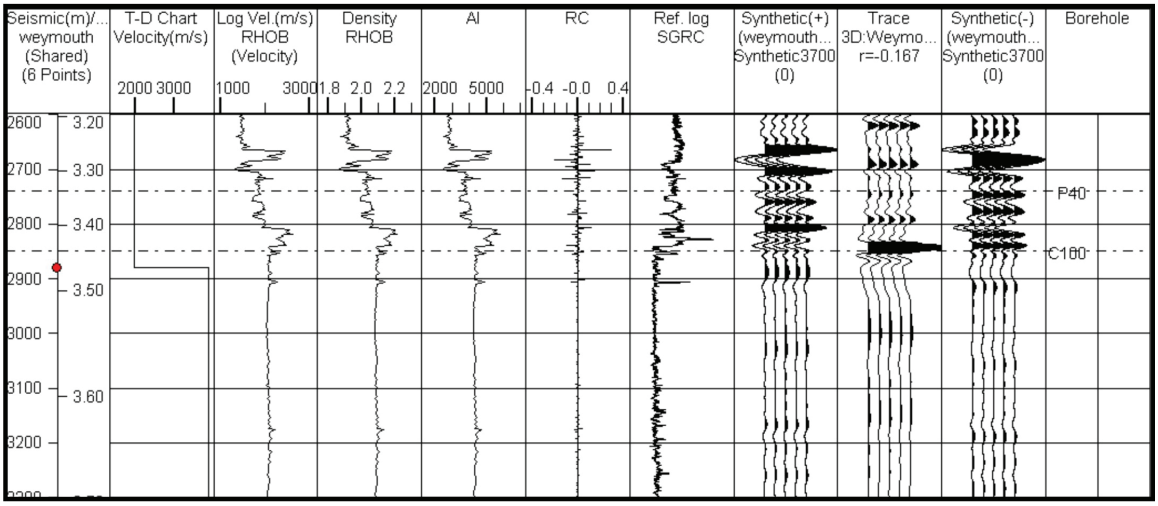

Location	43.06705 -60.603909
Drilling reference	Rotary table
Reference elevation (for measured depths)	25 m
Water depth	1689.7 m
Total depth	6520 m

APPENDIX III- COPYRIGHT PERMISSION FOR CAMPBELL AND MOSHER (2010) (CH. 3)

SPRINGER LICENSE
TERMS AND CONDITIONS

May 05, 2011

This is a License Agreement between Calvin Campbell ("You") and Springer ("Springer") provided by Copyright Clearance Center ("CCC"). The license consists of your order details, the terms and conditions provided by Springer, and the payment terms and conditions.

All payments must be made in full to CCC. For payment instructions, please see information listed at the bottom of this form.

License Number	2662590705602
License date	May 05, 2011
Licensed content publisher	Springer
Licensed content publication	Springer eBook
Licensed content title	Middle to Late Miocene Slope Failure and the Generation of a Regional Unconformity Beneath the Western Scotian Slope, Eastern Canada
Licensed content author	D. C. Campbell
Licensed content date	Jan 1, 2010
Type of Use	Thesis/Dissertation
Portion	Full text
Number of copies	40
Author of this Springer article	Yes and you are the sole author of the new work
Order reference number	
Title of your thesis / dissertation	The Late Cretaceous and Cenozoic Geological History of the Outer Continental Margin off western Nova Scotia, Canada
Expected completion date	Jul 2011
Estimated size(pages)	250
Total	0.00 CAD
Terms and Conditions	

Introduction
The publisher for this copyrighted material is Springer Science + Business Media. By clicking "accept" in connection with completing this licensing transaction, you agree that the following terms and conditions apply to this transaction (along with the Billing and Payment terms and conditions established by Copyright Clearance Center, Inc. ("CCC"), at the time that you opened your Rightslink account and that are available at any time at http://myaccount.copyright.com).

Limited License
With reference to your request to reprint in your thesis material on which Springer Science and Business Media control the copyright, permission is granted, free of charge, for the use indicated in your enquiry. Licenses are for one-time use only with a maximum distribution equal to the number that you identified in the licensing process.

This License includes use in an electronic form, provided it is password protected or on the university's intranet, destined to microfilming by UMI and University repository. For any other electronic use, please contact Springer at (permissions.dordrecht@springer.com or permissions.heidelberg@springer.com)

The material can only be used for the purpose of defending your thesis, and with a maximum of 100 extra copies in paper.

Although Springer holds copyright to the material and is entitled to negotiate on rights, this license is only valid, provided permission is also obtained from the (co) author (address is given with the article/chapter) and provided it concerns original material which does not carry references to other sources (if material in question appears with credit to another source, authorization from that source is required as well). Permission free of charge on this occasion does not prejudice any rights we might have to charge for reproduction of our copyrighted material in the future.

Altering/Modifying Material: Not Permitted
However figures and illustrations may be altered minimally to serve your work. Any other abbreviations, additions, deletions and/or any other alterations shall be made only with prior written authorization of the author(s) and/or Springer Science + Business Media. (Please contact Springer at permissions.dordrecht@springer.com or permissions.heidelberg@springer.com)

Reservation of Rights
Springer Science + Business Media reserves all rights not specifically granted in the combination of (i) the license details provided by you and accepted in the course of this licensing transaction, (ii) these terms and conditions and (iii) CCC's Billing and Payment terms and conditions.

Copyright Notice:
Please include the following copyright citation referencing the publication in which the material was originally published. Where wording is within brackets, please include verbatim.
"With kind permission from Springer Science+Business Media: <book/journal title, chapter/article title, volume, year of publication, page, name(s) of author(s), figure number(s), and any original (first) copyright notice displayed with material>."

Warranties: Springer Science + Business Media makes no representations or warranties with respect to the licensed material.

Indemnity
You hereby indemnify and agree to hold harmless Springer Science + Business Media and CCC, and their respective officers, directors, employees and agents, from and against any and all claims arising out of your use of the licensed material other than as specifically authorized pursuant to this license.

No Transfer of License
This license is personal to you and may not be sublicensed, assigned, or transferred by you to any other person without Springer Science + Business Media's written permission.

No Amendment Except in Writing

This license may not be amended except in a writing signed by both parties (or, in the case of Springer Science + Business Media, by CCC on Springer Science + Business Media's behalf).

Objection to Contrary Terms
Springer Science + Business Media hereby objects to any terms contained in any purchase order, acknowledgment, check endorsement or other writing prepared by you, which terms are inconsistent with these terms and conditions or CCC's Billing and Payment terms and conditions. These terms and conditions, together with CCC's Billing and Payment terms and conditions (which are incorporated herein), comprise the entire agreement between you and Springer Science + Business Media (and CCC) concerning this licensing transaction. In the event of any conflict between your obligations established by these terms and conditions and those established by CCC's Billing and Payment terms and conditions, these terms and conditions shall control.

Jurisdiction
All disputes that may arise in connection with this present License, or the breach thereof, shall be settled exclusively by the country's law in which the work was originally published.

Other terms and conditions:

v1.2

Gratis licenses (referencing $0 in the Total field) are free. Please retain this printable license for your reference. No payment is required.

If you would like to pay for this license now, please remit this license along with your payment made payable to "COPYRIGHT CLEARANCE CENTER" otherwise you will be invoiced within 48 hours of the license date. Payment should be in the form of a check or money order referencing your account number and this invoice number RLNK10981946.
Once you receive your invoice for this order, you may pay your invoice by credit card. Please follow instructions provided at that time.

Make Payment To:
Copyright Clearance Center
Dept 001
P.O. Box 843006
Boston, MA 02284-3006

For suggestions or comments regarding this order, contact Rightslink Customer Support: customercare@copyright.com or +1-877-622-5543 (toll free in the US) or +1-978-646-2777.

APPENDIX IV- COPYRIGHT PERMISSION FOR CAMPBELL AND DEPTUCK (IN PRESS) (CH. 5)

SEPM
Society for Sedimentary Geology

May 5, 2011

D. Calvin Campbell
Geological Survey of Canada
P O Box 1006
Dartmouth NS B2Y 4A2
Canada
cacampbe@nrcan.gc.ca

Mr. Campbell:

In response to your request for permission reprint the article listed below from an SEPM publication. I am sending this formal approval. The specific figures requested are:

Campbell, D.C., and Deptuck, M.E., 2011, Alternating bottom current dominated and gravity flow dominated deposition in a lower slope and rise setting – Insights from the seismic geomorphology of the western Scotian margin, Eastern Canada *in* Prather, B.E., Deptuck, M.E., Mohrig, D., van Hoorn, B., Wynn, R.B., eds., Application of Seismic Geomorphology Principles to Continental Slope and Base-of-Slope Systems: Case Studies from Seafloor and Near-Seafloor Analogues. SEPM Special Publication *in press*.

This is to inform you that non-exclusive world rights are hereby granted for both print and electronic media on the condition that proper credit is provided. A standard credit line for SEPM (Society for Sedimentary Geology) is acceptable.

Sincerely,

[redacted]

Michele Tomlinson
SEPM Publications & Technology Coordinator
4111 S Darlington, Suite 100
Tulsa, OK 74135-6373